2013

Design, synthesis, and characterization of porphyrin derivatives for biological applications

Raja Gabadage Waruna Eranga Jinadasa
Louisiana State University and Agricultural and Mechanical College, rjinad1@lsu.edu

DESIGN, SYNTHESIS, AND CHARACTERIZATION OF PORPHYRIN DERIVATIVES FOR BIOLOGICAL APPLICATIONS

A Dissertation

Submitted to the Graduate Faculty of the
Louisiana State University and
Agricultural and Mechanical College
in partial fulfillment of the
requirements for the degree of
Doctor of Philosophy

in

The Department of Chemistry

by
R. G. Waruna Jinadasa
B.Sc., University of Colombo, 2006
December 2013

Dedicated with love to my parents

And my wife and son

ACKNOWLEDGEMENTS

First and foremost I offer my sincerest gratitude to my doctoral mentor, Professor Kevin M. Smith, who has supported me throughout my Ph.D study with his patience and unsurpassed knowledge whilst allowing me the room to work in my own way. I could not have imagined having a better advisor and mentor for my Ph.D studies. I also want give my sincere appreciations to Professor M. Graça H. Vicente for her guidance and support; she always encouraged me to do my best, and was always there for me to help me with my research. Without their guidance and persistent help, this Dissertation would not have been possible.

I would like to thank my doctoral committee members: Professor Carol M. Taylor and Professor William E. Crowe, and Professor John R. White for taking time out from their busy schedules and agreeing to serve on my advisory committee. I am deeply thankful to Dr. Xiaoke Hu and Dr. Zehua Zhou for in vitro cellular investigations, to Dr. Frank R. Fronczek for the crystal structure determinations, to Connie David for the support in mass spectrometry and especially to the late Dr. W. Dale Treleaven and Dr. Thomas Weldegheorghis for all their help in the NMR facility.

In my daily work I have been blessed with a friendly and cheerful group of fellow students. Heartiest thanks go to past and present fellow doctoral colleague in my group, Dr. N. V. S. Dinesh Bhupathiraju, Dr. Timsy Uppal, Dr. Alecia M. McCall, Dr. Krystal R. Fontenot, Dr. Javoris V. Hollingsworth, Dr. Benson G. Ongarora, Moses I. Ihachi, Haijun Wang, Jamie Hayes, Qianli Meng, Tyrslai Williams, Ning Zhao, Elizabeth Okoth for friendship, and for sharing their enthusiasm and suggestions on my work.

I am very much grateful to my family, my wife Chamini Karunaratne and son Yevin Deemitha, who supported me in every possible way to see the completion of this work. Finally, I take this opportunity to express the profound gratitude from my deep heart to my beloved parents and my siblings for their love, encouragement and help, at every stage of my personal and academic life; they longed to see this achievement come true.

TABLE OF CONTENTS

GLOSSARY OF ABBREVIATIONS

δ	Chemical shift
Ac	Acetyl
Boc	N-*tert*-butoxycarbonyl
BoDIPY	Boron-dipyrromethene
Bn	Benzyl
br	broad
^{13}C NMR	Carbon 13 Nuclear Magnetic Resonance
d	doublet
DCC	N,N'-Dicyclohexylcarbodiimide
DCE	Dichloroethane
DDQ	2,3-Dichloro-5,6-dicyano-1,4-benzoquinone
DIEA	N,N-Diisopropylethylamine
DMAP	Dimethylaminopyridine
DMSO	Dimethylsulfoxide
ER	Endoplasmic reticulum
ESI	Electrospray ionization
EtOAc	Ethyl acetate
EtOH	Ethyl alcohol
^{1}H NMR	Proton Nuclear Magnetic Resonance
HCC	Hepatocellular carcinoma
HEp2	Human epithelial type 2
HOBt	1-Hydroxybenzotriazole
HPLC	High Performance Liquid Chromatography

HPPH	2-[1-Hexyloxyethyl]-2-devinyl-pyropheophorbide-*a*
HRMS	High Resolution Mass Spectrometry
IC_{50}	Half maximal inhibitory concentration
J	Coupling constant
MALDI	Matrix Assisted Laser Desorption Ion Ionization
MeOH	Methanol
MS	Mass Spectrometry
m/z	mass to charge ratio
NBS	N-bromosuccinimide
NIS	N-iodosuccinimide
NMR	Nuclear Magnetic Resonance
PDT	Photodynamic Therapy
PEG	Polyethylene glycol
Ph	Phenyl
PMe	Methyl propionate
ppm	parts per million
q	quartet
RT	room temperature
s	singlet
SaO_2	Oxygen saturation
t	triplet
TBTU	N,N,N′,N′-Tetramethyl-O-(benzotriazol-1-yl)uronium tetrafluoroborate
TCCA	Trichloroisocyanuric acid
TCT	Trichlorotriazine

TEA	Triethylamine
TFA	Trifluoroacetic acid
THF	Tetrahydrofuran
TLC	Thin Layer Chromatography
p-TSA	p-Toluenesulfonic acid

ABSTRACT

Chapter 1 of this Dissertation presents a brief introduction to the basic properties of porphyrins and their derivatives (hydroporphyrins), their abundance and functions in the nature, and their applications in photodynamic therapy.

Chapter 2 reports the synthesis, characterization, conformational analysis and cellular studies of novel mono conjugated regioisomers of chlorin e_6 derivatives that are promising photosensitizers for photodynamic therapy. All three regioisomers were synthesized from pheophytin a, which was extracted from the alga *Spirulina pacifica*. *In vitro* investigations using human carcinoma HEp2 cells show that the 15^2-lysyl regioisomers accumulate the most within cells, and the most phototoxic are the 13^1 regioisomers. Cellular studies revealed that the 13^1-aspartylchlorin e_6 conjugate could be a more efficient photosensitizer for PDT than the currently used commercial 15^2 derivative.

Chapter 3 describes the synthesis, characterization and cellular investigation of water soluble regioisomers of di-conjugated chlorin e_6 derivatives for photodynamic therapy. New synthetic routes were developed to synthesize all three regioisomes. Both the 15^2,17^3-diamino and 13^1,17^3-diamino derivatives were synthesized starting from chlorin e_6 and the 13^1,15^2-diamino derivatives were synthesized from pheophytin a. The effects of position and number of amino acid substituents on their *In vitro* photodynamic properties are described.

Chapter 4 discussed the design, synthesis and characterization of electron deficient symmetric porphyrin for incorporation into a synthetic cytochrome to mimic the activity of native cytochrome. It also presents a brief introduction of basic synthetic routes to obtain porphyrin macrocycles. The importance of the construction of artificial hemoproteins to understand the cytochromes activity is also discussed. Various synthetic routes and strategies to obtain the symmetric porphyrin are reported in detail.

CHAPTER 1: INTRODUCTION

1.1 Porphyrins

Porphyrin is a macrocycle which consists of four pyrrole units, and each of these pyrrole units is connected with each other by methine (=CH-) bridges. The macrocycle is fully conjugated and has 22π electrons but only 18π electrons participate in the delocalized aromatic system according to Hückel's 4n+2 rule.[1-3] As a result of the extended conjugation, porphyrins absorb light in the visible region and are highly colored. Porphyrins obeys Hückel's rule of aromaticity (n=4) and they are usually planar according to their crystal structures. Their aromaticity has been confirmed using heat of combustion measurements, bond distances (X-ray crystal structures),[4,5] and chemical shifts in ^{1}H NMR spectroscopy.[1,6]

The classical nomenclature for porphyrin was first introduced by H. Fischer.[7] The four methine positions between the pyrrole units were assigned as α, β, ϒ and δ: in general, they are named the *meso* positions. The peripheral β pyrrolic positions were numbered from 1 to 8. Later the four pyrrole rings in the pophyrin were labeled as A, B, C and D and all the carbons and nitrogens in the macrocycle were numbered from 1 to 24 (Figure 1.1). This nomenclature was accepted by IUPAC and is currently also used to designate porphyrinoid derivatives such as isoporphyrin, chlorin, etc.[8]

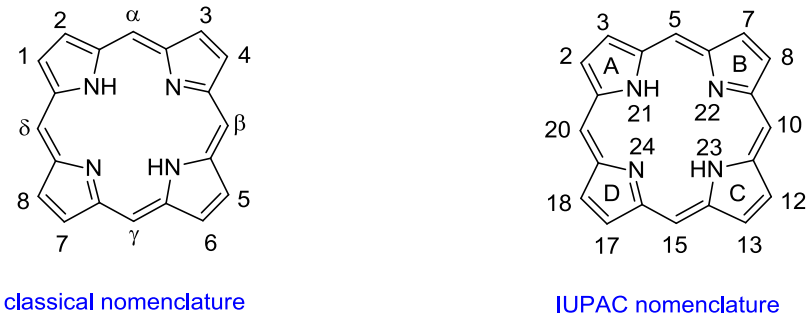

Figure 1.1: Porphyrin nomenclature

Unsubstituted porphyrin (porphin) can exist in two different tautermeric forms (Figure 1.2). Spectroscopic and computational calculations proved tautomer **1** which holds two hydrogens on two

opposite pyrrole rings; this is more stable than the tautomer **2** with two hydrogens at adjacent pyrrole rings.[9]

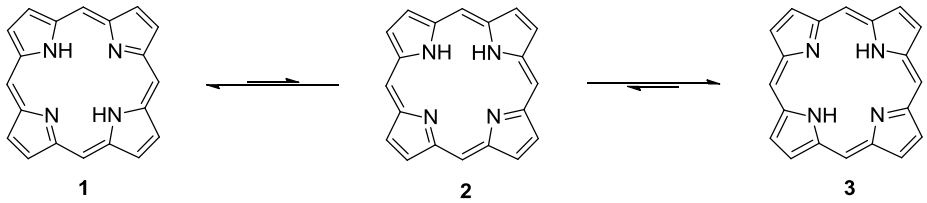

Figure 1.2: Tautermerization of porphyrin

Porphyrin acts as a tetradentate ligand while binding with metal ions. The macrocyclic cavity of the porphyrin can coordinate with metal ions having a maximum radius of 2 Å.[10] The geometry of these complexes and number of additional ligands is a property of the metal ion.[11] Depending on the metal, they can form square planar (Cu^{2+}, Ni^{2+}), square-pyramidal (Mg^{2+}, Zn^{2+}) or octahedral (Fe^{2+}, Mn^{2+}) complexes. Almost all metal ions form a 1:1 complex with porphyrin. Upon coordination of metal, two protons on the inner nitrogens will leave and form neutral complexes with divalent metals. Central metal ions can coordinate with porphyrins through σ-coordination with nitrogen lone pairs and π-interaction of metal pπ or dπ orbitals with other nitrogens π orbitals. σ-Coordination of the inner nitrogens always acts as an electron donor to the metal ion but π-coordination can act as either a π-donor or acceptor depending on the metal and the substituents on the porphyrin. These metalloporphyrins play vital roles in biological systems associating with globular proteins. Hemoglobin, myoglobin, chlorophyll, cytochromes, catalases and peroxidases are well known examples. They play a very important role not only in biological systems but also in chemical, industrial and technological fields as biosensors, semiconductors and catalysts.[12]

1.2 Spectroscopic Character of Porphyrins

Due to their highly conjugated π system, porphyrins show very characteristic absorption spectra. They show intense absorption around 380 to 420 nm, called the Soret band or B-band, and a few weaker absorption bands in the longer wavelength region (500 to 750 nm) of visible light, called Q bands or β –

α bands.[13] According to Gouterman's four orbital model (Figure 1.3), the Soret band corresponds to excitation of the porphyrin from its ground state to its second excited state (S_0 to S_2) and Q bands correspond to excitation from the ground state to the first excited state (S_0 to S_1). Because of x and y polarization of free base porphyrin the HOMO (e_{gx}) and HOMO-1 energy levels are not degenerate; hence the Q band is further split in to four bands.[14,15] Upon formation of a metalloporphyrin, the symmetry of the porphyrin changes from D_{2V} to D_{4h} (4-fold symmetry) as it removes the protons on the inner nitrogens. As a result of higher symmetry the HOMO and HOMO-1 energy levels are degenerate and the absorption spectrum of metalloporphyrins shows only two Q bands in the visible region. Protonation of the macrocycle also results in an effective 4-fold symmetry and gives rise to spectra displaying only two Q-bands (Figure1.4).

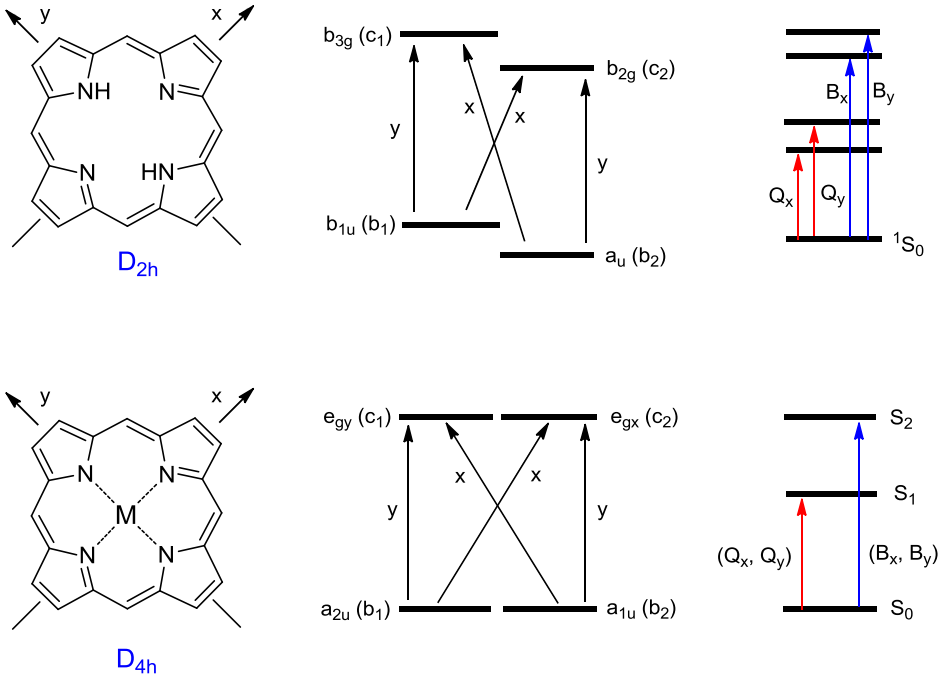

Figure 1.3: Simplified Gouterman four-orbital model for D_{2h} symmetry free-base porphyrins (top) and transition-metal D_{4h} symmetry porphyrins (bottom).[14]

The characteristic changes in the absorption spectrum during chemical reactions provide evidence about the possible alteration of the structure. While variations of the peripheral substituents

on the porphyrin ring often cause minor changes to the intensity and wavelength of the absorption features, protonation of two of the inner nitrogen atoms or the insertion/change of metal atoms into the macrocycle usually strongly changes the visible absorption spectrum.[16]

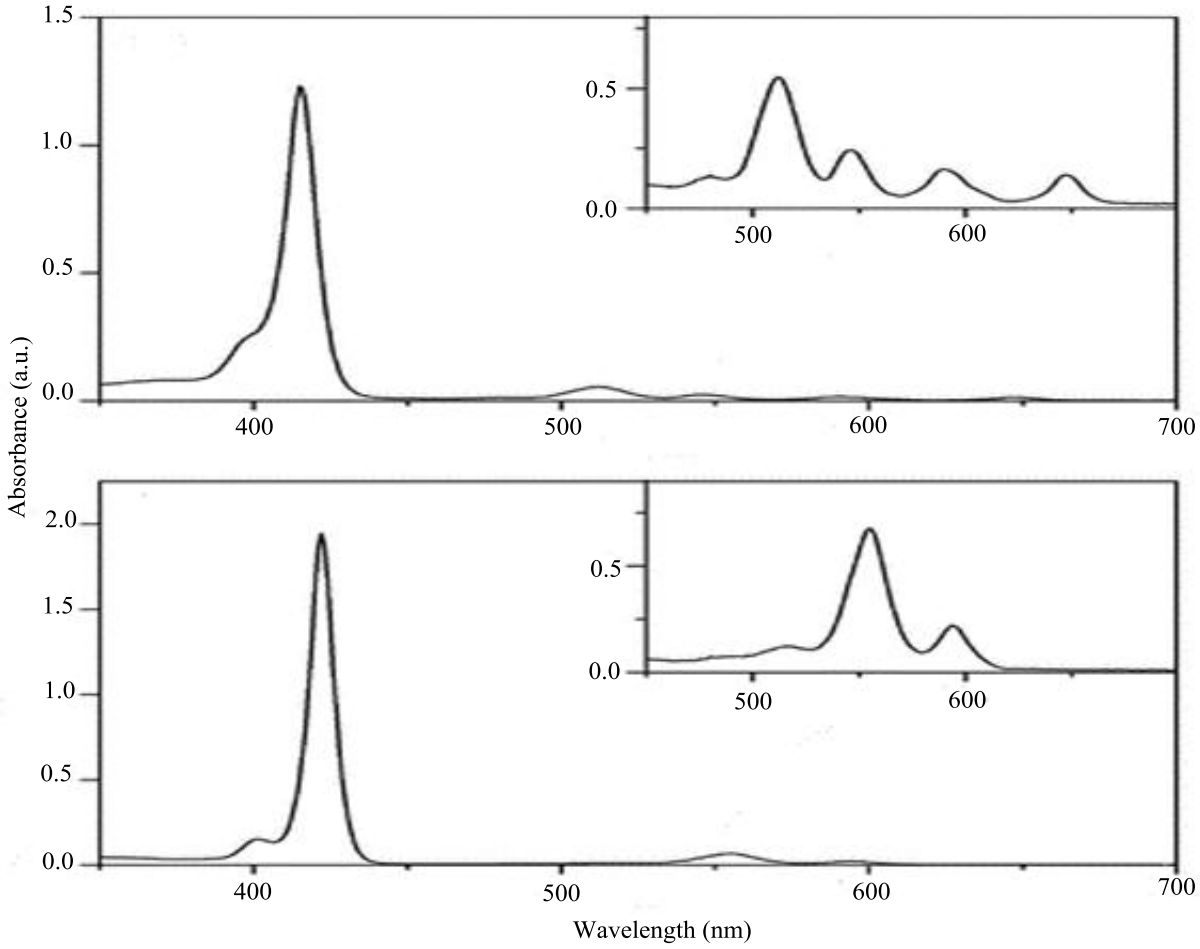

Figure 1.4: Typical UV–Vis spectra for a free-base porphyrin (top) and a porphyrin-metal complex (bottom). [Adapted with permission from reference 12. Copyright (2010) American Chemical Society.]

As in benzene, the chemical shifts of the proton signals of porphyrins are strongly affected by the aromatic ring current. ^{1}H NMR signals for *meso* protons (5, 10, 15, 20) appear far down field (around 10 ppm) in the ^{1}H NMR spectrum compared with normal sp^2 hybridized CH protons. Protons at beta positions are also shifted further downfield than normal sp^2 hybridized CH protons and are slightly shifted upfield compared to the *meso* protons. All these peripheral protons are positioned in the

deshielded region of the porphyrin spectrum. As a consequence of the induced diamagnetic ring current, the inner NH protons are shifted to the negative region of the ^{1}H NMR spectrum as they are in the shielded region. Also, substituents on the porphyrin show the same behavior. The closer the substituent to the ring, the more downfield the protons appear relative to its normal position.

1.3 Hydroporphyrins

Hydroporphyrins are partially reduced derivatives of porphyrins (Figure 1.5). Saturation of one or more of the porphyrin double bonds by hydrogen atoms or alkyl groups will form the various hydroporphyrins. Generally, oxidation of the hydroporphyrin macrocycle back to porphyrin is easier than further reduction. The most common hydroporphyrins in nature are chlorins (dihydroporphyrins), bacteriochlorins and isobacteriochlorins (tetrahydroporphyrins) which all retain their macrocyclic conjugation. Reduction of one pyrrole double bond in the porphyrin ring leads to a dihydroporphyrin (chlorin). Further reduction of the dihydroporphyrin will result in the tetrahydroporphyrin in which the reduced pyrrole double bonds occur either in opposite pyrrole units (called bacteriochlorins) or in adjacent pyrroles (called isobacteriochlorins). As reported in the recent literature, all these porphyrins, chlorins and bacteriochlorins show aromatic character[17] as they have conjugated 18π electron systems and further reduction of pyrrole double bonds in bacteriochlorins is energetically unfavored.[18] Saturation of the bridging methine positions of porphyrin will lead to loss of their macrocyclic conjugation and results in non-aromatic *meso*-hydrogenated systems like porphodimethene and porphyrinogen.

The class of dihydroporphyrins or chlorins includes chlorophyll, pheophytin and bacteriochlorophylls c, d, e and f which regulate the photosynthesis of green plants and phototrophic bacteria. Bacteriochlorophylls a, b, and g belong to the class of bacteriochlorins. Due to their photophysical properties, some members of the chlorin and bacteriochlorin families are of great interest

in the medicinal field for photodynamic therapy (PDT). Siroheme is a heme-like prosthetic group found in sulfite and nitrite reductase enzymes; it belongs to the class of isobacteriochlorins.

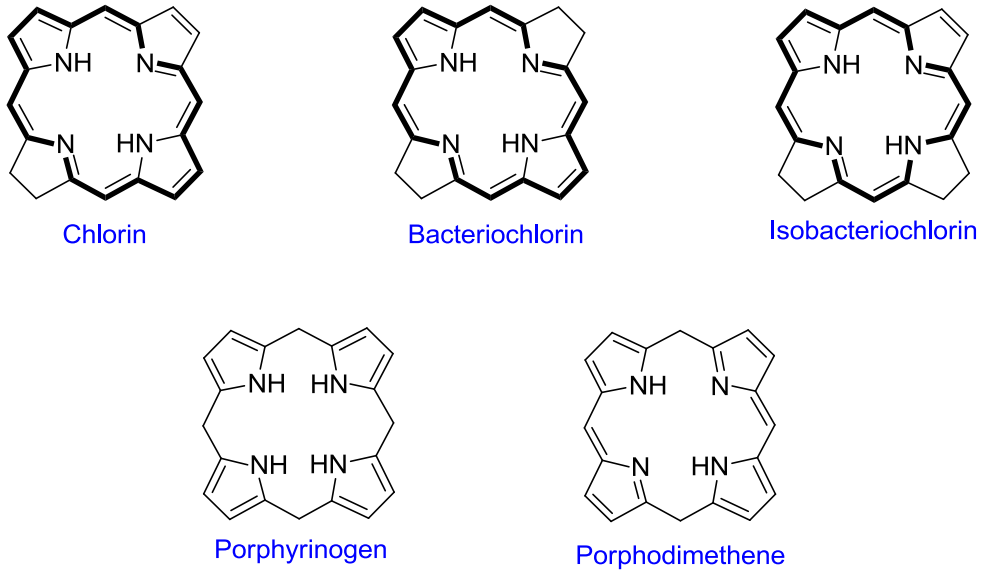

Figure 1.5: Structures of hydroporphyrins

1.4 Naturally Occurring Porphyrins

Porphyrin derivatives, especially metal complexes, play a vital role in several life processes. Their functions vary and depend on the protein environment and the central metal ion. For example hemeproteins, which contain a porphyrin prosthetic group, are responsible for oxygen transport in hemoglobin, oxygen storage in myoglobin, electron transport in cytochromes and oxygen reduction in cytochrome oxidase. The variations in the function of hemeproteins mainly come from the interaction between the protein and heme prosthetic group. Chlorophyll is another very important porphyrin-based natural system, which is a catalyst in the process of converting light energy to chemical energy in plants, photosynthesis.

1.4.1 Hemoglobin and Myoglobin

Hemoglobin and myoglobin are two of the most important proteins in the body. They are high molecular weight protein systems containing an iron(II) protoporphyrin IX prosthetic group (heme group, Figure 1.6a). Their function is to facilitate transport and storage of molecular oxygen in higher animals. Hemoglobin binds with O_2 and transports it from the lungs to the muscle cells. Then it transfer O_2 to myoglobin which has higher affinity for O_2 than does hemoglobin. By itself, heme is not a good oxygen carrier. It must be part of a larger protein to prevent oxidation of the Fe^{2+} to Fe^{3+} in the porphyrin core.

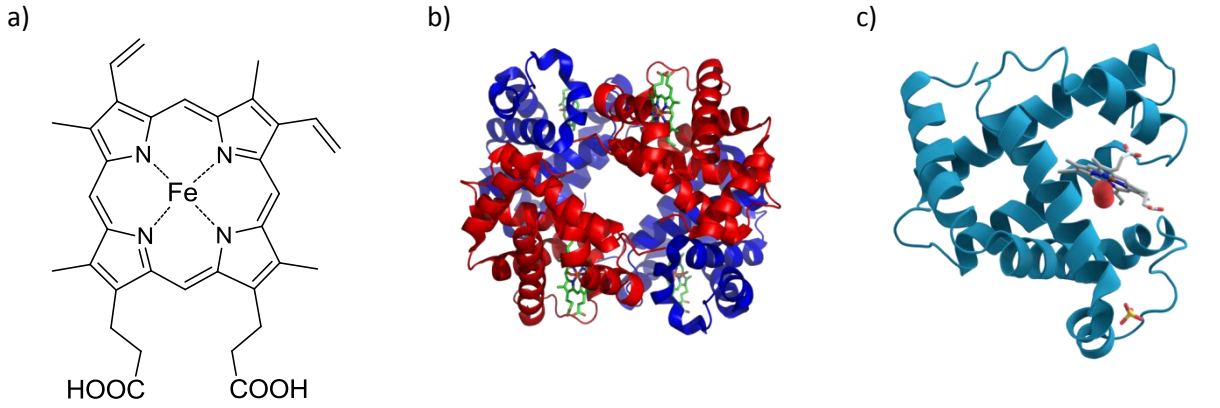

Figure 1.6: a) Heme prosthetic group, the iron(II) protoporphyrin-IX complex; b) Structure of human hemoglobin.[19] The protein α and β subunits are in red and blue, and the iron-containing heme groups in green; c) Structure of oxymyoglobin.[20] Modified from references 19 and 20.

Hemoglobin consists of four subunits (two α and two β) and each holds one heme group (Figure 1.6b). In the lungs the partial pressure of O_2 is high and the pH is low due to low CO_2 concentration. These factors favor the formation of a hemoglobin-O_2 complex. Once the first O_2 molecule binds with the heme group, that changes the shape of the protein in a way favorable for binding (relaxed state) of the second O_2 molecule. This special property, called the cooperative effect, is mainly caused by the decrease in the size of Fe^{2+} after binding with O_2. It is due to a change in the spin state of Fe^{2+} (Figure1.7).

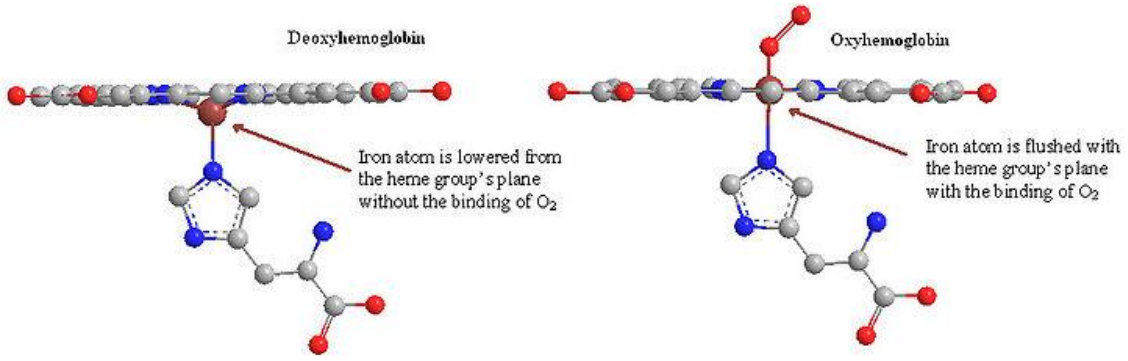

Figure 1.7: Iron(II) slight orientation changes from deoxyhemoglobin to oxyhemoglobin.[21]

As shown in Figure 1.6, four of the six coordination sites of Fe^{2+} are occupied by nitrogen atoms from a planar porphyrin ring. The fifth coordination site is occupied by a nitrogen atom of an imidazole ring of the histidine amino acid. In deoxyhemoglobin (Hb) the sixth coordination site is available for coordination with dioxygen. Because of lower crystal field splitting, the iron(II) in deoxyheamoglobin is in a high spin state and has a radius of 92 pm. Therefore the ferrous ion is positioned slightly out of the porphyrin plane. When dioxygen, which is a weak ligand, binds to the ferrous of the hemoglobin (HbO_2) it increases the crystal field slightly, increasing the splitting just enough tip the iron into a low spin state - its radius contracts to 75 pm and the ion moves into the plane of the porphyrin along with the histidine residue.[22] That changes the conformation of the protein and increases the binding affinity for dioxygen (cooperative effect) to the other units, probably by breaking some salt bridges in the protein. Inside the cells, the partial pressure of O_2 is low and the pH is high due to higher concentration of CO_2. These conditions favor the tense state which has low affinity for O_2 and leads to release of dioxygen.

Myoglobin is a single-chain globular protein containing an iron(II) protoporphyrin IX prosthetic group in the center (Figure 1.6c). Myoglobin has a higher affinity for O_2 than hemoglobin, even at lower O_2 concentration. The active site of myoglobin is very similar to that of hemoglobin. A proximal histidine group is attached directly to the iron center and there is a histidine group on the opposite face, not

bonded to the iron. This is called the distal histidine, and influences the affinity for O_2 by increasing the O_2 binding constant by hydrogen bonding to dioxygen (Figure 1.8). This histidine residue serves two very important functions in the polypeptide; 1) It prevents oxidation of the Fe^{2+} to Fe^{3+} by any number of possible oxidizing agents. If it is oxidized to ferric, the O_2 affinity will be lost; 2) the position of this histidine side chain makes it difficult to bind carbon monoxide (CO) to the iron in a linear fashion, while allowing oxygen to bind easily as it binds to iron in a bent fashion. Formally, free heme has a much higher (23,000 times) affinity for CO than O_2, but in hemoglobin and myoglobin, CO has a lower binding constant compared to free heme.

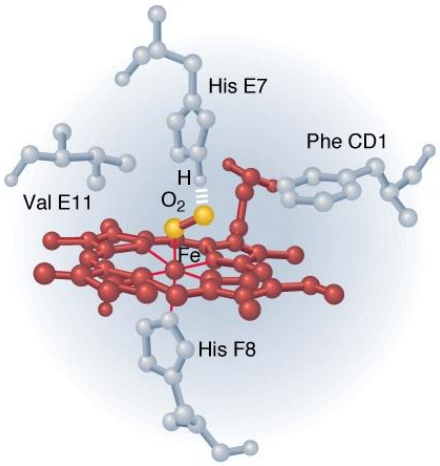

Figure 1.8: The distal histidine amino acid from the hemoglobin protein molecule further stabilizes the O_2 molecule by hydrogen-bonding interactions.[23]

1.4.2 Chlorophyll

Chlorophyll is vital for photosynthesis, which allows plants and cyanobacteria to absorb energy from light and convert it into chemical energy. Chlorophylls are mainly found in chloroplasts of plants and cyanobacteria. Most of the chlorophylls (*a*, b, d, and f) are chlorin pigments containing a magnesium as a central metal ion, but few of them (chlorophyll c1 and c2) remain as unreduced porphyrin derivatives. Slight changes in peripheral substituents in chlorin and porphyrin macrocycles result in different classes of chlorophylls as shown in Figure 1.9.

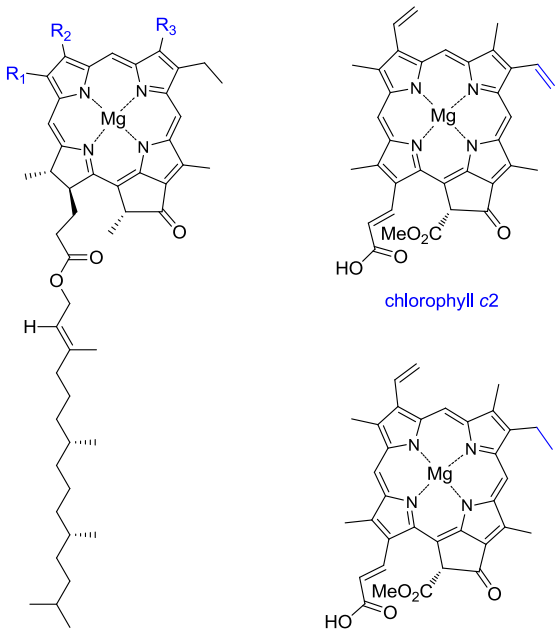

	Chlorophyll a	Chlorophyll b	Chlorophyll d	Chlorophyll f
R_1	$-CH_3$	$-CH_3$	$-CH_3$	-CHO
R_2	$-CH=CH_2$	$-CH=CH_2$	-CHO	$-CH=CH_2$
R_3	$-CH_2CH_3$	-CHO	$-CH_2CH_3$	$-CH_2CH_3$

Figure 1.9: Structures of different chlorophylls

As shown in Figure 1.9, chlorophyll derivatives consist of a porphyrinoid macrocycle with a central magnesium ion. All chlorophylls contain the isocyclic β-keto ester ring that is biosynthetically derived from the C13 propionic acid side chain of protoporphyrin IX. Peripheral substituents in chlorophylls vary widely. There are more than 50 derivatives that have been isolated and identified from photosynthetic organisms. The chlorophyll c structure deviates from other chlorophylls; it has an unreduced porphyrin macrocycle compared to the dihydroporphyrin in other chlorophylls and a free unsaturated propionic acid chain at C17 compared to the phytol esterified propionic acid.

Chlorophylls absorb strongly in the blue (mostly at 430 nm) and red (mostly at 660 nm) regions of the electromagnetic spectrum (Figure 1.10). Thus, their absorption bands significantly overlap with the emission spectrum of the solar radiation reaching the biosphere, resulting in efficient tools for conversion of radiation into chemical energy.

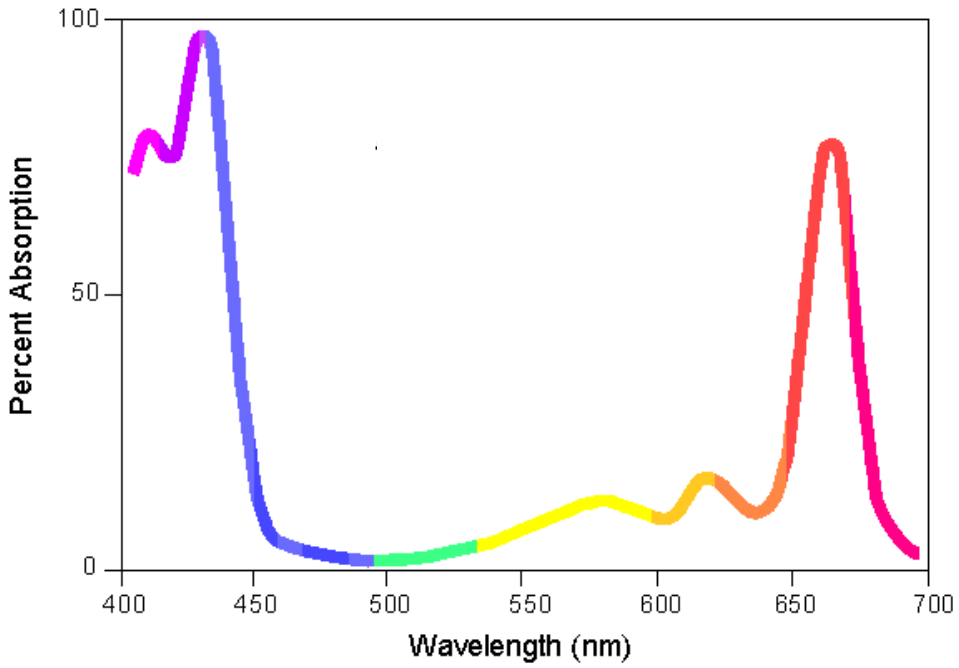

Figure 1.10: Absorption spectrum of chlorophyll a.[24]

Bacteriochlorophylls which are related to chlorophylls, are photosynthetic pigments that are found in various phototropic bacteria. Bacteriochlorophylls c, d, and e are dihydroporphyrin (chlorin) structures like chlorophylls, being reduced in ring D only. Bacteriochlorophylls a (Figure 1.11), b, and g are tetrahydroporphyrin (bacteriochlorins), which have two reduced pyrrole rings (ring B and D). In general, bacteriochlorophylls absorb light of a longer wavelength than do the chlorophylls. The position of the absorption maximum is observed in the red or infra-red region and depends on the conjugation of the macrocycle and its protein environment.

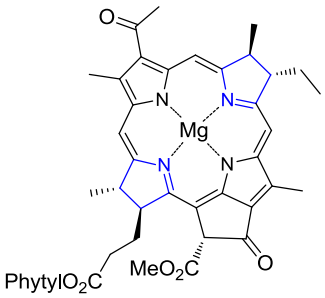

Bacteriochlorophyll a

Figure 1.11: Structure of bacteriochlorophyll a

All of these chlorophyll derivatives (chlorophylls and bacterochlorophylls) share a number of modifications in the macrocycle to achieve their main function; light harvesting. These common structural modifications include 1) usage of Mg^{2+} as the central metal ion; 2) addition of an extra ring (five membered isocyclic ring) to the tetrapyrrole structure; 3) loss of one or more double bonds from the conjugated system, but while still maintaining their aromaticity; and 4) with an elongated nonpolar phytol group. These modifications impart unique properties to chlorophylls, such as longer wavelength light absorption compared with heme groups, and increased lipophilicity and electron transfer ability.

1.4.2.1 Chemical Degradation of Chlorophylls

Chlorophyll a and b are the most common and predominant pigments in all oxygen-evolving photosynthetic organisms such as higher plants, red and green algae. The ratio of chlorophyll a to b in the chloroplast is normally 3:1. It is known that the ratio of chlorophyll a to b varies with the amount of light received by the plant, for example, the ratio is higher in high-light growth conditions than in low-light growth conditions. These pigments can be extracted from plant leaves and from alga in large quantities. Chlorophyll a and b can be separated by classical and high performance liquid chromatography. Also more convenient large scale separation methods by solvent partition have been reported.[4] The reagent Girard 'T' (carboxymethyltrimethylammonium chloride hydrazide) readily reacts

with the 3-formyl group of chlorophyll b to form the water soluble derivative and makes the separation easier.

Pheophytin a (**5**) and b (a chlorophyll molecule lacking a central Mg^{2+} ion) can be obtained from chlorophyll a (**4**) and b respectively by treating with a mild acid. Effective hydrolysis of the phytol ester group of pheophytin **5** to achieve pheoporbide **6** has been reported under acidic, alkaline and enzymatic conditions. In addition both the phytyl residue and the magnesium atom of chlorophyll **4** (in ether) can be removed under acidic conditions (30% HCl) to form pheophorbide **6** (Scheme 1.1).

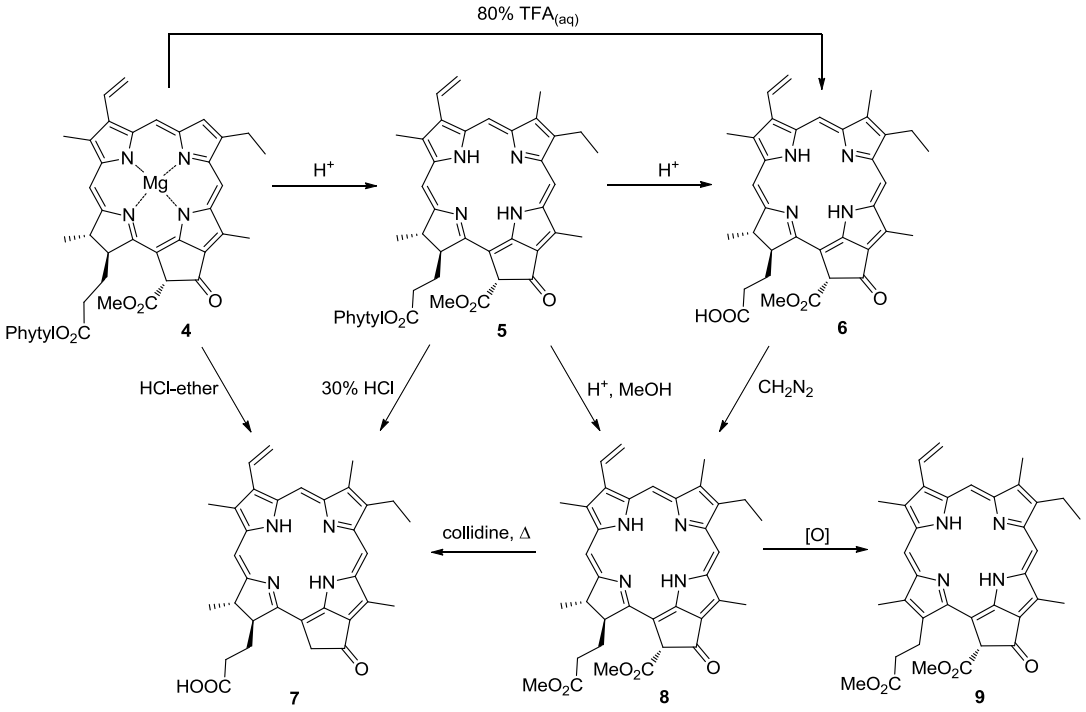

Scheme 1.1: Pathways for hydrolysis and transesterification of phytol ester group of pheophytin a

As reported, hydrolysis of the phytyl propionate group of chlorophyll b requires a higher concentration of HCl than does the hydrolysis of the phytyl propionate group of chlorophyll a (**4**) and this fact has been used successfully to separate chlorophyll a (**4**) from b.[9] But with HCl-ether conditions, the hydrolysis of both phytol residue and 13^2-CO_2Me group of chlorophyll **4** to its acid and subsequent

decarboxylation of the 13^2-COOH group with formation of the corresponding pyropheophorbide **7** was reported.[9] Then the regioselective hydrolysis of the phytyl propionate residue of chlorophyll **4** was performed using 80% aqueous trifluoroacetic acid at 0 ^{0}C by Wasielewski and Svec.[25] Transesterification of pheophytin **5** by the action of methanol in the presence of sulfuric acid produced methyl pheophorbide **8** in quantitative yield.[8] Also esterification of pheophorbide **6** with diazomethane produced methyl pheophorbide **8** in high yield. Oxidation of any chlorin with dichlorodicyanobenzoquinone (DDQ) gives the corresponding porphyrin. For example, methyl pheophorbide a (**8**) gives 2-vinylpheoporphyrin a_5 dimethyl ester (**9**) where in the subscript number indicates the number of oxygen atoms in the molecule. If methyl pheophorbide **8** is refluxed in collidine it gives the corresponding 'pyro' derivative **7**.

Air oxidation of pheophorbide a (**6**) under alkaline conditions initially forms the hydroperoxide intermediate **10** and subsequent fragmentation of the hydroperoxide and loss of the phytol residue results in Fisher's so-called "unstable chlorin" **11** (Scheme 1.2).[8]

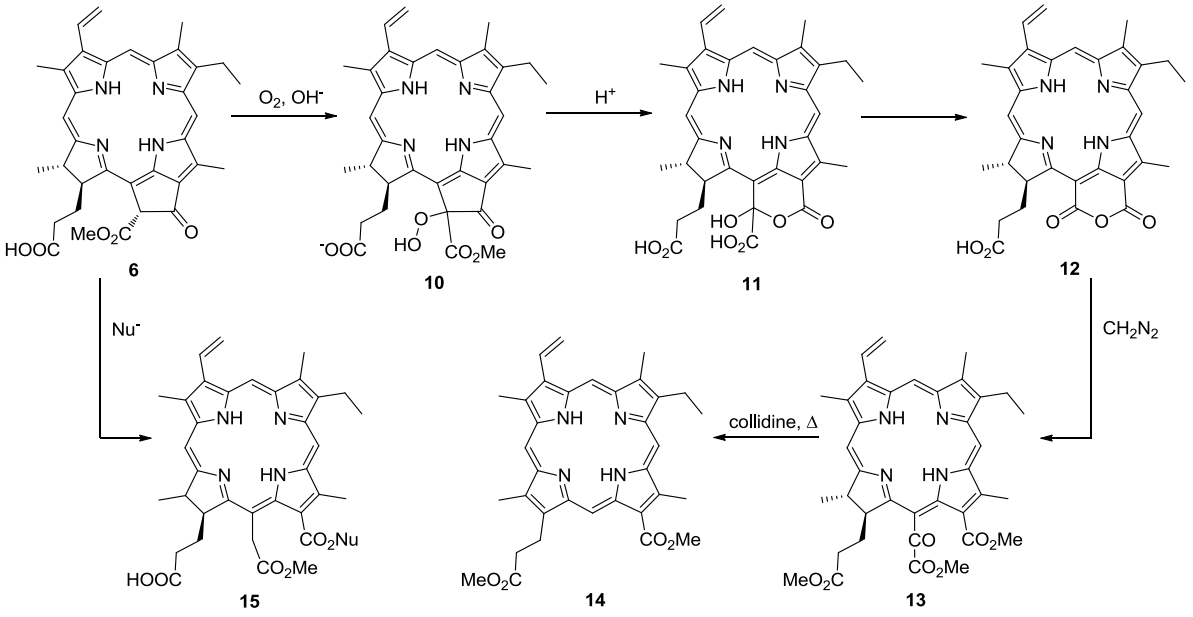

Scheme 1.2: Pathways for modification of the isocyclic ring of pheophorbide a (**6**)

On evaporation of the solvent this chlorin **11** is converted into purpurin-18 (**12**) and subsequent esterification with diazomethane gives the purpurin 7 trimethyl ester (**13**). Further refluxing of purpurin 7 trimethyl ester (**13**) in collidine produces rhodoporphyrin-XV dimethyl ester (**14**) in 81% yield. Base catalyzed nucleophilic addition to the β-keto ester group of pheophorbide-*a* (**6**) under an inert atmosphere (without involvement of oxygen) leads to the isocyclic ring-opened chlorin derivative **15** through intermediate formation of a 15[2] enol.

Under alkaline conditions pheophorbide a (**6**) is converted into chlorin e_6 (**16**) by cleaving the isocyclic ring. Chlorin e_6 features prominently in this Dissertation. Opening of the isocyclic ring of pheophorbide a (**6**) by methoxide followed by esterification with diazomethane affords the chlorin e_6 trimethyl ester (**17**, Scheme 1.3).

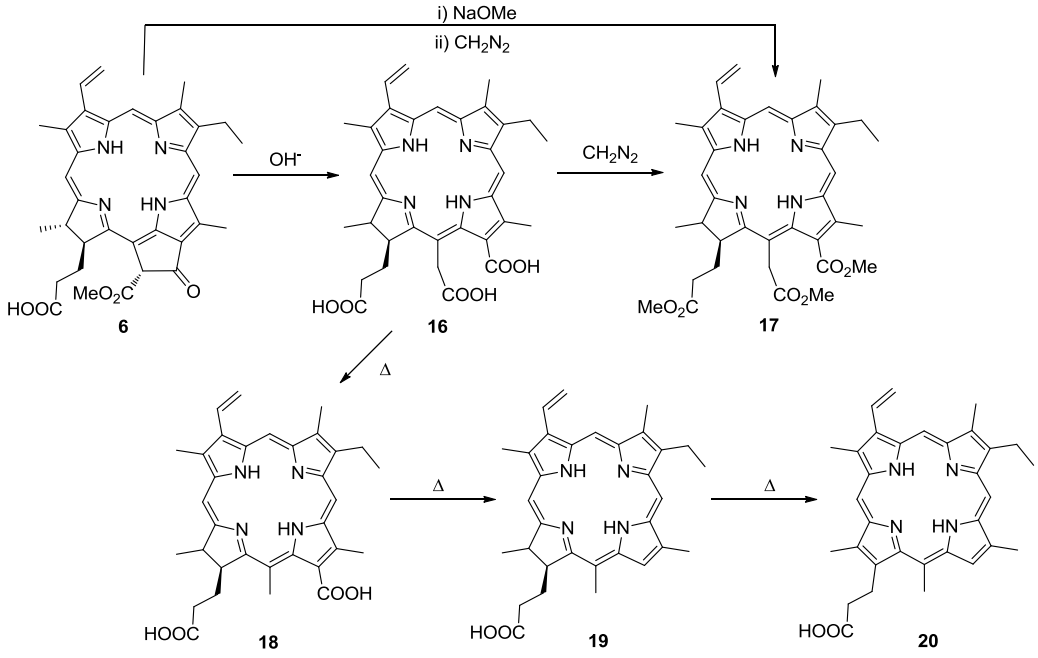

Scheme 1.3: Modifications of chlorin e_6

Methanolysis of methyl pheophorbide a (**8**) affords chlorin e_6 trimethyl ester (**17**) in quantitative yield. Decarboxylation of the free acid groups of chlorin e_6 (**16**) sequentially forms chlorin **18** and **19**. Upon further heating of chlorin **19** the stable phylloporphyrin XV (**20**) is formed.

Treatment of chlorin e_6 (**16**) with potassium permanganate and subsequent esterification of the resulting diacid **21** leads to formation of the formyl derivative **22**. When heated with hydroxylamine hydrochloride in aqueous pyridine, the formyl derivative **22** leads to deformylation to afford rhodochlorin **23**. Intramolecular aldol condensation of the formyl derivative **22** results in introduction an extra six membered ring to the chlorin core. The formyl derivative **22** can be treated with hydrogen cyanide to afford cyanolactone **25** and subsequent reduction with a zinc/acetic acid system followed by esterification gives the nitrile derivative **26**. Hydrolysis of the nitrile derivative **26** followed by esterification can afford chlorine e_6 trimethyl ester (**17**).

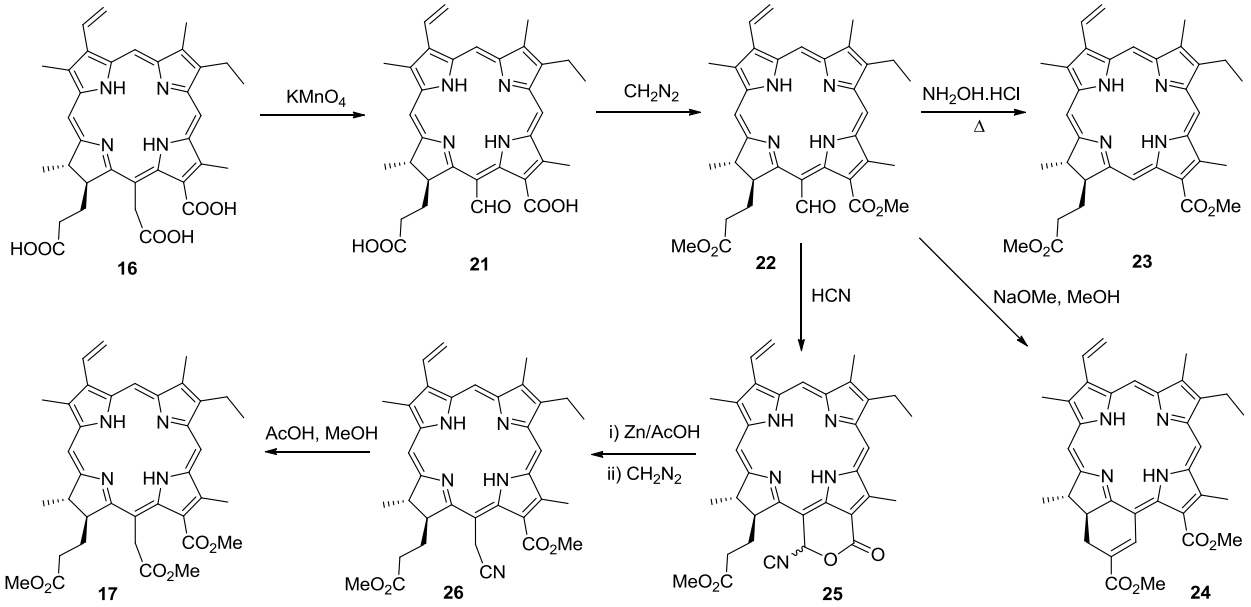

Scheme 1.4: Further modifications of the carboxyl groups on the chlorin e_6 (**16**)

1.4.3 Cytochromes

Cytochromes are proteins with heme prosthetic groups that take part in oxidation/reduction reactions by carrying electrons. They can be found in the inner mitochondrial membrane or in the endoplasmic reticulum in cells.

In the past these pigments were classified into groups based on the position of the lowest energy absorption band in the reduced state. For example cytochrome-*a* (605 nm), cytochrome-*b* (565 nm) and cytochrome-*c* (550 nm). But nowadays cytochromes are subdivided into four classes depending on the nature and the mode of binding of the heme prosthetic groups to protein. At least 30 different cytochromes have been identified.

There are four major established subclasses (Figure 1.12):

(1) Cytochromes-*a* contain heme-*a* as the prosthetic group.

(2) Cytochromes-*b* contain heme-*b* (protoheme) as the prosthetic group, not covalently bound to the protein.

(3) Cytochromes-*c* contain a prosthetic group very similar to heme-*b* but there are covalent thioether linkages between the heme side-chains and the protein.

(4) Cytochromes-*d* contain a tetrapyrrolic chelate of iron as the prosthetic group, in which the degree of conjugation of double bonds is less than is found in porphyrin.[26]

Both heme-*a* and heme-*c* are biosynthetically derived from heme-*b*. Conversion of the vinyl group at position 2 in heme-*b* to a hydroxylethylfarnesyl side chain followed by oxidation of the methyl group at position 8 to a formyl group will result in heme-*a*. The porphyrin macrocycle of cytochrome *c*, which is very similar to the porphyrin macrocycle of cytochrome-*b*, linked to the protein via two cysteine residues of the protein with the two vinyl groups of the porphyrin. All other cytochrome heme groups are covalently bound to the protein. Unlike in hemoglobin and myoglobin, in cytochromes all six coordination sites of iron are occupied by specific amino acid residues of the protein and the nitrogens in the porphyrin. Therefore cytochromes cannot bind to ligands such as O_2 and CO. Their function involves transfer of a single-electron, in a reversible equilibrium between the Fe^{2+} and Fe^{3+} states of the

central iron atom. Even though they have very similar prosthetic groups, their reduction midpoint potentials span an 800 mV range, from cytochrome-c_3 (-400 mV) to cytochrome-b_{559} (+400 mV); this gives the electron chain its "directionality" so that electrons move from one carrier to another in the chain. These changes in redox potentials are mainly influenced by the protein environment. Other factors such as nature of axial ligation with iron, peripheral substituents of the porphyrin, solvent accessibility to the metal site, electrostatic interactions with amino acid side chains of proteins and protonation state of neighboring amino acids also influence the redox potential of the cytochrome.

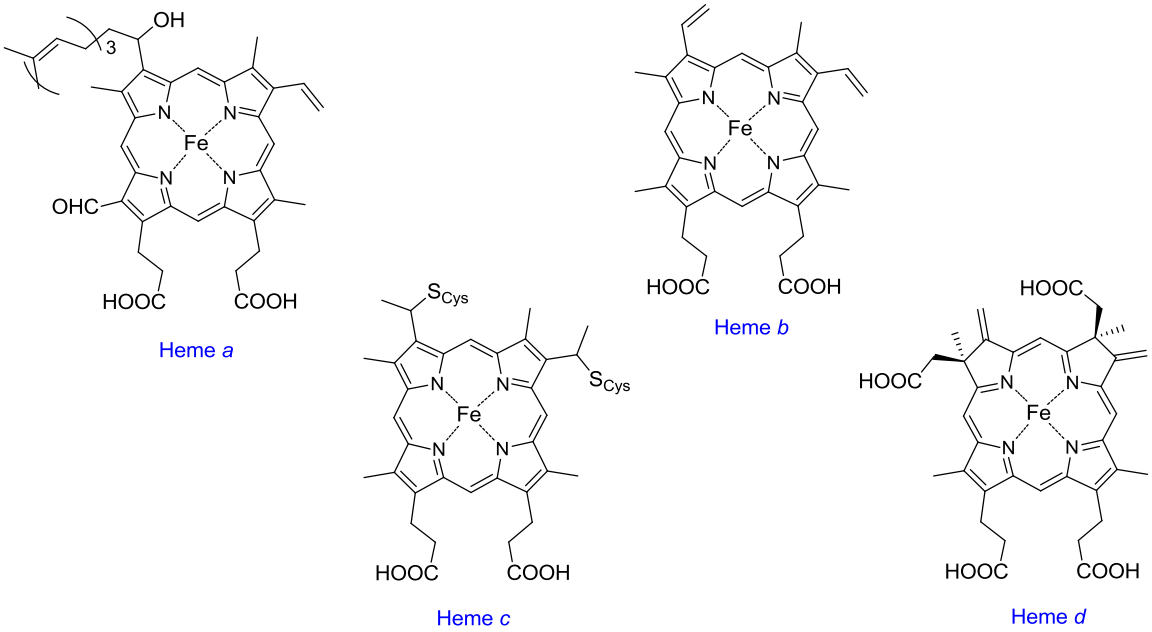

Figure 1.12: Structures of commonly occurring natural hemes -*a*, -*b*, -*c*, and -*d*.

1.5 Photodynamic Therapy (PDT)

PDT is a binary cancer therapy, which relies on selective uptake of a photosensitizer into the cancer cells which upon irradiation with light of an appropriate wavelength produce highly toxic singlet oxygen and other cytotoxic species.[27,28] Singlet oxygen can readily react with electron rich biomolecules such as unsaturated lipids, amino acids and DNA.[29] Its limited diffusion prevents damage to the normal cells next to the tumor. The selectivity of the PDT treatment depends upon both the tumor-targeting

ability of the photosensitizer and the light used to activate it. The most coherent light sources are lasers and since the maximum of skin permeability occurs in the range of approximately 620-850 nm called the "therapeutic window", light of this spectral range is predominantly used in PDT.[30] Hence, photosensitizers with a strong absorption band in this region can be activated to gather light that penetrates deeper into the tissues.

The photophysical processes of PDT are illustrated in the simplified Jablonski diagram shown in Figure 1.13. In the presence of laser radiation, a photosensitizer (P^0) which is in the ground state, is excited to a singlet excited state. Relaxation of the singlet exited state yields the short-lived lowest excited singlet state ($^1P^*$). There is little opportunity for it to react with another molecule via either electron or energy transfers because the excited singlet state has a very short life-time. Most of the singlets will return to the ground state by emitting energy in the form of fluorescence, which helps to visualize the tumor. A few of the singlet excited photosensitizers will undergo intersystem crossing to the triplet state ($^3P^*$) which has a longer life time (10^{-3} s) than the singlet state (10^{-8} s).[31] Normally these triplet state molecules will return to the ground state by emitting their energy via phosphorescence. But in the cell the excited triplet state can undergo two types of reactions; defined as types I and II mechanisms. 1) It can transfer electrons to a biological substrate to form radicals. Ultimately these electrons can interact with molecular oxygen to form superoxide (type I mechanism). 2) In the presence of ground state oxygen, which is in the triplet state, the energy will transfer from the excited triplet state of photosensitizer to ground state triplet oxygen ($^3O_2$). This will produce a short lived and highly reactive excited singlet oxygen ($^1O_2$) which can readily react destructively with any nearby biomolecules (type II mechanism). Each photosensitizer molecule can typically generate 10^3-10^5 molecules of singlet state oxygens before being degraded through photobleaching by excited singlet oxygen or by some other process.[31] In water, lifetimes of singlet oxygen are much shorter than in organic solvents and their lifetime gets even shorter in the cells due to rapid reactions with subcellular substrates. Therefore the

diffusion of singlet state oxygen from the site of generation is very limited (0.01-0.02 µm).[32] Such limited diffusion of singlet state oxygen provides a huge advantage in PDT.[33] Ultimately, these destructive reactions lead to cell death through apoptosis or necrosis.

$$P^0 + hv \longrightarrow {}^1P^*$$

$${}^1P^* \xrightarrow{ISC} {}^3P^*$$

$${}^3P^* + {}^3O_2 \longrightarrow {}^1O_2 + P^0$$

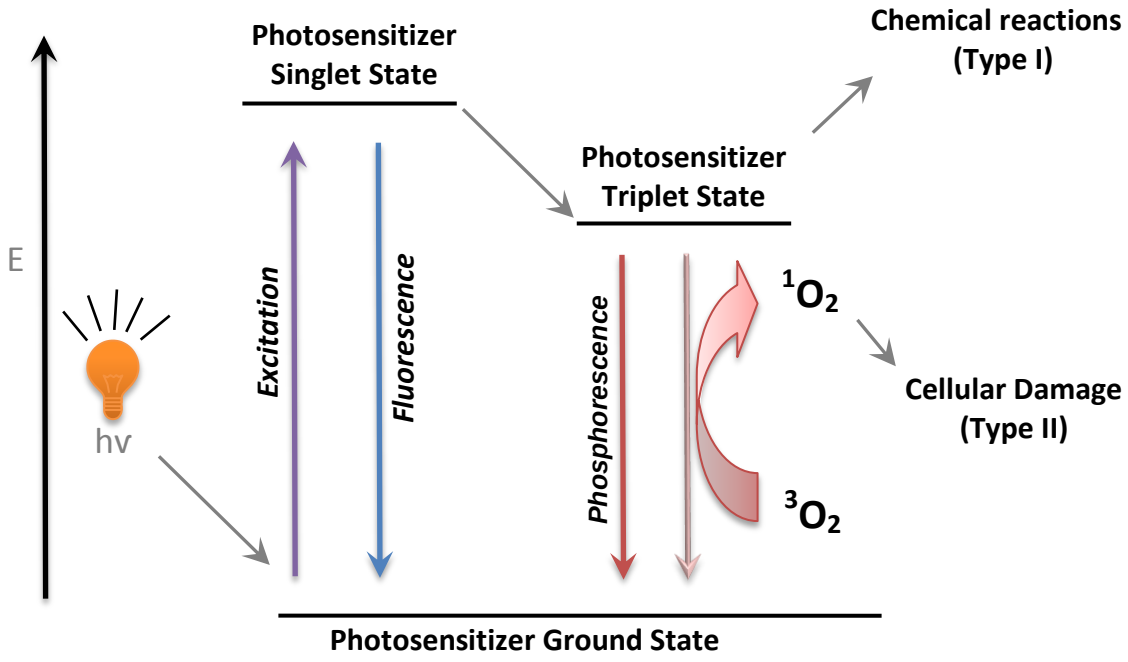

Figure 1.13: Production of singlet oxygen by PDT

In the first step of PDT (Figure 1.14), the photosensitizer or the drug is administered into the blood stream through a vein or else placed directly on the skin. Then the photosensitizer will be absorbed by the cells all over the body. But it will accumulate in cancer cells more than normal cells and

also the photosensitizer stays longer in cancer cells than normal cells. Within 72 – 96 hours after injection much of the photosensitizers accumulate in the cancer cells. Then the tumor is exposed to light of an appropriate wavelength to activate the photosensitizer. After absorbing light the photosensitizer will excite and generate singlet oxygen and eventually shrink or destroy the tumor. The major mechanism of tumor destruction is damaging the blood vessels in the tumor that prevent the tumor from receiving its essential oxygen and nutrients.

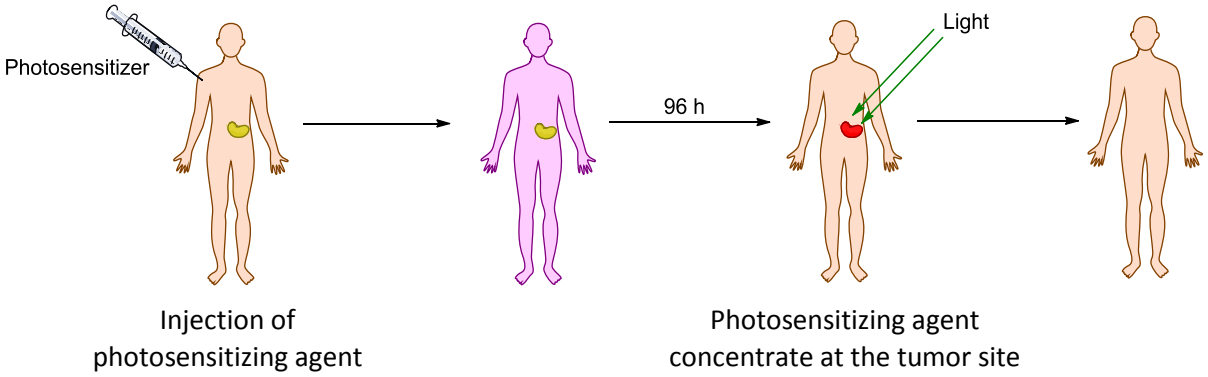

Figure 1.14: The stages of photodynamic therapy

Studies are now being performed to test the use of PDT for several types of cancer and pre-cancerous conditions, including cancers of the: skin, cervix, bladder, prostate, bile duct, pancreas, stomach, brain, mouth, and larynx (voice box). The main advantages of PDT are:

1) It is less invasive than surgery.
2) It has few long-term side effects.
3) It is a tumor targeted therapy that causes less damage to normal cells.
4) It is cost-effective compared to other cancer treatment methods.
5) It can be combined with other cancer treatments.

The usage of an external light source makes PDT limited to areas where light can reach. Therefore PDT is limited to treat cancers on or just under the skin, or in the lining of organs that can be reached

with the light source as the light can be directed through fiber optic cables to internal organs. PDT is less effective in treating larger and widely spread cancers. The poor selectivity of current photosensitizers for tumor tissue remains another main drawback in photodynamic therapy.

The selectivity toward cancer cells over normal cells in the PDT treatment depends upon both the tumor-targeting ability of the photosensitizer and the light used to activate it. Extensive research is underway to develop modern photosensitizers that meet the following criteria for an ideal photosensitizer.[34,35] It should have;

1) Minimal dark toxicity and only be cytotoxic in the presence of light
2) High quantum yield of singlet oxygen production in vivo
3) High selectivity for tumor cells over normal cells
4) Fast elimination from the skin and epithelium
5) Strong absorption peaks in the therapeutic window (the far-red and near-infrared regions)
6) Available manufacturing and synthesis
7) Homogeneous composition
8) Storage and application light stability.

The effective destruction of tumor cells requires a high concentration of singlet state oxygen in the tumor. To achieve this, the photosensitizer should have a high quantum yield of singlet oxygen production and also should have high accumulation of the photosensitizer in the tumor site.

It is well known that the 650-800 nm region is the optimal wavelength absorption for an efficient photosensitizer. Lower and upper limits are set by the absorption and scattering of tissue and the minimum energy required to excite the ground state oxygen. Lower wavelengths will increase the absorption by tissue and reduce the penetration of light. Heme proteins in the tissue absorb more light at the lower region and are maximal around 400 nm. Therefore light penetration through tissue

increases with longer wavelengths, but above 1000 nm water in the biological tissue starts to absorb light heavily (Figure 1.15).

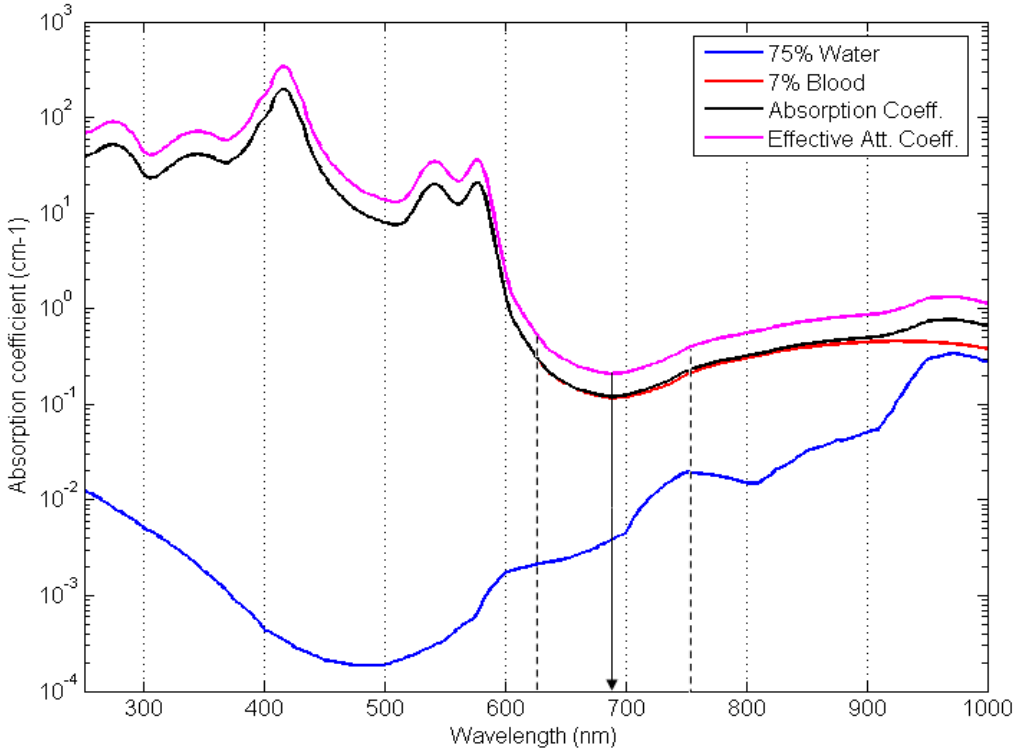

Figure 1.15: The absorption spectrum for arteries ($SaO_2 \approx 98\%$)[36]

As shown in Figure 1.16, molecular oxygen has two low-lying singlet excited states, $^1\Delta_g$ and $^1\Sigma_g^+$. Where, transition from excited state $^1\Delta_g$ to ground state ($^1\Sigma_g^-$) is spin forbidden, therefore excited state $^1\Delta_g$ Oxygen has relatively longer lifetime. Energy difference between ground state ($^1\Sigma_g^-$) and excited states, $^1\Delta_g$ and $^1\Sigma_g^+$ are 95 kJ mol^{-1} (22.5 kcal mol^{-1}) and 158 kJ mol^{-1} (31.5 kcal mol^{-1}), respectively. However, porphyrins which absorb light in the longer wavelength region emit low energy when it comes to the ground state. The energy level often mentioned for photosensitizer is that for the excitation of it to singlet state. Therefore the energy of the triplet state is even lower than that of the singlet state. If the triplet state energy is lower than the energy required to excite ground state oxygen to the singlet state (95 kJ mol^{-1}), it is not possible for it to act as an effective photosensitizer.

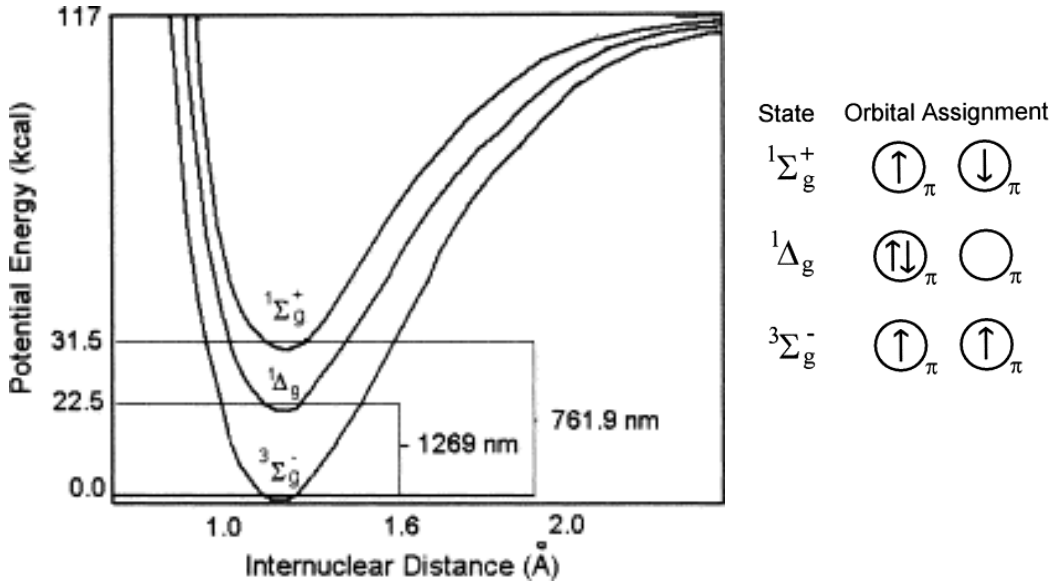

Figure 1.16: Potential energy curves for the three low-lying electronic states of molecular oxygen. [Adapted with permission from reference 31. Copyright (2002) Elsevier.]

Tumor-selectivity of photosensitizers can be increased by targeting the distinctive features of tumor tissue over normal tissue, such as increased low-density lipoprotein receptors, macrophages, acidic environment and tumor stroma with large interstitial space, leaky vasculature, increased lipids and newly-synthesized collagen. The mechanism for selectivity of porphyrin towards cancer cells is still unclear. According to our research (see later) amphiphilic character, overall charge, and spatial conformation of the molecule play a vital role in tumor selectivity.

Maintaining the proper balance between hydrophilicity and hydrophobicity is the most important factor when designing an optimal-porphyrin based photosensitizer. Previous studies revealed that hydrophobic photosensitizers readily accumulate in tumors more than hydrophilic photosensitizers, as they bind with LDL, enter into the cytoplasm via endocytosis, or binding with lipoprotein receptors, and subsequently redistribute in the membrane domain, mitochondria, Golgi apparatus, and lysosomes. However, poor solubility of these compounds in aqueous media prevents their circulation in the blood

stream and also hydrophobic drugs are retained in the body for a longer time and result in adverse skin photosensitivity reactions in the body. Conversely hydrophilic photosensitizers excrete easily from the body after the therapy. They can bind with serum albumin and accumulate in the stroma of the tumor cells.[4]

The following attributes of the porphyrin derivatives make them powerful and versatile chromophores for PDT studies:

1) The presence of main absorption bands in the therapeutic window, the Q bands, around 600-700 nm. It is advantageous to use red-shifted chromophores in order to get better penetration of exciting laser source;

2) Intense extinction coefficients. Singlet oxygen production depends on the extinction coefficient of the chromophore; and

3) Ease of modification of substituent groups. Porphyrins have several distinct functionalization sites, i.e., the *meso* position, β-position. The solubility of porphyrin derivatives in nonpolar or polar solvents can be modified by varying the porphyrin substituents.

1.5.1 Clinical Photosensitizers

Photofrin (porfimer sodium, hematoporphyrin, HpD, Figure 1.17) has been commercially developed and approved in a number of countries as a first generation photosensitizer. But it is far from an ideal photosensitizer. It is not a single compound; it consists of a mixture of monomers and oligomers of porphyrins linked by ether and ester linkages.[7] Its long wavelength absorption (Q band) is not situated within the therapeutic window. The longest wavelength absorption maximum is at 630 nm, typical for porphyrin. Therefore it has limited use due to poor light penetration. It also has longer retention times in the body and causes skin photosensitivity.

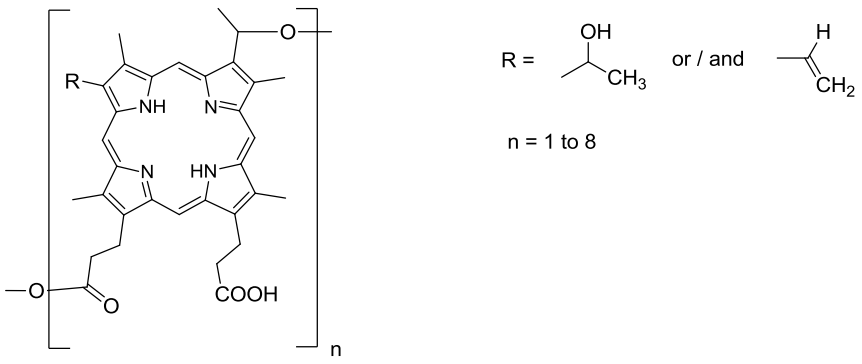

Figure 1.17: Structure of Photofrin

Levulan (5-aminolevulinic acid or ALA, Figure 1.18), which is the first unique compound in the porphyrin biosynthesis pathway, is a naturally occurring prodrug which converts enzymatically in to protoporphyrin (active photosensitizer) after administration[37,38] and it has received approval for the treatment of cancerous lesions in 1999. The active drug belongs to the porphyrin category like Photofrin and therefore suffers from weak absorption in the therapeutic window. The drug is applied superficially on the tumor because of lack of selectivity when it is administered systemically.[39] The use of ALA in PDT has several advantages over Photofrin: there is a more rapid clearance (limiting skin photosensitivity to 1–2 days), it can be applied topically for the treatment of skin cancer and orally for cancer in the oral cavity or digestive tract.

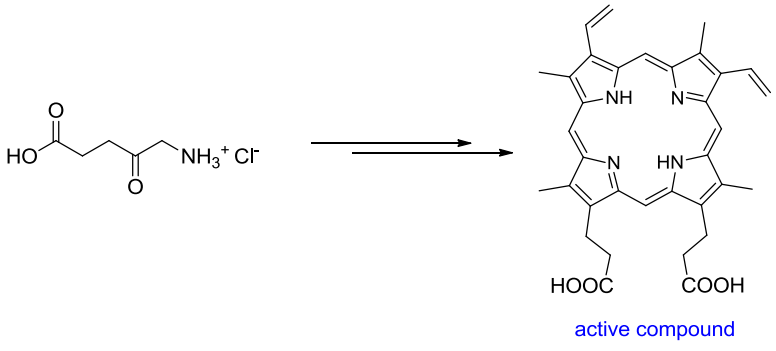

Figure 1.18: Conversion of 5-aminolevulinic acid to protoporphyrin IX

Verteporfin (Visudyne, BPD, 1.19) is a benzoporphyrin derivative. It absorbs at 690 nm; this longer wavelength allows deeper penetration due to extended conjugation of the macrocycle. The free carboxylic acid groups and ester groups provide the necessary amphiphilicity, allowing rapid accumulation and excretion from tumors. Difficulty of its synthesis is one of the major drawbacks.

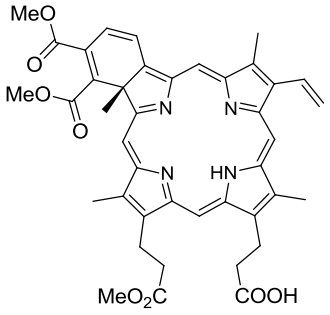

Figure 1.19: Structure of one isomer Verteporfin

To overcome the major drawbacks in porphyrin based photosensitizers, low excitation coefficient in the therapeutic window and persistence in skin, so called second generation chlorin based photosensitizers (Figure 1.20), such as Foscan (Temoporfin) NPe_6 (LS11, mono-aspartylchlorin e_6) and HPPH [Photochlor, 2-(1-hexyloxyethyl)-2-devinyl-pyropheophorbide a] have been developed.[35] Chlorins are particularly promising photosensitizers for PDT because of their distinctive ability to accumulate in tumorous tissues,[40] intense absorptions at 664 nm, high stability, low dark toxicity and ability to generate singlet oxygen in the light.[41-43] Amphiphilicity, another favorable trait, has been shown to improve the effectiveness of photosentizers. Chlorophyll a derivatives of the chlorin e_6 series possess three carboxylic side chains, making them an ideal substrate for synthesis of novel amphiphilic photosensitizers.

As mentioned earlier, chlorins are reduced porphyrins; hydrogenation of one of the pyrrole double bonds provides its characteristic absorption spectrum. Their strong absorption in the long wavelength region (around 650 nm, inside the therapeutic window) and high molar extinction coefficient make them more promising photosensitizers than Photofrin.[44,45] For an example Talaporfin

shows absorption peaks at 400 and 654 nm with molar absorption coefficients of 180 000 and 40 000 M^{-1} cm^{-1} respectively.[45] These properties of chlorins allow for deeper photodamage of tissue and a better therapeutic effect compared with porphyrins.[46] As reported in the literature, chlorin derivatives have higher quantum yields for singlet oxygen production and long triplet lifetimes, which may help to increase singlet oxygen production.[47] The measured lifetime of the triplet state in buffer solution is 760 µS for chlorin e_6[44] and 300 µS for Talaporfin.[45] But the quantum yield of singlet oxygen production of Talaporfin (0.77) is similar to the reported value of chlorin e_6 (0.7).[45]

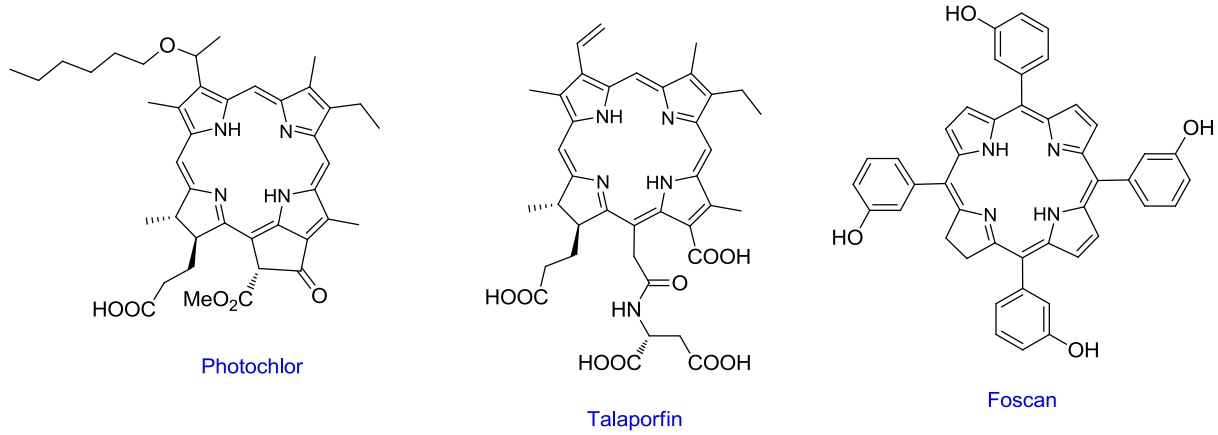

Figure 1.20: Second generation chlorin photosensitizers

Aizawa and coworkers reported that Talaporfin has 10 times greater uptake in malignant tissue cells than in normal organs.[48] It transports through the body by binding to the plasma proteins and lipoproteins. The previous studies revealed that Talaporfin bound more strongly to plasma proteins than to lipoproteins.[49] They are also rapidly cleared from the body; this would be of great advantage in clinical studies. Because of that, the therapeutic dosage of Talaporfin causes very little skin sensitization compared to most porphyrin-based photosensitizers, and it clears quickly from tissue.[11,21,50] However the future of photodynamic therapy highly depends on the development of more tumor selective and more efficient photosensitizers. Development of improved derivatives of Talaporfin is a major objective of the research work reported in this Dissertation.

1.6 References

(1) *Aromaticity and Tautomerism in Porphyrins and Porphyrinoids*; Stępień, M.; Latos-Grażyński, L., Eds.; Springer Berlin Heidelberg: Wrocław, 2009; Vol. 19.

(2) Wu, J. I.; Fernández, I.; Schleyer, P. v. R. *J. Am. Chem. Soc.* **2012**, *135*, 315.

(3) Lash, T. D.; Jones, S. A.; Ferrence, G. M. *J. Am. Chem. Soc.* **2010**, *132*, 12786.

(4) Wetherell, H.; Hendrickson, M. *J. Org. Chem.* **1959**, *24*, 710.

(5) Aizawa, K.; Okunaka, T.; Ohtani, T.; Kawabe, H.; Yasunaka, Y.; O'Hata, S.; Ohtomo, N.; Nishimiya, K.; Konaka, C.; Kato, H.; Hayata, Y.; Saito, T. *Photochem. Photobiol.* **1987**, *46*, 789.

(6) Sondheimer, F.; Wolovsky, R.; Amiel, Y. *J. Am. Chem. Soc.* **1962**, *84*, 274.

(7) Dougherty, T. J. *Photochem. Photobiol.* **1987**, *46*, 569.

(8) Kenner, G. W.; McCombie, S. W.; Smith, K. M. *J. Chem. Soc, Perkin Tran. 1* **1973**, 2517.

(9) Hynninen, P. H.; Lötjönen, S. *Synthesis* **1980**, *1980*, 539.

(10) Sessler, J. L.; Tomat, E. *Acc. Chem. Res.* **2007**, *40*, 371.

(11) Nelson, J. S.; Roberts, W. G.; Berns , M. W. *Cancer Res.* **1987**, *47*, 4681.

(12) *Metalloporphyrin based Biomimetic Catalysts for Materials Synthesis and Biosensing*; Subhalakshmi, N.; Ferdinando, F. B.; Lynne, S.; Jayant, K.; Ramaswamy, N., Eds.; American Chemical Society, 2010; Vol. 1054.

(13) Rio, Y.; Rodriguez-Morgade, S. M.; Torres, T. *Org. Bio. Chem.* **2008**, *6*, 1877.

(14) Nemykin, V. N.; Hadt, R. G. *J. Phys. Chem. A* **2010**, *114*, 12062.

(15) Gouterman, M. *J. Mol. Spec.* **1961**, *6*, 138.

(16) Giovannetti, R. In *The Use of Spectrophotometry UV-Vis for the Study of Porphyrins*; Uddin, J., Ed.; InTech: 2012; Vol. 6.

(17) Fliegl, H.; Sundholm, D. *J. Org. Chem.* **2012**, *77*, 3408.

(18) Otero, N.; Fias, S.; Radenkovic´, S.; Bultinck, P.; Grana, A. M.; Mandado, M. *Chem. Eur. J.* **2011**, *17*, 3274.

(19) Wheeler, R. In *http://commons.wikimedia.org/wiki*; Haemoglobin.png, G., Ed. 2007.

(20) Toth, A. In *http://en.wikipedia.org/wiki/*; Myoglobin.png, Ed. 2008.

(21) Roberts, W. G.; Smith, K. M.; McCuliough, J. L.; Berns, M. W. *Photochem. Photobiol.* **1989**, *49*, 431.

(22) Hardison, R. *Am. Scientist Class.* **1999**, *87*, 126.

(23) Thomas, J. H. In *http://www.bio.miami.edu/tom/courses/protected/ECK/CH13*; figure-13-02c.jpg, Ed. 2005.

(24) Shakhashiri, B. Z. In *http://scifun.chem.wisc.edu/chemweek/chlrphyl/chlrphyl.html*; clrphlsp, Ed.

(25) Wasielewski, M. R.; Svec, W. A. *J . Org. Chem.* **1980**, *45*, 1969.

(26) Reedy, C. J.; Gibney, B. R. *Chem. Rev.* **2004**, *104*, 617.

(27) Dolmans, D. E. J. G. J.; Fukumura, D.; Jain, R. K. *Nat. Rev. Cancer* **2003**, *3*, 380.

(28) Dougherty, T. J.; Gomer, C. J.; Henderson, B. W.; Jori, G.; Kessel, D.; Korbelik, M.; Moan, J.; Peng, Q. *J. Natl. Cancer Inst.* **1998**, *90*, 889.

(29) Vicente, M. G. H. *Curr. Med. Chem. AntiCancer Agents* **2001**, *1*.

(30) Szaciłowski, K.; Macyk, W.; Drzewiecka-Matuszek, A.; Brindell, M.; Stochel, G. *Chem. Rev.* **2005**, *105*, 2647.

(31) DeRosa, M. C.; Crutchley, R. J. *Coord. Chem. Rev.* **2002**, *233–234*, 351.

(32) Triesscheijn, M.; Baas, P.; Schellens, J. H. M.; Stewart, F. A. *The Oncologist* **2006**, *11*, 1034.

(33) Moan, J.; Berg, K. *Photochem. Photobiol.* **1991**, *53*, 549.

(34) Li, H.; Jensen, T. J.; Fronczek, F. R.; Vicente, M. G. H. *J. Med. Chem.* **2008**, *51*, 502.

(35) Allison, R. R.; Downie, G. H.; Cuenca, R.; Hu, X.; Sibata, C. H.; Childs, C. *Photodiag. Photodynamic Therapy* **2004**, *1*, 27.

(36) Zhun310 In *http://commons.wikimedia.org/wiki/File:Fig_6_The_absorption_spectrum for_arteries.png* 2009.

(37) Kennedy, J. C.; Pottier, R. H. *J. Photochem. Photobiol. B.* **1992**, *14*, 275.

(38) Peng, Q.; Warloe, T.; Berg, K.; Moan, J.; Kongshaug, M.; Giercksky, K.-E.; Nesland, J. M. *Cancer.* **1997**, *79*, 2282.

(39) Loh, C. S.; MacRobert, A. J.; Bedwell, J.; Regula, J.; Krasner, N.; Bown, S. G. *Br. J. Cancer* **1993**, *68*, 41.

(40) Aizawa, K.; Okunaka, T.; Ohtani, T.; Kawabe, H.; Yasunaka, Y.; O'Hata, S.; Ohtomo, N.; Nishimiya, K.; Konaka, C.; Kato, H.; Hayata, Y.; Saito, T. *Photochem. Photobiol.* **1987**, *46*, 789.

(41) Kostenicha, G. A.; Zhuravkina, I. N.; Zhavrid, E. A. *J. Photochem. Photobiol. B.* **1994**, *22*, 211.

(42) Kessel, D. *Photochem. Photobiol.* **2008**, *49*, 447.

(43) Palma, M.; Cárdenas-Jirón, G. I.; Menéndez Rodríguez, M. I. *J. Phys. Chem. A* **2008**, *112*, 13574.

(44) Spikes, J. D. *J. Photochem. Photobiol. B.* **1990**, *6*, 259.

(45) Spikes, J. D.; Bommer, J. C. *J. Photochem. Photobiol. B.* **1993**, *17*, 135.

(46) Ol'shevskaya, V. A.; Nikitina, R. G.; Savchenko, A. N.; Malshakova, M. V.; Vinogradov, A. M.; Golovina, G. V.; Belykh, D. V.; Kutchin, A. V.; Kaplan, M. A.; Kalinin, V. N.; Kuzmin, V. A.; Shtil, A. A. *Bio. Med. Chem.* **2009**, *17*, 1297.

(47) Kimel, S.; Tromberg, B. J.; Roberts, W. G.; Berns, M. W. *Photochem. Photobiol.* **1989**, *50*, 175.

(48) Aizawa, K.; Okunaka, T.; Ohtani, T.; Kawabe, H.; Yasunaka, Y.; O'Hata, S.; Ohtomo, N.; Nishimiya, K.; Konaka, C.; Kato, H.; Hayata, Y.; Saito, T. *Photochem. Photobiol.* **1987**, *46*, 789.

(49) Kessel, D. *Photochem. Photobiol.* **1989**, *49*, 447.

(50) Gomer, C. J.; Ferrario, A.; Rucker, N.; Wong, S.; Morinelli, E.; Liu, G.; Szirth, B. C. In *Advances in Photochemotherapy*; Hasan, T., Ed. Boston, MA, 1989; Vol. 0997, p 8.

CHAPTER 2: SYNTHESIS AND CHARACTERIZATION OF CHLORIN e_6 DERIVATIVES FOR PHOTODYNAMIC THERAPY[1]

2.1 Introduction

Mono-L-aspartyl chlorin e_6 (**1,** Talaporfin, also known as, NPe_6, or LS11) is a photosensitizer used in photodynamic therapy (PDT). It was approved in Japan (in 2004) but not yet in the USA, for PDT of lung cancer and marketed as Laserphyrin.[1] It is trademarked as Aptocine by Light Sciences Oncology and is a second generation photosensitizer in advanced-stage clinical trials. Light Sciences Oncology (LSO) has completed treatment of patients in a phase III trial of NPe_6 in hepatocellular carcinoma (HCC), a phase III trial for metastatic colorectal cancer (MCRC) and in phase I and Phase II clinical trials in benign prostatic hyperplasia (BPH), or enlargement of the prostate.[2]

As shown in Scheme 2.1, NPe_6 (**1**) is synthesized starting from pheophytin a (**4**) which is extracted from alga. Transesterification of the phytyl group of the pheophytin a (**4**) with methanol in acidic conditions afforded methyl pheophorbide a (**3**). Subsequent isocyclic ring opening of methyl pheophorbide a (**3**) with methoxide produced chlorine e_6 trimethyl ester. Hydrolysis of all three methyl esters then yielded chlorin e_6 (**2**). The final product NPe_6 (**1**) can be obtained after carboxylic acid activation of chlorin e_6 (**2**) and then coupling with aspartic acid.[3]

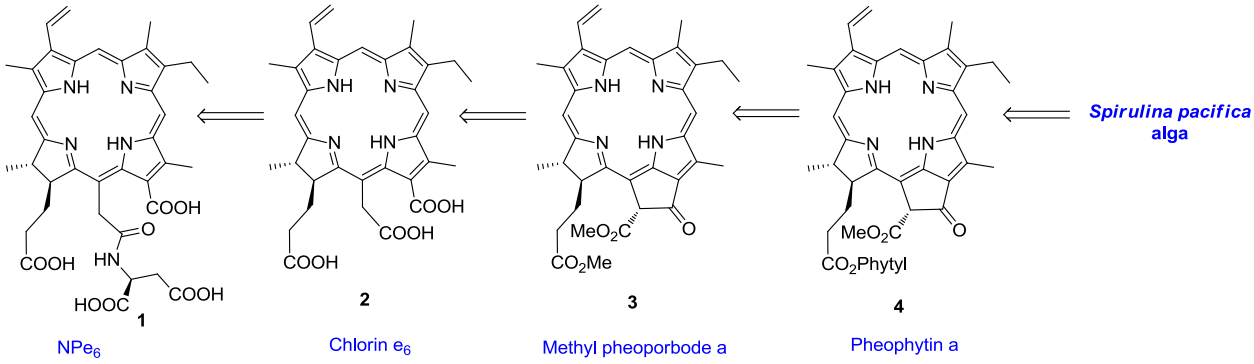

Scheme 2.1: Synthesis of NPe_6 from *Spirulina pacifica*

[1] This chapter reprinted with permission from Jinadasa, R. G. W.; Hu, X.; Vicente, M. G. H.; Smith, K. M. *J. Med. Chem.* **2011**, 54, 7464. Copyright (2011) American Chemical Society.

Chlorin e_6 (**2**) possesses three carboxylic acid side chains. Of the three carboxylic acids, the propionic acid chain seems more accessible for activation and for nucleophilic attack than the acetic or formic acid chains under classical coupling reaction conditions. Therefore academic papers published since 1997 assumed NPe_6 (**1**) was the propionic acid regioisomer of chlorin e_6 (**5**). But in 1998, Gomi and coworkers claimed NPe_6 (**1**) is actually the acetic acid regioisomer not the propionic acid regioisomer, according to 2D NMR studies.[4] But this discovery was not accepted by the porphyrin community because it was against chemical logic, and the NMR work was done in D_2O which is known to cause aggregation. In this synthesis, protecting groups or any other strategies were not used to do a selective coupling reaction. All three carbocyclic acid side chains in chlorin e_6 (**2**) are susceptible to activation followed by conjugation with amino acid. The classical coupling reagent, DCC and DMAP were used to activate the carboxylic acid and then nucleophilic addition of the free amine group of aspartic acid followed by elimination of activator as urea produced the final product (Scheme 2.2).

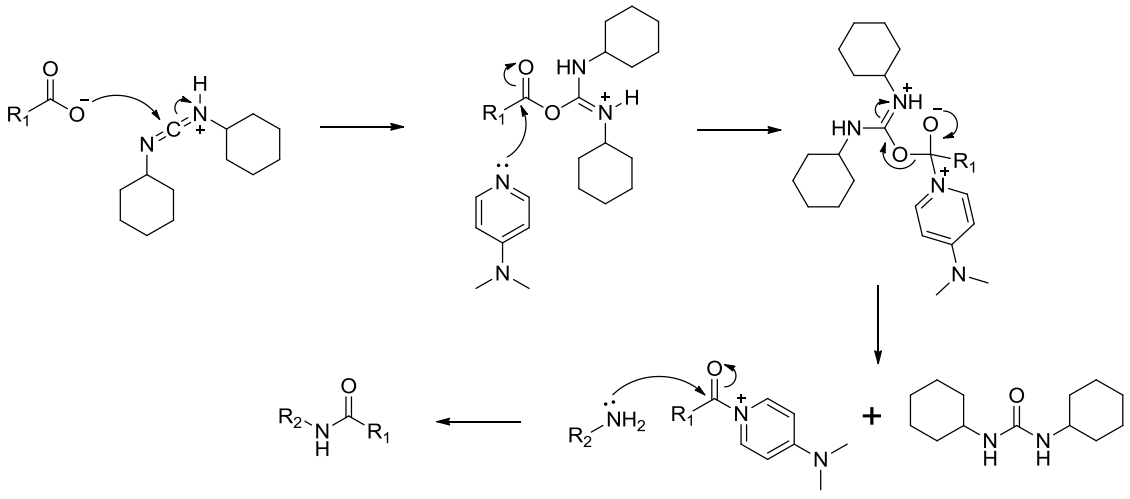

Scheme 2.2: Mechanism of DCC/ DMAP coupling reaction

According to the mechanism in Scheme 2.2, it is reasonable to assume that the propionic side chain, which is located far away from the macrocycle and is more accessible than the other acidic side chains, will activate first to give the conjugated product. Additionally, the propionic side chain is located

perpendicular to the macrocycle and this makes it less stericaly hindered. The acetic acid and formic acid chains are more sterically hindered by both substituents and by the macrocycle compared to the propionic side chain. Apart from that, the formic acid is deactivated during esterification under acidic conditions because it is directly attached to the macrocycle and conjugated with it. Under acidic conditions, the inner nitrogens of the macrocycle are protonated and this makes it electron deficient. That prevents the activation of the conjugated carboxylic acid to undergo nucleophilic attack. It seems that neither the formic nor the acetic side chains were considered serious competition to the propionic carboxyl chain.

With the intention to establish the true isomeric identity of NPe_6, all three regioisomers **5**, **6** and **7** were prepared by total synthesis from chlorin e_6 (**2**) or methyl pheophorbide a (**3**), and the acetic regioisomer **6** was shown to be identical with NPe_6.[5] In 2007, our group was also able to obtain the X-ray structure of this ambiguous compound **6** which was prepared using the same method with DCC as a coupling agent.[5] Surprisingly, the crystal structure confirmed that the aspartyl group is attached to the acetic acid position in chlorin e_6. It was really a surprise to see highly regioselective coupling at the acetic acid position without any carboxylic protecting groups. It seems this coupling follows a different path than classical coupling reactions. This highly regioselective coupling provides an easy, short and high yielding route to synthesize acetic acid derivative without any protecting groups. It was possible to synthesis all three regio-isomers (Figure 2.1) of chlorin e_6 starting from pheophytin a (**4**) in reasonable yield.

Our particular interest is to synthesize various regioisomers (Figure 2.1) of chlorin e_6, since such molecules could selectively accumulate in specific organelles within cancer cells and cause effective photodamage. Their biological efficacy could be modulated based on the position and the type of amino acids (nature of the side chain). Furthermore, introducing spacer groups such as ethylene diamine, to

the formic acid chain should significantly influence the chemical and biological properties of the photosensitizer,[6] as they alter the aggregation behavior and hydrophilic character of the conjugates.[7,8]

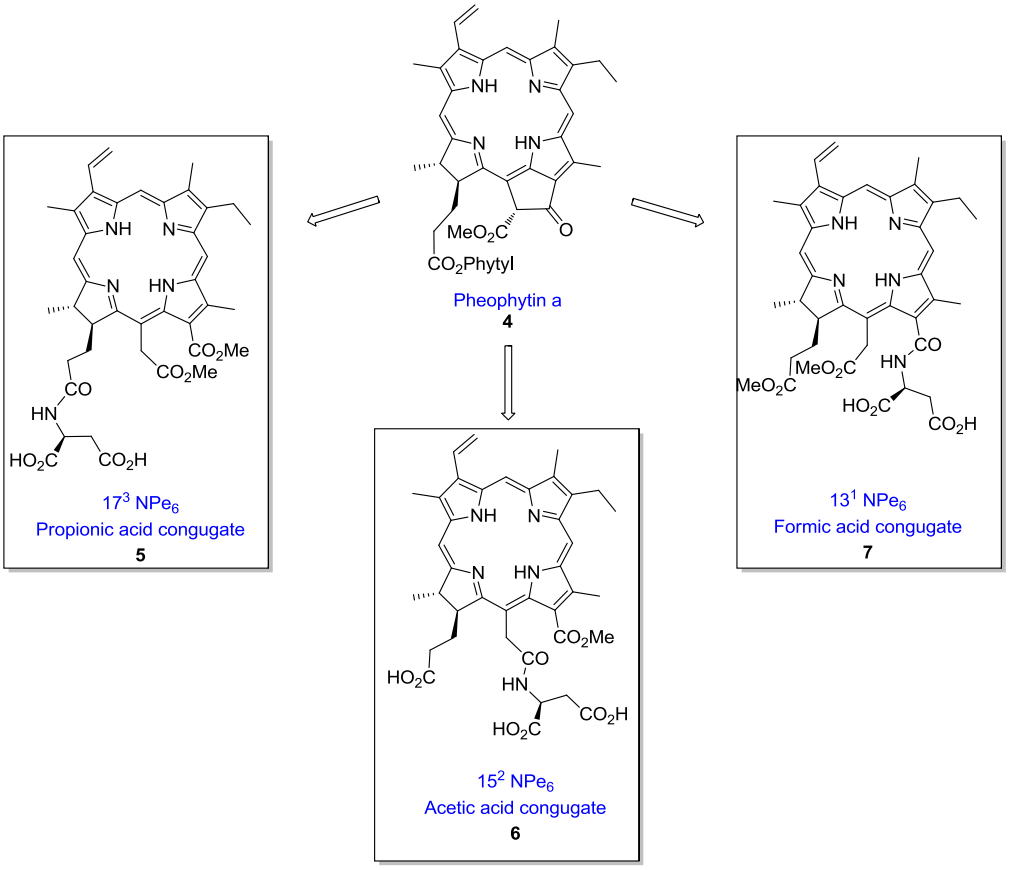

Figure 2.1: Synthesis of NPe_6 regioisomers

It was recently reported that the photosensitizing properties of the conjugate can be improved by introduction of metal ions into the coordination sphere of chlorins.[9,10] Heavy metal atoms in tetrapyrroles will enhance the intersystem crossing rates and consequently the singlet oxygen quantum yields.[10] Unfortunately, metal coordination with chlorophylls also results in a blue shift of the Q band in the absorption spectrum.[11]

2.2 Mechanistic Studies

The synthetic, X-ray[5] and spectroscopic[4] work mentioned above confirmed the formation of the acetic acid derivative from reaction between DCC activated chlorin e_6 and carboxyl protected aspartic

acid. To discover the path of this coupling reaction, several reactions were designed and ^{1}H NMR and mass spectroscopy were used to characterize the intermediates.

In this reaction one equivalent of chlorin e_6, one equivalent of DCC and one equivalent of DMAP were suspended in DCM under argon for two hours at room temperature. After 30 minutes TLC with 10% acetone/CH_2Cl_2 showed two newly formed spots. Chlorin e_6 does not move on TLC with less polar solvent systems such as 10% acetone/CH_2Cl_2. These observations confirmed the formation of a less polar highly reactive intermediate of chorin e_6 in the reaction with DCC. Isolation of these fractions failed due to the high reactivity of the product. The colors of the fractions changed from purple to green during column chromatography. Once the color had changed to green, the material refused to elute from the column, even with high polar solvent systems. Mass spectroscopy of the reaction mixture showed two main peaks at m/z 785 and 578.

Based on the mass spectrum and TLC, it was hypothesized[12] that the intermediate could be a seven-membered anhydride intermediate **8** which has high reactivity and can easily undergo a ring-opening reaction with nucleophiles to produce acetic acid derivatives **10**. The other possible intermediate is the nine-membered anhydride intermediate **8'** which has the same mass as the seven-membered intermediate, but was not seriously considered because of lower stability compared to the seven membered ring and the color change to purple during formation of anhydride (Scheme 2.3). Formation of the seven membered anhydride ring can clearly change a part of the conjugation of the compound and that can result in the color change. The ring opening of the isocyclic ring of methyl pheophorbide a also had resulted in a blue shift in CH_2Cl_2. Contrasting to ring-opening of pheophorbide a, the red shift in this case is attributable to the formation of an anhydride ring between the formic and acetic acid chains.

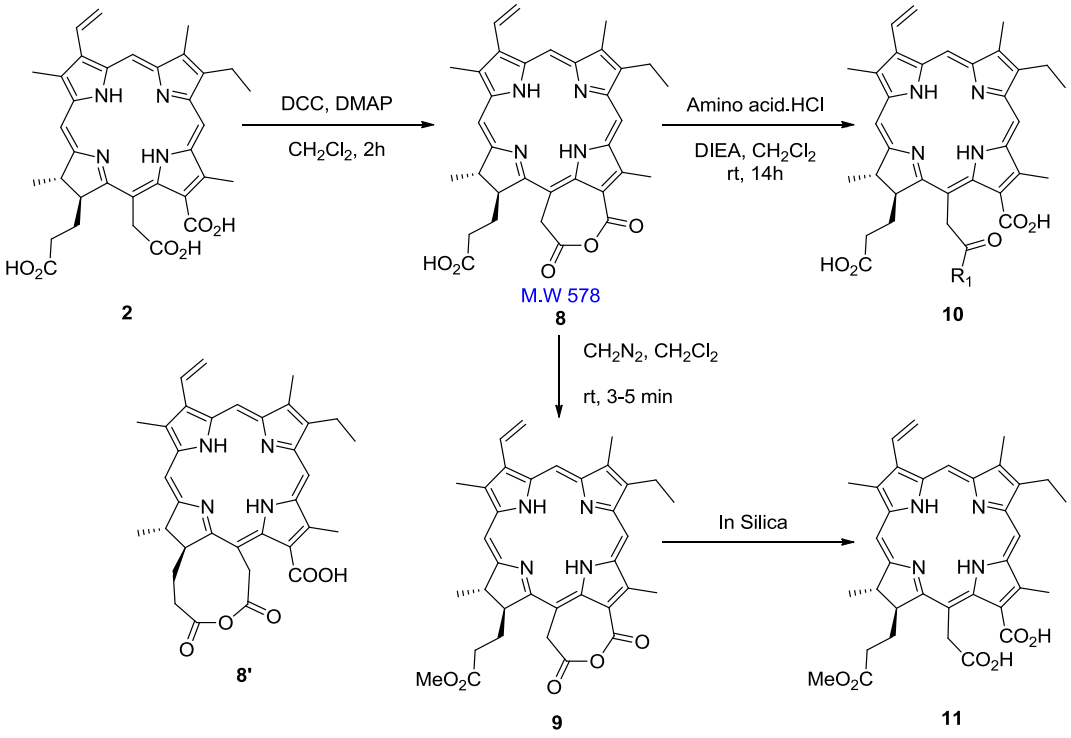

Scheme 2.3: Proposed intermediate during DCC/DMAP coupling with chlorin e_6

Due to the high reactivity and polarity associated with the presence of the free acid chain in anhydride **8**, isolation was very challenging. In order to reduce its polarity, esterification was performed using diazomethane under argon, to obtain methyl protected anhydride **9**. Esterification was done without any purification directly following the coupling reaction due to the high sensitivity of the anhydride towards moisture. Excess amounts of diazomethane gas were bubbled through the reaction mixture for 3-5 minutes. TLC indicated the formation of the methyl protected anhydride **9**. After the reaction, column chromatography was performed in order to purify the intermediate. But during the column chromatography the color of the mixture changed to green and the material became stuck to the column. Upon applying to a silica gel chromatography, the anhydride ring could be opened easily and this changed the color from purple to green, forming the very polar molecule **11** bearing two free acids. Although attempts were made using different column supports such as Sephadex or alumina, still no practical way was found to isolate the pure compound **9**.

Then it was decided to prove the regioselectivity of the coupling reaction using NMR spectroscopy. A small nucleophile like ethoxide was selected to open the anhydride to minimize the complications in the ^{1}H NMR spectrum (Scheme 2.4). So once we obtained the intermediate seven membered anhydride **8** using DCC and DMAP as was discussed before, it was reacted with one equivalent of freshly prepared sodium ethoxide to obtain chlorin e_6 ethyl ester (**12**). Then the remaining free acids were protected with diazomethane gas and purified via column chromatography. Mass spectroscopy confirmed the the product chlorin e_6 dimethyl ethyl ester (**13**). Then the ^{1}H NMR spectrum of chlorin e_6 dimethyl ethyl ester (**13**) was compared with ^{1}H NMR spectrum of chlorine e_6 trimethyl ester to confirm the regioisomer.

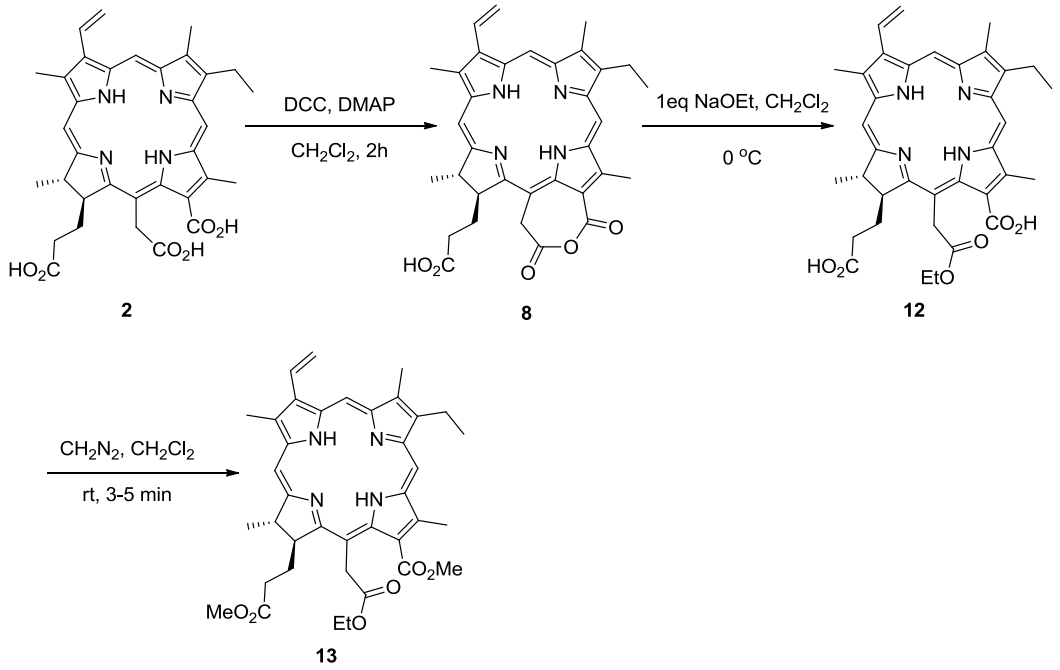

Scheme 2.4: Synthesis of 15[2] ethyl ester chlorin e_6 dimethyl ester

As shown in Figure 2.2, the ^{1}H NMR spectrum of chlorin e_6 trimethyl ester shows six singlets between 3 to 4.5 ppm for six methyl groups. Of these six singlets, three belong to the methyl ester groups and the other three peaks belong to the methyl groups directly connected to the macrocycle. All of these methyl groups are found in the deshielded region of the macrocycle due to its ring current.

Hence all the peaks are downfield from their normal position in the NMR spectrum. The first three peaks (a,b,c) belong to three methyl esters and the one most downfield is the that closest to the macrocycle, the 13^1 ester. Likewise, the 15^2 ester is more downfield compared to the 17^3 ester. These peaks had been assigned in previous studies using 2D NMR. Upon comparison of the two NMR spectra of chlorin e_6 trimethyl ester and chlorin e_6 dimethyl ethyl ester (**13**), it was possible to verify the ethyl ester had been definitely added at the 15^2 (acetic acid) position, because of disappearance of the 15^2 methyl ester peak (b) and the appearance of two new peaks (d & e) for the ethyl group in the chlorin e_6 dimethyl ethyl ester. This also provides evidence that the ring opening reaction of the anhydride **8** was occurring at the 15^2 position instead of 13^1 position, regardless of the size or nucleophilicity of the molecule.

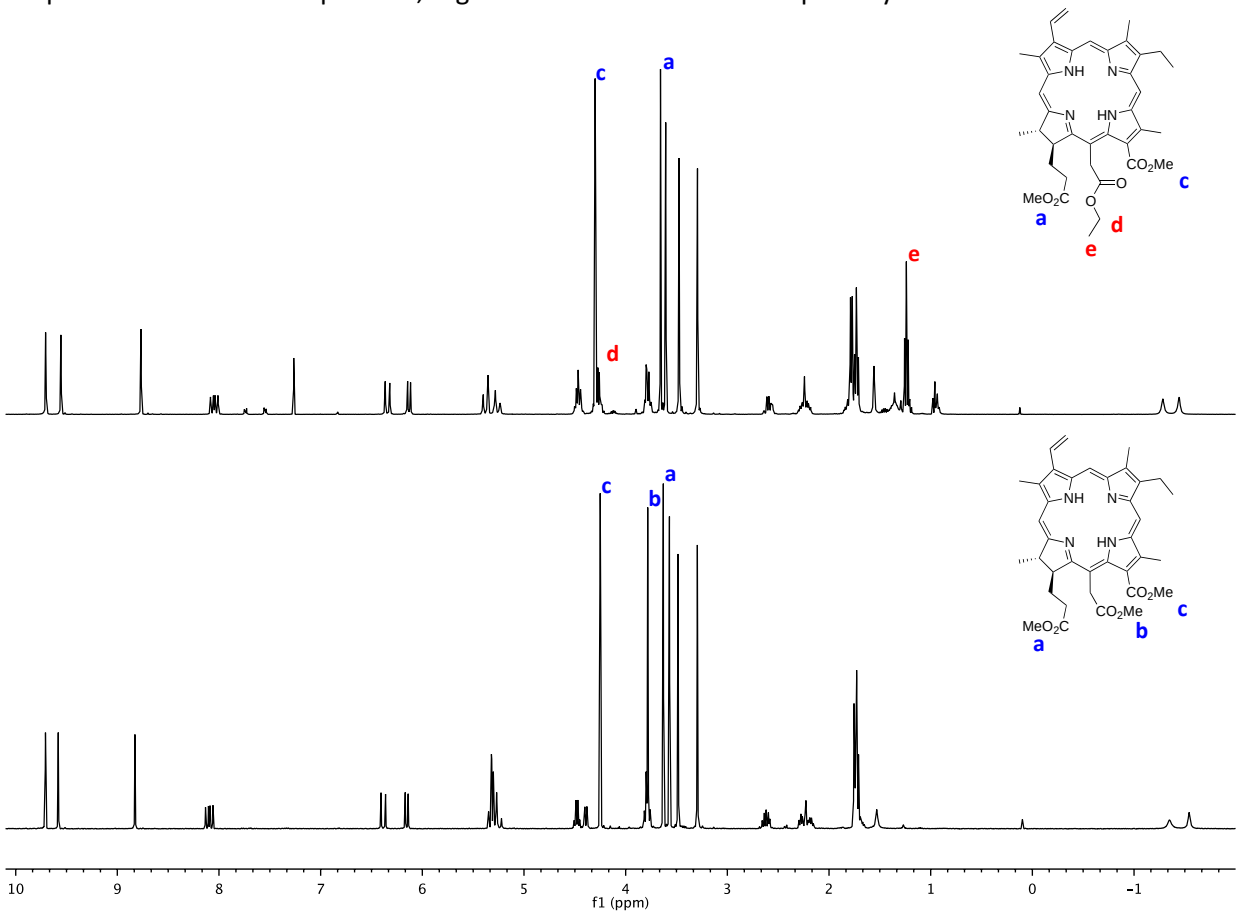

Figure 2.2: ^{1}H NMR spectral Comparison of 15^2 ethyl ester chlorin e_6 (**13**) and chlorin e_6 trimethyl ester

It is worth noticing that the amount of DCC plays an important role in the mechanism of the reaction. When we increase the amount of DCC in the coupling reaction, the appearance of new spot in

the TLC was apparent. This new spot is less polar compared to the anhydride **8**. The reaction with one equvelent of aspartic acid *tert*-butyl ester hydrochloride followed by esterification with diazomethane formed the expected mono aspartyl chorin e_6 dimethyl ester (**14**). Hence it was decided to add 2.5 equivalents of aspartic acid *tert*-butyl ester hydrochloride with DIEA to the activated chlorin e_6. After three hours diazomethane gas was bubbled through the mixture to esterify any remaining free acid groups. TLC indicated the formation of two new spots. Both fractions were isolated and characterized by ^{1}H NMR spectroscopy. Based on NMR and mass spectra, the major fraction is the expected monoaspartylchorin e_6 dimethyl ester (**14**) and the second fraction is the diaspartylchlorine e_6 methyl ester (**16**). Existence of a peak for the 13^1 methyl group (peak c, Figure 2.2) confirmed that the two aspartyl groups were inserted at the 17^3 and 15^2 positions. Increasing the amount of DCC helped to increase the yield of diaspartyl derivative **16** but the monoaspartyl derivative **14** was always the major product. This observation also supports the conclution that the two free acids 13^1 and 15^2 had been fused to form the anhydride seven membered ring, keeping the 17^3 free for DCC activation (Scheme 2.5). The activation with DCC forms a seven-membered anhydride intermediate **8** between the formic and acetic acid chains, and if there is excess DCC, it will activate the remaining propionic acid to form intermediate **15.** This structure corresponds with the mass spectrum peak at m/z 785. Then, the free amine group of the aspartic acid can attack both of the activated positions of intermediate **15** to form diaspartylchlorin e_6 methyl ester (**16**). Formation of monoaspartylchorin e_6 dimethyl ester (**14**) as the major product even with excess aspartic acid provides the evidence that the acetic acid activation follows a different path and forms a more active functional group than does the propionic acid activation with DCC. This supports the suggested intermediate **8**; the somewhat strained seven-membered ring anhydride is more reactive towards nucleophilic attack than the activated propionic side chain.

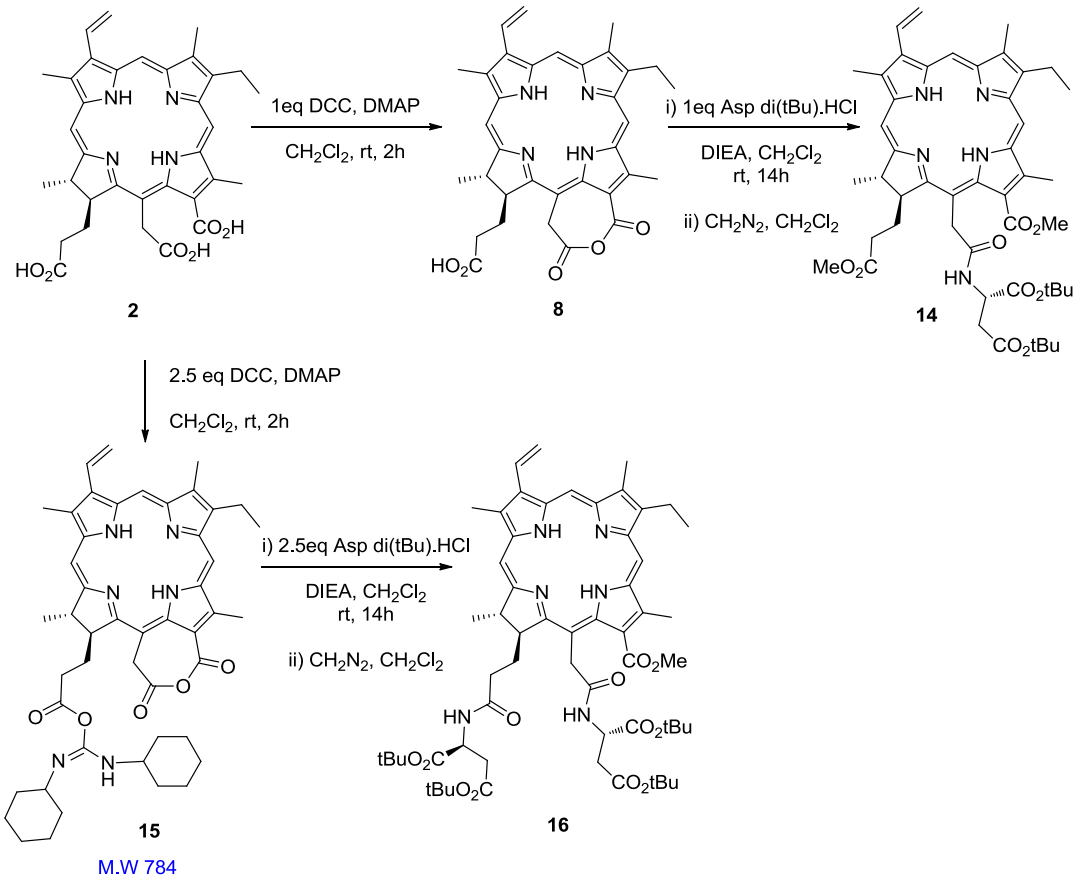

Scheme 2.5: Formation of mono and diaspartic acid chlorin e_6 derivatives with DCC/DMAP

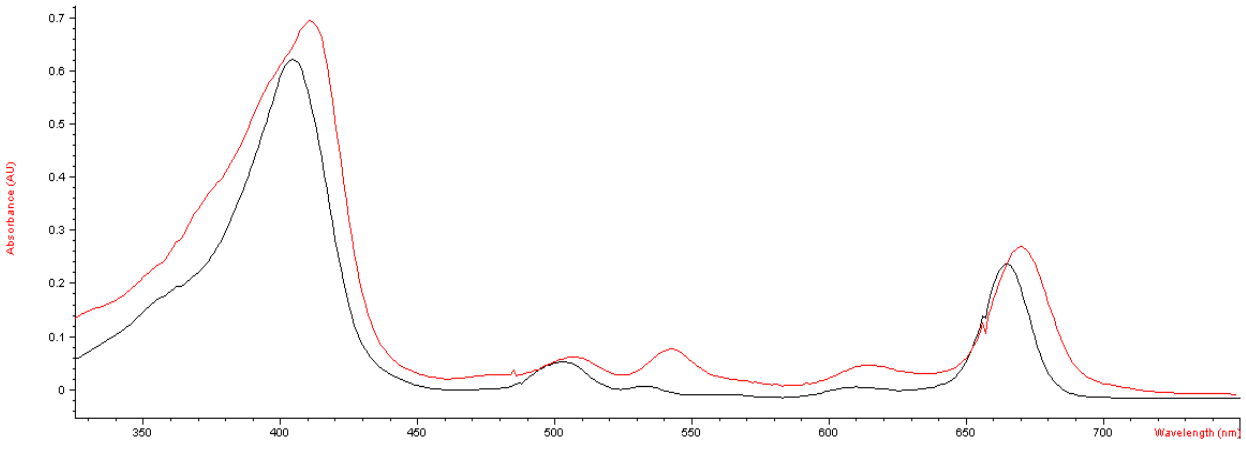

Figure 2.3: UV-Vis spectra of chlorin e_6 (**2,** black) and anhydride intermediate **8** (red) in CH_2Cl_2

After confirming the mechanism for the unique regioselective coupling reaction, the yield of the reaction was improved. In this synthetic route, formation of the seven-membered anhydride intermediate can be monitored through TLC and UV-Visible spectroscopy (Figure 2.3). Once it formed, an amino acid or other nucleophile was added and the reaction was monitored by TLC, following the disappearance of the intermediate or by the visible color change from purple to green.

2.3 Structural Elucidation and Synthesis of Chlorin e_6 Derivatives

2.3.1 Synthesis of 17^3 Chlorin e_6 Conjugates

The synthetic route to 17^3 monolysinechlorin e_6 trimethyl ester (**20**) is shown in Scheme 2.6. It was possible to obtain monolysinechlorin e_6 trimethyl ester (**20**) in 33% overall yield from pheophorbide a (**17**). Pheophytin a (**4**) was obtained by extraction from *S. pacifica* alga, an ideal source for chlorophyll a that greatly simplifies the purification of the algal extract because of the absence of chlorophyll b in the alga.[13] Pheophorbide a (**17**) was obtained by selective hydrolysis of the phytyl ester group of pheophytin a (**4**) using the Wasielewski and Svec procedure, without affecting the β-keto-ester of the isocyclic ring.[14] This ring serves as a natural protecting group during the coupling reactions. In the literature an effective hydrolysis of the phytyl ester group under acidic,[15] basic,[16] and under the influence of enzymes can be found.[17] There are some drawbacks to the reaction done under alkaline hydrolysis. It tends to eliminate the phytyl group with retention of the magnesium ion in the macrocycle, to hydrolyze the 13^2 methyl ester to carboxyl with formation of chlorophyllins, and also tends to open the isocyclic ring to give chlorin derivatives.[18] But under acidic hydrolysis both the phytyl group and the magnesium ion can be removed in a single step without affecting the isocyclic ring. After acid hydrolysis, the structure of compound **17** was confirmed by ^{1}H NMR and mass spectroscopy. The presence of peaks for the central NH protons of macrocycle in the ^{1}H NMR confirmed the elimination of central magnesium atom. These central NH protons resonate around δ -2 to -3 ppm due to significant shielding from the induced ring current of the large π system of the macrocycle. Likewise the *meso* protons appear

considerably downfield because they are situated outside the ring in the deshielded region. In addition to the characteristic chlorin peaks, the most significant peak in the structure elucidation of pheophorbides are the peak that confirms the presence of isocyclic ring. The only proton in the isocyclic ring appears as a sharp singlet at δ 6.26. It is much more deshielded than is a normal β-keto-ester proton, due to the induced macrocycle ring current.

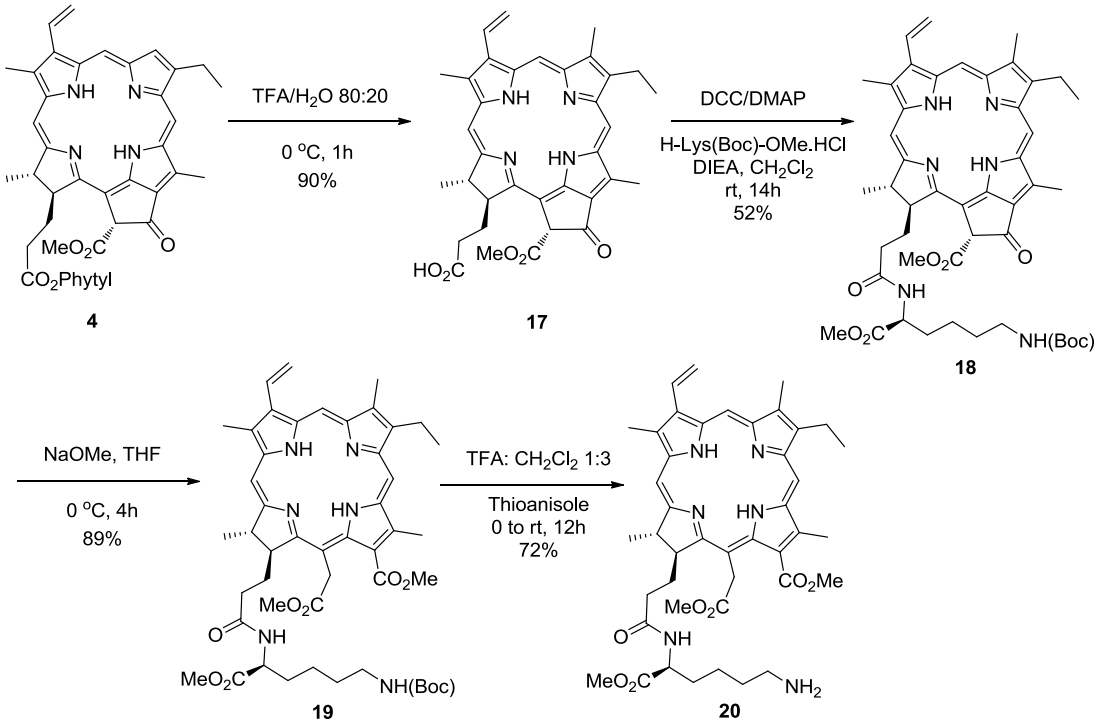

Scheme 2.6: Synthesis of propionic acid derivative of chlorin e_6

Selective hydrolysis of the phytyl ester produced the free 17^3 carboxylic acid group which was used to couple pheophorbide a (**17**) with H-lysine(boc) methyl ester. Numerous coupling conditions were tested to form the amide bond between lysine and 17^3 carboxyl group of pheophorbide **17** and it was found that the DCC/DMAP combination provided the best yield. Coupling with modern coupling reagents like HOBt and TBTU did not change the yield and formed unwanted side products from opening of the isocyclic ring. In the literature an alternate path has been reported for the production of the 17^2

amide derivative **23** (Scheme 2.7). Treatment of natural chorin derivative **21** with 2,3-dichloro-5,6-dicyano-1,4-benzoquinone (DDQ) leads to the formation of the lactone **22** by oxidizing the chlorin ring.[19] Then, opening of the lactone with nucleophiles formed the desired ester **23** in good yield.[20] But it seems to be challenging to get rid of extra hydroxyl formed after ring opening of the lactone group while keeping the dihydrochlorin ring; dehydration may lead to the more stable porphyrin system. The optimum strategy for the coupling of pheophobide **17** with lysine is activation of the free acid with DCC and DMAP in dichloromethane. DIEA was used to neutralize the H-Lysine(Boc).HCl salt.

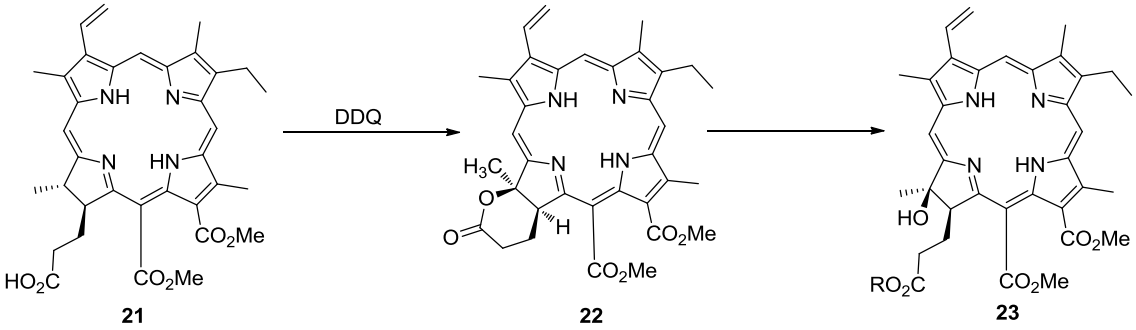

Scheme 2.7: Alternate method to obtain propionic acid derivative of chlorin e_6

Coupling of H-Lysine(Boc)-OH with pheophorbide **17** provided lysine(boc) methyl ester pheophorbide a (**18**) in 52% yield. ^{1}H NMR spectroscopy demonstrated the existence of the isocyclic ring and new peaks are apparent for the lysine moiety.

Next it was necessary to open the isocyclic ring to obtain the desired chlorin e_6 derivative **19** (Scheme 2.8). The isocyclic ring in phephorbide **17** is easily opened with cleavage of the β-keto-ester by the action of various nucleophiles. The ease of opening of the isocyclic ring is due to the release of ring strain and the formation of a resonance stabilized carbanion as an intermediate. In the literature, both O- and N-nucleophiles have been use to open the ring successfully. Methanolysis of the isocyclic ring of pheophorbide has been reported under several sets of reaction conditions. Chlorin e_6 trimethyl ester (**24**) was formed when the pheophorbide is treated with methanol and diazomethane in the presence of

pyridine under nitrogen for 24 hours.[21] Treatment with 0.5% KOH in methanol in the presence of pyridine also leads to the expected product **24**.[22] Methanolysis with sodium methoxide in THF provided an excellent yield compared to the other two conditions.

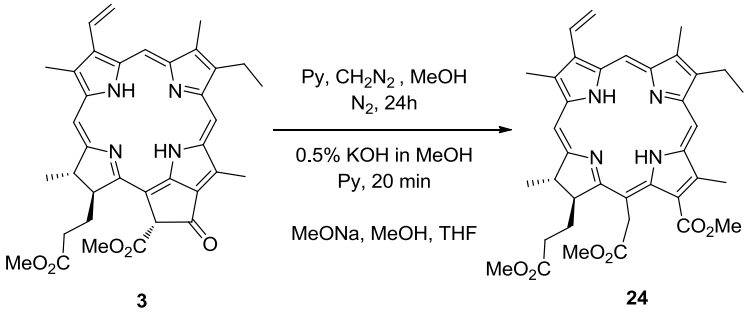

Scheme 2.8: Opening of the isocyclic ring

Apart from nucleophilic attack, this ring is susceptible to various reactions like allomerization and decarboxymethylation (Figure 2.3). In the presence of a base, the acidification of the 13^2 proton by the two neighboring carbonyl groups initiates easy enolization. This leads to a rapid irreversible oxidation of the isocyclic ring by atmospheric oxygen, this is called allomerization, or autoxidation.[23] At higher temperatures, the ester group (COOMe) of the β-keto-ester can undergo decarboxymethylation and form the corresponding stable pyro derivative.[24]

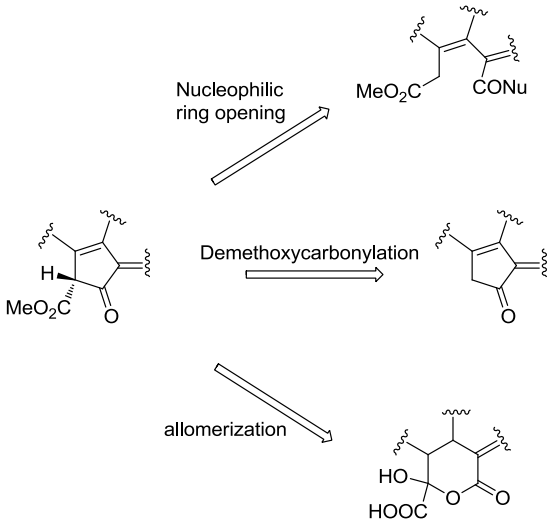

Figure 2.3: Reactions of isocyclic ring

Due to the high yield and short reaction times, it was decided to use sodium methoxide to open up the isocyclic ring to obtain the chorin e_6 derivative **19**. This reaction was carried out under argon to prevent allomerization and in an ice bath to prevent the racemization of the lysine. Previous literature has reported that under strong basic conditions amino acids can undergo racemization.[25] A dilute solution of sodium methoxide (0.5 M) was freshly prepared each time, by reacting dry methanol with sodium metal. The ring opening step was easy to follow by using its UV-Vis spectrum. Chorin e_6 compounds have a much sharper Soret band compared to the pheophorbides. Once the ring opens, the Soret band is blue shifted from 413 to 404 nm and reaction mixture quickly turns from brown to green upon addition of the sodium methoxide mixture. Subsequent isocyclic ring opening with sodium methoxide[26] in THF produced 17^3-monolysine(boc)chlorin e_6 trimethyl ester (**19**) in high yield (89%). The identity of the molecule **19** was confirmed using ^{1}H NMR, mass spectrometry and UV-Vis spectrometry. Disappearance of characteristic sharp singlet at δ 6.33 for the single proton in the isocyclic ring and the appearance of a multiplet for two protons a δ 5.38 confirmed the formation of chlorine e_6 derivative.

Deprotection of the amine[27] of the lysine side chain with TFA: CH_2Cl_2 yielded the desired molecule 17^3-monolysinechlorin e_6 trimethyl ester (**21**) in 33% overall yield from pheophorbide a (**17**) (Scheme 1).

2.3.2 Synthesis of Chlorin e_6

Previously discussed mechanistic studies revealed that selective coupling at the acetic acid side chain of chlorin e_6 (**2**) yielded the 15^2 chlorin e_6 derivatives. The target is to synthesize all three isomers starting from a natural inexpensive source: *S. pacifica* alga. To achieve the target it is nesassary to synthesize chlorin e_6 (**2**) from pheophytin a (**4**). The synthetic route to chlorin e_6 (**2**) from pheophytin a (**4**) is shown in Scheme 2.8. Transesterification of the phytyl ester group of pheophytin a (**4**) was accomplished with 5% sulfuric acid in methanol at room temperature. In spite of the convenient

hydrolysis of the phytyl ester to carboxylic acid, it was decided to do a transesterification to simplify the purification process. Methyl pheophorbide a (**3**) was obtained in quantitative yield and its identity was confirmed using NMR and mass spectroscopy.

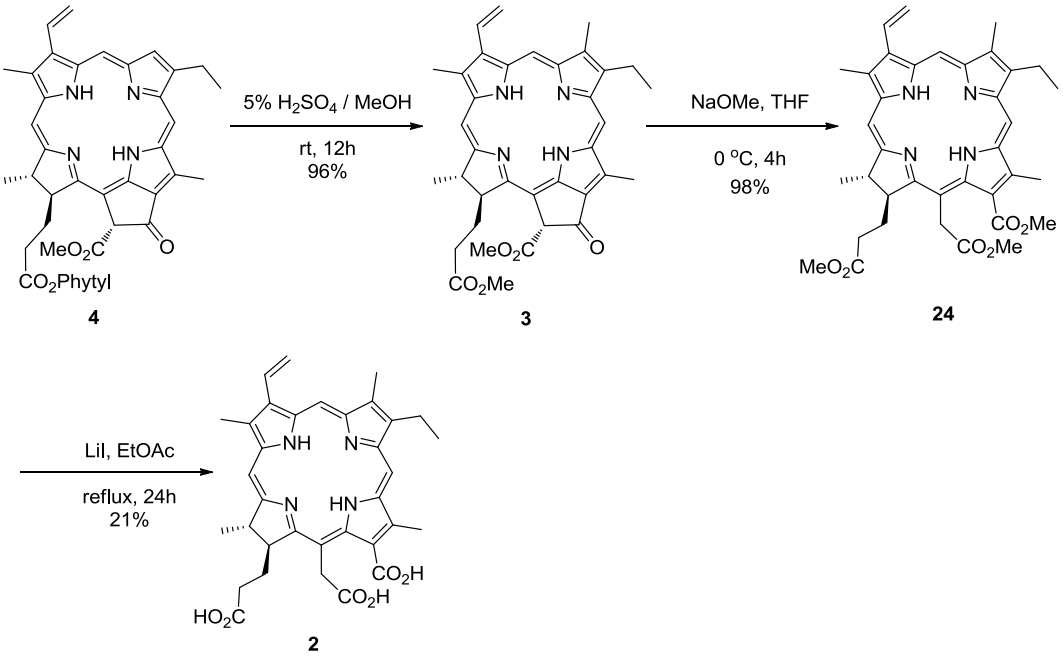

Scheme 2.8: Synthesis of chlorin e_6 (**2**) from pheophytin a (**4**)

The ring opening of the isocyclic ring of methyl pheophorbide a (**3**) with methoxide produced chlorin e_6 trimethyl ester (**24**). The first few attempts of the Isocyclic ring opening reaction failed with sodium methoxide in CH_2Cl_2. An optimized yield of 98% of chlorin e_6 trimethyl ester (**24**) was obtained with 1.1 equivalents of freshly prepared sodium methoxide in THF. The ^{1}H NMR spectrum and mass spectrum confirmed the existence of the extra methyl group for the methylated formic group.

Chlorin e_6 (**2**) can be obtained by hydrolysis of all three methyl esters of chlorin e_6 trimethyl ester (**24**). Methyl ester hydrolysis has been attempted with numerous reagents and conditions. Hydrolysis with stronger bases such as NaOH, LiOH and KOH under different conditions yields an inseparable mixture of compounds. Esters can be hydrolyzed with various protic or Lewis acids, e.g.,

CH_3SO_3H, p-TSA, BCl_3,[28] or BBr_3.[29] Hydrolysis with BBr_3 in CH_2Cl_2 formed a mixture of partially hydrolyzed products and various by products. These reagents are highly reactive and are not tolerated by many functional groups, which seriously limits their utility. Apart from numerous methods based on saponification/hydrolysis reaction pathways, this conversion can be carried out with various strong nucleophilic reagents capable of cleaveing the esters by dealkylation (S_N2 -type) reactions.[30] Among them, LiCl, LiBr and LiI have been described as effective reagents for conversion of esters derived from primary and secondary alcohols. Little success was achieved using a large excess of LiI in ethyl acetate under reflux conditions for 24 hours.[15] The main problem is partial hydrolysis of these which results in a mixture of mono, di and tri acids which is hard to purify using normal column chromatography. Only 21% maximum yield of chlorin e_6 (**2**) was obtained after purification via Sephadex LH 20 column chromatography (100% MeOH) on a small scale.

2.3.3 Synthesis of 15^2-Chlorin e_6 Conjugates

The final steps in the synthesis of 15^2-amino acid derivatives **27c** and **27d** of chlorin e_6 require the coupling of chlorin e_6 with a protected amino acid followed by deprotection. According to previous studies[5] with three free carboxylic acids, the 15^2-carboxylic acid is activated regardless of the coupling reagent employed. A detailed mechanism was discussed at the beginning of this Chapter. As was proposed, the reaction goes through a seven-membered anhydride intermediate **8** which forms between the acetic and formic acid chains. The free amine of the amino acid selectively attacked the more accessible carbonyl group of the anhydride **8**. DIEA was used to activate the amino acid by neutralizing the salt. To minimize the loss of the product during the chromatography and to simplify the characterization of the product, both the 17^3- and 13^1- acids were converted into methyl esters with diazomethane. Classical esterification with methanol under acidic conditions only reacts with the propionic side chain and leaves the formic side chain unchanged. Not only that, all these acid labile protecting groups can be cleaved during esterification under acidic conditions. Freshly prepared

diazomethane was bubbled through the reaction mixture and the reaction was monitored by TLC. Both products **26a** and **26b** were characterized by ^{1}H NMR and mass spectroscopy. An optimum yield of 45% of the 15^2-monoaspartylchlorin e_6 di(*tert*)butyl dimethyl ester (**26a**) and 77% of of 15^2-monolysine(boc) chlorin e_6 trimethyl ester (**26b**) were obtained with 1.2 equivalents of DCC and DMAP in CH_2Cl_2 at room temperature for 12 hours (Scheme 2.9).

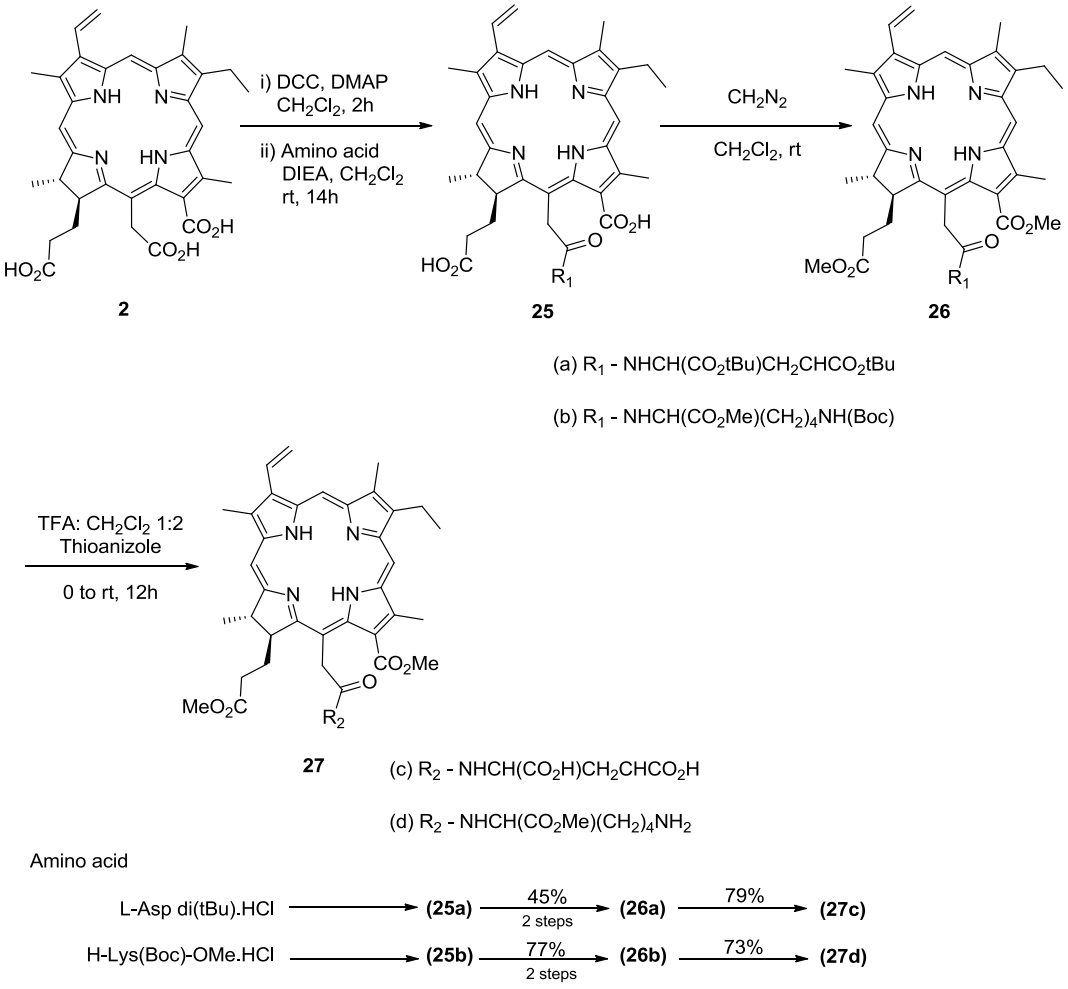

Scheme 2.9: Synthesis of acetic acid derivatives of chlorin e_6 (**2**)

Yields are extremely variable for the aspartyl derivative compared to the lysine derivative, possiblly due to steric bulkiness of the *tert*-butyl protecting group of the aspartic acid. Excess DCC and aspartic acid reduced the yield significantly by forming the diaspartic acid conjugate as a side product. Deprotection of the amine of the lysine conjugate **26b** and both acids of the aspartyl conjugate **26a** have

been achieved under acidic conditions. Deprotection using TFA in CH_2Cl_2 afforded 15^2-monoaspartylchlorin e_6 dimethyl ester (**27c**) and 15^2-monolysinechlorin e_6 trimethyl ester (**28b**) in 79% and 73% yields, respectively.

Insertion of palladium into the chlorin ring was done before the deprotection step to simplify the purification, but a good ^{1}H NMR spectrum of deprotected palladium chlorin derivative could not be obtained. Several deprotection methods were tested. *tert*-Butyl deprotection with TFA/CH_2Cl_2,[31] ZnBr/ CH_2Cl_2[32] and with HCl gas in CH_2Cl_2, but all were unsuccessful. Product was difficult to identify using ^{1}H NMR due to peak broadening. This may be due to a paramagnetic species which is produced during the deprotection step. To solve this problem, palladium insertion was done after deprotection. Both palladium acetate and palladium chloride worked well in the insertion reaction. An optimized yield of 98% of palladium inserted chlorin derivatives **28a** and **28b** was consistently obtained with 1.2 equivalents of palladium acetate in THF at 40 ^{o}C (Scheme 2.10). A significant blue shift in the UV-Vis spectrum was observed (Figure 2.4). ^{1}H NMR and mass spectroscopy also confirmed the insertion of palladium.

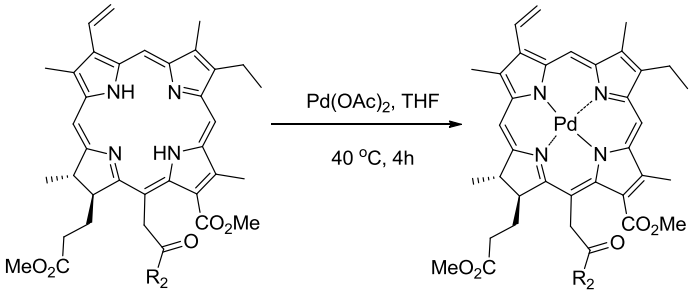

27 **28**

(a) R_2 - $NHCH(CO_2H)CH_2CHCO_2H$

(b) R_2 - $NHCH(CO_2Me)(CH_2)_4NH_2$

Scheme 2.10: Palladium insertion reaction

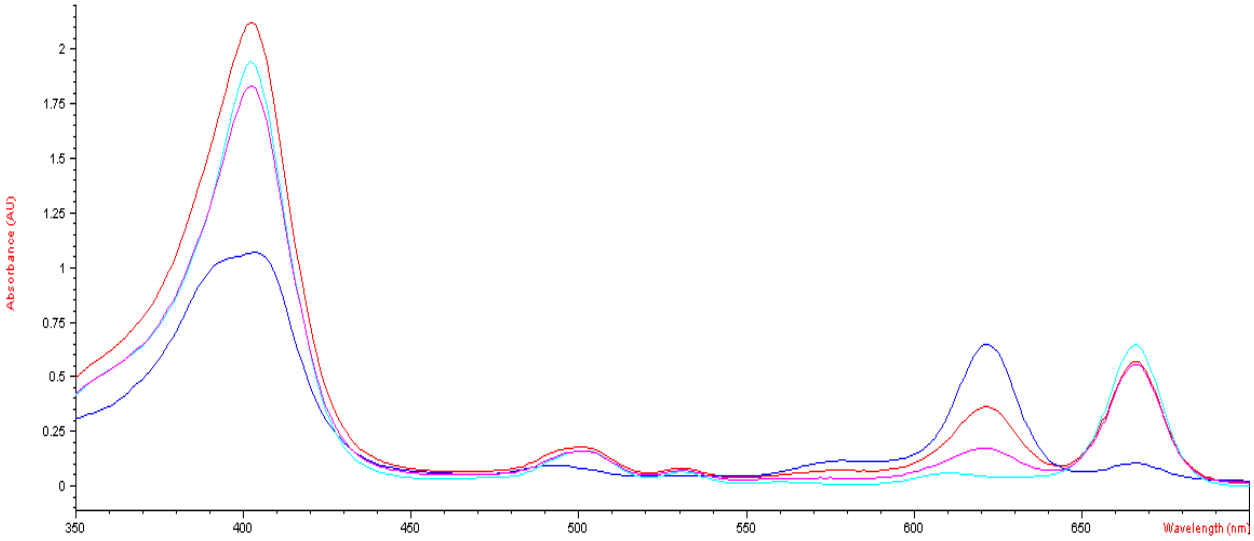

Figure 2.4: UV-Vis spectroscopic progression of the palladium insertion reaction in THF. 15^2-Monoaspartylchlorin e_6 dimethyl ester (**27a**, green) and palladium inserted 15^2-Monoaspartylchlorin e_6 dimethyl ester (**28a**, blue)

2.3.4 Synthesis of 13^1 Chlorin e_6 Conjugates

There are two possible ways to synthesize 13^1 conjugates. These are: (1) selective esterification of 17^3 and 15^2 carboxylic acids of chlorin e_6 (**2**) followed by coupling,[33] and (2) isocyclic ring-opening of methyl pheophorbide a (**3**) with a nucleophile. By using the second method we will be able to avoid the low yielding chlorin e_6 (**2**) synthesis and enhance the yield of the overall reaction. Unfortunately, the ring opening-reaction was only successful with ethylene diamine. Coupling with any other linker or direct coupling of amino acids has to follow the first route.

Under acidic conditions, the inner nitrogen atoms of the chlorin ring are fully protonated and the 13^1-carboxylic acid becomes severely deactivated. The protonated chlorin core is inductively electron-withdrawing from the 13^1-carbonyl, making the carbonyl double bond stronger. This prevents the formation of protonated 13^1-carbonyl intermediate during the esterification. This permits selective esterification of the 15^2- and 17^3- carboxylic acids. These carboxylic acids were selectively methylated with 5% H_2SO_4/MeOH to give chlorin e_6 dimethyl ester (**29**) in quantitative yield. The remaining 13^1-

carboxylic acid was activated using HOBt/TBTU under basic conditions and coupled directly with L-aspartic di(*tert*)butyl ester to give (**30**) in 66% yield. With DCC/DMAP a lower yield was obtained compared to HOBt/TBTU. Product **30** was isolated using silica gel column chromatography and characterized by ^{1}H NMR and mass spectroscopy. Subsequent deprotection of both carboxylic acid groups in the aspartic chain provided compound **7** in 57% overall yield from chlorin e_6 (Scheme 2.11).

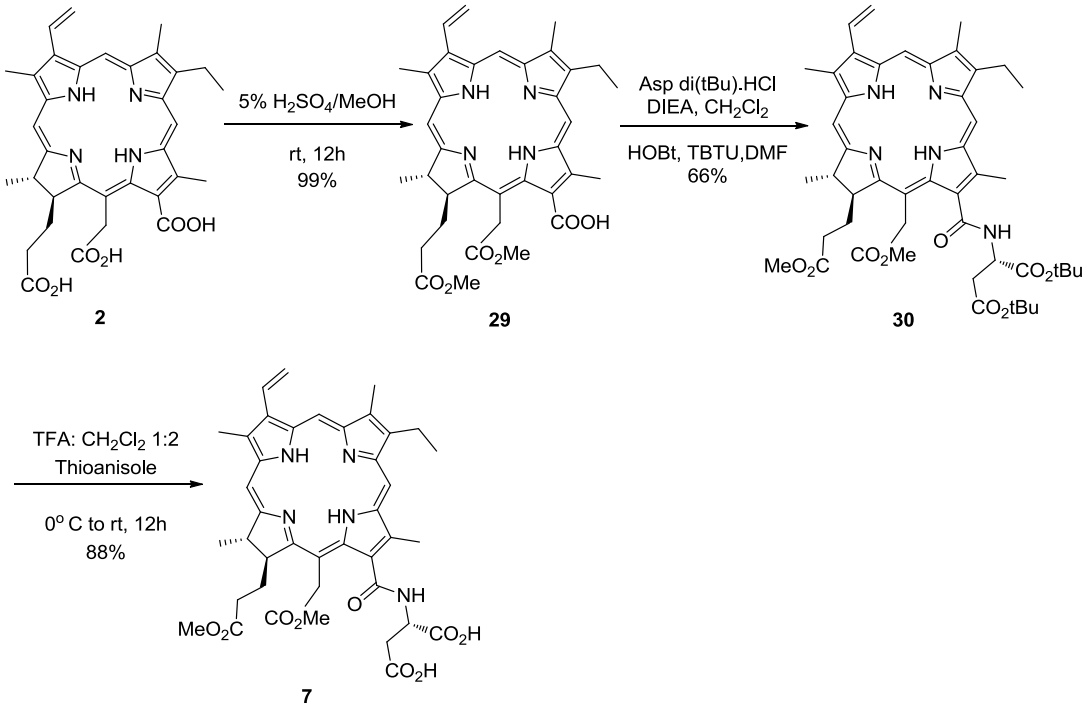

Scheme 2.11: Synthesis of 13^1 aspartic acid derivative of chlorin e_6 **7**

Nucleophilic opening of the isocyclic ring in pheophorbide a (**17**) with ethylenediamine and ethanolamine has been reported.[34] The same reaction was carried out with β-alanine(*tert*)butyl ester to produce a link to couple aspartic acid to the chlorin e_6 dimethyl ester **29**. Isocyclic ring-opening with β-alanine(*tert*)butyl ester was unsuccessful, presumably because of its lower nucleophilcity and its bulkiness compared to ethylenediamine. Coupling β-alanine(*tert*)butyl ester with the remaining 13^1-carboxylic acid of the chlorin e_6 dimethyl ester **(29)** followed by deprotection of the *tert*-butyl group provided 13^1-mono-β-alanylchlorin e_6 dimethyl ester **(32)** in 64% yield over two steps. Aspartic

di(*tert*)butyl ester was coupled through the linker to the chlorin e_6 to produced 13^1-mono-β-alanylaspartylchlorin e_6 dimethyl ester **33**; subsequent deprotection of the *tert*-bytyl group provided **34** in 54% overall yield (Scheme 2.12).

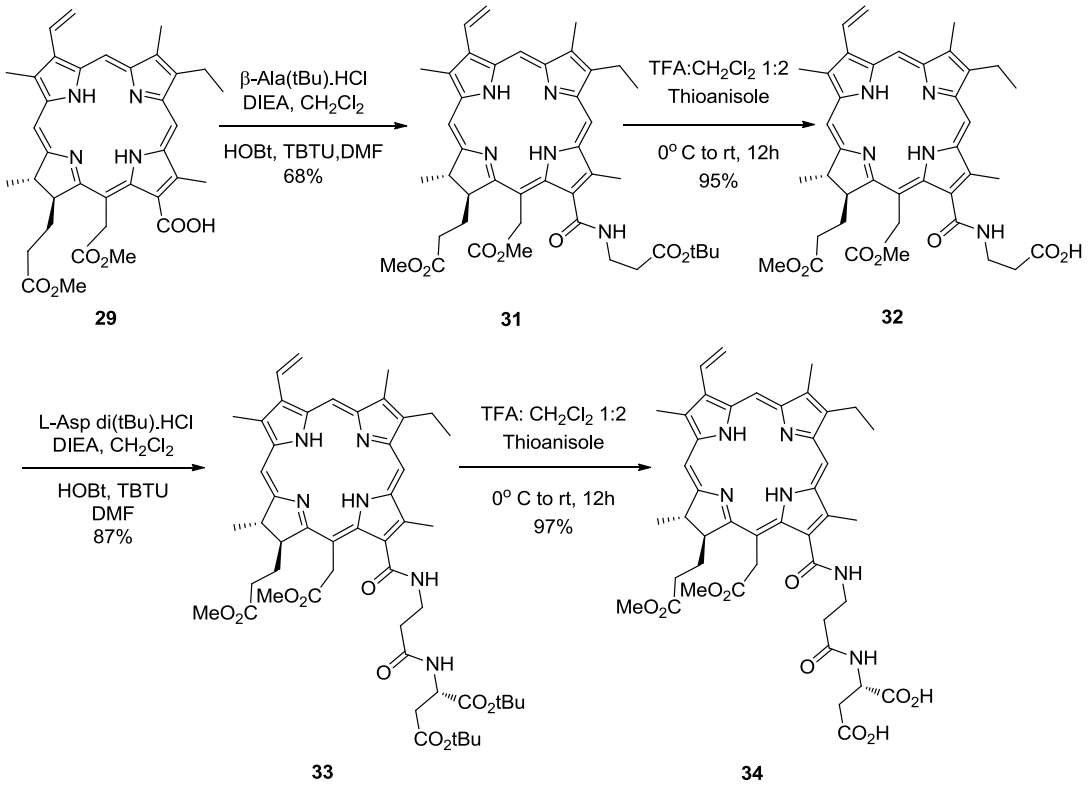

Scheme 2.12: Synthesis of 13^1-β-alanylaspartylchlorin e_6 **34**

The high yielding isocyclic ring-opening reaction with ethylenediamine was used to develop a potentially high yielding way to synthesize novel chlorin e_6 photosensitizers directly from pheophytin a **(2)** in four steps. Nucleophilic opening of the isocyclic ring of methyl pheoporbide **3** with ethylenediamine led to molecule **35** which was isolated in 91% yield. The reaction was monitored using TLC and UV-Vis spectroscopy. Due to the change in conjugation of the molecule, the color changed from dark green to bright green during ring-opening. Recently it was found possible to reduce the reaction time by half at 40 ^{o}C using toluene as a solvent. ^{1}H NMR, UV-Vis and mass spectroscopy confirmed the

presence of the product **35**. Subsequent coupling of protected lysine followed by deprotection provided the desired product **37** in four steps and in 55% yield from pheophytin a **(2)** (Scheme 2.13).

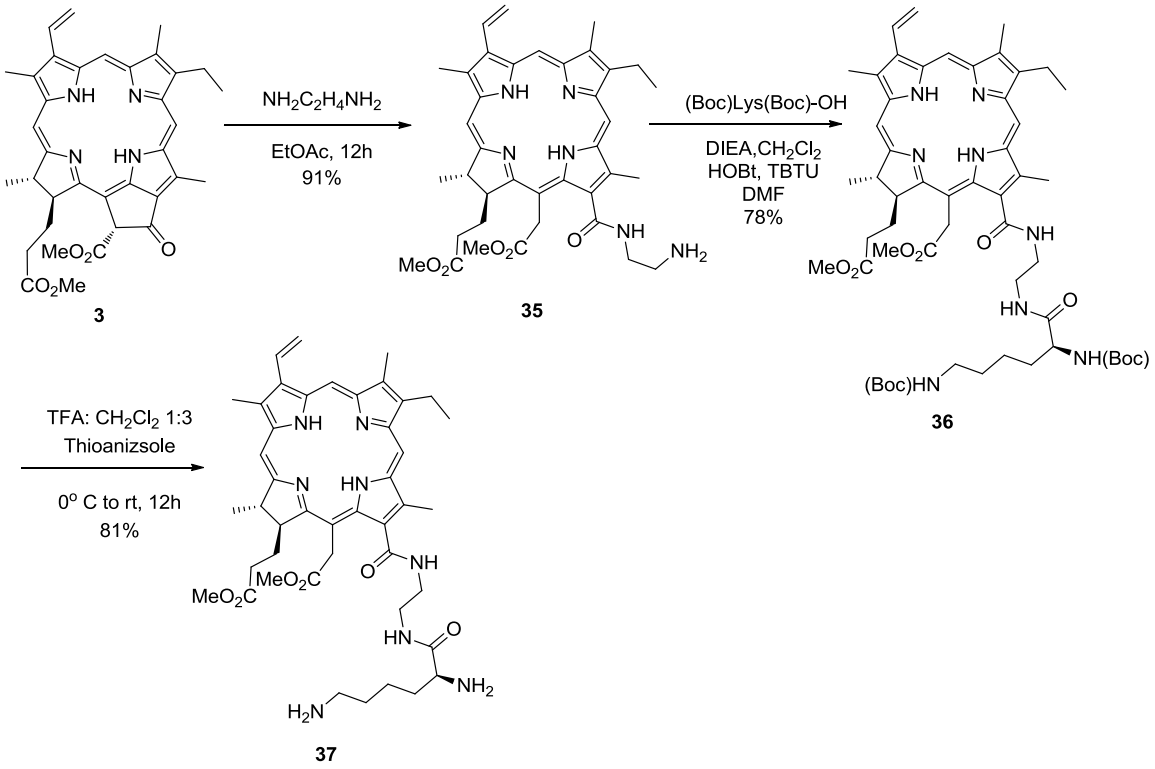

Scheme 2.13: Synthesis of 13^1-ethylenediaminylchlorin e_6 **37**

2.4 Molecular Modeling

Conformation analysis calculations for all three regioisomers (17^3, 15^2 and 13^1) of lysine derivatives of chlorin e_6 **20**, **27b** and **37** was achieved in the gas phase at the HF/6-31G level and the minimum energy conformations were obtained (Figure 2.5). In addition, the minimum energy conformation of a mono-cationic 13^1-lysinyl chlorin e_6 derivative without a linker (Figure 2.5d) was also examined for direct comparison with the propionic acid derivative **20** and the acetic acid derivative **27b.** These calculations were done using atom coordinates from the X-ray structure of 15^2-aspartylchlorin e_6 tetramethyl ester.[12] As shown in Figure 2.5, the lysine attached propionic side chain in the 17^3-lysinyl derivative **20** is nearly perpendicular to the macrocyclic plane (Figure 2.5a). The lysine residue in the 15^2-

lysinyl derivative **27b** forms approximately a 120^{o} angle (Figure 2.5b). On the other hand, as shown in Figure 2.5c and 2.5d, the lysine-attached formic acid side chain extends away from the macrocycle in the 13^{1}-lysinyl derivatives, with and without the short spacer. Subsequently, in the L-shape conformation of the 17^{3}-lysinylchlorin e_6 derivative **20** the amino acid covers one face of the chlorin ring, while in the case of the 15^{2}- and 13^{1}-lysinyl derivatives, it extends away from the macrocycle resulting in nearly a linear conformation for the 13^{1} derivatives. According to the minimum energy conformations in the gas phase, the use of a short linker and the presence of two (rather than one) positive charges, as a result of conjugation to the C-terminus rather than the N-terminus of the amino acid, do not appear to have a substantial effect on the preferred conformation; the main factor affecting the molecule conformation is the site of substitution. Water effects were also evaluated for the 13^{1}-lysinylchlorin e_6 derivative **37.** There was no significant difference in the minimum energy conformation for the aquous phase compared with the conformation in the gaseous phase.

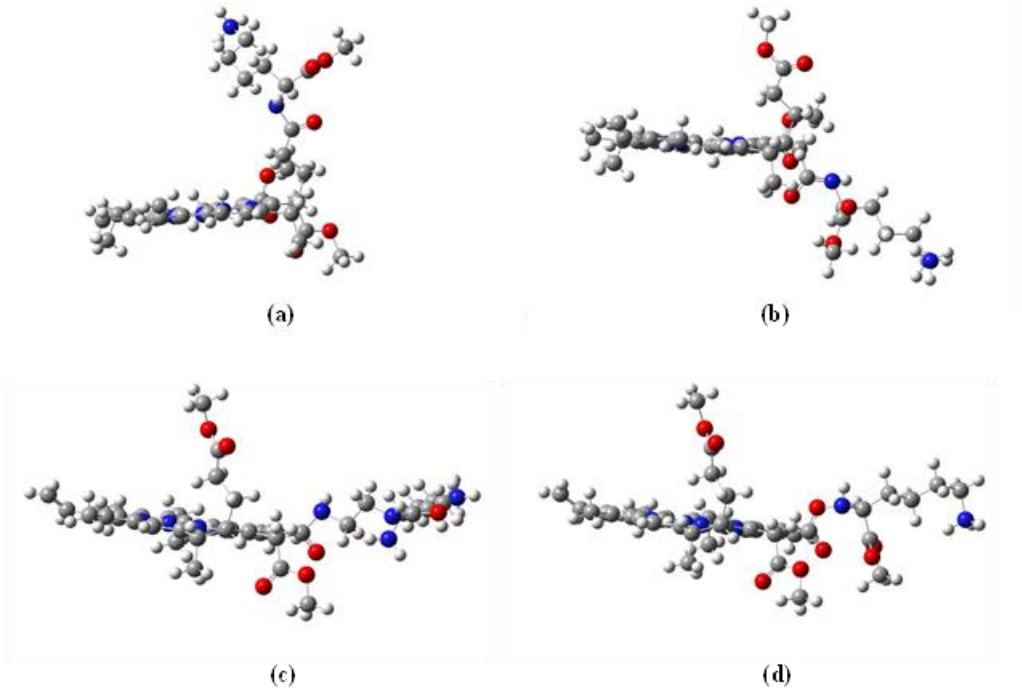

Figure 2.5: Energy minimized conformations in gas phase for chlorin e_6 derivatives (a) **20**, (b) **27b**, (c) **37** and (d) [13^{1} LysCe_6TME]$^{+}$. Optimization by energy was carried out at HF/6-31G level.

2.5 Cell Culture Studies

2.5.1 Time-dependent Cellular Uptake

The results obtained for the time-dependent uptake of chlorin e_6 and its derivatives at a concentration of 10 μM in human HEp2 cells are shown in Figure 2.6. All amino acid conjugates of chlorin e_6 were readily taken up by cells and showed similar uptake kinetics to unconjugated chlorin e_6. Interestingly, the 15^2-lysinylchlorin e_6 derivatives **27b** and its palladium complex **28b** accumulated to a much higher extent than all other compounds, at all time points studied. In comparison with chlorin e_6 (**2**), the lysinyl derivatives **27b** and **28b** showed 18-fold and 4-fold higher cellular uptake, respectively, after 24 hours. The observed high uptake for derivatives **27b** and **28b** is probably due to the lysine residue in position 15^2 since the corresponding aspartyl derivatives **27a** and **28a** accumulated to a significantly lower extent within cells. Presumably, the stronger interactions between the positively charged lysine derivatives, (compared with the corresponding aspartyl derivatives), with the negatively charged plasma membrane leads to enhanced cellular uptake. On the other hand a lysine residue in position 17^3, as in derivative **20**, showed a dramatic decrease in cellular uptake compared with the same residue in position 15^2, suggesting that the molecular conformation plays an important role on the mechanism of cellular uptake. Indeed the extended conformation of the 15^2-lysinylchlorin e_6 derivative **27b** (Figure 2.5b) might be the most favored for penetration across the plasma membrane, compared with the L-shape and linear conformations of the 17^3- and 13^1-lysinyl derivatives (Figures 2.5a,c), respectively. The presence of a chelated palladium ion, as well as the more linear structure of the 13^1-lysinyl side chain might lead to enhanced π-π stacking of the macrocycles, decreasing cellular uptake.

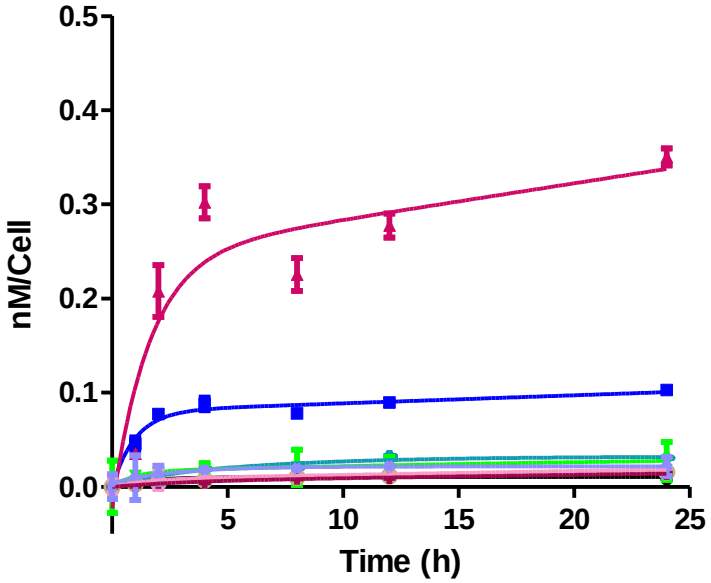

Figure 2.6: Time-dependent uptake of chlorin e_6 (**2**, black line) and its derivatives 17^3-LysCe_6TME (**20**, brown line), 15^2-AspCe_6DME (**27a**, light blue line), 15^2-LysCe_6TME (**27b**, red line), 15^2-AspPdCe_6DME (**28a**, green line), 15^2-LysPdCe_6TME (**28b**, blue line), 13^1-AspCe_6DME (**7**, maroon line), 13^1-β-AlaAspCe_6DME (**34**, purple line) and 13^1-EDLysCe_6DME (**37**, pink line) at 10 μM by HEp2 cells.

2.5.2 Cytotoxicity

The dark cytotoxicity and phototoxicity of chlorin e_6 and its derivatives was evaluated in HEp2 cells exposed to increasing concentrations of each compound up to 400 μM; the results are shown in Figures 2.8 and 2.7, respectively, and summarized in Table 2.1. Chlorin e_6 and its lysinyl derivatives **20**, **27b** and **28b** were found to be non-toxic in the dark up to the highest concentration of 400 μM investigated. All other amino acid derivatives showed very low dark cytotoxicities (Figure 2.7), with IC_{50} > 320 μM except for the 13^1-chlorin e_6 derivatives **7** and **37**, which showed IC_{50} of 285 and 268 μM, respectively. However, upon exposure to low light dose (1 J/cm), all chlorin e_6 derivatives were found to be highly toxic to HEp2 cells (Figure 2.8). The most phototoxic were the 13^1-chlorin e_6 derivatives **7**, **34** and **37**, with estimated IC_{50} values of 0.61, 0.82 and 1.34 μM, respectively. Among these, the most promising aspartyl derivatives for PDT applications are compounds **7** and **34**, because they have the

highest dark cytotoxicity/phototoxicity ratio, > 466:1. The presence of the β-alanine spacer between the 13^1 carbonyl group and the aspartic acid residue seems to have only a small effect, slightly decreasing compound cytotoxicity. On the other hand the 15^2-aspartylchlorin e_6 derivative **27a** was less phototoxic than its 13^1 regioisomer **7** by approximately 7-fold, and the introduction of palladium further reduced its phototoxicity. The positively charged 17^3- and 15^2-lysinylchlorin e_6 derivatives **20** and **27b** were the least phototoxic, and the introduction of palladium increased the phototoxicity of the 15^2 derivative by about 10-fold. These results show for the first time that the phototoxicity of amphiphilic conjugates of chlorin e_6 depends mainly on the site of conjugation, probably as a result of molecule conformation; the nature of the amino acid, the molecule overall charge, and the presence of palladium(II) also affect phototoxicity, but apparently to a smaller extent. Our results suggest that the most extended, nearly linear conformation of the 13^1 regioisomers facilitates binding to biological substrates, enhancing their toxic effect.

Table 2.1: Cytotoxicity (HEp2 cells) for chlorin e_6 and its derivatives using the MTT assay

Compound	**Dark toxicity (IC_{50}, μM)**	**Phototoxicity (IC_{50}, μM)**	**Ratio**
Chlorin e_6 (**2**)	>400	20.8	>19.2
17^3-LysCe_6TME (**20**)	>400	26.2	>15.3
15^2-AspCe_6DME (**27a**)	373.1	4.0	93.4
15^2-LysCe_6TME (**27b**)	>400	28.8	>13.9
15^2-AspPdCe_6DME (**28a**)	324.8	16.7	19.4
15^2-LysPdCe_6TME (**28b**)	>400	3.3	>121.2
13^1-AspCe_6DME (**7**)	284.6	0.61	466.6
13^1-βAlaAspCe_6DME (**34**)	383.9	0.82	468.2
13^1-EDLysCe_6DME (**37**)	268.4	1.34	200.3

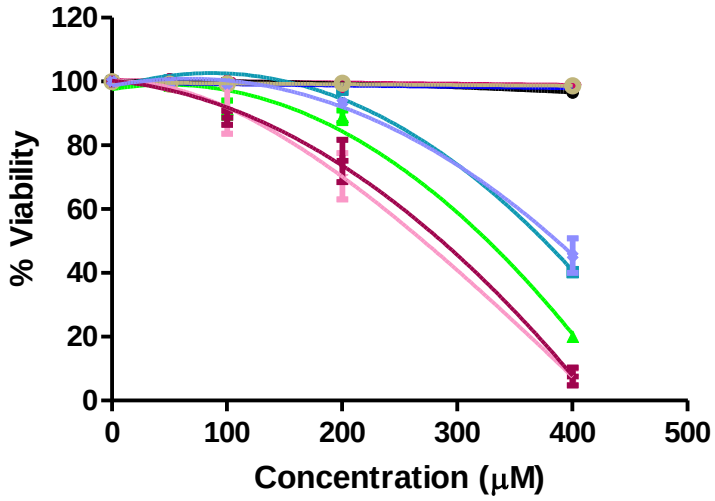

Figure 2.7: Dark toxicity of chlorin e_6 (**2**, black line) and its derivatives 17^3-LysChlorin e_6TME (**20**, brown line), 15^2-AspChlorin e_6DME (**27a**, light blue line), 15^2-LysChlorin e_6TME (**27b**, red line), 15^2-AspPdChlorin e_6DME (**28a**, green line), 15^2-LysPdChlorin e_6TME (**28b**, blue line), 13^1-AspChlorin e_6DME (**7**, maroon line), 13^1-βAlaAspChlorin e_6DME (**34**, purple line), and 13^1-EDLysChlorin e_6DME (**37**, pink line) toward HEp2 cells using 1 J/cm2 light dose and the Cell Titer Blue assay.

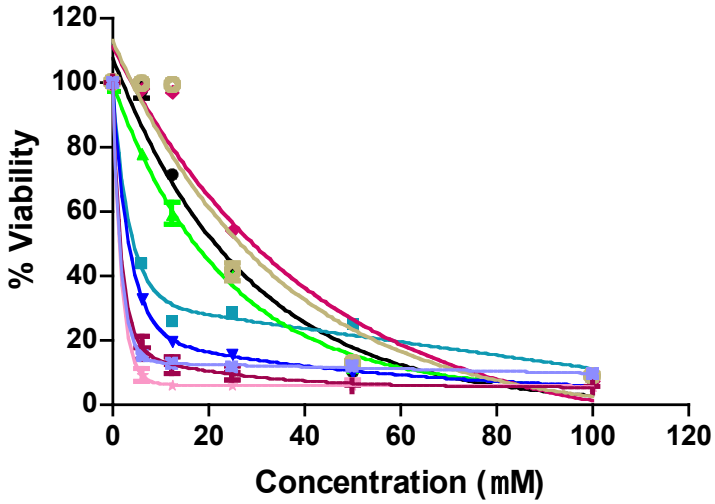

Figure 2.8: Phototoxicity of chlorin e_6 (**2**, black line) and its derivatives 17^3-LysChlorin e_6TME (**20**, brown line), 15^2-AspChlorin e_6DME (**27a**, light-blue line), 15^2-LysChlorin e_6TME (**27b**, red line), 15^2-AspPdChlorin e_6DME (**28a**, green line), 15^2-LysPdChlorin e_6TME (**28b**, blue line), 13^1-AspChlorin e_6DME (**7**, maroon line), 13^1-βAlaAspChlorin e_6DME (**34**, purple line), and 13^1-EDLysChlorin e_6DME (**37**, pink line) toward HEp2 cells using 1 J/cm2 light dose and the Cell Titer Blue assay.

2.5.3 Intracellular Localization

The preferential sites of subcellular localization of this series of chlorin e_6 derivatives were evaluated by fluorescence microscopy, upon exposure of HEp2 cells to 10 μM compound concentrations for six hours. Figure 2.9 to 2.17 in supporting information shows the fluorescence pattern observed for all compounds and Table 2.2 summarizes their main sites of subcellular localization.

Table 2.2: Main subcellular sites of localization for chlorin e_6 and its derivatives in HEp2 cells

Compound	Lysosomes	ER	Golgi	Mitochondria
Chlorin e_6 (**2**)	+	++	-	-
17^3-LysCe_6TME (**20**)	+	++	+	-
15^2-AspCe_6DME (**27a**)	++	++	-	+
15^2-LysCe_6TME (**27b**)	++	++	+	-
15^2-AspPdCe_6DME (**28a**)	++	+	++	-
15^2-LysPdCe_6TME (**28b**)	+	++	-	-
13^1-AspCe_6DME (**7**)	+	++	++	++
13^1-βAlaAspCe_6DME (**34**)	++	++	++	-
13^1-EDLysCe_6DME (**37**)	++	++	++	-

Overlay experiments using the organelle specific fluorescence probes BoDIPY Ceramide (Golgi), LysoSensor Green (Lysosomes), MitoTracker Green (mitochondria), and ER tracker Blue/White fluorescence (ER) were conducted to evaluate the preferential sites of compound localization. All the chlorin e_6 derivatives were found to localize in the lysosomes and the ER. This is not surprising, since the structurally-related LS-11 (**1**, 15^2-aspartyl chlorin e_6) is a known lysosomal localizer, and HPPH (2-[1-hexyloxyethyl]-2-devinyl-pyropheophorbide a) localizes preferentially in the ER.[35] Photodamage to ER and/or lysosomes has been shown to lead to activation of apoptotic pathways.[35,36] In addition, the most phototoxic 13^1 chlorin e_6 regioisomers were also found in Golgi and mitochondria; presumably, the

photodamage effect to multiple organelles caused by the 13^1 derivatives can trigger various apoptotic pathways, leading to effective cell destruction. The multiple sites of intracellular localization observed for the 13^1 chlorin e_6 derivatives might again be due to their linear conformations that may facilitate their binding to various intracellular sites.

2.6 Conclusion

A series of chlorin e_6 derivatives, conjugated directly or with a spacer group with either an aspartic or a lysine residue at the propionic (17^3), acetic (15^2) or formic (13^1) side chains of the chlorin macrocycle, have been synthesized in good yields from pheophytin a (**4**) extracted from *S. pacifica.* In comparison with chlorin e_6 (**2**), all amino acid derivatives readily accumulated in human HEp2 cells. Cytotoxicity results revealed that none of these compounds is toxic in the absence of light in the range of therapeutic dose. However after exposure to light all of these derivatives showed high phototoxicity. According to the phototoxicity results, the most phototoxic compounds were found to be the formic acid regioisomers, bearing either an aspartic acid or a lysine residue directly conjugated to position-13 of the chlorin macrocycle, or connected via a short spacer group. 13^1-Aspartylchlorin e_6 (**7**) showed the lowest IC_{50} value of 0.61 μM. Computational conformational analysis revealed that the 13^1 regioisomer has an extended, nearly linear, conformation in comparison with the 15^2 and 17^3 regioisomers. This linear conformation might facilitate the binding to multiple intracellular and internal components and subsequent photodamage to multiple cellular sites. These results show that the site of amino acid conjugation in the chlorin e_6 macrocycle is the major determinant of its phototoxicity. Therefore, we conclude that the 13^1 regioisomer of mono-L-aspartylchlorin e_6 (**7**) is a more efficient photosensitizer for PDT than is the commercially available 15^2 regioisomer (LS-11, **1**)

2.7 Experimental

Isolation of pheophytin a (**4**) from *Spirulina pacifica*:

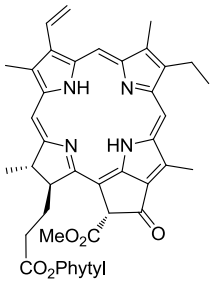

Approximately 300 g of dried *Spirulina pacifica* algae was wetted with acetone and subsequently slurried with 2 L of liquid nitrogen in a resistant 2 gallon bucket to form a frozen slush. The algae were then transferred to a 3 L reaction vessel and 2 L of acetone was added. The vessel was fitted with a Fisher jumbo mechanical stirrer with a 46 cm impeller shaft and a 3-neck lid was clamped to the vessel. The reaction mixture was heated at reflux under argon with mechanical stirring for 3 h. The supernatant was then filtered through Whatman 1 paper on a Buchner funnel and more acetone was added to the solid. This slurry was allowed to sit overnight protected from light. Then the extraction and filtration processes were repeated twice. The green filtrates were combined and evaporated and then purified by flash column chromatography on silica gel. Elution first with CH_2Cl_2 removed the fast-running yellow carotenoid band. Then elution with 95:5 CH_2Cl_2/acetone eluted the major blue-grey pheophytin a band (**4**, $C_{55}H_{74}N_4O_5$, 1.5g); UV-Vis (CH_2Cl_2): λ_{max} ($\varepsilon/M^{-1}cm^{-1}$) 668 nm (44,600) , 611 (8,600), 538 (9,700), 507 (10,800), 414 (106,000); ^{1}H NMR (chloroform-*d*, 400 MHz): δ 9.50 (s, 1H), 9.35 (s, 1H), 8.57 (s, 1H), 8.0 (m, 1H), 6.28 (m, 1H), 6.26 (s, 1H), 6.18 (s, 1H), 4.48 (m, 1H), 4.21 (m, 1H), 3.88 (s, 3H), 3.64 (s, 3H), 3.60 (q, J = 7.5 Hz, 2H), 3.40 (s, 3H), 3.20 (s, 3H), 2.63 (m, 2H), 2.34 (m, 2H), 1.74(d, J = 7.5 Hz, 3H), 1.61 (t, J = 7.5 Hz, 3H) Phytyl: 5.13 (m, 1H), 4.50 (m, 1H), 1.90 (m, 2H), 1.56 (m, 3H), 1.0-1.3 (m, 2H), 0.85 (m, 6H) 0.71 (m, 6H). MS (MALDI-TOF) *m/z* 872 $[M+H]^+$, calcd. for $C_{55}H_{75}N_4O_5$ 872.256.

Pheophorbide a (**17**):

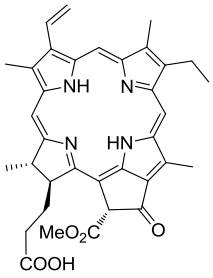

Pheophytin a (**4**, 250 mg, 0.29 mmol) was selectively hydrolyzed to give the 17^3-carboxylic acid without affecting the 13^1-carbomethoxy group via the Wasielewski and Svec procedure which requires stirring pheophytin a in 25 ml of degassed TFA/H_2O 80:20 at 0 °C overnight. The reaction mixture was poured into 150 ml of H_2O and extracted with $CHCl_3$. The extract was washed three times with H_2O and once with 10% $NaHCO_3$ to remove TFA. This formed a precipitate in the organic layer. Then it was washed with 10% citric acid until the precipitate was dissolved. The organic layer was dried over anhydrous Na_2SO_4. Evaporation of solvent provided a brown residue that was purified via silica gel column chromatography with 50% ethyl acetate in CH_2Cl_2. After evaporation of solvent pheophorbide a (**17**, $C_{35}H_{36}N_4O_5$, 155 mg, 0.26 mmol, 90%) was obtained. UV-Vis (DCM): λ_{max} ($\varepsilon/M^{-1}cm^{-1}$) 667 nm (55,200), 609 (7,900), 535 (9,500), 505(12, 100), 413 (119, 200); ^{1}H NMR (acetone-d_6, 400 MHz): δ 9.53 (s, 1H), 9.20 (s, 1H), 8.85 (s, 1H), 7.99 (dd, J = 17.86, 11.61 Hz, 1H), 6.34 (s, 1H), 6.26 (d, J = 16.82 Hz, 1H), 6.26 (dd, J = 11.61, 1.13 Hz, 1H), 4.66 (m, 1H), 4.23 (m, 1H), 3.88 (s, 3H), 3.59 (s, 3H), 3.47 (q, J = 7.5 Hz, 2H), 3.38 (s, 3H), 3.01 (s, 3H), 2.59 (m, 2H), 2.35 (m, 2H), 1.85 (d, J = 7.5 Hz, 3H), 1.55 (t, J = 7.5 Hz, 3H), -1.3 (s, 1H), -1.5 (s, 1H). MS (MALDI-TOF) *m/z* 593 $[M+H]^+$, calcd. for $C_{35}H_{37}N_4O_5$ 593.276.

Lysine(boc) methyl ester pheophorbide a (**18**):

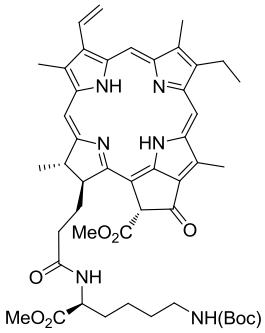

Pheophorbide a (**17**, 100 mg; 0.169 mmol) was dissolved in 10 ml of CH_2Cl_2. Then DCC (42 mg) and DMAP (10 mg) were added and the mixture was left for 15 min. H-Lysine (boc) methyl ester.HCl (60 mg, 0.20 mmol) and DIEA (0.07 ml, 0.40 mmol) were dissolved in 5 ml of CH_2Cl_2, added to the reaction mixture and it was stirred for 4 h. [Note: this reaction is favored by dilute conditions. Concentrated conditions favor the formation of the anhydride (bispheophorbide), and will slow the reaction.] The reaction mixture was washed with 10% citric acid, water and brine, dried over anhydrous Na_2SO_4 and purified on a silica gel column (eluted with 10% acetone in CH_2Cl_2). After the major brown band was eluted from the column, the solvent was evaporated and the solid was dissolved in ethyl acetate and filtered. (DCC precipitates in ethyl acetate.) Evaporation of the ethyl acetate gave lysine (boc) methyl ester pheophorbide a (**18**, $C_{47}H_{58}N_6O_8$, 74 mg, 0.085 mmol, 51%); UV-Vis (DCM): λ_{max} (rel. inten.) 667 nm (0.463), 609 (0.066), 535 (0.080), 505(0.100), 413 (1.000); ^{1}H NMR (acetone-d_6, 400 MHz): δ 9.12 (s, 1H), 8.71 (s, 1H), 8.70 (s, 1H), 7.64 (dd, J = 17.8, 11.63 Hz, 1H), 7.20 (d, J = 7.2 Hz, 1H), 6.33 (s, 1H), 6.02 (d, J = 17.85 Hz, 1H), 5.93 (d, J = 11.61 Hz, 1H), 5.77 (s, 1H), 4.65 (m, 1H), 4.41 (m, 1H), 4.21 (m, 1H), 3.91 (s, 3H), 3.59 (s, 3H), 3.47 (s, 3H), 3.19 (s, 3H) 3.09 (q, J = 7.5 Hz, 2H), 2.92 (3H, s), 2.83 (m, 2H), 2.66 (m, 1H), 2.48 (m, 1H), 2.25 (m, 1H), 1.85-1.62 (br , 4H), 1.86 (d, J = 7.24, 3H), 1.37 (t, J = 7.58, 3H), 1.43 (m, 2H), 1.26 (s, 9H), - 1.95 (s, 1H), -2.23 (s, 1H) MS (MALDI-TOF) *m/z* 835 $[M+H]^+$, calcd. for $C_{47}H_{59}N_6O_8$ 835.439.

17^3-Monolysine(boc)chlorin e_6 trimethyl ester (**19**):

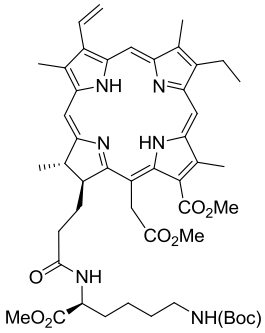

Lysine(boc) methyl ester pheophorbide a (**18**, 74 mg, 0.085 mmol) was dissolved in a dry 2:1 THF/MeOH solvent system and stirred under argon for 10 min. Sodium methoxide (0.17 mL of a 0.5 M solution, 0.085 mmol) was added and the reaction mixture was allowed to stir at 0 °C for 1 h. The reaction was followed by UV-Vis spectroscopy. The solution turns from brown to green as the isocyclic ring opens. The reaction mixture was then poured into water. The mixture was extracted with CH_2Cl_2 and the organic layer was washed with water and 5% citric acid, dried over anhydrous Na_2SO_4 and then evaporated. The residue was dissolved in 2% methanol/CH_2Cl_2 and purified on a silica gel plug with the same mobile phase. The solvent was evaporated and 17^3-monolysine(boc)chlorin e_6 trimethyl ester (**19**, $C_{48}H_{62}N_6O_9$, 68 mg, 0.078 mmol, 89%) was obtained. ^{1}H NMR (acetone-d_6, 400 MHz): δ 9.80 (s, 1H), 9.65 (s, 1H), 9.03 (s, 1H), 8.19 (dd, J = 17.87, 11.58 Hz, 1H), 7.44 (d, J = 7.6 Hz, 1H), 6.40 (d, J = 17.87, 1.33 Hz, 1H), 6.13 (d, J = 11.61, 1.36 Hz, 1H), 5.89 (s, 1H), 5.38 (m, 2H), 4.63 (q, J = 7.22 Hz, 1H), 4.55 (dd, J = 10.34, 1.95 Hz, 1H), 4.44 (m, 1H), 4.25 (s, 3H), 3.78 (q, J =7.67, 2H) 3.75 (s, 3H), 3.69 (s, 3H), 3.56 (s, 3H) 3.49 (s, 3H), 3.27 (3H, s), 3.00 (m, 2H), 2.66 (m, 1H), 2.33 (m, 1H), 2.20 (m, 1H), 1.85-1.62 (br , 4H), 1.78 (d, J = 7.24, 3H), 1.69 (t, J = 7.58, 3H), 1.43 (m, 2H), 1.32 (s, 9H), - 1.32 (s, 1H), -1.52 (s, 1H). MS (MALDI-TOF) *m/z* 867 $[M+H]^+$, calcd. for $C_{48}H_{63}N_6O_9$ 867.466.

17^3-Monolysinechlorin e_6 trimethyl ester (**20**):

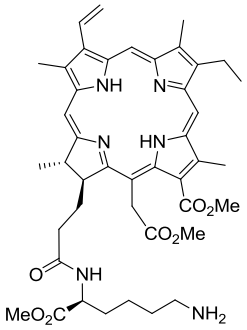

Monolysine(boc) chlorin e_6 trimethyl ester (**19**, 68mg, 0.078 mmol) was dissolved in 2 ml of dry CH_2Cl_2 in an ice bath under argon. Thioanisole (0.057 mmol) and 1 ml of TFA were added and the reaction mixture was allowed to stir overnight. The reaction mixture was rotavaped several times with diethyl ether to remove TFA. The resulting precipitate was washed several times with diethyl ether to remove thioanisole. Then the precipitate was dissolved in CH_2Cl_2 which was washed three times with H_2O and once with 10% $NaHCO_3$ to remove TFA. The organic layer was dried over anhydrous Na_2SO_4. Solvent was evaporated to give 17^3-monolysinechlorin e_6 trimethyl ester (**20**, $C_{43}H_{54}N_6O_7$, 43 mg, 0.056 mmol; 72%) was obtained. UV-Vis (acetone): λ_{max} ($\varepsilon/M^{-1}cm^{-1}$) 664 (65,000), 608 (4,900), 528 (4,500), 500 (16,100), 400 (213,000); ^{1}H NMR (acetone-d_6, 400 MHz): δ 9.79 (s, 1H), 9.63 (s, 1H), 9.03 (s, 1H), 8.17 (dd, *J* = 17.87, 11.58 Hz, 1H), 7.59 (d, *J* = 7.6 Hz, 1H), 6.38 (d, *J* = 17.87, 1.33 Hz, 1H), 6.12 (d, *J* = 11.61, 1.36 Hz, 1H), 5.37 (m, 2H), 4.63 (q, *J* = 7.22 Hz, 1H), 4.55 (dd, *J* = 10.34, 1.95 Hz, 1H), 4.44 (m, 1H), 4.25 (s, 3H), 3.76 (m, 2H) 3.75 (s, 3H), 3.69 (s, 3H), 3.55 (s, 3H) 3.48 (s, 3H), 3.25 (3H, s), 3.09 (m, 2H), 2.67 (m, 1H), 2.30 (m, 1H), 2.20 (m, 1H), 1.85-1.62 (br , 3H), 1.78 (d, *J* = 7.24, 3H), 1.68 (t, *J* = 7.58, 3H), 1.51 (m, 2H), 1.39 (m, 2H), - 1.33 (s, 1H), -1.53 (s, 1H). ^{13}C NMR (dichloromethane-d_2, 400 MHz) δ 173.8, 173.3, 172.6, 170.9, 169.9, 167.9, 155.3, 149.4, 145.6, 140.0, 136.8, 136.6, 135.9, 135.7, 135.2, 131.4, 129.7, 129.6, 124.1, 122.1, 103.1, 102.6, 99.0, 94.2, 53.5, 53.4, 52.5, 50.0, 41.7, 38.9, 34.4, 32.8, 32.2, 31.1, 30.8, 23.4, 22.9, 20.0, 18.0, 12.6, 12.4, 11.5. MS (MALDI-TOF) *m/z* 767 $[M+H]^+$, calcd. for $C_{43}H_{55}N_6O_7$ 767.414.

Methyl pheophorbide a (**3**):

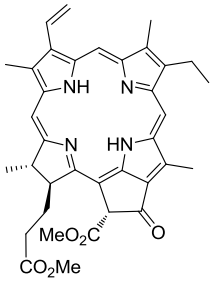

Pheophytin a (**4**, 250 mg, 0.29 mmol) was treated with 5% sulfuric acid in methanol (degassed by bubbling with argon) overnight at room temperature under argon and protected from light. It was diluted with CH_2Cl_2, washed with water and then with 10% saturated aqueous sodium bicarbonate. The organic layer was dried over anhydrous Na_2SO_4, filtered and then evaporated. Purification was achieved via silica gel chromatography with 5% acetone in CH_2Cl_2 to obtain methyl pheophorbide a (**3**, $C_{36}H_{38}N_4O_5$, 170 mg, 0.28 mmol, 96%) was obtained. UV-Vis (CH_2Cl_2): λ_{max} ($\varepsilon/M^{-1}cm^{-1}$) 668 nm (40,700), 610 (8,100), 560 (3,200), 538 (9400), 506 (10,400), 412 (93,400); ^{1}H NMR (acetone-d_6, 400 MHz): δ 9.33 (s, 1H), 9.11 (s, 1H), 8.61 (s, 1H), 7.83 (dd, *J* = 17.86, 11.61 Hz, 1H), 6.21 (s, 1H), 6.19 (dd, *J* = 17.85, 1.26 Hz, 1H), 6.09 (dd, *J* = 11.57, 1.37 Hz, 1H), 4.50 (q, *J* = 7.32 Hz, 1H), 4.19 (m, 1H), 3.90 (s, 3H), 3.62 (s, 3H), 3.58 (s, 3H), 3.44 (q, *J* = 7.5 Hz, 2H), 3.61 (s, 3H), 3.59 (s, 3H), 2.66 (m, 1H), 2.56 (m, 1H), 2.32 (m, 2H), 1.85 (d, *J* = 7.5 Hz, 3H), 1.59 (t, *J* = 7.5 Hz, 3H), -1.8 (br, 2H). MS (MALDI-TOF) *m/z* 607 $[M+H]^+$, calcd. for $C_{36}H_{39}N_4O_5$ 607.292.

Chlorin e_6 trimethyl ester (**24**):

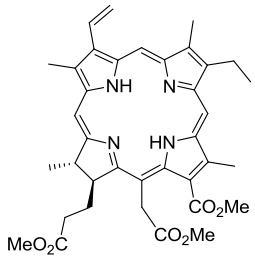

Methyl pheophorbide a (**3**, 921 mg, 1.52 mmol) was dissolved in dry THF and stirred under argon for 10 min. Then 1.65 ml of a 1 M sodium methoxide solution (1.65 mmol) was added to the solution which

was allowed to stir for 2 h at 0 °C (the reaction was monitored using UV-Vis spectroscopy). The solution was diluted with H_2O and extracted with CH_2Cl_2. The organic layer was dried over anhydrous Na_2SO_4, filtered and then evaporated. The solid obtained was dissolved in CH_2Cl_2 and chromatographed on a short silica gel column eluted with the 5% acetone/CH_2Cl_2. After evaporation of solvent, chlorin e_6 trimethyl ester (**24**, $C_{37}H_{42}N_4O_6$, 948 mg, 1.48 mmol, 98% of) was obtained. UV-Vis (CH_2Cl_2): λ_{max} ($\varepsilon/M^{-1}cm^{-1}$) 666 nm (43,700), 608 (4,500), 558 (1,800), 530 (4,700), 500 (11,200), 404 (123,400); ^1H NMR (acetone-d_6, 400 MHz): δ 9.72 (s, 1H), 9.53 (s, 1H), 9.03(s, 1H), 7.08 (dd, *J* = 17.86, 11.61 Hz, 1H), 6.31 (dd, *J* = 17.85, 1.26 Hz, 1H), 6.06 (dd, *J* = 11.57, 1.37 Hz, 1H), 5.36 (s, 2H), 4.63 (q, *J* = 7.32 Hz, 1H), 4.52 (dd, *J* = 10.50, 2.21 Hz, 1H), 4.25 (s, 3H), 3.77 (s, 3H), 3.67 (q, *J* = 7.5 Hz, 2H), 3.61 (s, 3H), 3.54 (s, 3H), 3.44 (s, 3H), 3.17 (s, 3H), 2.72 (m, 1H), 2.35 (m, 1H), 2.26 (m, 1H), 2.06 (m, 1H), 1.75 (d, *J* = 7.5 Hz, 3H), 1.64 (t, *J* = 7.5 Hz, 3H), -1.34 (s, 1H), -1.52 (s, 1H); MS (MALDI-TOF) *m/z* 639 $[M+H]^+$, calcd. for $C_{37}H_{43}N_4O_6$ 639.318.

Chlorin e_6 (**2**):

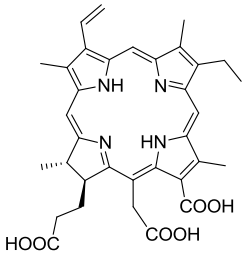

Chlorin e_6 trimethyl ester (**24**, 50 mg, 0.078 mmol) was dissolved in anhydrous ethyl acetate under argon. Lithium iodide (124 mg, 0.94 mmol) was added. The reaction mixture was refluxed for 48 h under argon. The reaction mixture was diluted with water and adjusted to pH 3 with aqueous citric acid and then washed with CH_2Cl_2. The solution was evaporated and redissolved in acetone and evaporated several times. The solid was washed with water and then dried under vacuum. The residue was dissolved in methanol and purified on a Sephadex LH20 column to yield chlorin e_6 (**2**, $C_{34}H_{36}N_4O_6$, 10 mg, 0.017 mmol, 21%); UV-Vis (MeOH): λ_{max} ($\varepsilon/M^{-1}cm^{-1}$) 666 nm (45,300), 610 (8,700), 558 (7,800), 530

(9,700), 502 (15,500), 402 (145,100); ^{1}H NMR (acetone-d_6, 400 MHz): δ 9.73 (s, 1H), 9.51 (s, 1H), 9.04(s, 1H), 8.05 (dd, *J* = 17.86, 11.61 Hz, 1H), 6.28 (dd, *J* = 17.85, 1.26 Hz, 1H), 6.02 (dd, *J* = 11.57, 1.37 Hz, 1H), 5.60 (d, *J* = 18.94 Hz, 1H), 5.40 (d, *J* = 18.94 Hz, 1H), 4.65 (m, 1H), 4.55 (m, 1H), 3.64 (m, 2H), 3.63 (s, 3H), 3.42 (s, 3H), 3.15 (s, 3H), 2.72 (m, 1H), 2.35 (m, 1H), 2.26 (m, 1H), 2.06 (m, 1H), 1.75 (d, *J* = 7.5 Hz, 3H), 1.64 (t, *J* = 7.5 Hz, 3H), -1.6 (s, 2H); MS (MALDI-TOF) *m/z* 597 $[M+H]^+$, calcd. for $C_{34}H_{37}N_4O_6$ 597.271.

15^2-Monoaspartylchlorin e$_6$ di(*tert)*butyl dimethyl ester (**26a**):

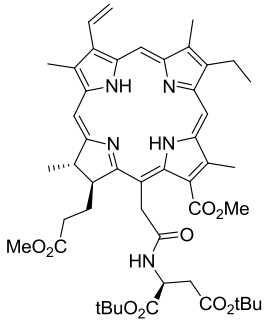

Chlorin e$_6$ (**2**, 100 mg, 0.168 mmol) was dissolved in dry CH_2Cl_2. DCC (35 mg, 0.168 mmol) and DMAP (9 mg, 0.074) were added and the mixture was allowed to stir until reagents were completely dissolved. After 3 h, aspartic acid di(*tert*)butyl ester hydrochloride (47.2 mg, 0.168 mmol) and DIEA (0.03 ml, 0.18 mmol) were mixed in CH_2Cl_2 and added to the reaction mixture which was allowed to stir overnight. The mixture was diluted with CH_2Cl_2 and then washed with 5% aqueous citric acid, followed by a wash with brine and water. It was dried over anhydrous Na_2SO_4 and then evaporated. Then it was dissolved in CH_2Cl_2 and treated with excess ethereal diazomethane. The residue was dissolved in 2% methanol/ CH_2Cl_2 and purified via silica gel column chromatography with the same mobile phase to afford 15^2-monoaspartylchlorin e$_6$ di(*tert*)butyl dimethyl ester(**26a**, $C_{48}H_{61}N_5O_9$, 65 mg, 0.076 mmol, 45%); ^{1}H NMR (aceton-d_6, 400 MHz) δ 9.64 (s, 1H), 9.32 (s, 1H), 9.02 (s, 1H), 7.81 (dd, *J* = 11.58, 17.85 Hz, 1H), 7.00 (s, 1H), 6.09 (dd, *J* = 17.87, 1.26 Hz, 1H), 5.85 (dd, *J* = 11.60, 1.29 Hz, 1H), 5.38 (s, 2H), 4.6 (br, 3H), 4.32 (s, 3H), 3.62 (s, 3H), 3.54 (s, 3H), 3.52 (q, *J* = 7.3 Hz, 2H), 3.30 (s, 3H), 3.02 (s, 3H), 2.78 (m, 3H), 2.44 (m, 2H),

1.87 (m, 1H), 1.65 (d, *J* = 7.3 Hz, 3H), 1.58 (t, *J* = 7.7 Hz, 3H), 1.26 (s, 9H), 1.16 (s, 9H), -1.42 (s, 1H), -1.53 (s, 1H); MS (MALDI-TOF) *m/z* 852 $[M+H]^+$, calcd. for $C_{48}H_{62}N_5O_9$ 852.454.

15^2-Monoaspartylchlorin e_6 dimethyl ester (**27a**):

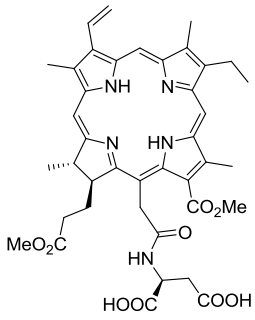

15^2-Monoaspartylchlorin e_6 di(*tert*)butyl dimethyl ester (**26a**, 65 mg, 0.076 mmol) was dissolved in 2 ml of dry CH_2Cl_2 in a ice bath under argon. Thioanisole (0.006 ml) and 2 ml of TFA were added and the reaction mixture was allowed to stir overnight. The reaction mixture was rotavaporated several times with diethyl ether to remove TFA. The resulting precipitate was washed several times with diethyl ether to remove thioanisole. Then the precipitate was dissolved in CH_2Cl_2 which was washed three times with H_2O and once with 10% $NaHCO_3$ to remove TFA. (This may form a precipitate. If so, the organic layer is washed with citric acid until the precipitate dissolves in the organic layer). The organic layer was dried over anhydrous Na_2SO_4. The solvent was evaporated to obtain 15^2-monoaspartylchlorin e_6 dimethyl ester (**27a**, $C_{40}H_{45}N_5O_9$, 44 mg, 0.06 mmol, 79%); UV-Vis (acetone) λ_{max} ($\varepsilon/M^{-1}cm^{-1}$) 664 (48,400), 609 (6,000), 560 (2,000), 529 (6,300), 500 (14,200), 402 (151,800); ^{1}H NMR (acetone-d_6, 400 MHz) δ 9.76 (s, 1H), 9.58 (s, 1H), 9.04 (s, 1H), 8.10 (dd, *J* = 17.85, 11.59 Hz, 1H), 6.33 (dd, *J* = 17.87, 0.98 Hz, 1H), 6.07 (dd, *J* = 11.61, 1.09 Hz, 1H), 5.32 (m, 2H), 4.84 (m, 1H), 4.60 (m, 2H), 4.26 (s, 3H), 3.72 (q, *J* = 7.3 Hz, 2H), 3.57 (s, 3H), 3.54 (s, 3H), 3.45 (s, 3H), 3.21 (m, 3H), 2.95 (dd, *J* = 16.85, 5.53 Hz, 1H), 2.88 (dd, *J* = 16.85, 5.09 Hz, 1H) 2.68 (m, 1H) 2.32 (m, 2H), 1.78 (m, 1H), 1.74 (d, *J* = 7.3 Hz, 3H), 1.66 (t, *J* = 7.7 Hz, 3H), -1.39 (s, 1H), -1.58 (s, 1H); ^{13}C NMR (acetone-d_6, 100 MHz) δ 174.5, 173.5, 173.2, 172.6, 171.7, 170.4, 169.4, 155.8, 150.3, 146.3, 140.4, 137.4, 136.6, 136.3, 135.8, 132.0, 130.6, 126.0, 122.6, 104.2, 103.1, 99.7,

95.4, 54.2, 54.0, 52.2, 50.4, 41.2, 37.8, 32.1, 31.0, 26.1, 23.8, 20.3, 18.4, 12.6, 11.6; MS (MALDI-TOF) *m/z* 740 $[M+H]^+$, calcd. for $C_{40}H_{46}N_5O_9$ 740.3296.

Palladium 15^2-monoaspartylchlorin e_6 dimethyl ester (**28a**):

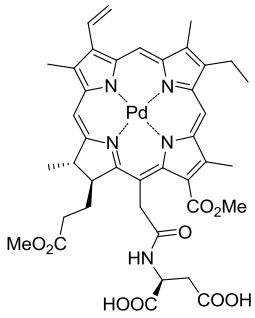

15^2-Monoaspartylchlorin e_6 dimethyl ester (**27a**, 44 mg, 0.06 mmol) was dissolved in 2 ml of dry THF. Palladium acetate (14.2 mg, 0.063 mmol) was dissolved in THF and added to the reaction vessel and it was allowed to stir at 40 °C for 3 h. The reaction was followed by UV-Vis spectroscopy. The solution turned from green to bluish green as the complex formed. After evaporation of solvent, the residue was dissolved in methanol and purified via sephedex LH-20 chromatography with the same mobile phase to afford palladium 15^2-monolysine chlorin e_6 trimethyl ester (**28a**, $C_{40}H_{43}N_5O_9Pd$, 50 mg, 0.059 mmol, 98%); UV-Vis (acetone-d_6): λmax (ε/$M^{-1}cm^{-1}$) 619 (31,200), 579 (6,200), 489 (4,000), 393 (44,200); ^{1}H NMR (acetone-d_6, 400 MHz) δ 9.53 (s, 1H), 9.54 (s, 1H), 8.93 (s, 1H), 8.03 (dd, *J* = 17.82, 11.54 Hz, 1H), 6.17 (d, *J* = 17.79 Hz, 1H), 6.00 (dd, *J* = 11.61, 1H), 5.19 (d, *J* = 18.77 Hz, 1H), 5.04 (d, *J* = 18.59 Hz, 1H), 4.92 (m, 1H), 4.63 (m, 2H), 4.20 (s, 3H), 3.62 (s, 3H), 3.57 (m, 2H), 3.57 (s, 3H), 3.37 (s, 3H), 3.07 (m, 3H), 2.68 (m, 2H) 2.38 (m, 1H) 2.12 (m, 1H), 1.78 (m, 2H), 1.74 (d, *J* = 7.3 Hz, 3H), 1.50 (t, *J* = 7.7 Hz, 3H). MS (MALDI-TOF) *m/z* 845 $[M+H]^+$, calcd. for $C_{40}H_{44}N_5O_9Pd$ 845.217.

15^2-Monolysine(boc)chlorin e_6 trimethyl ester (**26b**):

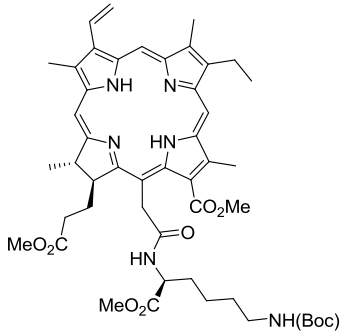

Chlorin e_6 (**2**, 75 mg, 0.12 mmol) was dissolved in dry CH_2Cl_2 (10 ml). DCC (31.3 mg, 0.15 mmol) and DMAP (11 mg, 0.09 mmol) were added and the mixture was allowed to stir until completely dissolved. After 3 h, H-lysine(boc)-OMe hydrochloride (45 mg, 0.15 mmol) and DIEA (0.03 ml, 0.17 mmol) were mixed in CH_2Cl_2 (2 ml) and added to the reaction mixture. The reaction was allowed to stir overnight. The mixture was diluted with CH_2Cl_2 and then washed with 5% aqueous citric acid, followed by a wash with brine and water. It was dried over anhydrous Na_2SO_4 and then evaporated. Then it was dissolved in CH_2Cl_2 and treated with excess ethereal diazomethane. The residue was dissolved in 12% acetone/CH_2Cl_2 and purified via silica gel column chromatography with the same mobile phase to afford 15^2-monolysine(boc)chlorin e_6 trimethyl ester (**26b**, $C_{48}H_{62}N_6O_9$, 84 mg, 0.097 mmol, 77%); ^{1}H NMR (acetone-d_6, 400 MHz) δ 9.77 (s, 1H), 9.55 (s, 1H), 9.04 (s, 1H), 8.08 (dd, *J* = 17.87, 11.58 Hz, 1H), 7.07 (m, 1H), 6.31 (dd, *J* = 17.87, 1.33 Hz, 1H), 6.06 (dd, *J* = 11.61, 1.36 Hz, 1H), 5.87 (s, 1H), 5.32 (s, 2H), 4.65 (q, *J* = 7.22 Hz, 1H), 4.60 (dd, *J* = 10.34, 1.95 Hz, 1H), 4.49 (m, 1H), 4.26 (s, 3H), 3.71 (q, *J* =7.67, 2H) 3.57 (s, 3H), 3.54 (s, 3H), 3.47 (s, 3H) 3.44 (s, 3H), 3.19 (3H, s), 2.97 (m, 2H), 2.71 (m, 1H), 2.37 (m, 2H), 1.80 (m, 3H), 1.77 (d, *J* = 7.24, 3H), 1.66 (t, *J* = 7.58, 3H), 1.39 (s, 9H), 1.27 (m, 2H), - 1.35 (s, 1H), -1.56 (s, 1H); MS (MALDI-TOF) *m/z* 867 $[M+H]^+$, calcd. for $C_{48}H_{63}N_6O_9$ 867.450.

15^2-Monolysinechlorin e_6 trimethyl ester (**27b**):

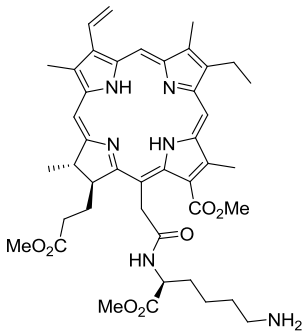

15^2-Monolysine(boc)chlorin e_6 trimethyl ester (**26b**, 84 mg 0.097 mmol) was dissolved in dry CH_2Cl_2 (3 ml) in an ice bath under argon. Thioanisole (0.01 ml) and TFA (1 ml) were added and the reaction mixture was allowed to stir overnight. The reaction mixture was rotavaporated several times with diethyl ether to remove TFA. The resulting precipitate was washed several times with diethyl ether to remove thioanisole. Then the precipitate was dissolved in CH_2Cl_2 and washed three times with H_2O and once with 10% $NaHCO_3$ to remove TFA. The organic layer was dried over anhydrous Na_2SO_4. Solvent was evaporated to obtain 15^2-monolysinechlorin e_6 trimethyl ester (**27b**, $C_{43}H_{54}N_6O_7$, 56 mg, 0.071 mmol, 73%); UV-Vis (acetone) λ_{max} ($\varepsilon/M^{-1}cm^{-1}$) 664 (57,800), 608 (4,600), 529 (4,900), 500 (14,800), 400 (187,200); ^{1}H NMR (acetone d_6, 400 MHz) δ 9.68 (s, 1H), 9.42 (s, 1H), 9.02 (s, 1H), 7.95 (dd, *J* = 17.87, 11.58 Hz, 1H), 7.12 (d, *J* = 6.8 Hz, 1H), 6.20 (dd, *J* = 17.87, 1.33 Hz, 1H), 5.95 (dd, *J* = 11.61, 1.36 Hz, 1H), 5.35 (s, 2H), 4.65 (q, *J* = 7.22 Hz, 1H), 4.61 (dd, *J* = 10.34, 1.95 Hz, 1H), 4.53 (m, 1H), 4.27 (s, 3H), 3.59 (m, 2H) 3.55 (s, 6H), 3.48 (s, 3H) 3.37 (s, 3H), 3.09 (3H, s), 2.99 (m, 3H), 2.73 (m, 1H), 2.38 (m, 2H), 1.80 (m, 3H), 1.78 (d, *J* = 7.24, 3H), 1.61 (t, *J* = 7.58, 3H), 1.43 (m, 2H), - 1.40 (s, 1H), -1.57 (s, 1H); ^{13}C NMR (dichloromethane-d_2, 100 MHz) δ 173.0, 172.7, 170.7, 170.0, 168.2, 167.8, 155.5, 149.5, 145.7, 140.2, 136.9, 136.8, 136.0, 135.5, 135.4, 131.5, 129.7, 129.6, 124.3, 122.2, 102.8, 102.5, 99.2, 94.4, 53.3, 52.4, 52.3, 52.0, 49.7, 40.8, 40.2, 34.4, 32.5, 31.4, 29.8, 28.2, 23.3, 22.5, 20.0, 18.0, 12.5, 12.4, 11.5; MS (MALDI-TOF) *m/z* 767 $[M+H]^+$, calcd. for $C_{43}H_{55}N_6O_7$ 767.413.

Palladium 15^2-monolysinechlorin e_6 trimethyl ester (**28b**):

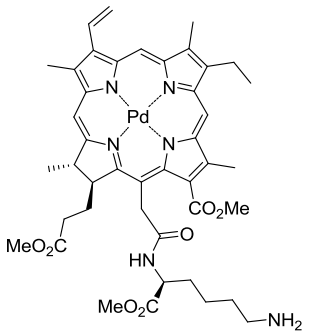

15^2-Monoysinechlorin e_6 trimethyl ester (**27b**, 56 mg, 0.071 mmol) was dissolved in 5 ml of dry THF. Palladium acetate (16.13 mg, 0.072 mmol) was dissolved in THF and added to the reaction vessel and allowed to stir at 60 °C for 3 h. The reaction was followed by UV-Vis spectroscopy. The solution turned from green to bluish green as the complex formed. After evaporation of solvent, the residue was dissolved in methanol and purified via Sephadex LH-20 chromatography with the same mobile phase to afford palladium 15^2-monolysinechlorin e_6 trimethyl ester (**28b**, $C_{43}H_{52}N_6O_7Pd$, 61 mg, 0.07 mmol, 99%); UV-Vis (acetone): λ_{max} ($\varepsilon/M^{-1}cm^{-1}$) 620 (97,520), 581 (14,500), 490 (7,600), 394 (140,900); ^1H NMR (acetone d_6, 400 MHz) all the peaks were broad due to the paramagnetic nature of the compound. MS (MALDI-TOF) *m/z* 871 $[M+H]^+$, calcd. for $C_{43}H_{53}N_6O_7Pd$ 871.301.

13^1-Aspartylchlorin e_6 di(*tert*)butyl dimethyl ester (**30**):

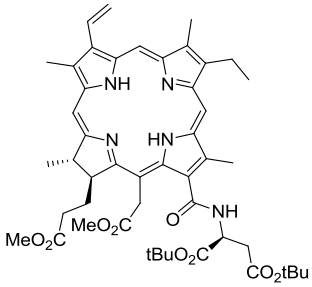

Chlorin e_6 dimethyl ester (**29**, 55 mg, 0.088 mmol) was dissolved in dry CH_2Cl_2. A mixture of HOBt (12 mg, 0.089 mmol), TBTU (29 mg, 0.089 mmol) and DIEA (0.017 ml, 0.1 mmol) in DMF (3 ml) was added and the mixture was allowed to stir for 30 min. H-Asp(tBu)$_2$.HCl (60 mg, 0.21 mmol) and DIEA (0.037 ml,

0.21 mmol) were mixed in CH_2Cl_2 and added to this reaction mixture. The mixture was stirred overnight. It was diluted with CH_2Cl_2 and then washed with 5% aqueous citric acid, followed by a wash with brine and water. It was dried over anhydrous Na_2SO_4 and then evaporated. The residue was dissolved in 5% acetone/CH_2Cl_2 and purified via silica gel column chromatography using the same mobile phase to afford 13^1-aspartylchlorin e_6 di(*tert*)butyl dimethyl ester (**30**, $C_{48}H_{61}N_5O_9$, 50 mg, 0.058 mmol, 66%); UV-Vis (acetone): λ_{max} ($\varepsilon/M^{-1}cm^{-1}$) 663 nm (0.330), 607 (0.025), 528 (0.020), 500 (0.081), 399 (1.000); ^{1}H NMR (acetone-d_6, 400 MHz) δ 9.79 (s, 1H), 9.70 (s, 1H), 9.10 (s, 1H), 8.39 (d, *J* = 7.93 Hz, 1H), 8.19 (dd, *J* = 11.58, 17.85 Hz, 1H), 6.37 (dd, *J* = 17.85, 1.23 Hz, 1H), 6.10 (dd, *J* = 11.87, 1.26 Hz, 1H), 5.71 (d, *J* = 18.95 Hz, 1H), 5.30 (m, 2H), 4.67 (q, *J* = 7.22 Hz, 1H), 4.49 (dd, *J* = 10.34, 1.95 Hz, 1H), 3.76 (q, *J* = 7.3 Hz, 2H), 3.74 (s, 3H), 3.64 (s, 3H), 3.61 (s, 3H), 3.50 (s, 3H), 3.27 (s, 3H), 3.16 (dd, J = 5.8, 0.78 Hz, 2H), 2.73 (m, 1H), 2.32 (m, 2H), 1.79 (m, 1H), 1.69 (m, 6H), 1.64 (s, 9H), 1.53 (s, 9H), -1.57 (s, 1H), -1.85 (s, 1H); MS (MALDI-TOF) *m/z* 852 $[M+H]^+$, calcd. for $C_{48}H_{62}N_5O_9$ 852.454.

13^1-Aspartylchlorin e_6 dimethyl ester (**7**):

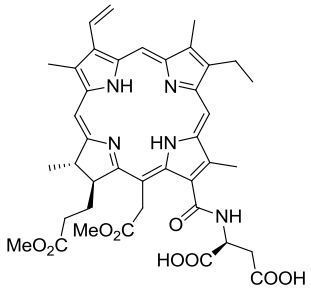

The 13^1-aspartylchlorin e_6 di(*tert*)butyl dimethyl ester (**30**, 50 mg, 0.058 mmol) was dissolved in 2 ml of dry CH_2Cl_2 in an ice bath under argon. Thioanisole (0.005 ml) and 2 ml of TFA were added and the reaction mixture was stirred overnight. The reaction mixture was evaporated several times with diethyl ether to remove residual TFA. The resulting precipitate was washed several times with diethyl ether to remove thioanisole. Then the precipitate was dissolved in CH_2Cl_2 and washed three times with H_2O and once with 10% $NaHCO_3$ to remove TFA. The organic layer was dried over anhydrous Na_2SO_4 and then

evaporated to afford 13[1]-aspartylchlorin e_6 dimethyl ester (**7**, $C_{40}H_{45}N_5O_9$, 38 mg, 0.051 mmol, 88%); UV-Vis (acetone): λ_{max} ($\varepsilon/M^{-1}cm^{-1}$) 663 nm (126,800), 607 (9,000), 528 (7,450), 500 (31,500), 399 (385,800); ^{1}H NMR (acetone-d_6, 400 MHz) δ 9.79 (s, 1H), 9.70 (s, 1H), 9.12 (s, 1H), 8.50 (d, *J* = 7.93 Hz, 1H), 8.19 (dd, *J* = 11.58, 17.85 Hz, 1H), 6.37 (d, *J* = 18.85 Hz, 1H), 6.10 (d, *J* = 11.87 Hz, 1H), 5.71 (d, *J* = 18.95 Hz, 1H), 5.45 (dd, *J* = 13.76, 5.80 Hz, 1H), 5.30 (d, *J* = 18.93 Hz, 1H), 4.67 (q, *J* = 7.22 Hz, 1H), 4.50 (dd, *J* = 10.34, 1.95 Hz, 1H), 3.76 (q, *J* = 7.3 Hz, 2H), 3.71 (s, 3H), 3.63 (s, 3H), 3.60 (s, 3H), 3.51 (s, 3H), 3.31 (dd, J = 5.76, 3.47 Hz, 2H), 3.26 (s, 3H), 2.70 (m, 2H), 2.31 (m, 2H), 1.79 (m, 1H), 1.71 (d, *J* = 7.24, 3H), 1.67 (t, *J* = 7.58, 3H), -1.57 (br s, 1H), -1.87 (s, 1H). ^{13}C NMR (acetone-d_6, 100 MHz) δ 174.0, 173.8, 172.6, 170.3, 169.1, 168.9, 154.5, 149.9, 145.4, 139.2, 137.0, 136.6, 136.4, 135.1, 131.0, 130.7, 130.3, 129.7, 122.0, 104.2, 101.8, 99.4, 95.0, 54.1, 52.3, 51.8, 50.4, 49.7, 43.2, 38.4, 36.6, 31.7, 30.7, 23.5, 20.0, 18.1, 12.3, 12.0, 11.3; HRMS (MALDI-TOF) *m/z* 740.344 $[M+H]^+$, Calcd. for $C_{40}H_{46}N_5O_9$ 740.330.

Chlorin e_6 dimethyl ester (**29**):

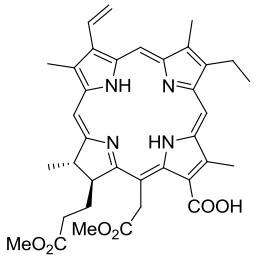

Chlorin e_6 (**2**, 50 mg, 0.083 mmol) was dissolved in 5% sulfuric acid and methanol (10 ml) and allowed to stir overnight protected from light, under argon. The reaction mixture was dilute with CH_2Cl_2 and poured into cold 5% aqueous $NaHCO_3$ (This may form a precipitate. If so, the organic layer is washed with citric acid until the precipitate dissolves in the organic layer). The organic layer was washed with water and brine, dried over anhydrous Na_2SO_4 and filtered. Solvent was removed to afford chlorin e_6 dimethyl ester ($C_{36}H_{40}N_4O_6$, 51 mg, 0.082 mmol, 99%); UV-Vis (chloroform): λ_{max} ($\varepsilon/M^{-1}cm^{-1}$) 666 nm (49,700), 610 (5,900), 562 (2,700), 523 (5,900), 502 (13,200) 402 (143,400); ^{1}H NMR (acetone-d_6, 400 MHz): δ 9.56 (s, 1H), 9.23 (s, 1H), 8.96(s, 1H), 7.75 (dd, *J* = 17.86, 11.61 Hz, 1H), 6.03 (dd, *J* = 17.85, 1.26 Hz, 1H), 5.80 (dd,

J = 11.57, 1.37 Hz, 1H), 5.64 (d, *J* = 18.91 Hz, 1H), 5.45 (d, *J* = 18.91 Hz, 1H), 4.62 (q, *J* = 7.32 Hz, 1H), 4.52 (dd, *J* = 10.50, 2.21 Hz, 1H), 3.81 (s, 3H), 3.61 (s, 6H), 3.40 (q, *J* = 7.5 Hz, 2H), 3.26 (s, 3H), 2.93 (s, 3H), 2.72 (m, 1H), 2.35 (m, 1H), 2.26 (m, 1H), 2.06 (m, 1H), 1.75 (d, *J* = 7.5 Hz, 3H), 1.53 (t, *J* = 7.5 Hz, 3H), -1.6 (s, 2H); MS (MALDI-TOF) *m/z* 625 $[M+H]^+$, calcd. for $C_{36}H_{41}N_4O_6$ 625.302.

13^1- β-Alanylchlorin e_6 (*tert)*butyl dimethyl ester (**31**):

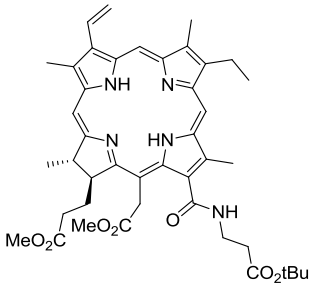

Chlorin e_6 dimethyl ester (**29**, 55 mg, 0.088 mmol) was dissolved in dry CH_2Cl_2. A mixture of HOBt (12 mg, 0.088 mmol), TBTU (29 mg, 0.089 mmol) and DIEA (0.017 ml, 0.10 mmol) in DMF (2 ml) was added and the mixture was stirred for 30 min. β-Alanine(tBu).HCl (18 mg, 0.1 mmol) and DIEA (0.017 ml, 0.1 mmol) were mixed in CH_2Cl_2 and added to the reaction mixture. The mixture was then allowed to stir overnight before being diluted with CH_2Cl_2 and then washed with 5% aqueous citric acid, followed by a wash with brine and water. It was dried over anhydrous Na_2SO_4 and then evaporated to dryness. The residue was dissolved in 5% acetone/CH_2Cl_2 and purified via silica gel column chromatography using the same mobile phase to afford 13^1-β-alanylchlorin e_6 (*tert)*butyl dimethyl ester (**31**, $C_{43}H_{53}N_5O_7$, 45 mg, 0.06 mmol, 68%); ^{1}H NMR (acetone-d_6, 400 MHz) δ 9.70 (s, 1H), 9.63 (s, 1H), 9.01 (s, 1H), 8.17 (t, *J* = 5.71 Hz, 1H), 8.11 (dd, *J* = 11.58, 17.85 Hz, 1H), 6.31 (d, *J* = 18.85 Hz, 1H), 6.04 (d, *J* = 11.87 Hz, 1H), 5.65 (d, *J* = 18.95 Hz, 1H), 5.38 (d, *J* = 19.06 Hz, 1H), 4.66 (q, *J* = 7.22 Hz, 1H), 4.52 (dd, *J* = 10.34, 1.95 Hz, 1H), 4.02 (m, 1H), 3.09 (m, 1H), 3.77 (s, 3H), 3.68 (q, *J* = 7.3 Hz, 2H), 3.61 (s, 3H), 3.51 (s, 3H), 3.46 (s, 3H), 3.21 (s, 3H), 2.71 (m, 2H), 2.31 (m, 2H), 1.79 (m, 1H), 1.72 (d, *J* = 7.24, 3H), 1.65 (t, *J* = 7.58, 3H), 1.54 (s, 9H), -1.62 (s, 1H), -1.91 (s, 1H); MS (MALDI-TOF) *m/z* 752 $[M+H]^+$, calcd. for $C_{43}H_{54}N_5O_7$ 752.402.

13^1-β-Alanylchlorin e_6 dimethyl ester (**32**):

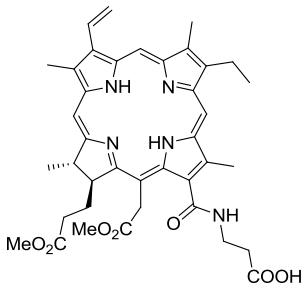

The 13^1- β-alanylchlorin e_6 (*tert*)butyl dimethyl ester (**31**, 45 mg, 0.059 mmol) was dissolved in 1.5 ml of dry CH_2Cl_2 in a ice bath under argon. Thioanisole (0.005 ml) and 1.5 ml of TFA were added and the reaction mixture was stirred overnight before being diluted with CH_2Cl_2 and washed three times with H_2O and once with 10% $NaHCO_3$. The organic layer was dried over anhydrous Na_2SO_4 and the solvent was evaporated to obtain 13^1-β-alanylchlorin e_6 dimethyl ester (**32**, $C_{39}H_{45}N_5O_7$, 39 mg, 0.056 mmol, 95%); ^{1}H NMR (acetone-d_6, 400 MHz) δ 9.74 (s, 1H), 9.72 (s, 1H), 9.10 (s, 1H), 8.22 (dd, *J* = 11.58, 17.85 Hz, 1H), 8.15 (t, *J* = 5.71 Hz, 1H), 6.39 (d, *J* = 18.85 Hz, 1H), 6.12 (d, *J* = 11.87 Hz, 1H), 5.65 (d, *J* = 18.95 Hz, 1H), 5.37 (d, *J* = 19.06 Hz, 1H), 4.66 (q, *J* = 7.22 Hz, 1H), 4.52 (dd, *J* = 10.34, 1.95 Hz, 1H), 4.07 (m, 1H), 3.95 (m, 1H), 3.77 (s, 3H), 3.68 (q, *J* = 7.3 Hz, 2H), 3.61 (s, 3H), 3.53 (s, 3H), 3.52 (s, 3H), 3.28 (s, 3H), 2.69 (m, 2H), 2.31 (m, 2H), 1.79 (m, 1H), 1.72 (d, *J* = 7.24, 3H), 1.65 (t, *J* = 7.58, 3H), -1.62 (s, 1H), -1.91 (s, 1H); MS (MALDI-TOF) *m/z* 696 $[M+H]^+$, calcd. for $C_{39}H_{46}N_5O_7$ 696.811.

13^1- β-Alanyl-aspartylchlorin e_6 di(*tert*)butyl dimethyl ester (**33**):

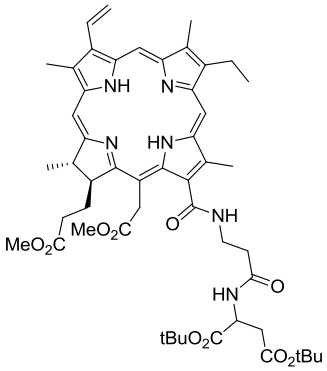

13^1-β-Alanylchlorin e_6 dimethyl ester (**32**, 39 mg, 0.056 mmol) was dissolved in dry CH_2Cl_2. A mixture of HOBt (8 mg, 0.06 mmol), TBTU (18 mg, 0.06 mmol) and DIEA (0.017 ml, 0.1 mmol) in DMF (2 ml) was

added and the mixture was stirred for 30 min. H-Asp(tBu)$_2$.HCl (40 mg, 0.14 mmol) and DIEA (0.025 ml, 0.14 mmol) were mixed in CH_2Cl_2 and added to the reaction mixture. The mixture was stirred overnight before being diluted with CH_2Cl_2 (10 ml) and then washed with 5% aqueous citric acid, followed by a wash with brine and water. It was dried over anhydrous Na_2SO_4 and then evaporated. The residue was dissolved in 10% acetone/CH_2Cl_2 and purified via silica gel column chromatography using the same mobile phase to afford 13^1- β-alanyl-aspartylchlorin e$_6$ di(*tert*)butyl dimethyl ester(**33**, $C_{51}H_{66}N_6O_{10}$, 45 mg, 0.048 mmol, 87%); ^{1}H NMR (acetone-d_6, 400 MHz) δ 9.74 (s, 1H), 9.70 (s, 1H), 9.10 (s, 1H), 8.19 (dd, *J* = 11.58, 17.85 Hz, 1H), 8.11 (t, *J* = 5.66 Hz, 1H), 7.64 (d, *J* = 8.11 Hz, 1H), 6.37 (d, *J* = 19.18 Hz, 1H), 6.10 (d, *J* = 12.94 Hz, 1H), 5.66 (d, *J* = 19.03 Hz, 1H), 5.38 (d, *J* = 19.09 Hz, 1H), 4.77 (dt, *J* = 8.14, 5.74 Hz, 1H), 4.66 (q, *J* = 7.22 Hz, 1H), 4.52 (dd, *J* = 10.34, 1.95 Hz, 1H), 4.07 (m, 1H), 3.95 (m, 1H), 3.75 (s, 3H), 3.76 (q, *J* = 7.3 Hz, 2H), 3.60 (s, 3H), 3.53 (s, 3H), 3.50 (s, 3H), 3.27 (s, 3H), 2.80 (d, *J* = 2.57 Hz, 1H), 2.79 (d, *J* = 3.06 Hz, 1H), 2.31 (m, 2H), 1.79 (m, 1H), 1.71 (d, *J* = 7.24, 3H), 1.68 (t, *J* = 7.58, 3H), 1.43 (s, 9H), 1.42 (s, 9H), -1.61 (s, 1H), -1.91 (s, 1H). MS (MALDI-TOF) *m/z* 923 $[M+H]^+$, calcd. for $C_{51}H_{67}N_6O_{10}$ 923.491.

13^1- β-Alanyl-aspartylchlorin e$_6$ dimethyl ester (**34**):

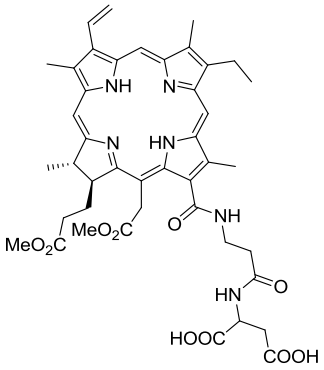

The 13^1- β-alanyl-aspartylchlorin e$_6$ di(*tert*)butyl dimethyl ester (**33**, 45 mg, 0.048 mmol) was dissolved in 2 ml of dry CH_2Cl_2 in an ice bath under argon. Thioanisole (0.004 ml) and 2 ml of TFA were added and the reaction mixture was stirred overnight before being evaporated several times with diethyl ether to remove residual TFA. The resulting precipitate was washed several times with diethyl ether to remove

more residual thioanisole. The precipitate was dissolved in CH_2Cl_2 and washed three times with H_2O and once with 10% $NaHCO_3$ to remove TFA. The organic layer was dried over anhydrous Na_2SO_4 and the solvent was evaporated to obtain 13^1- β-alanyl-aspartylchlorin e_6 dimethyl ester (**34**, $C_{43}H_{50}N_6O_{10}$, 38 mg, 0.046 mmol, 97%); UV-Vis (acetone): λ_{max} ($\varepsilon/M^{-1}cm^{-1}$) 663 (77,100), 607 (3,600), 528 (1,800), 500 (17,200), 399 (237,100); ^{1}H NMR (acetone-d_6, 400 MHz) δ 9.72 (s, 1H), 9.70 (s, 1H), 9.10 (s, 1H), 8.20 (dd, *J* = 11.58, 17.85 Hz, 1H), 8.11 (br t, *J* = 5.66 Hz, 1H), 7.64 (br d, *J* = 8.11 Hz, 1H), 6.32 (d, *J* = 19.18 Hz, 1H), 6.10 (d, *J* = 12.94 Hz, 1H), 5.63 (d, *J* = 19.03 Hz, 1H), 5.37 (d, *J* = 19.09 Hz, 1H), 4.92 (dt, *J* = 8.14, 5.74 Hz, 1H), 4.66 (q, *J* = 7.22 Hz, 1H), 4.51 (dd, *J* = 10.34, 1.95 Hz, 1H), 4.07 (m, 1H), 3.95 (m, 1H), 3.74 (s, 3H), 3.75 (q, *J* = 7.3 Hz, 2H), 3.60 (s, 3H), 3.51 (s, 3H), 3.50 (s, 3H), 3.25 (s, 3H), 2.96 (d, *J* = 5.27 Hz, 1H), 2.69 (d, *J* = 3.06 Hz, 1H), 2.31 (m, 2H), 1.79 (m, 1H), 1.71 (d, *J* = 7.24, 3H), 1.66 (t, *J* = 7.58, 3H), -1.61 (s, 1H), -1.91 (s, 1H). ^{13} C NMR (acetone-d_6, 100 MHz) δ 174.1, 173.9, 173.7, 173.4, 171.6, 170.5, 169.0, 168.4, 143.5, 139.8, 135.3, 134.8, 134.2, 130.7, 130.4, 129.5, 129.0, 128.7, 126.8, 125.2, 123.6, 122.3, 103.5, 100.5, 98.0, 95.0, 53.4, 52.5, 51.9, 49.4, 49.0, 38.8, 37.5, 36.6, 34.7, 31.2, 29.7, 23.3, 19.0, 17.0, 12.1, 11.5, 10.8; HRMS (MALDI-TOF) *m/z* 811.381 $[M+H]^+$, calcd. for $C_{43}H_{51}N_6O_{10}$ 811.367.

13^1-Ethylenediaminylchlorin e_6 dimethyl ester (**35**):

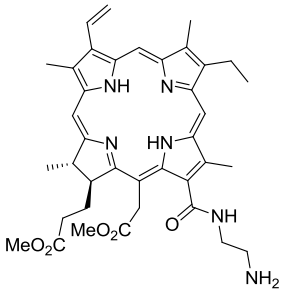

Methyl pheophorbide a (**3**, 100 mg, 0.164 mmol) was dissolved in dry $CHCl_3$ (5 ml) and stirred under argon for 10 min. Then ethylenediamine (0.2 ml, 3.0 mmol) was added to the solution and the mixture was stirred for 24 h. The reaction was monitored by spectrophotometry. The reaction mixture was evaporated and the residue was dissolved in 2.5% MeOH/CH_2Cl_2 and then chromatographed on a short

silica gel column using the same mobile phase to remove by-products, and then the product was eluted using 50% MeOH/CH_2Cl_2 to afford 13^1-ethylenediaminylchlorin e_6 dimethyl ester (**35**, $C_{38}H_{46}N_6O_5$, 100 mg, 0.150 mmol, 91%); ^{1}H NMR (acetone d_6, 400 MHz) δ 9.69 (s, 1H), 9.63 (s, 1H), 9.09 (s, 1H), 8.09 (dd, *J* = 17.78, 11.58 Hz, 1H), 8.07 (br s, 1H), 6.29 (d, *J* = 18.85 Hz, 1H), 6.02 (d, *J* = 11.87 Hz, 1H), 5.67 (d, *J* = 19.08 Hz, 1H), 5.39 (d, *J* = 19.11 Hz, 1H), 4.66 (q, *J* = 7.22 Hz, 1H), 4.51 (dd, *J* = 10.34, 1.95 Hz, 1H), 4.01 (m, 1H), 3.87 (m, 1H), 3.75 (s, 3H), 3.66 (q, *J* = 7.3 Hz, 2H), 3.61 (s, 3H), 3.50 (s, 3H), 3.45 (s, 3H), 3.20 (s, 3H), 2.71 (m, 1H), 2.31 (m, 2H), 1.95 (br m, 1H), 1.80 (m, 1H), 1.72 (d, *J* = 7.24, 3H), 1.64 (t, *J* = 7.58, 3H), -1.64 (s, 1H), -1.93 (s, 1H). ^{13}C NMR (acetone d_6, 100 MHz) δ 173.1, 173.0, 169.2, 168.3, 167.7, 153.6, 149.1, 144.4, 138.1, 136.0, 135.3, 134.7, 133.9, 130.1, 129.8, 129.3, 120.9, 103.2, 100.7, 98.4, 93.9, 53.1, 51.4, 50.8, 50.2, 48.8, 41.2, 37.2, 30.7, 29.6, 22.6, 19.0, 17.2, 11.3, 11.0, 10.3. HRMS (MALDI-TOF) *m/z* 667.395 $[M+H]^+$, calcd. for $C_{38}H_{47}N_6O_5$ 667.361.

13^1-Ethylenediaminyl(boc)lysyl(boc)chlorin e_6 dimethyl ester (**36**):

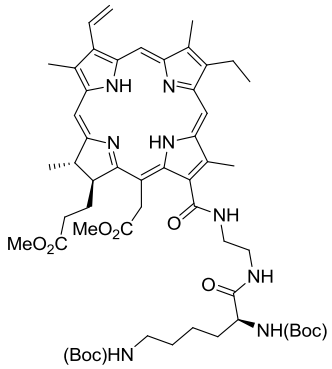

(boc)Lysine(boc)OH (55 mg, 0.082 mmol) was dissolved in dry CH_2Cl_2 (10 ml). A mixture of HOBt (15 mg, 0.11 mmol), TBTU (33 mg, 0.11 mmol) and DIEA (0.017 ml, 0.1 mmol) in DMF (3 ml) was added and then the mixture was stirred for 1 h. 13^1-Ethylenediaminylchlorin e_6 dimethyl ester (**35**, 50 mg, 0.075 mmol) was added to the reaction mixture, which was stirred overnight. The mixture was diluted with CH_2Cl_2 and then washed with 5% aqueous citric acid, followed by a wash with brine and water. It was dried over anhydrous Na_2SO_4 and then evaporated. The residue was dissolved in 2.5% MeOH/CH_2Cl_2 and

purified via silica gel column chromatography using the same mobile phase to afford 13^1-ethylenediaminyl(boc)lysyl(boc)chlorin e_6 dimethyl ester (**36**, $C_{54}H_{74}N_8O_{10}$, 65 mg, 0.065 mmol; 78%); ^{1}H NMR (acetone d_6, 400 MHz) δ 9.54 (s, 1H), 9.53 (s, 1H), 9.07 (s, 1H), 8.14 (br s, 1H) 7.94 (dd, *J* = 17.78, 11.58 Hz, 1H), 7.78 (br s, 1H), 6.18 (d, *J* = 18.85 Hz, 1H), 6.16 (br s, 1H), 5.93 (d, *J* = 11.87 Hz, 1H), 5.89 (br s, 1H), 5.63 (d, *J* = 19.08 Hz, 1H), 5.39 (d, *J* = 19.11 Hz, 1H), 4.67 (q, *J* = 7.22 Hz, 1H), 4.52 (dd, *J* = 10.34, 1.95 Hz, 1H), 4.17 (m, 1H), 3.85 (m, 1H), 3.75 (s, 3H), 3.66 (m, 3H), 3.61 (s, 3H), 3.52 (br q, *J* = 7.14 Hz, 2H), 3.41 (s, 3H), 3.39 (s, 3H), 3.11 (s, 3H), 3.00 (m, 2H), 2.71 (m, 1H), 2.32 (m, 2H), 1.95 (br m, 1H), 1.84 (m, 2H), 1.72 (d, *J* = 7.24, 3H), 1.67 (m, 1H), 1.59 (t, *J* = 7.58, 3H), 1.41 (m, 3H), 1.37 (s, 9H), 1.34 (s, 9H), -1.66 (s, 1H), -1.94 (s, 1H). MS (MALDI-TOF) *m/z* 995 $[M+H]^+$, calcd. for $C_{54}H_{75}N_8O_{10}$ 995.560.

13^1-Ethylenediaminyl-lysylchlorin e_6 dimethyl ester (**37**):

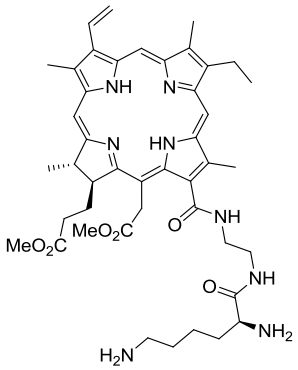

The 13^1-ethylenediaminyl(boc)lysyl(boc)chlorin e_6 dimethyl ester (**36**, 65 mg, 0.065 mmol) was dissolved in of dry CH_2Cl_2 (3 ml) in a ice bath under argon. Thioanisole (0.003 ml) and of TFA (2 ml) were added and the reaction mixture was stirred overnight. The reaction mixture was evaporated several times with diethyl ether to remove TFA. The resulting precipitate was washed several times with diethyl ether to remove thioanisole. Then the precipitate was dissolved in CH_2Cl_2 and washed three times with H_2O and once with 10% $NaHCO_3$ to remove TFA. The organic layer was dried over anhydrous Na_2SO_4 and the solvent was evaporated to afford 13^1-ethylenediaminyl-lysylchlorin e_6 dimethyl ester (**37**, $C_{44}H_{58}N_8O_6$, 42 mg, 0.052 mmol, 81%); UV-Vis (acetone): λ_{max} (ε/$M^{-1}cm^{-1}$) 663 nm (76,400), 607 (1,800), 527 (700), 500

(14,600), 399 (242,100); ^{1}H NMR (acetone d_6, 400 MHz) δ 9.76 (s, 1H), 9.69 (s, 1H), 9.10 (s, 1H), 8.29 (br s, 1H) 8.17 (dd, *J* = 17.78, 11.58 Hz, 1H), 7.86 (br s, 1H), 6.35 (d, *J* = 18.85 Hz, 1H), 6.07 (d, *J* = 11.87 Hz, 1H), 5.64 (d, *J* = 19.08 Hz, 1H), 5.40 (d, *J* = 19.11 Hz, 1H), 4.66 (q, *J* = 7.22 Hz, 1H), 4.52 (dd, *J* = 10.34, 1.95 Hz, 1H), 3.92 (m, 2H), 3.75 (br m, 5H), 3.74 (s, 3H), 3.60 (s, 3H), 3.53 (s, 3H), 3.49 (s, 3H), 3.26 (s, 3H), 2.96 (br t, 2H), 2.70 (m, 1H), 2.29 (m, 2H), 1.95 (br m, 1H), 1.84 (m, 2H), 1.72 (d, *J* = 7.24, 3H), 1.68 (t, *J* = 7.58, 3H), 1.45 (m, 2H), 1.31 (m, 2H) -1.60 (s, 1H), -1.89 (s, 1H). ^{13}C NMR (dichloromethane d_2, 100 MHz) δ 176.6, 174.2, 174.0, 169.9, 169.7, 167.7, 154.5, 149.5, 145.3, 139.3, 136.8, 135.4, 135.2, 134.9, 130.9, 130.2, 129.8, 129.7, 129.0, 122.2, 102.9, 101.8, 99.2, 94.4, 55.4, 52.6, 52.0, 49.7, 41.4, 41.1, 39.6, 38.2, 35.0, 31.5, 31.1, 30.2, 23.3, 23.0, 20.0, 18.0, 12.4, 12.2, 11.6, 11.5. HRMS (MALDI-TOF) *m/z* 795.492 $[M+H]^+$, calcd. for $C_{44}H_{59}N_8O_6$ 795.456.

2.8 Supporting information

^{1}H NMR spectrum of pheophorbide a (**17**) in acetone-d_6 at 400 MHz

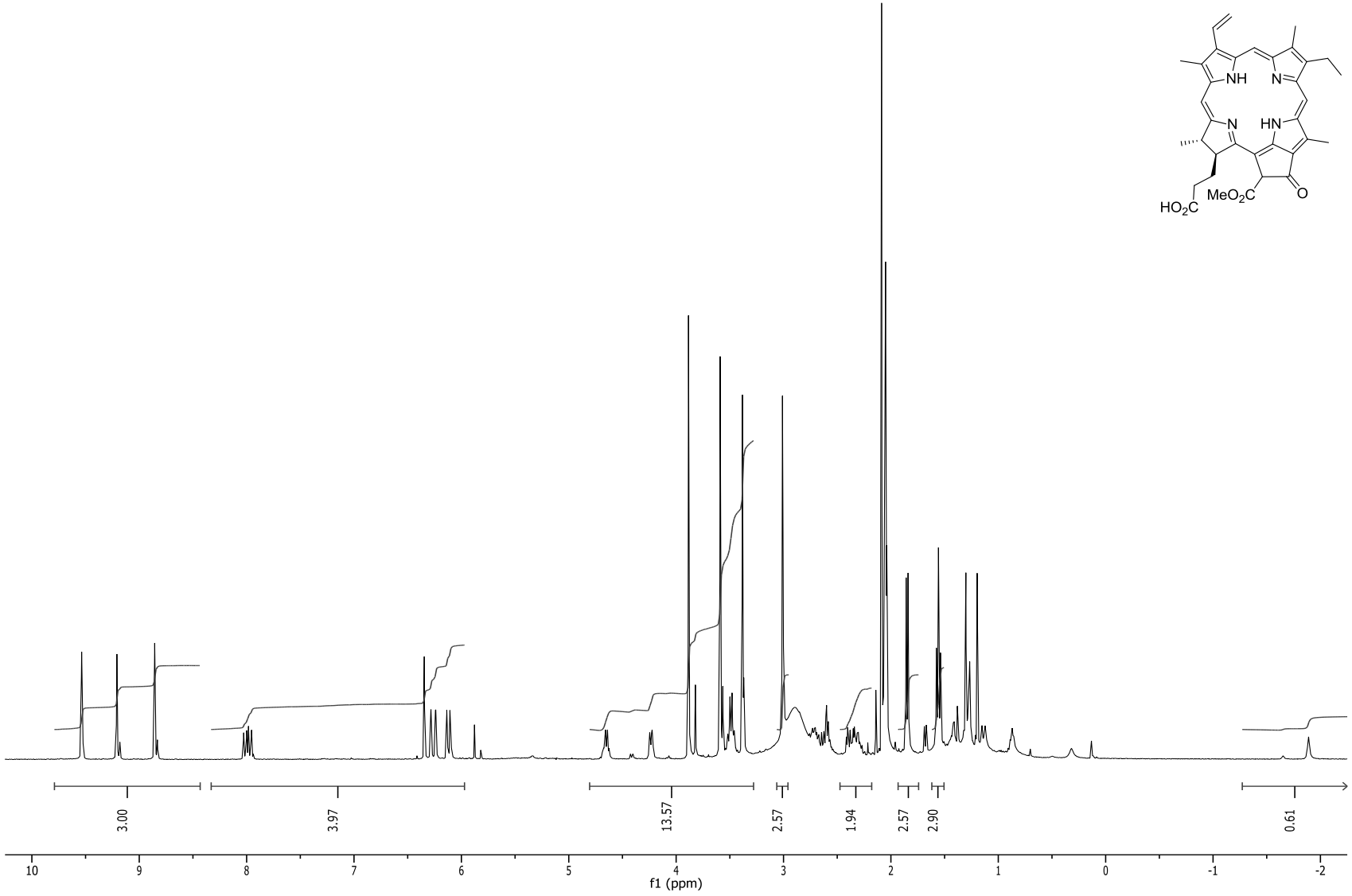

^{1}H NMR spectrum of Lys(Boc)OMe pheophorbide a **18** in acetone-d_6 at 400 MHz

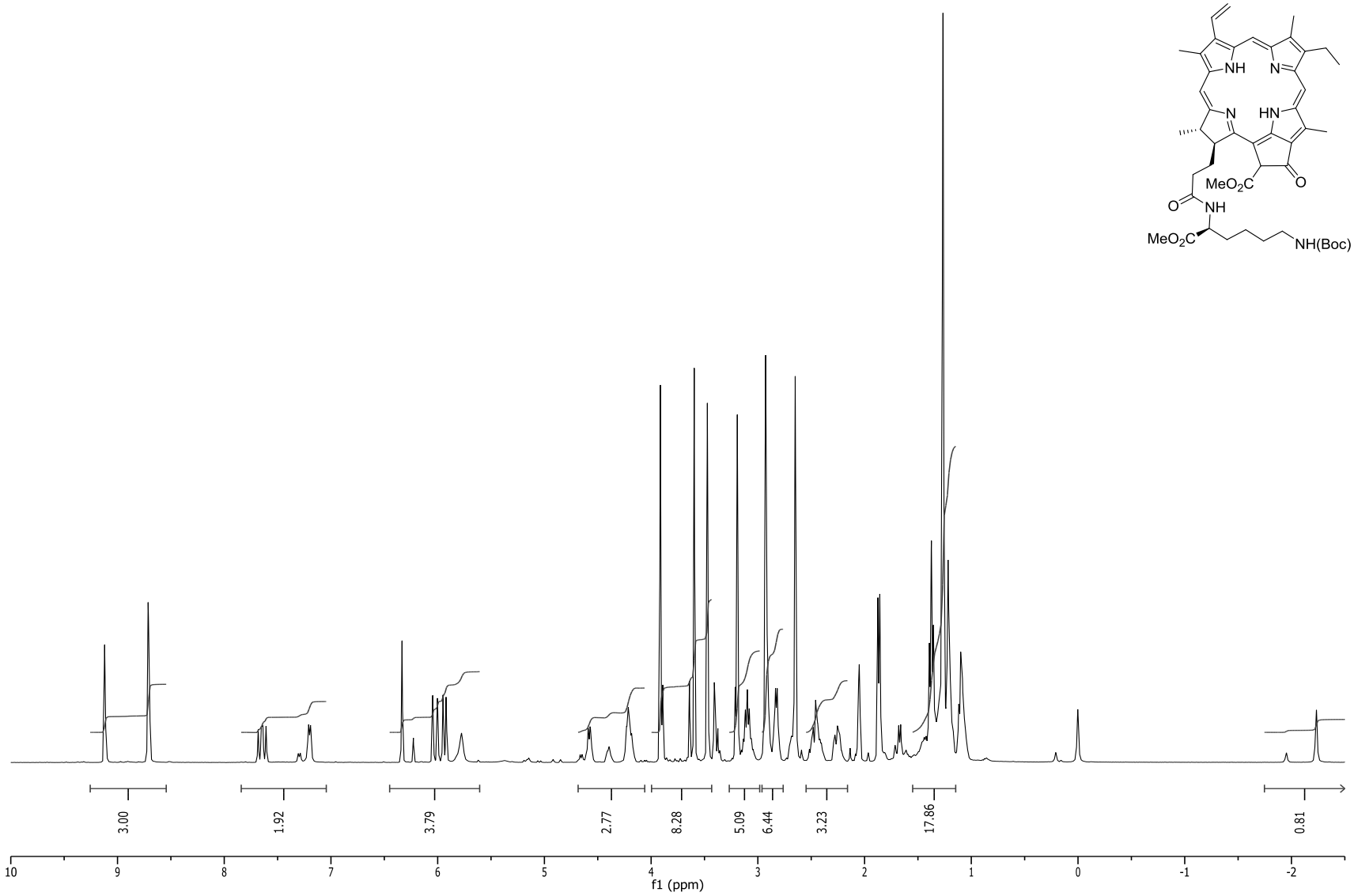

^{1}H NMR spectrum of 17^3-Lys(Boc)Ce$_6$ TME **19** in acetone-d_6 at 400 MHz

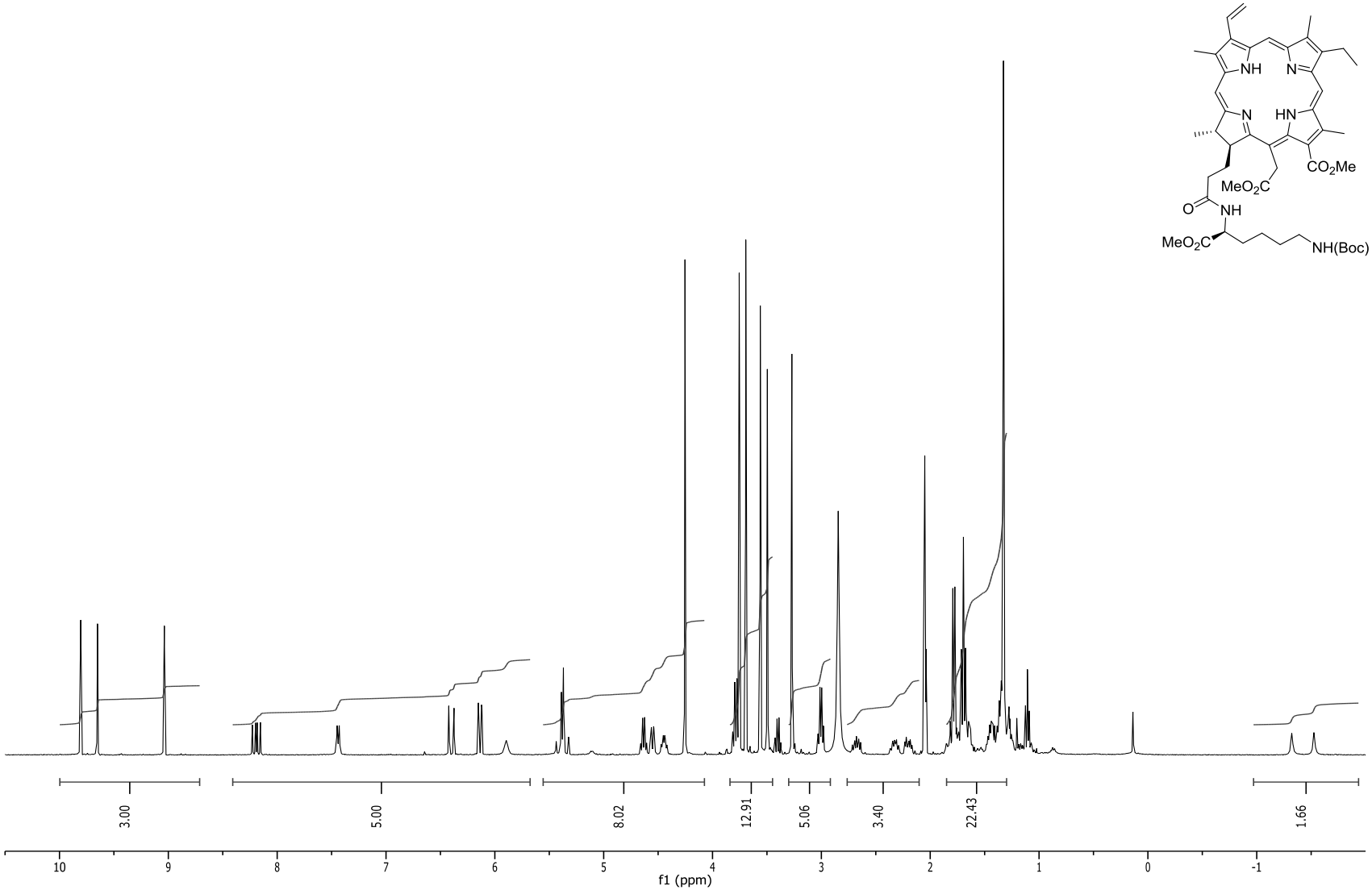

^{1}H NMR spectrum of 17^{3}-LysCe$_{6}$ TME **20** in acetone-d_6 at 400 MHz

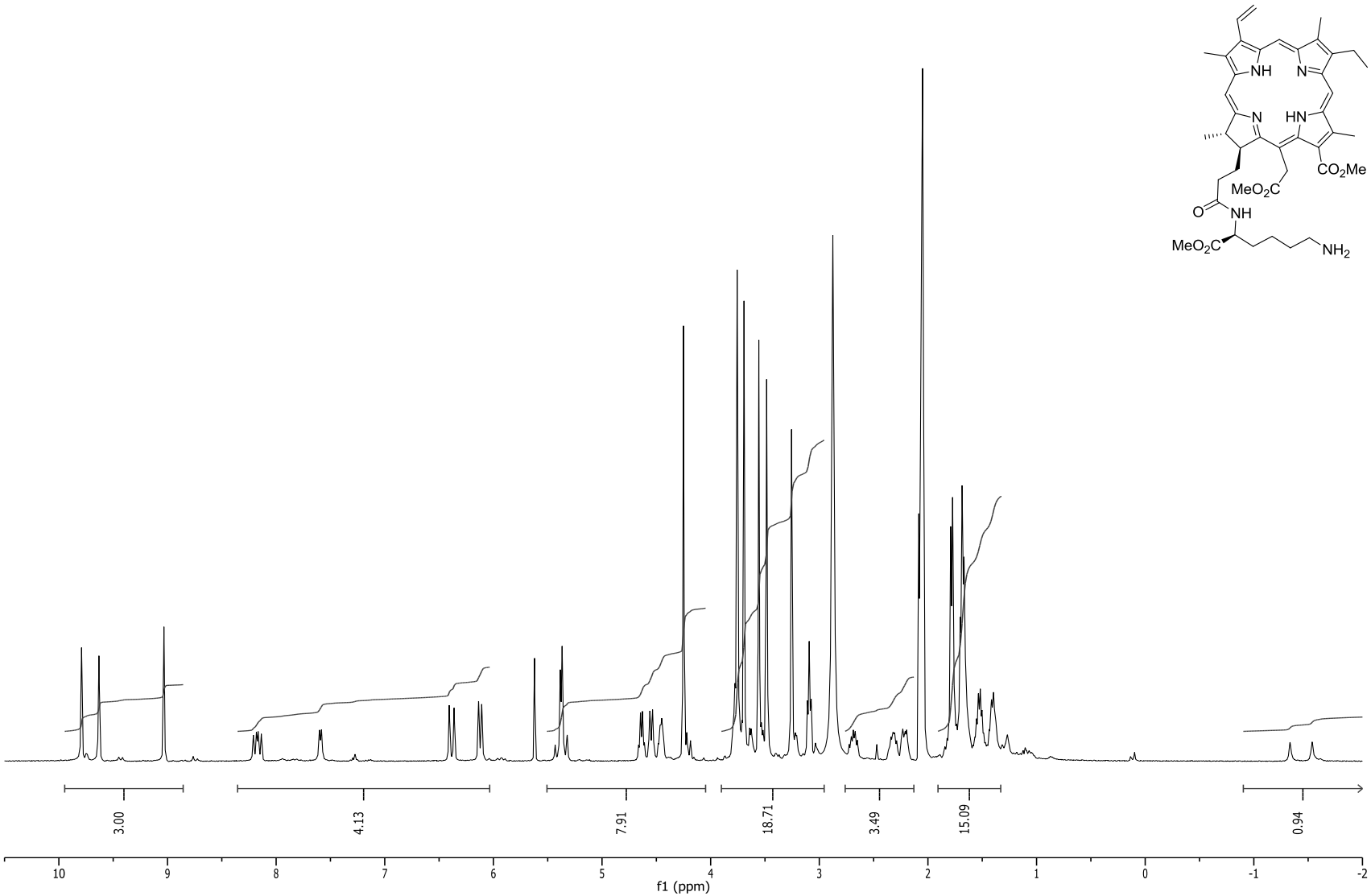

^{1}H NMR spectrum of methyl pheophorbide a (**3**) in acetone-d_6 at 400 Mhz

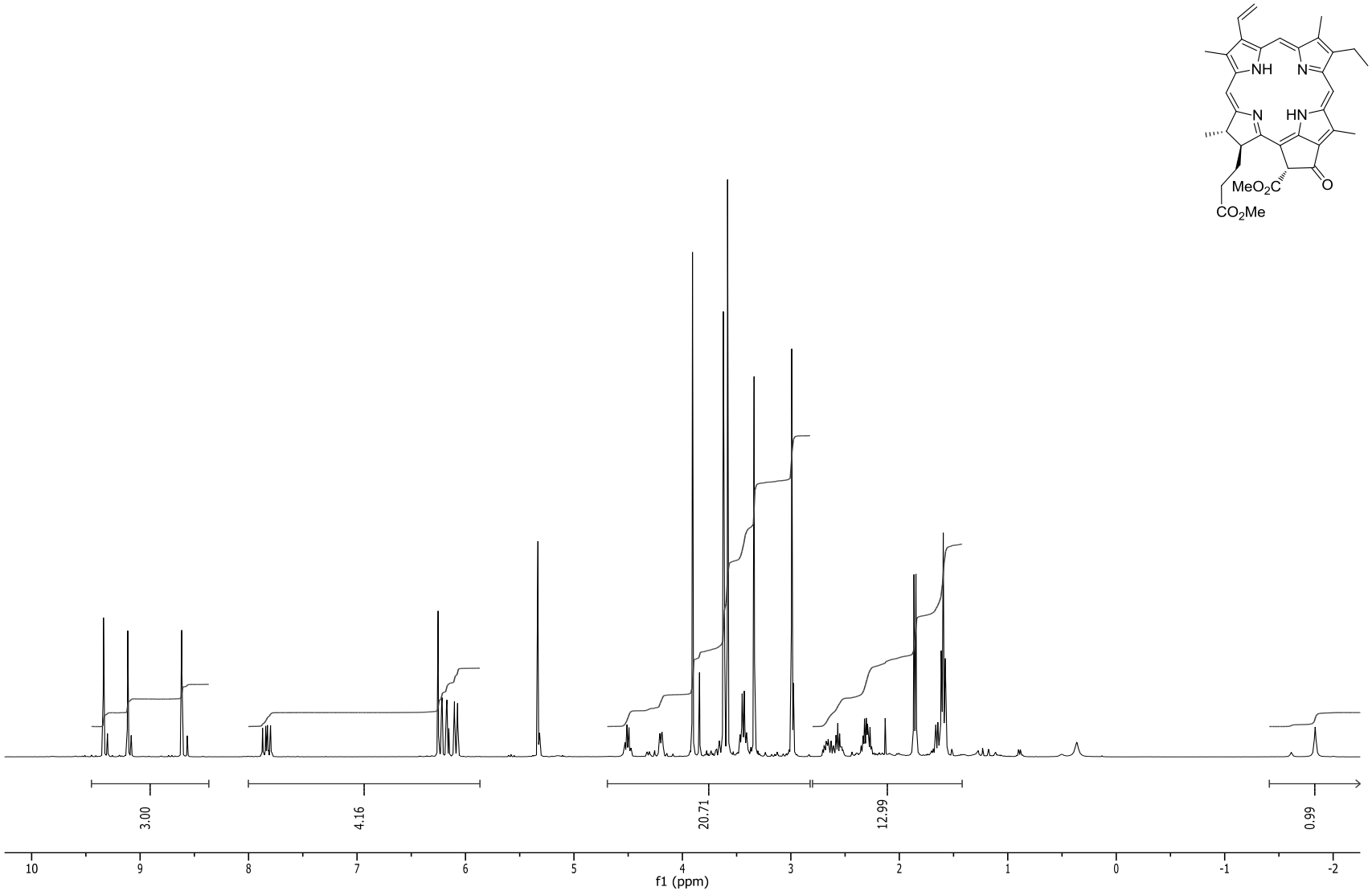

^{1}H NMR spectrum of Ce_6 TME (**24**) in acetone-d_6 at 400 MHz

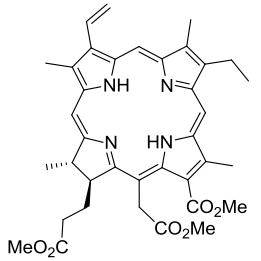

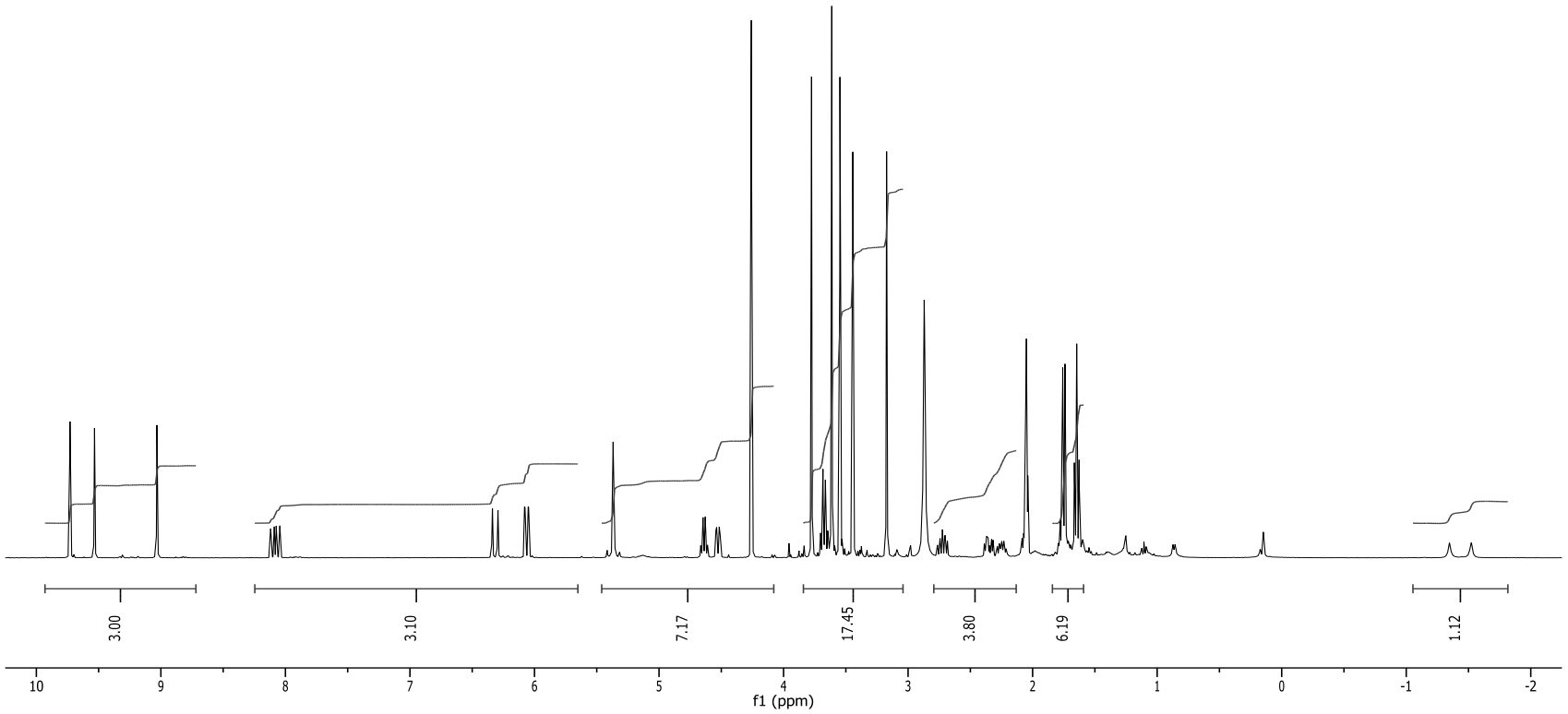

^{1}H NMR spectrum of Ce_6 (**2**) in dimethyl sulfoxide-d_6 at 400 MHz

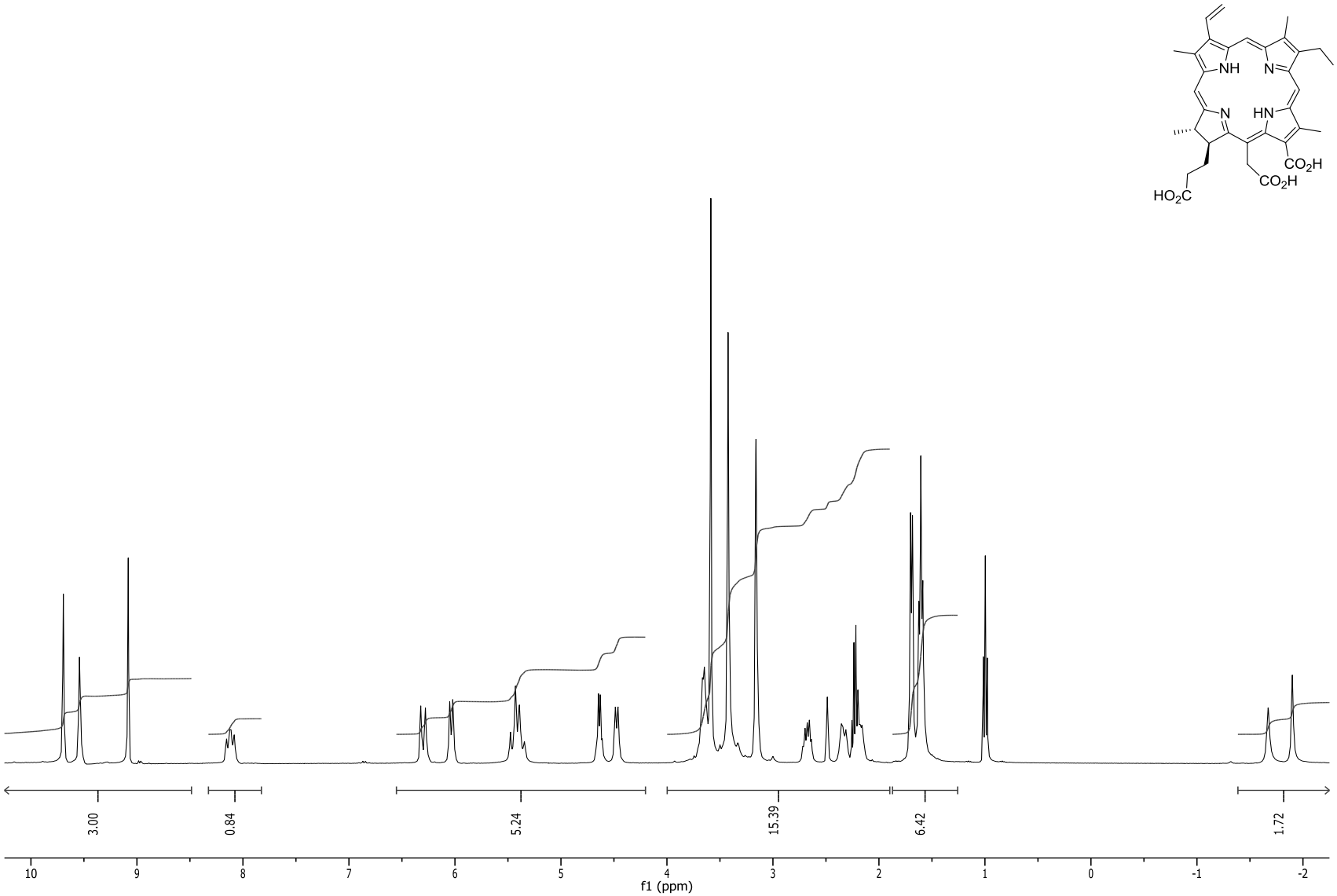

^{1}H NMR spectrum of 15^{2}-Aspdi(tBu)Ce$_{6}$ DME **26a** in acetone-d_6 at 400 MHz

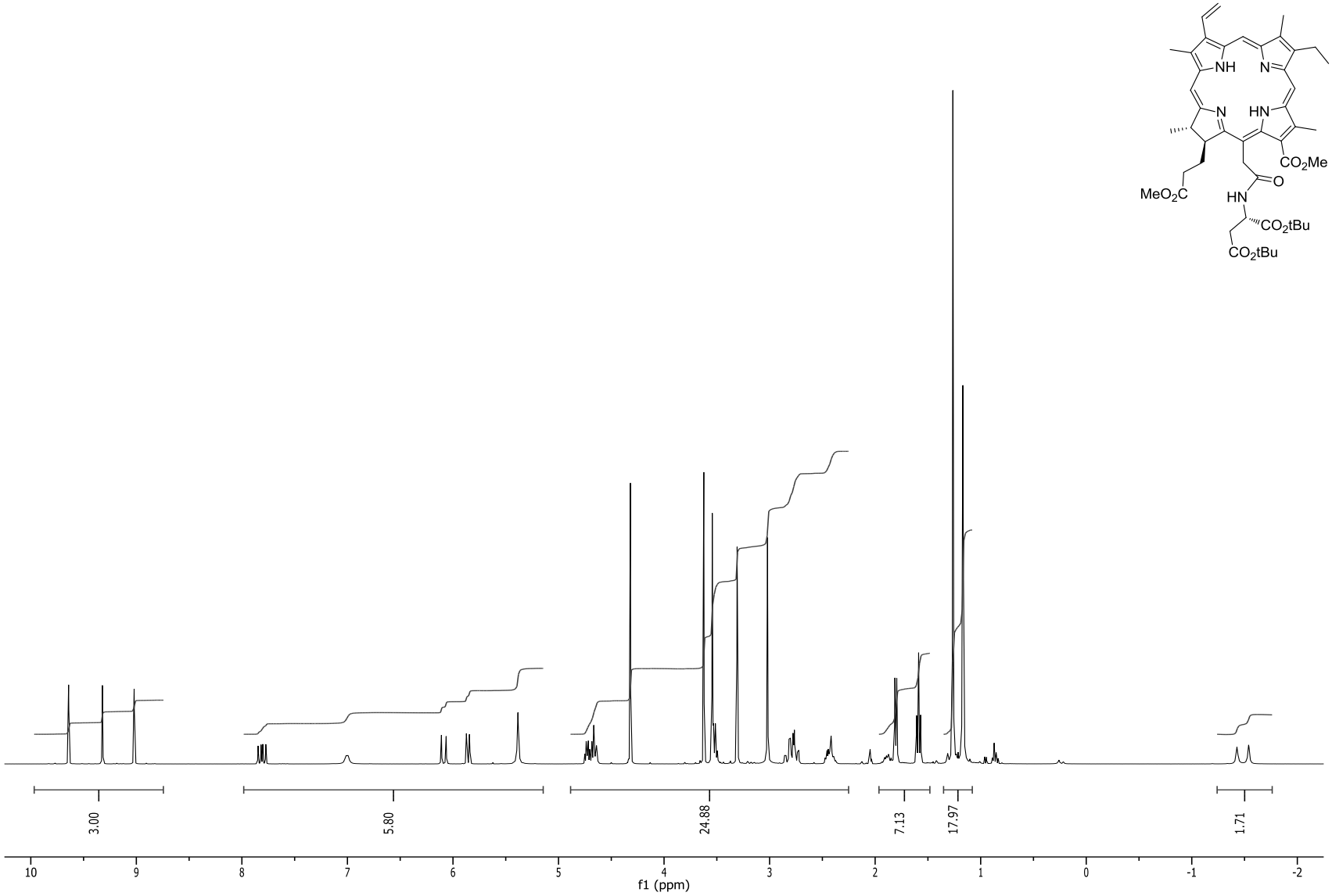

^{1}H NMR spectrum of 15^{2}-AspCe$_{6}$ DME **27a** in acetone-d_6 at 400 MHz

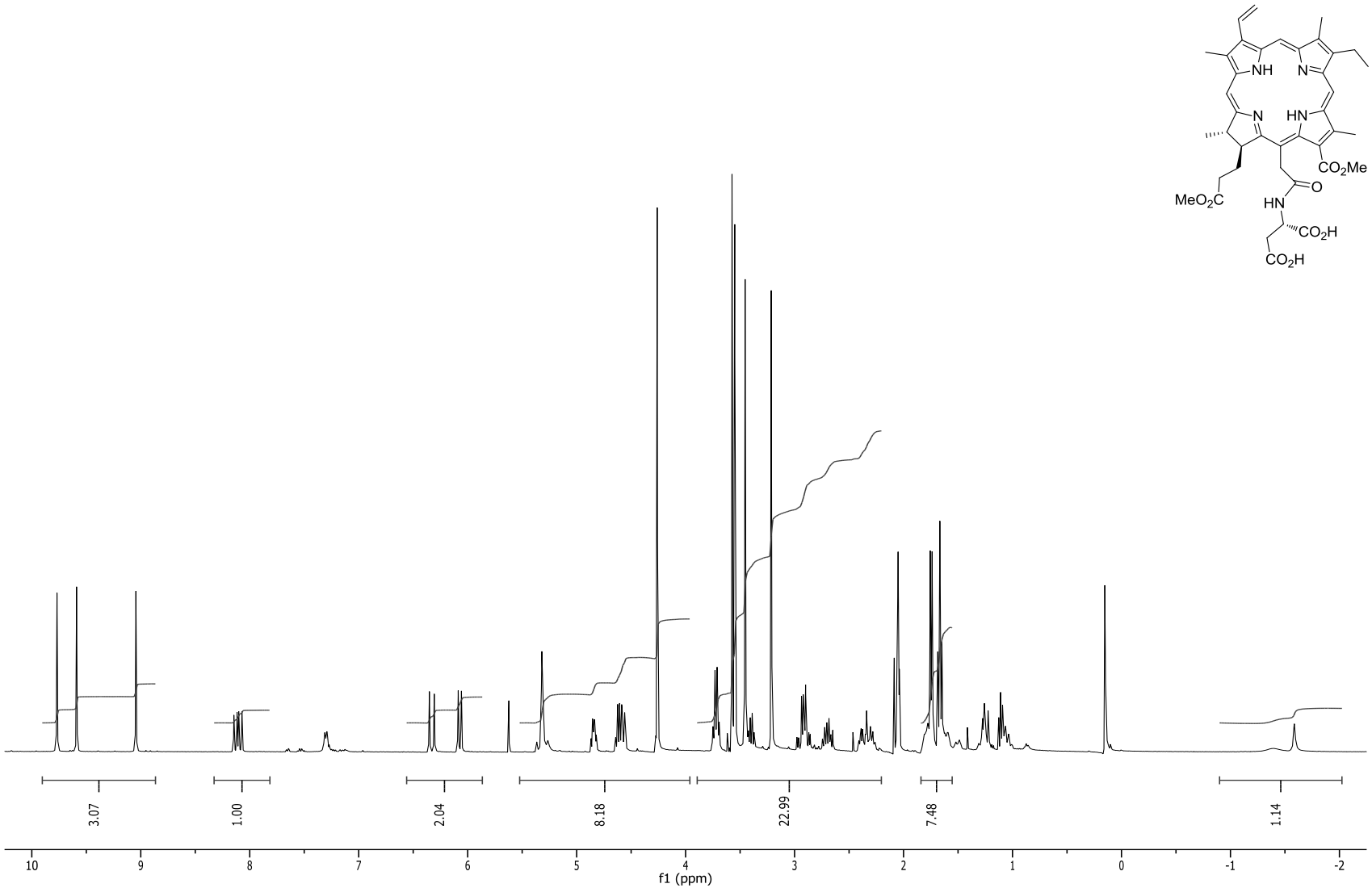

^{1}H NMR spectrum of 15^{2}-Lys(Boc)Ce$_6$TME **26b** in acetone-d_6 at 400MHz

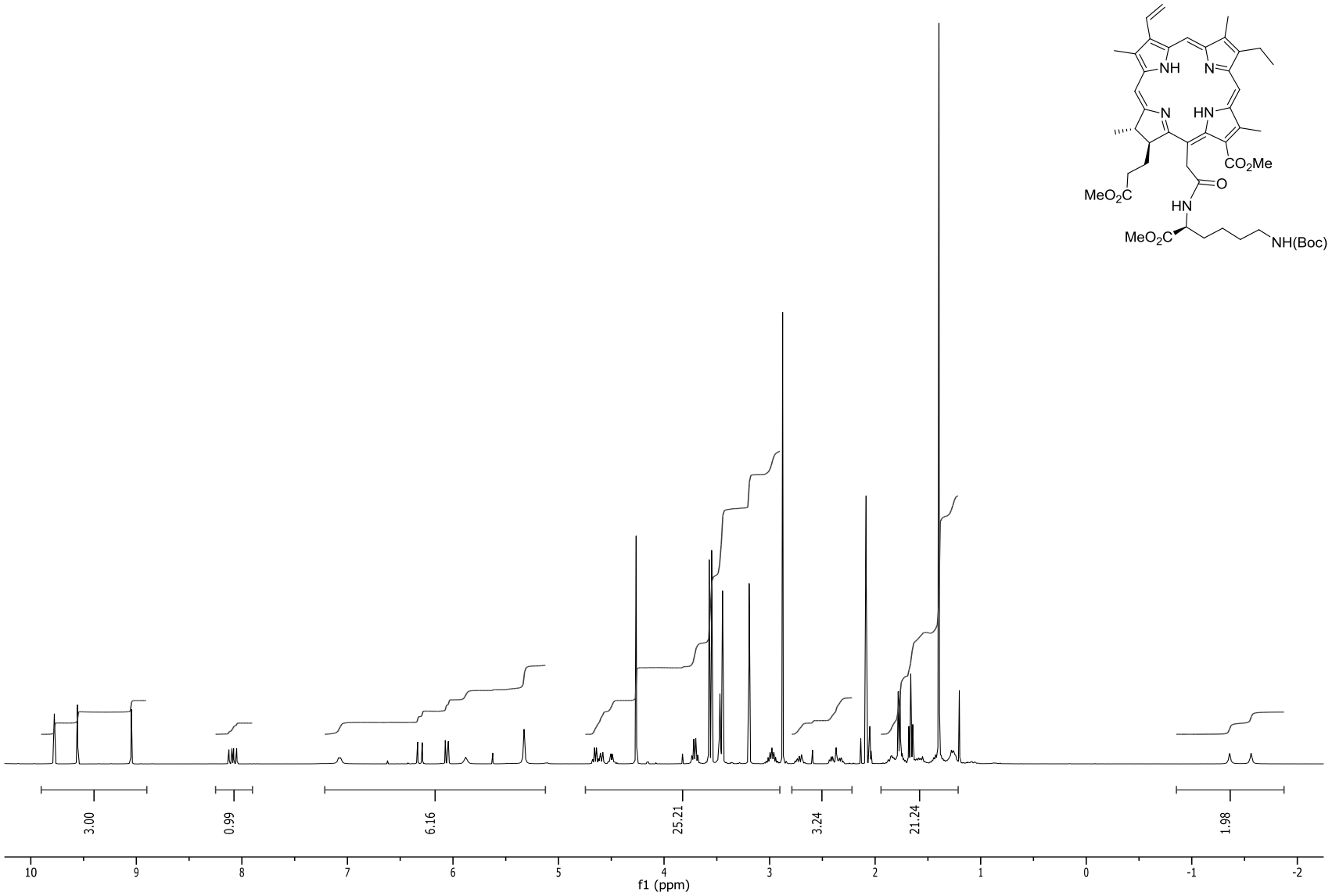

^{1}H NMR spectrum of 15^{2}-LysCe$_{6}$TME **27b** in acetone-d_6 at 400 MHz

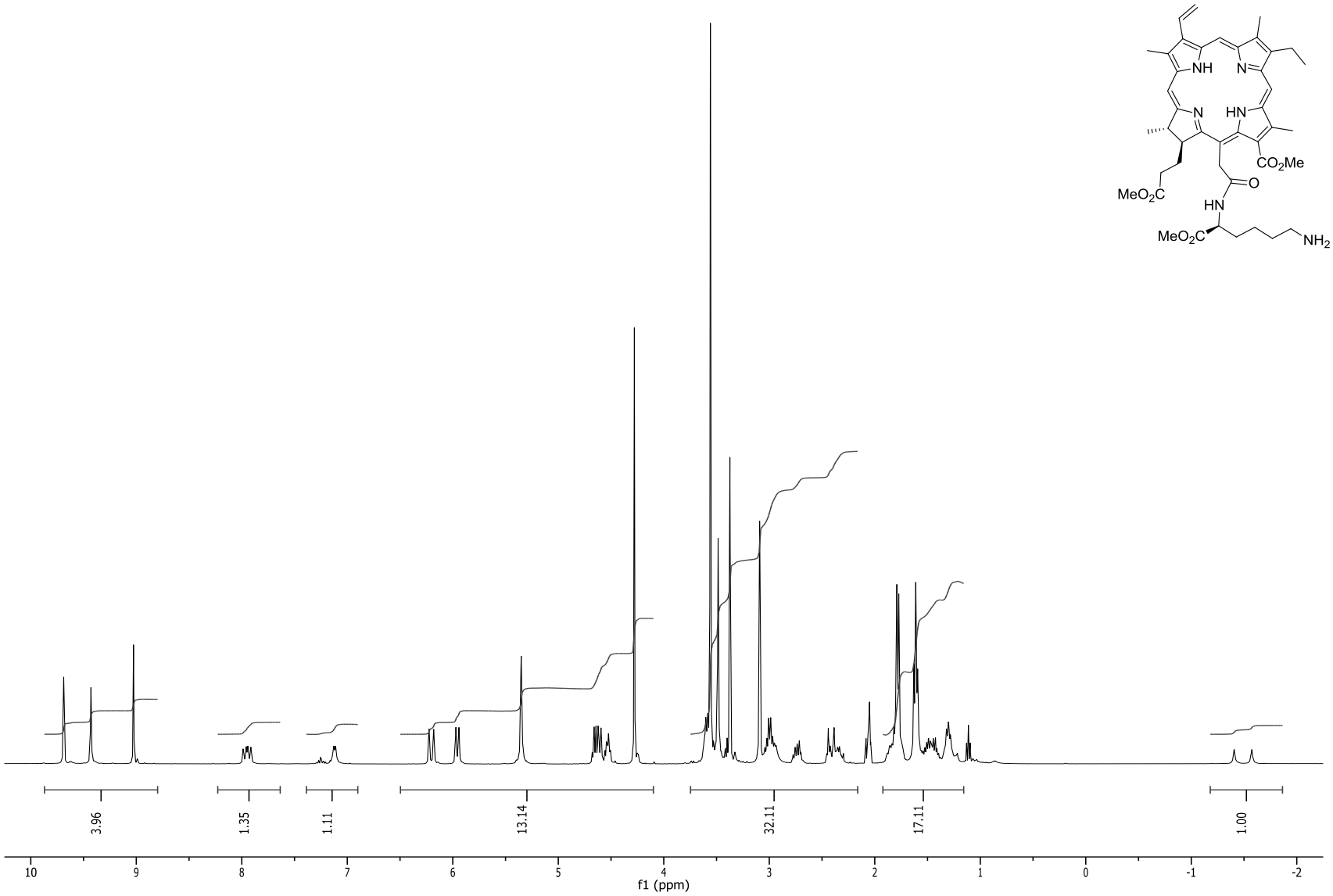

^{1}H NMR spectrum of Ce_6 DME (**29**) in acetone-d_6 at 400 MHz

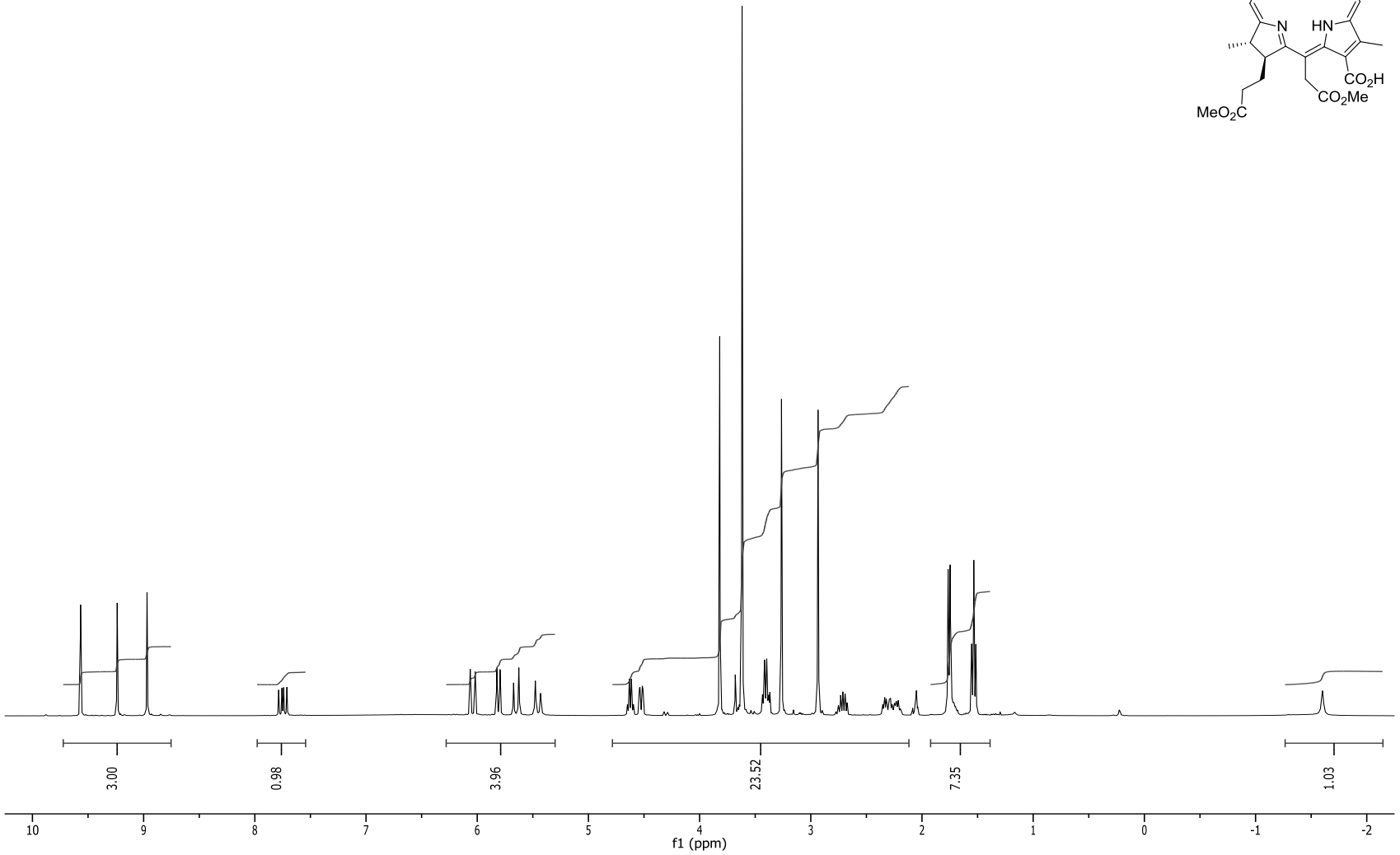

^{1}H NMR spectrum of 13^{1}-Aspdi(tBu)Ce$_6$ DME **30** in acetone-d_6 at 400 MHz

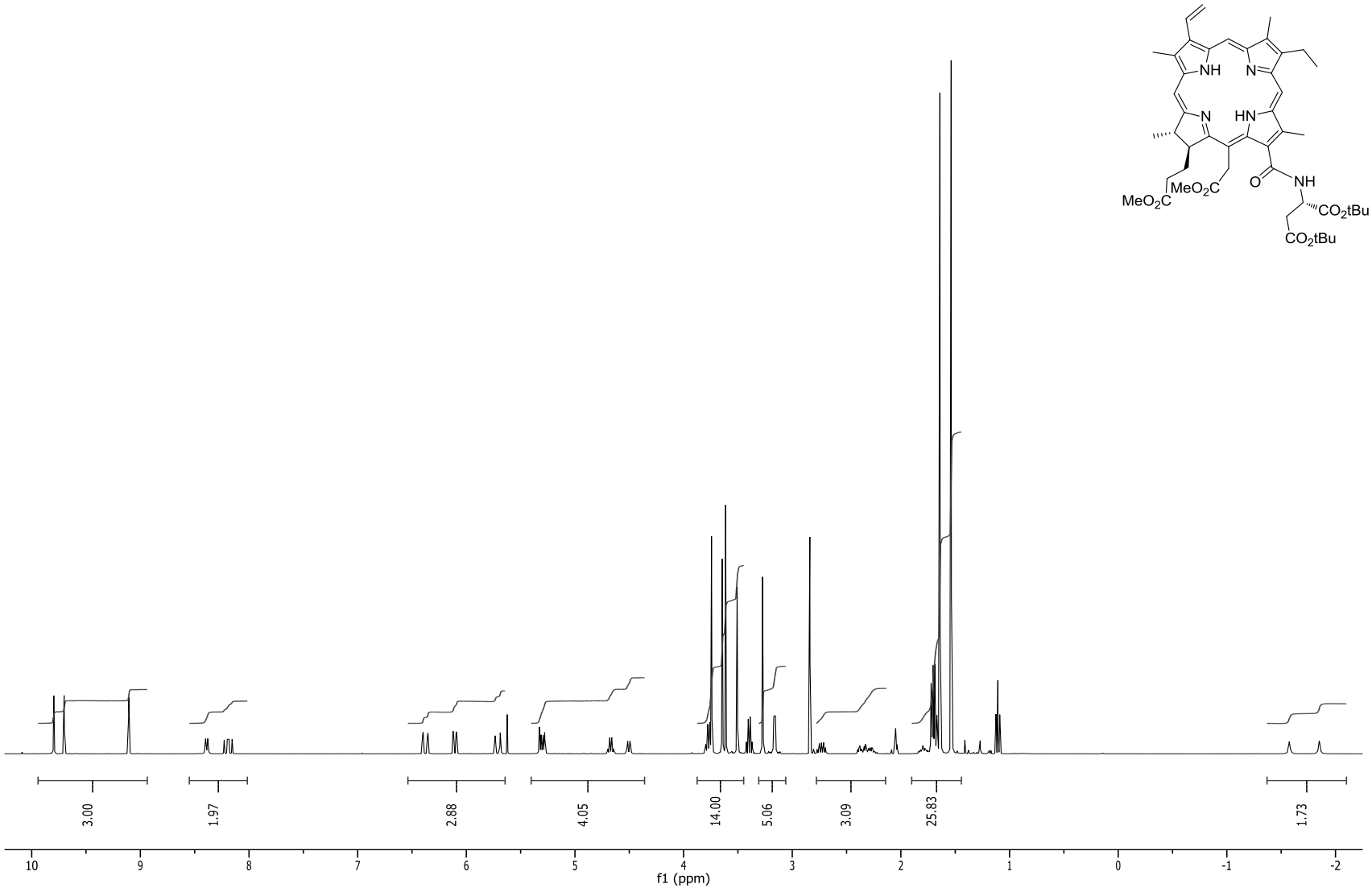

^{1}H NMR spectrum of 13[1] AspCe$_6$ DME **7** in acetone-d_6 at 400 MHz

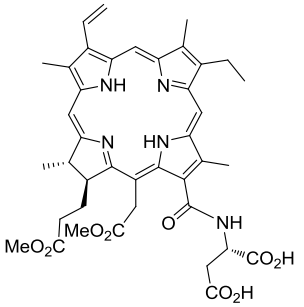

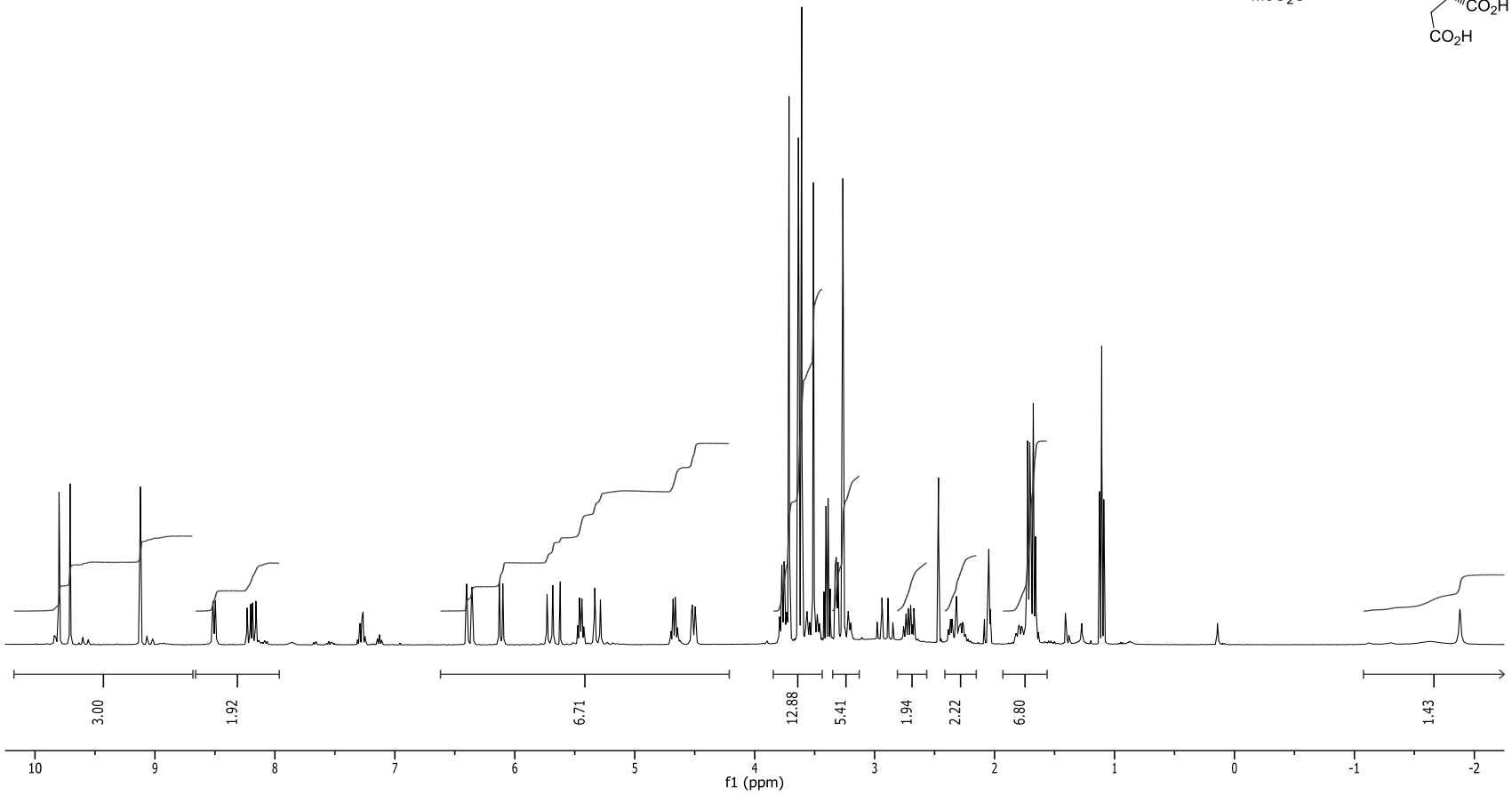

^{1}H NMR spectrum of 13^{1}-β-Ala(tBu)Ce$_6$ DME **31** in acetone-d_6 at 400 MHz

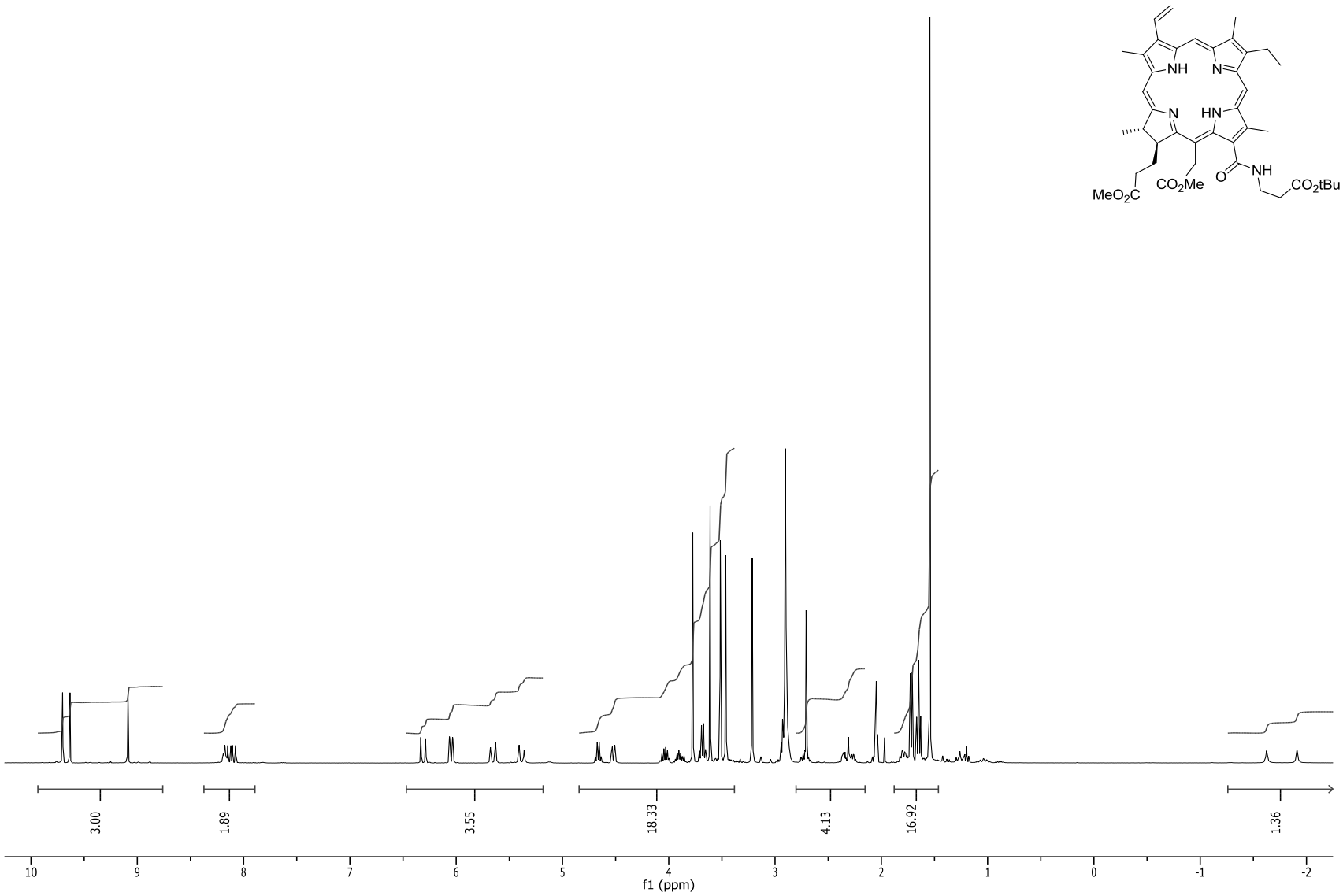

^{1}H NMR spectrum of 13[1] β-AlaCe$_6$ DME **32** in acetone-d_6 at 400 MHz

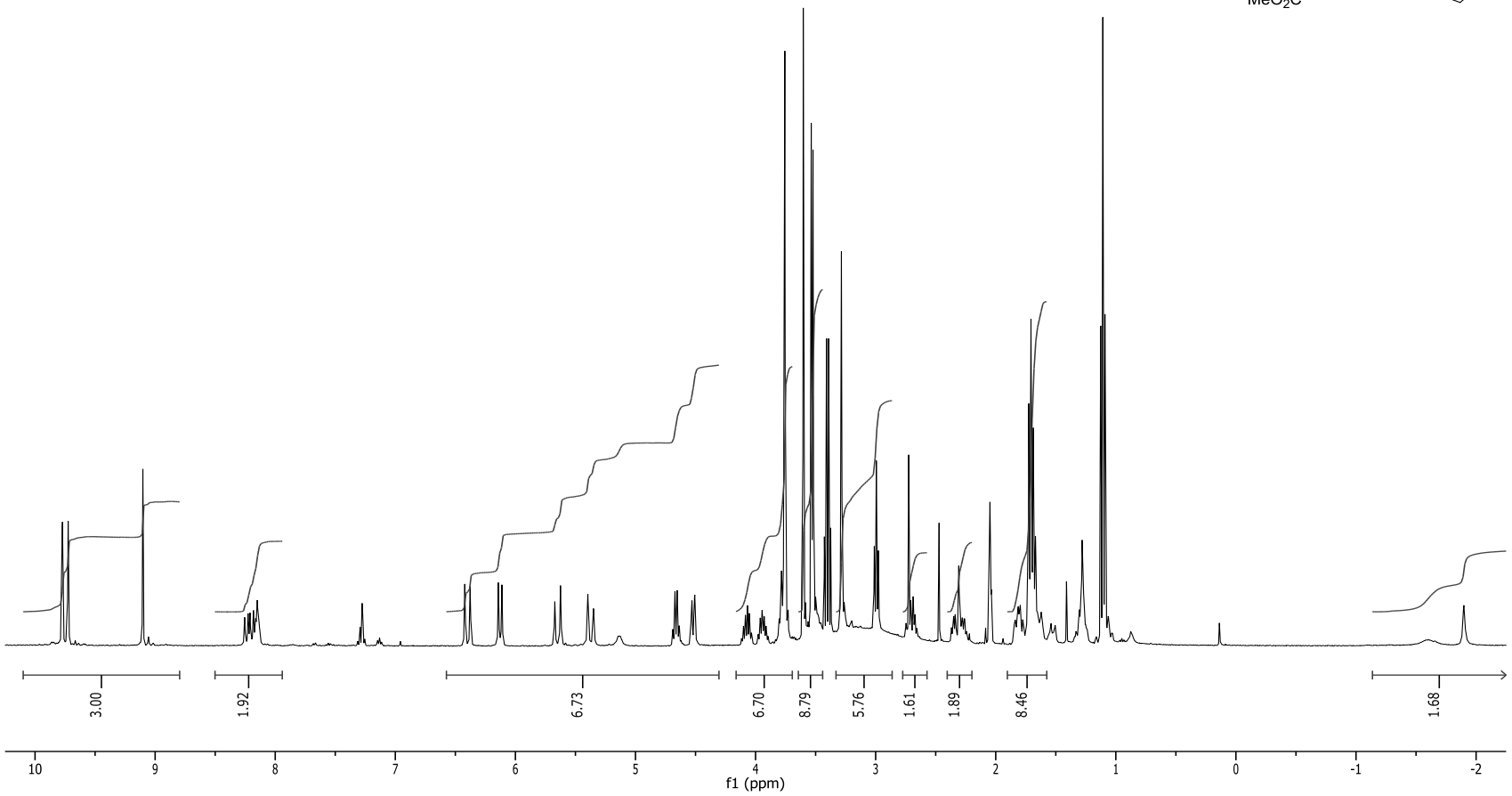

^{1}H NMR spectrum of 13^{1}-β-Ala-Aspdi(tBu)Ce$_6$ DME **33** in acetone-d_6 at 400 MHz

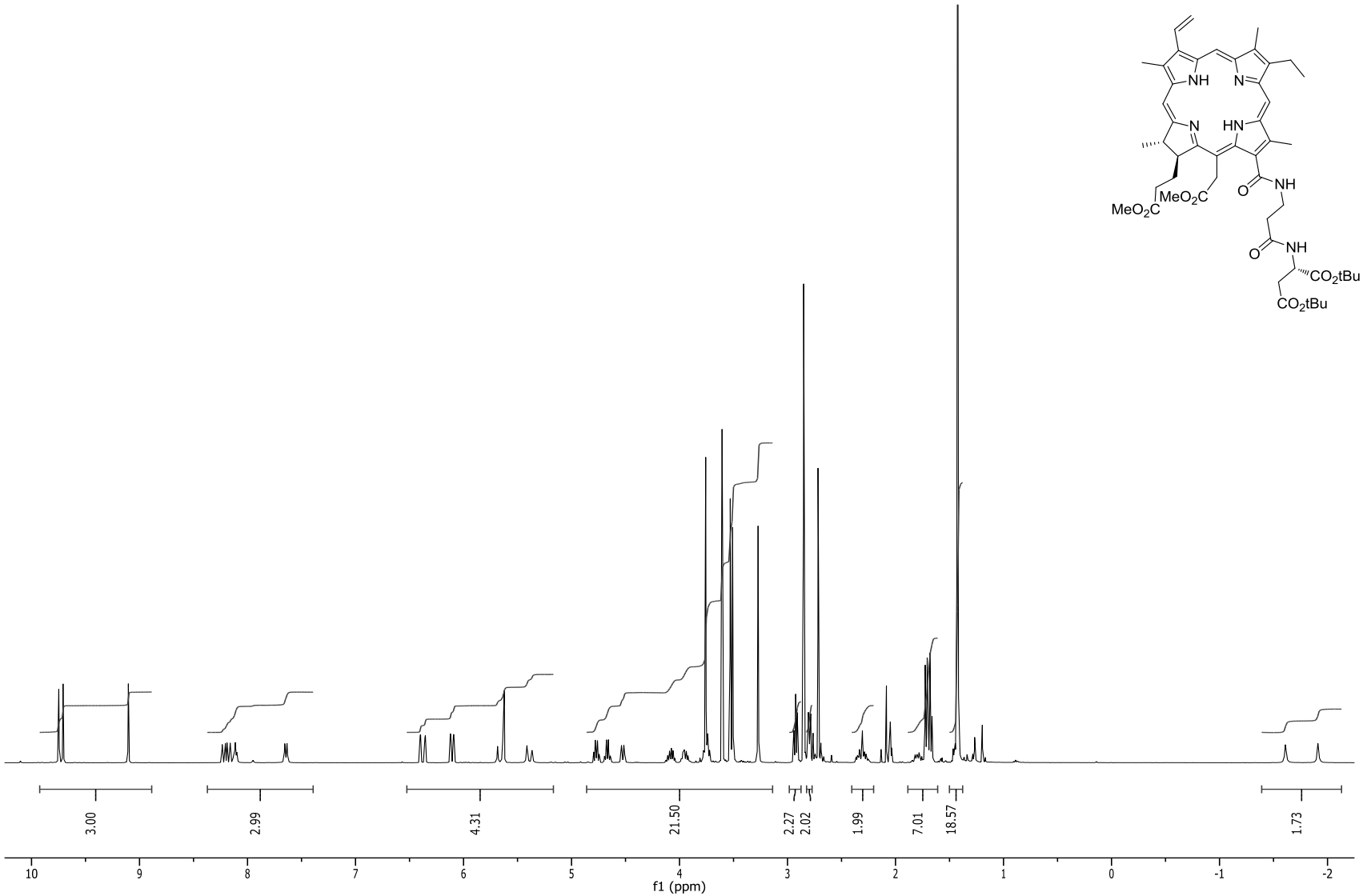

^{1}H NMR spectrum of 13^{1}-b-Ala-AspCe$_6$ DME **34** in acetone-d_6 at 400 MHz

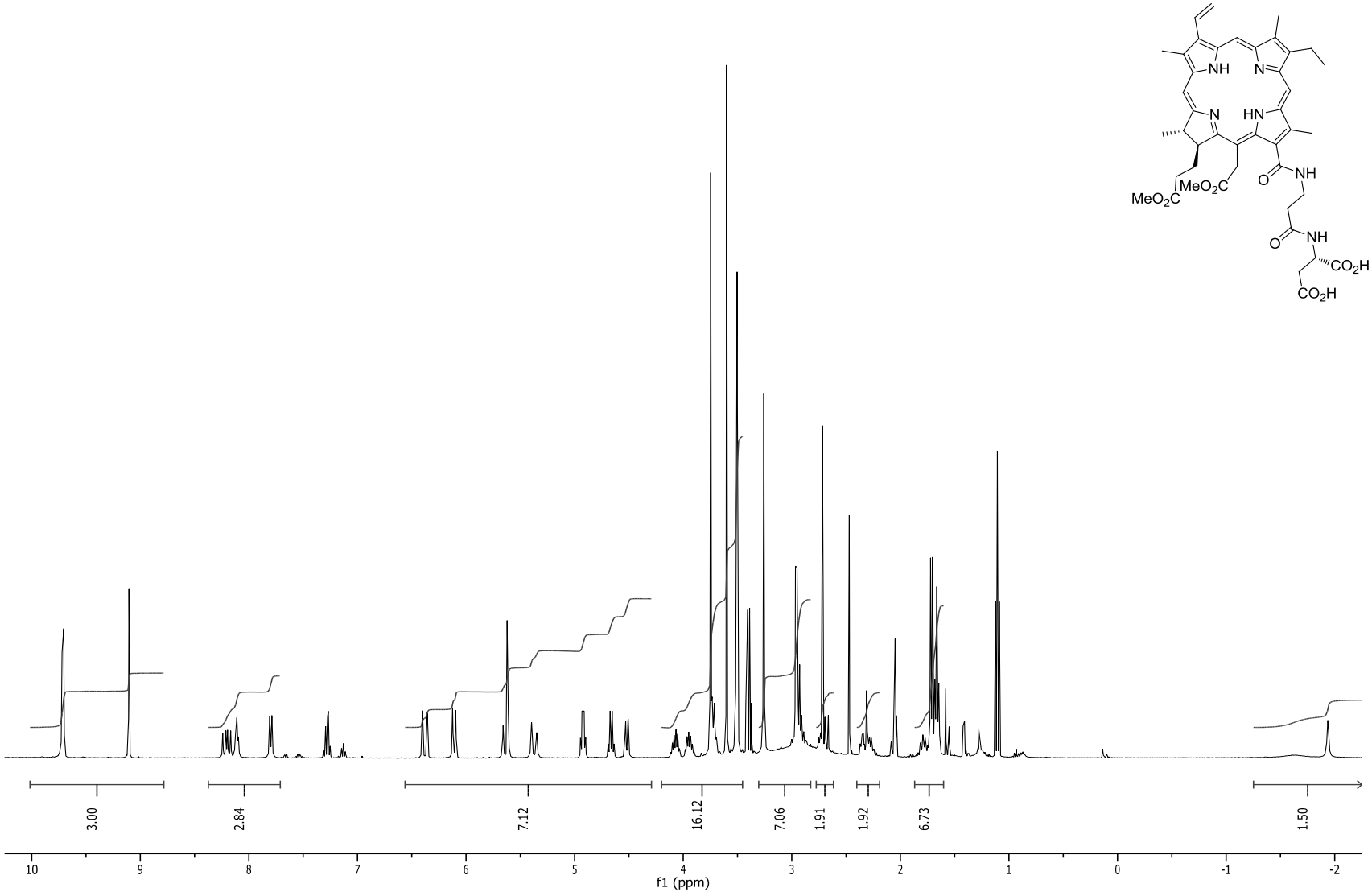

^{1}H NMR spectrum of 13^{1}-ED-Ce$_6$ DME **35** in acetone-d_6 at 400 Mhz

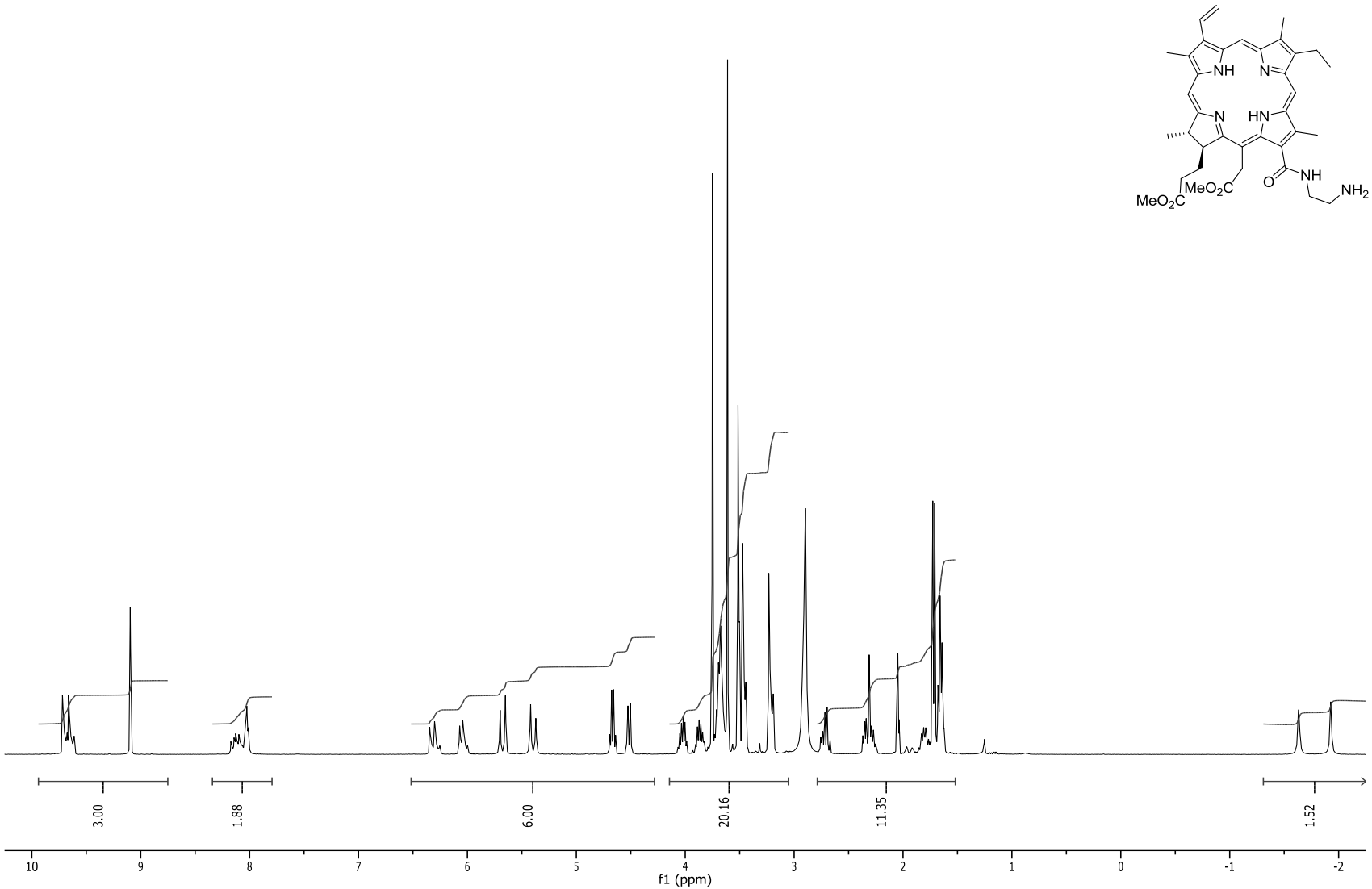

^{1}H NMR spectrum of 13^{1}-ED-(Boc)Lys(Boc)Ce$_6$ DME **36** in acetone-d_6 at 400 MHz

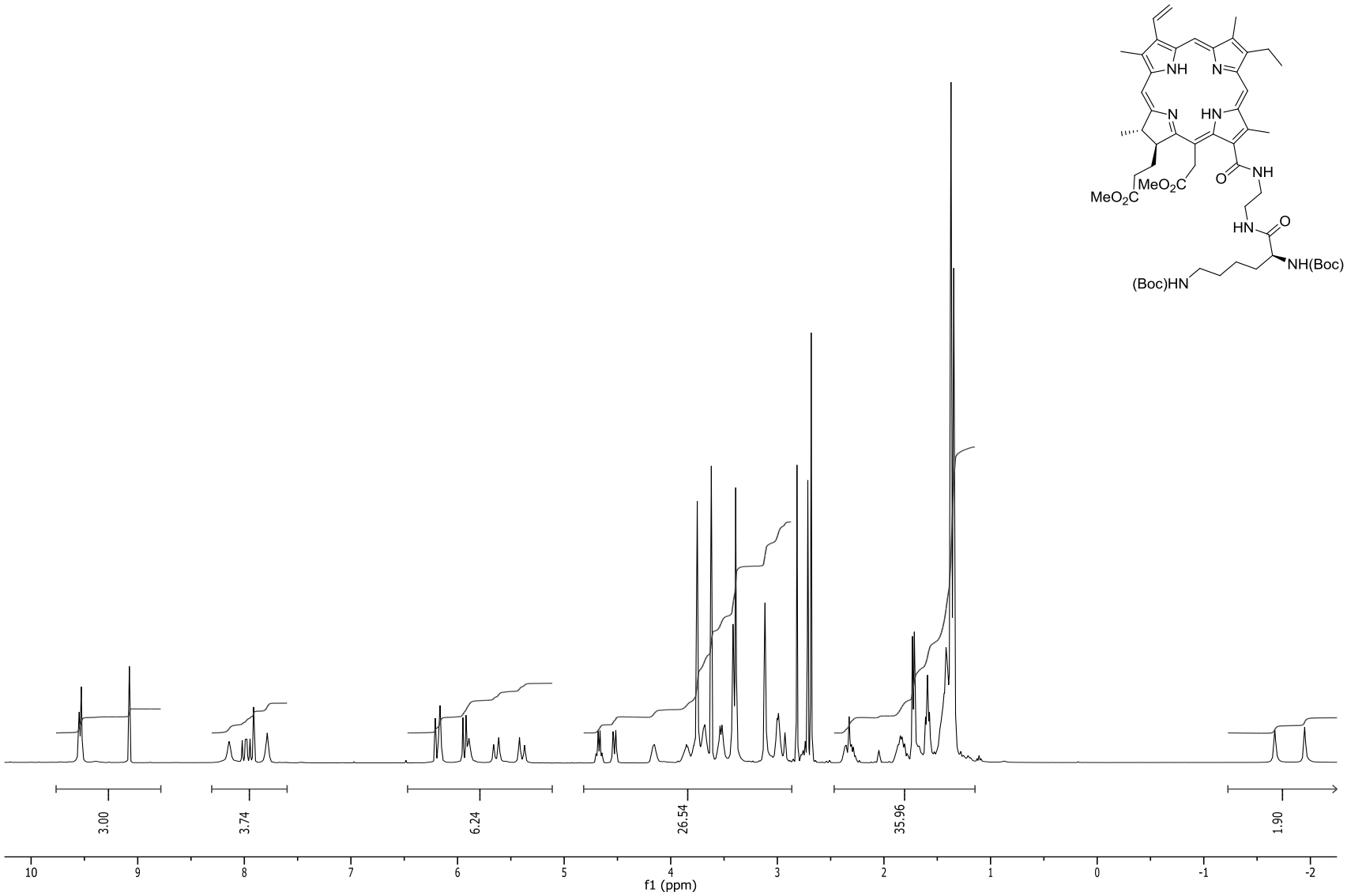

^{1}H NMR spectrum of 13^{1}-ED-LysCe$_6$ DME **37** in acetone-d_6 at 400 MHz

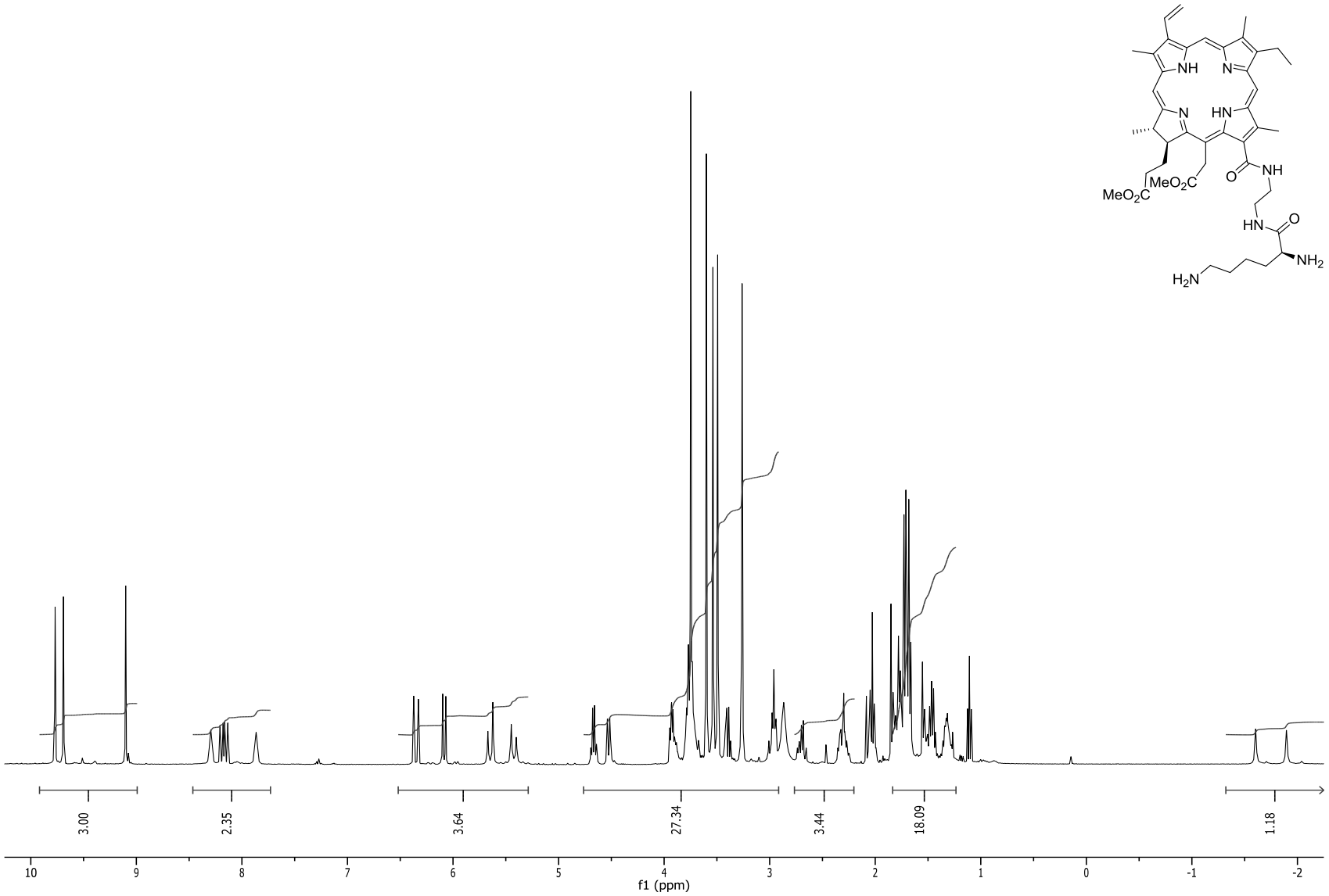

^{13}C NMR spectrum of 17^{3}-LysCe$_6$ TME **20** in dichloromethane-d_2 at 100 MHz

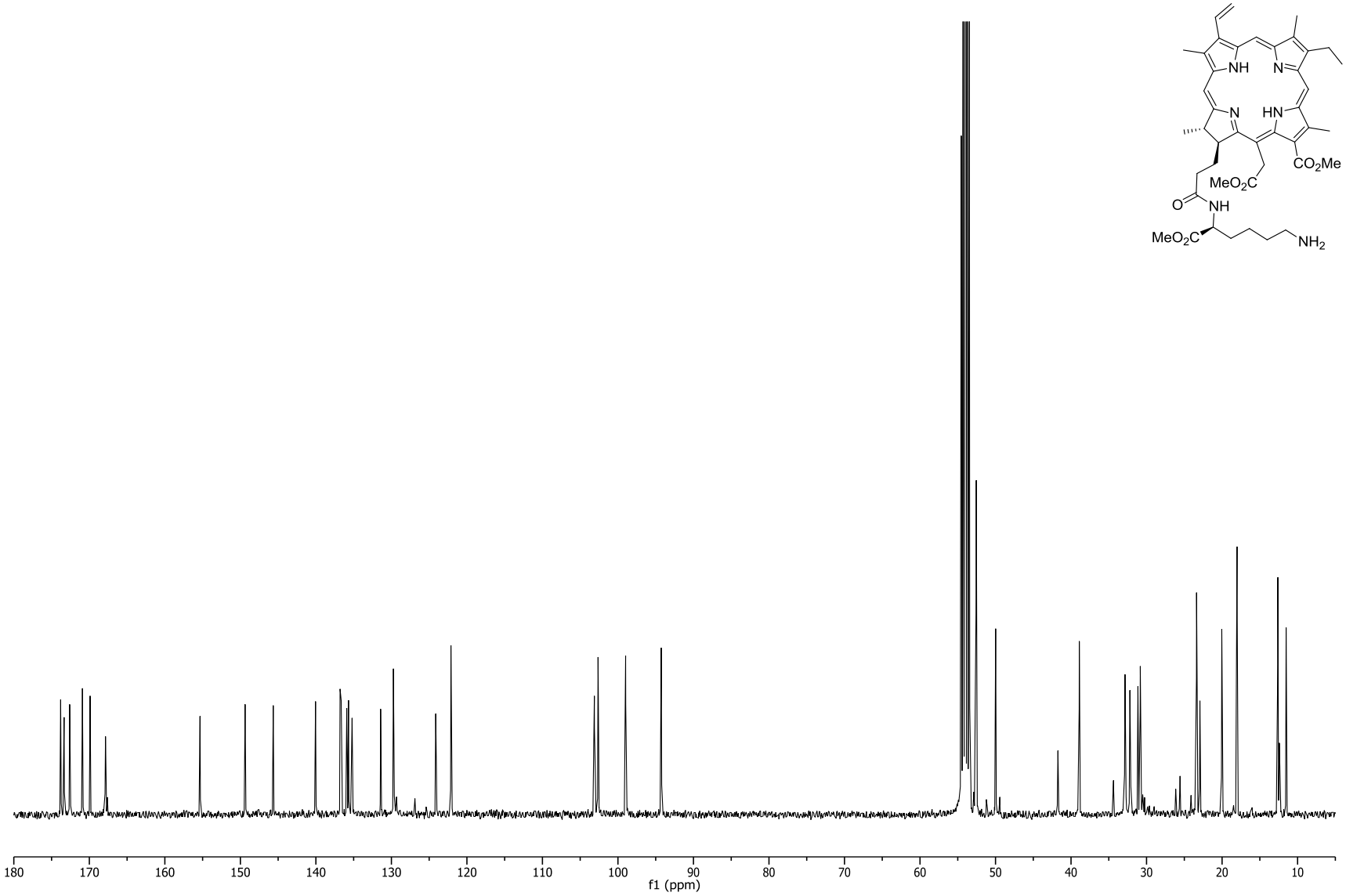

^{13}C NMR spectrum of Ce_6 TME **24** in dichloromethane-d_2 at 100 MHz

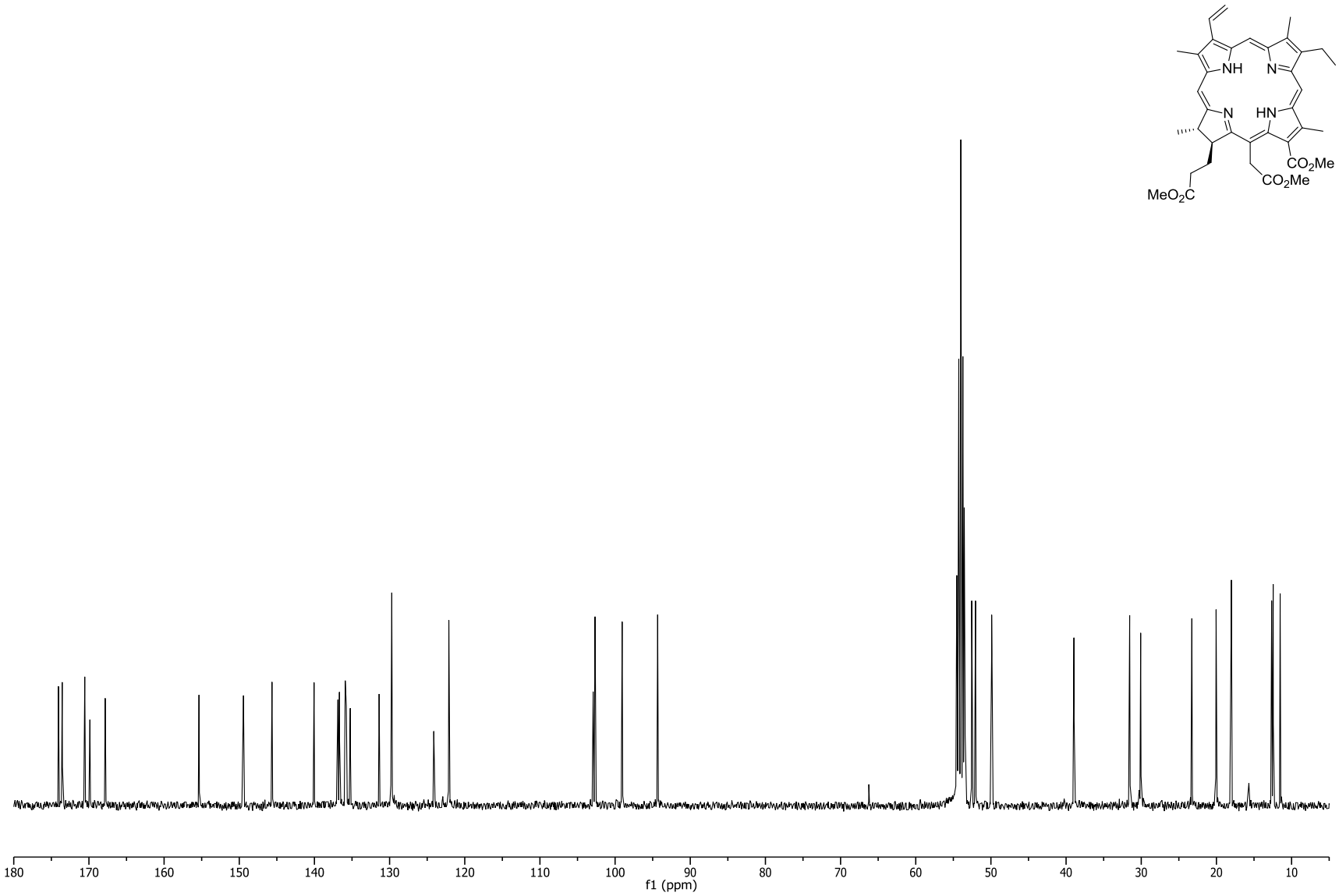

^{13}C NMR spectrum of Ce_6 **2** in dimethyl sulfoxide-d_6 at 100 MHz

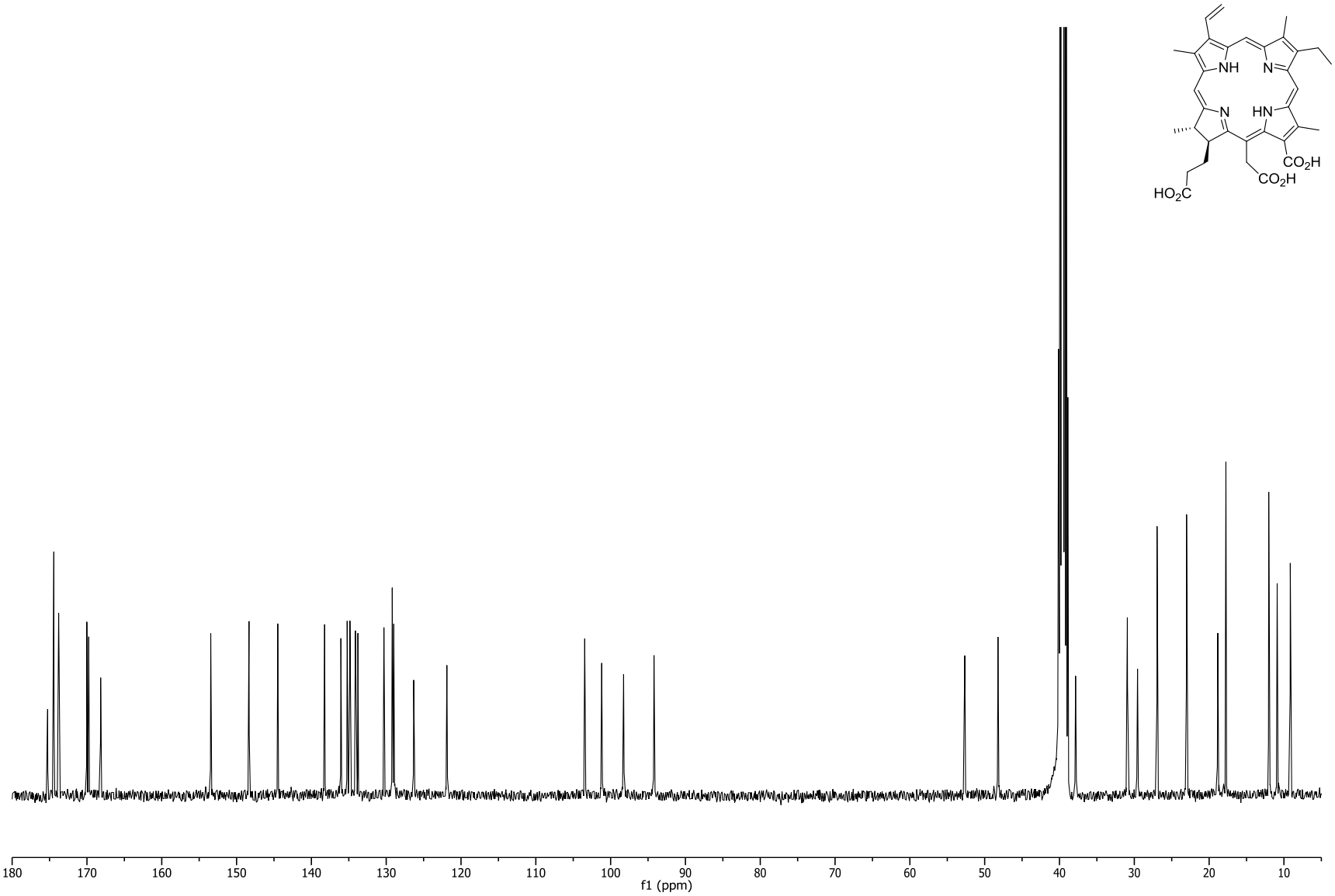

^{13}C NMR spectrum of 15^2-AspCe$_6$ DME **27a** in acetone-d_6 at 100 MHz

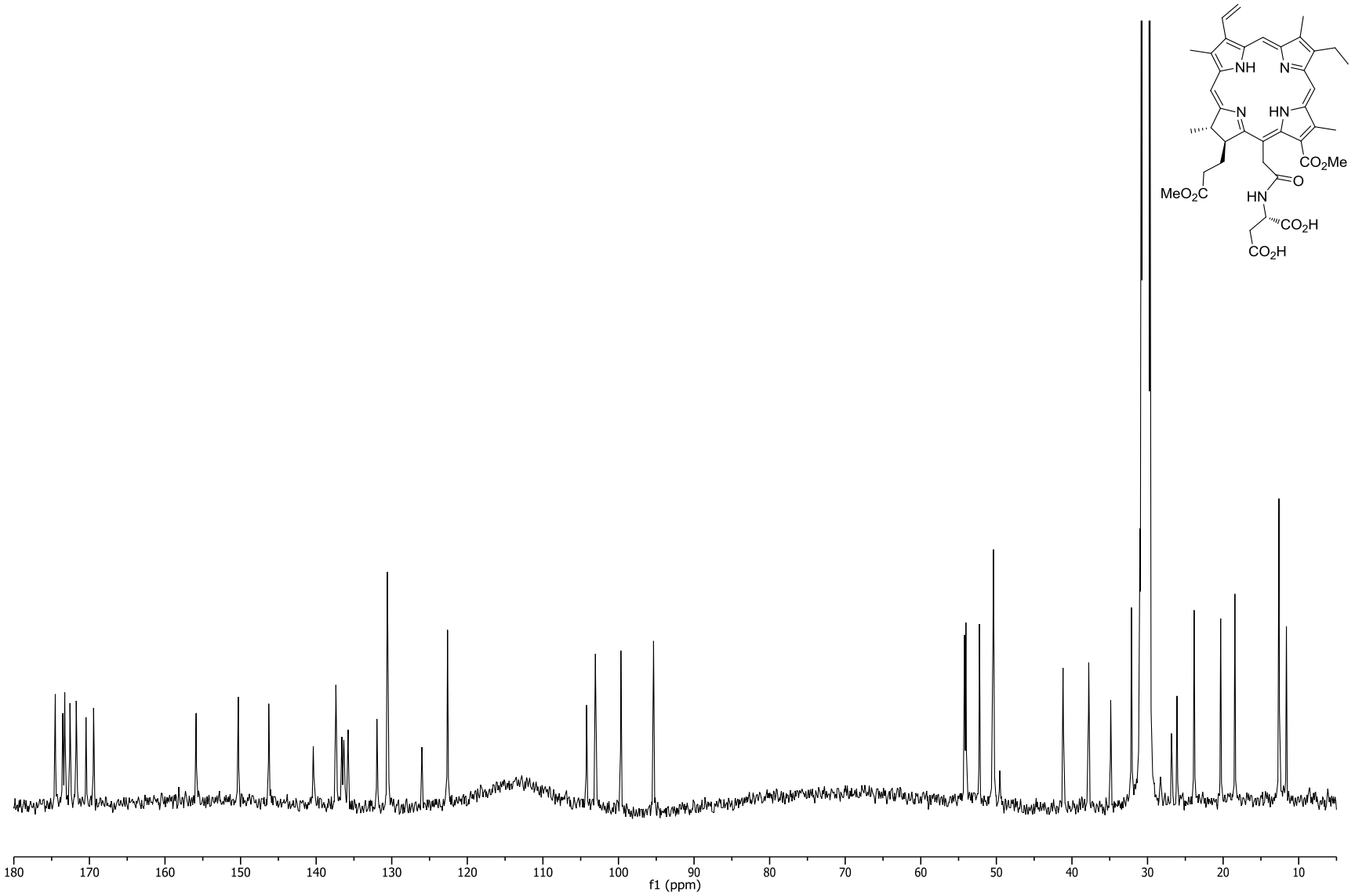

^{13}C NMR spectrum of 15^{2}-LysCe$_6$ TME **27b** in dichloromethane-d_2 at 100 MHz

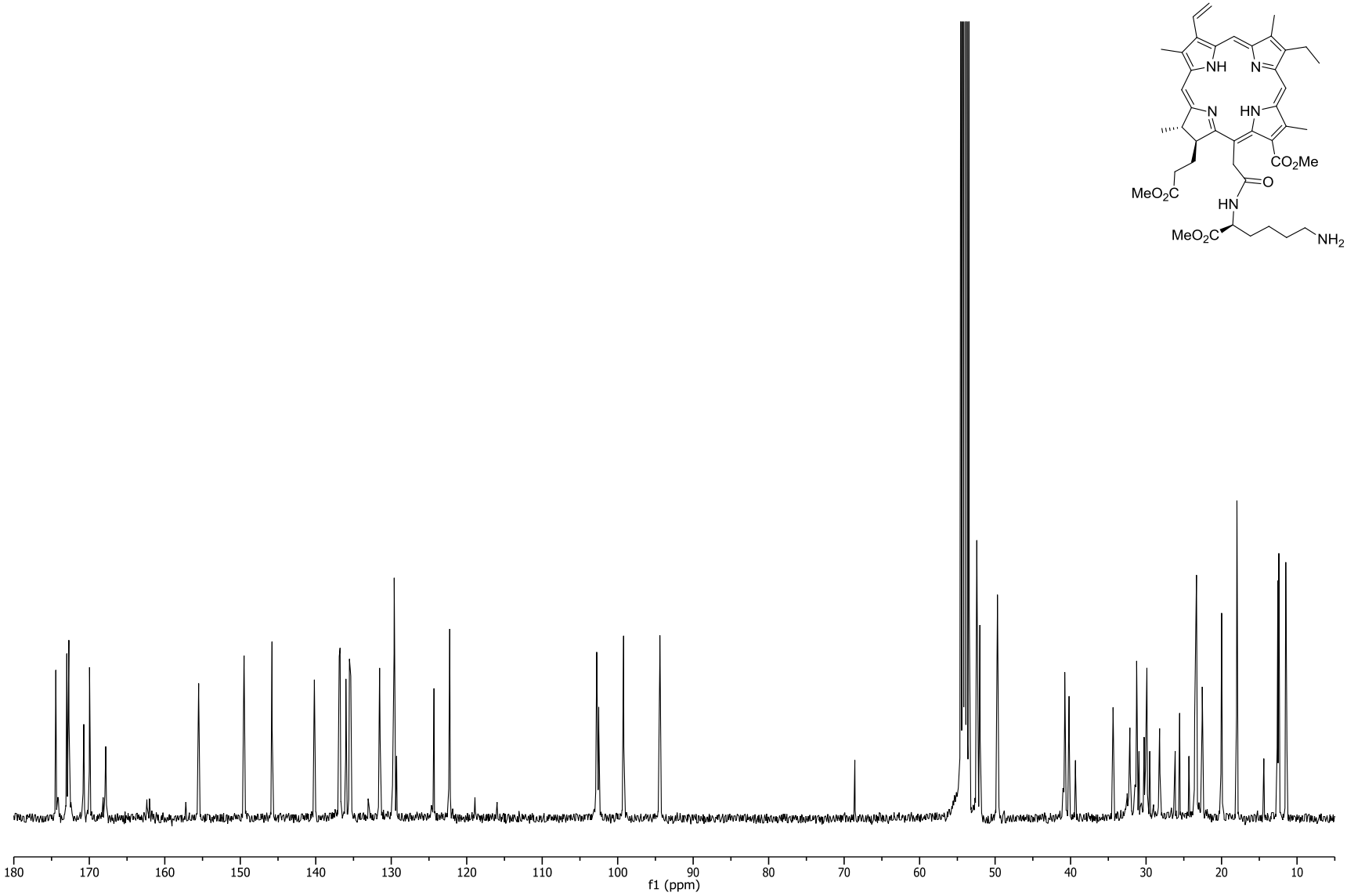

^{13}C NMR spectrum of 13^{1} AspCe$_6$ DME **7** in acetone-d_6 at 100 MHz

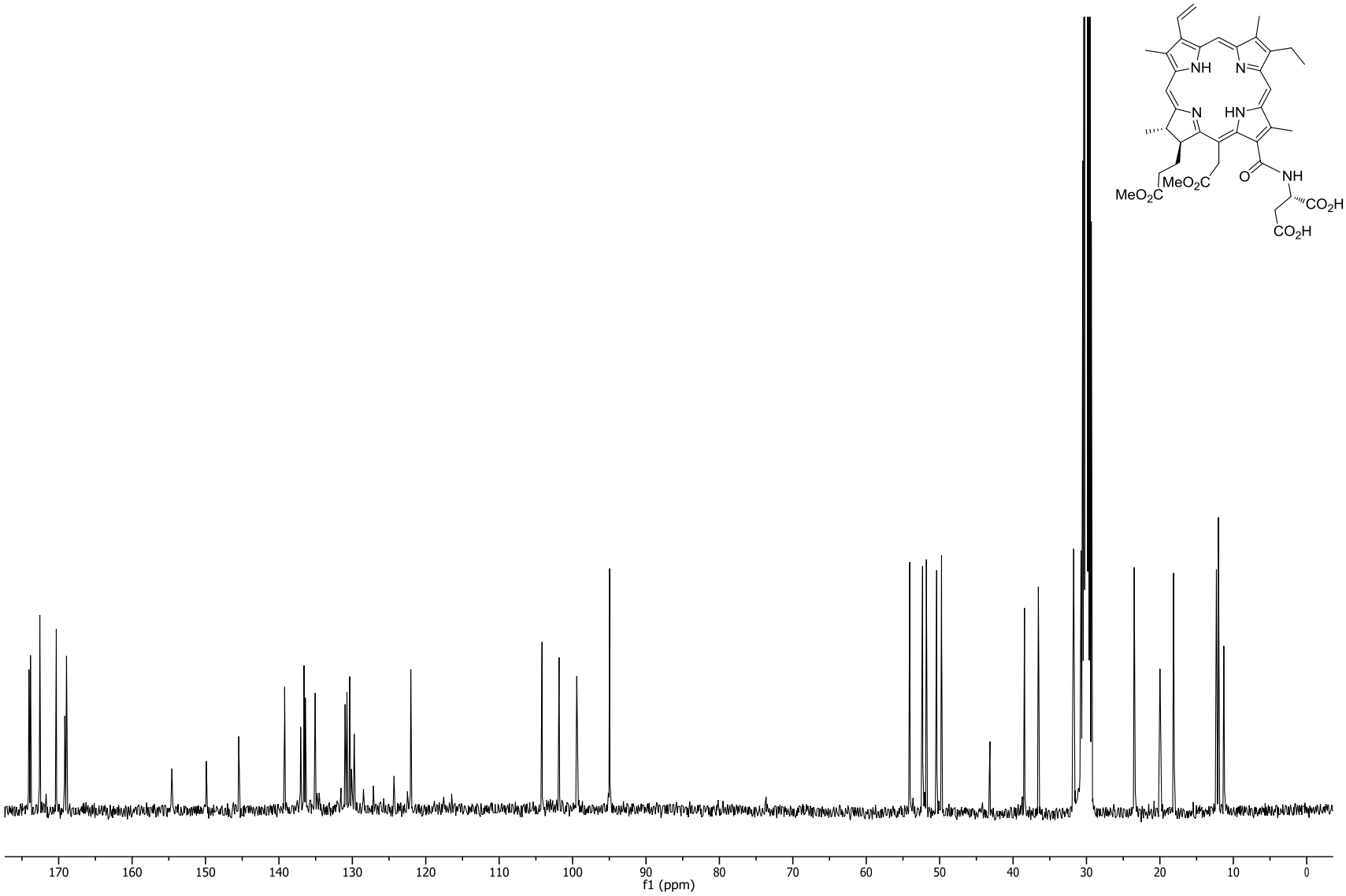

^{13}C NMR spectrum of 13^{1}-β-Ala-AspCe$_6$ DME **34** in chloroform-*d* at 100 MHz

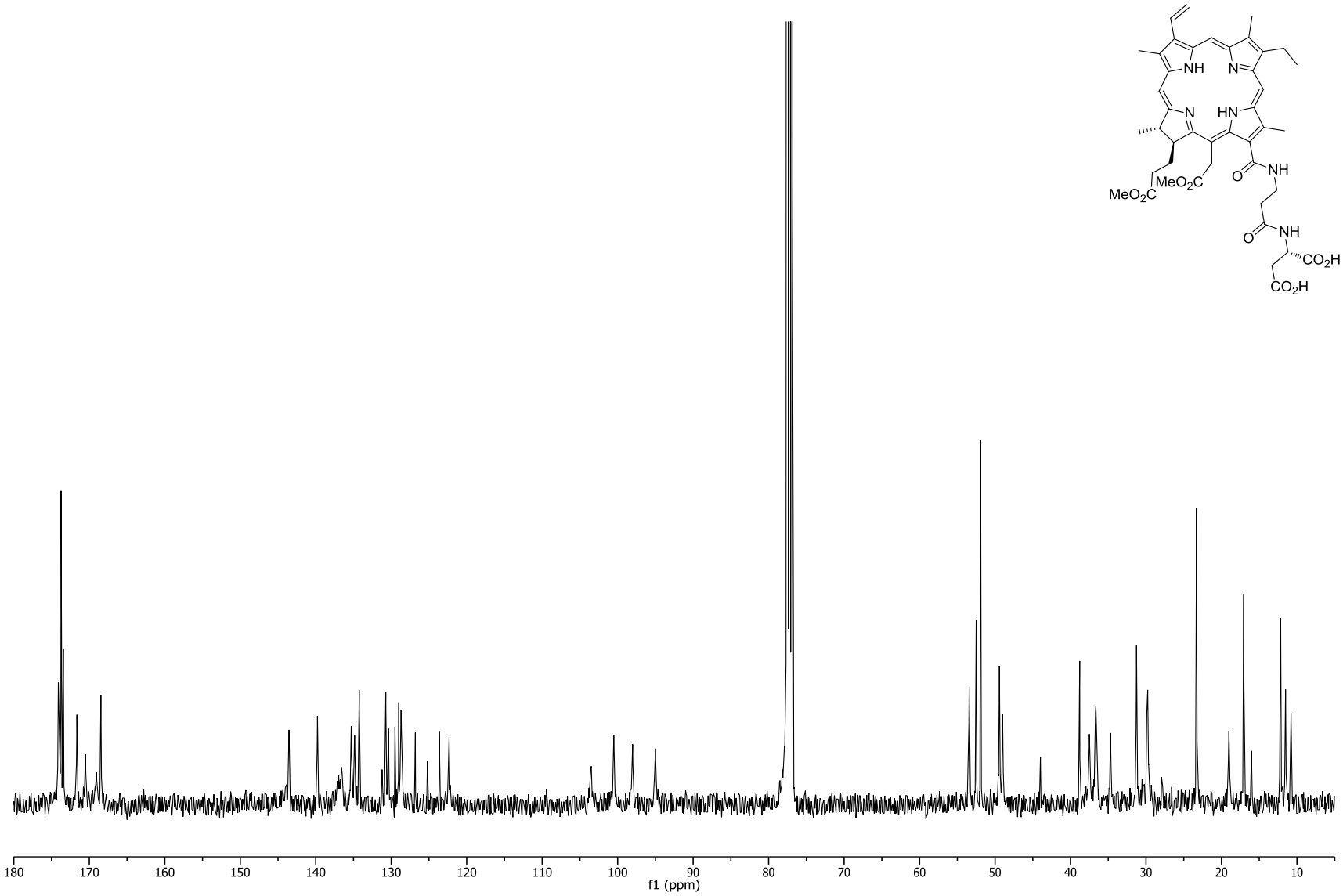

^{13}C NMR spectrum of 13^{1}-ED-Ce$_6$ DME **35** in acetone-d_6 at 100 MHz

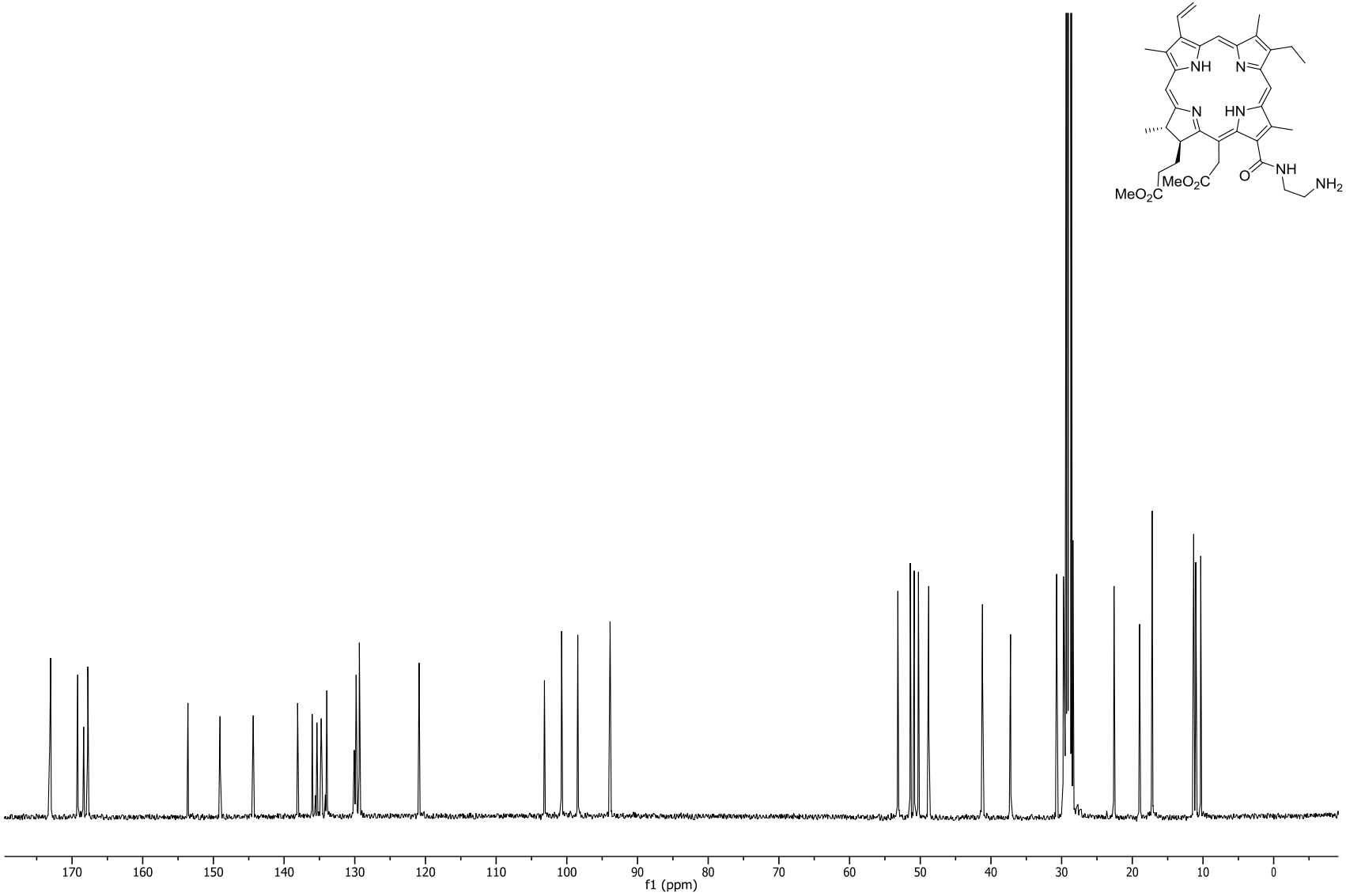

^{13}C NMR spectrum of 13^{1}-ED-LysCe$_6$ DME **37** in dichloromethane-d_2 at 100 MHz

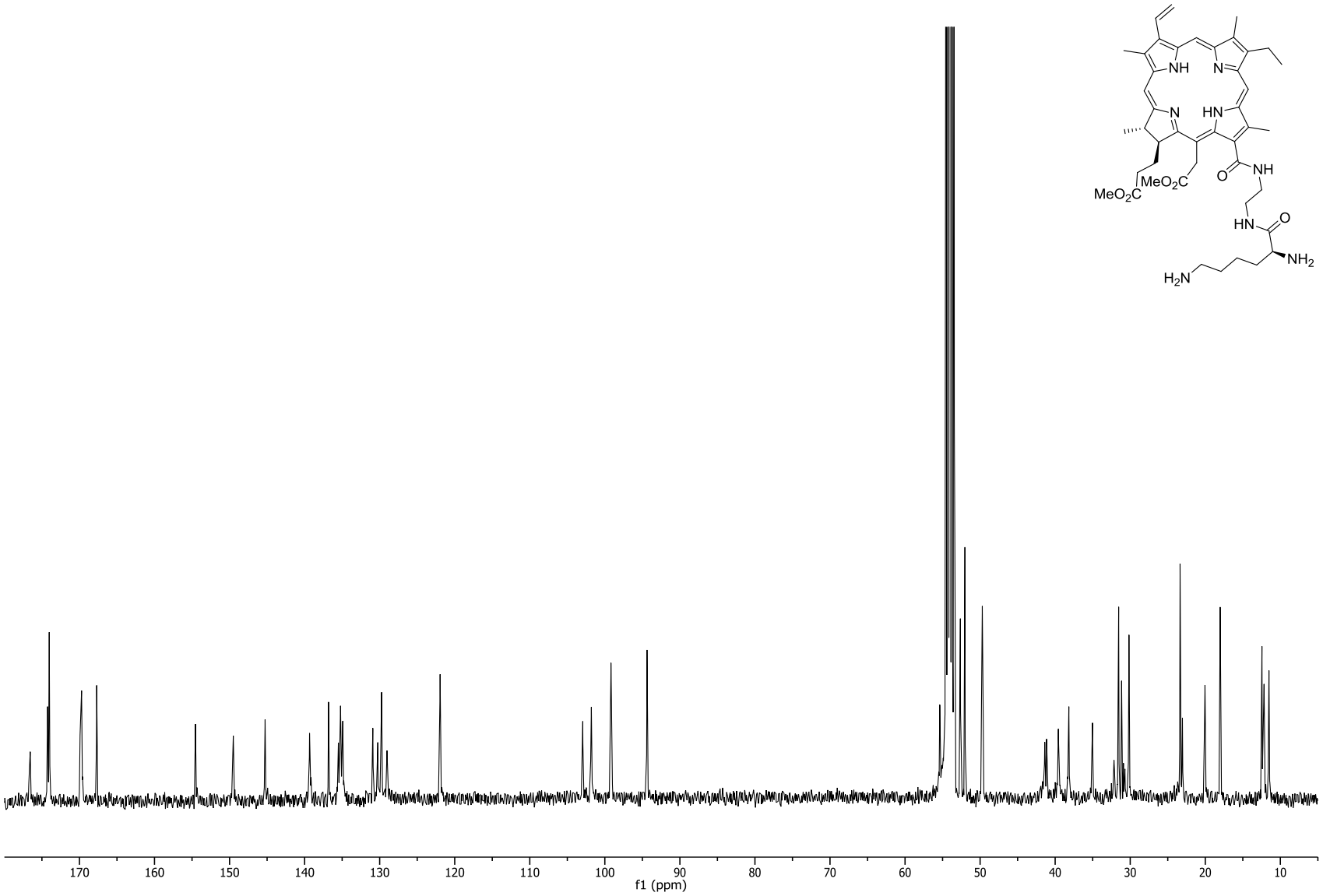

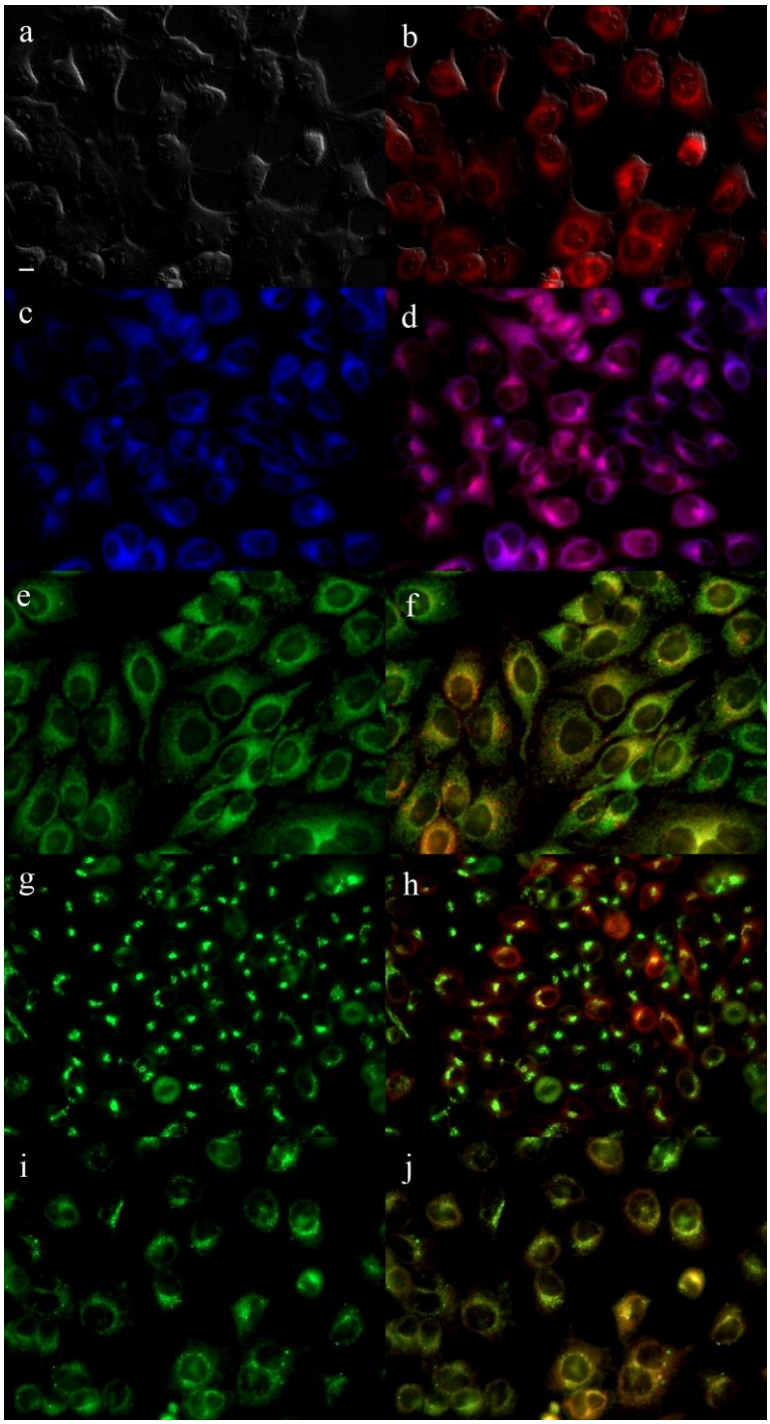

Figure 2.9: Subcellular localization of conjugate Ce_6 in HEp2 cells at 10 µM for 18 h (a) phase contrast, (b) overlay of compound Ce_6 compound and phase contrast, (c) ER tracker Blue/White fluorescence (e) MitoTracker Green fluorescence, (g) BoDIPY Ceramide, (i) LysoSensor Green fluorescence, and (d, f, h, j) overlays of organelle tracers with compound fluorescence. Scale bar: 10 µm.

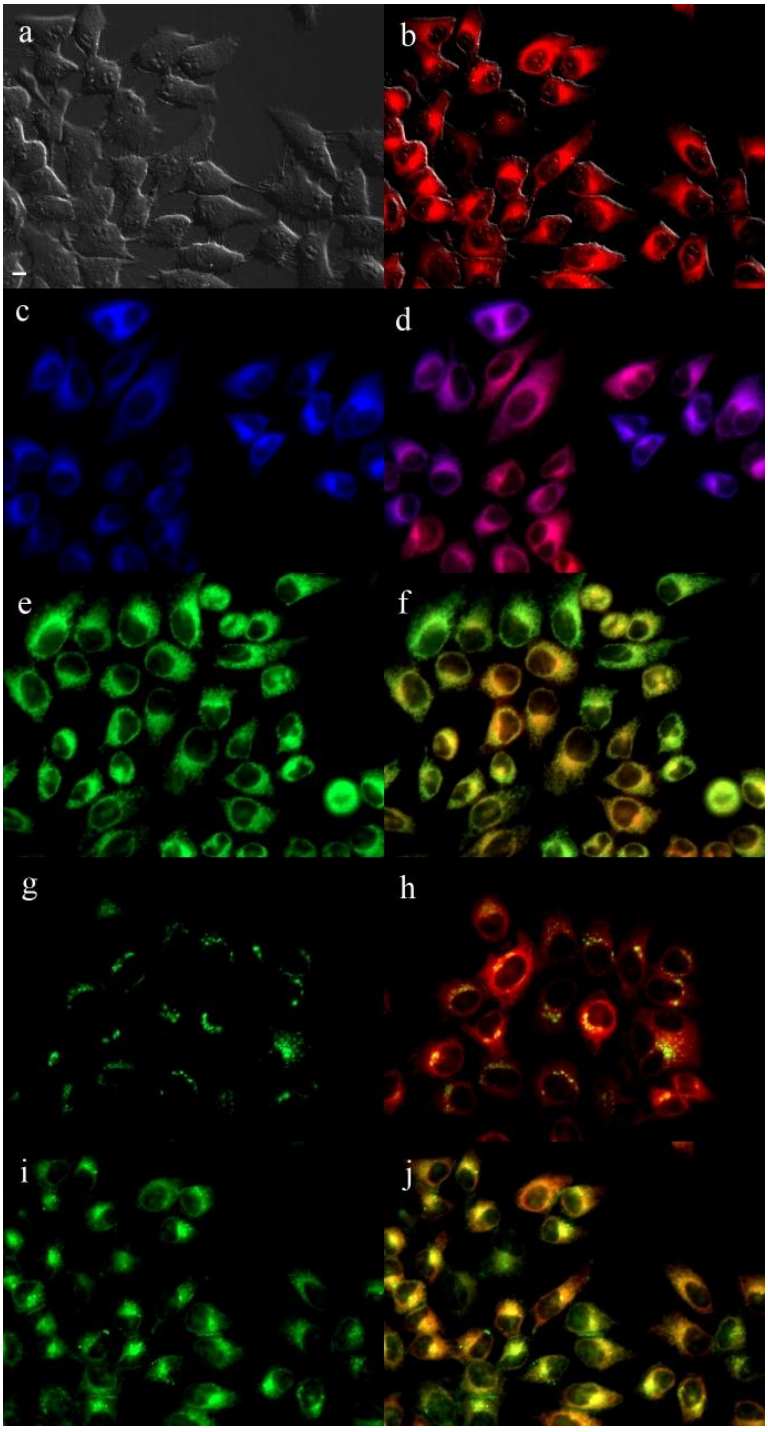

Figure 2.10: Subcellular localization of conjugate 15^2 $AspCe_6DME$ in HEp2 cells at 10 µM for 18 h (a) phase contrast, (b) overlay of compound 15^2 $AspCe_6$ compound and phase contrast, (c) ER tracker Blue/White fluorescence (e) MitoTracker Green fluorescence, (g) BoDIPY Ceramide, (i) LysoSensor Green fluorescence, and (d, f, h, j) overlays of organelle tracers with compound fluorescence. Scale bar: 10 µm.

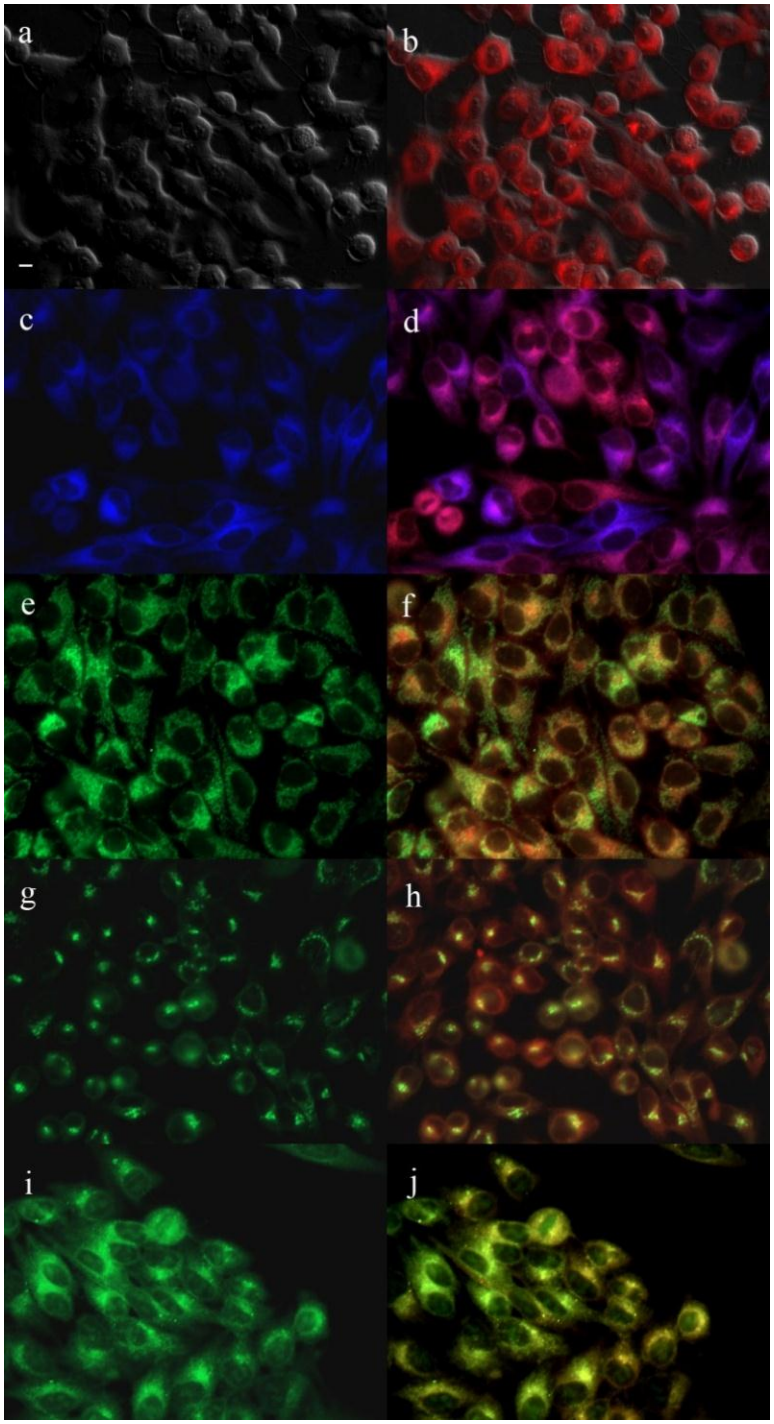

Figure 2.11: Subcellular localization of conjugate 15^2 PdAspCe$_6$DME in HEp2 cells at 10 µM for 18 h (a) phase contrast, (b) overlay of compound 15^2 PdAspCe$_6$ compound and phase contrast, (c) ER tracker Blue/White fluorescence (e) MitoTracker Green fluorescence, (g) BoDIPY Ceramide, (i) LysoSensor Green fluorescence, and (d, f, h, j) overlays of organelle tracers with compound fluorescence. Scale bar: 10 µm.

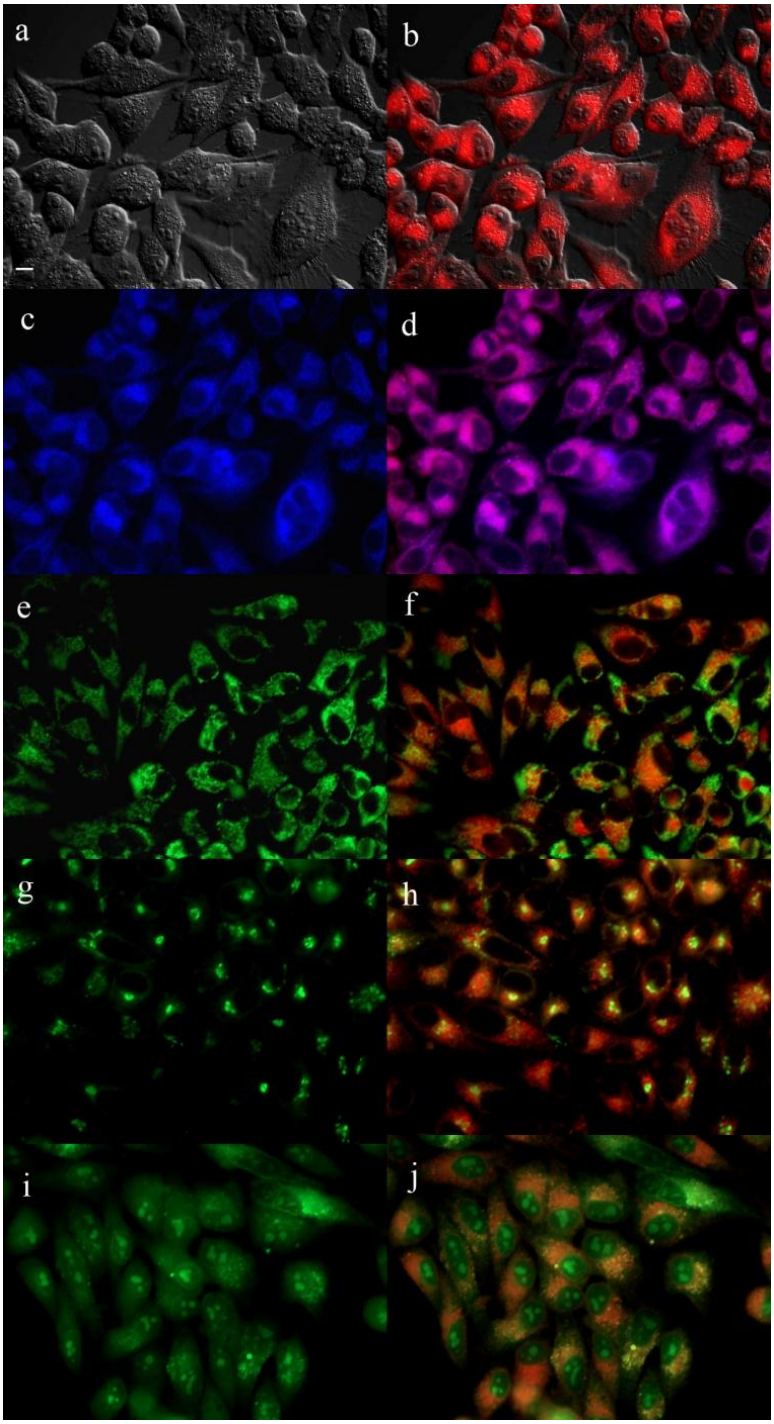

Figure 2.12: Subcellular localization of conjugate 15^2 LysCe_6TME in HEp2 cells at 10 µM for 18 h (a) phase contrast, (b) overlay of compound 15^2 LysCe_6 compound and phase contrast, (c) ER tracker Blue/White fluorescence (e) MitoTracker Green fluorescence, (g) BoDIPY Ceramide, (i) LysoSensor Green fluorescence, and (d, f, h, j) overlays of organelle tracers with compound fluorescence. Scale bar: 10 µm.

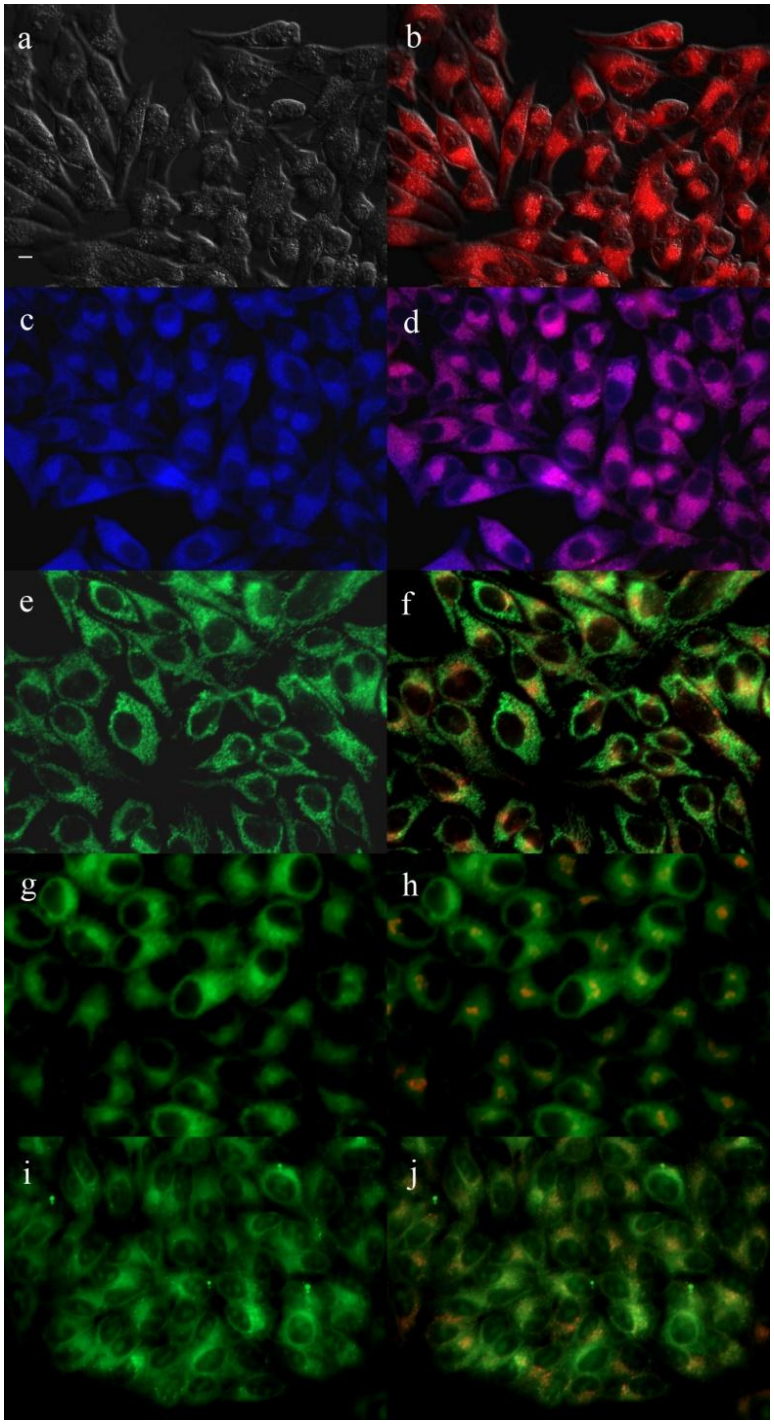

Figure 2.13: Subcellular localization of conjugate 15^2 PdLysCe$_6$TME in HEp2 cells at 10 µM for 18 h (a) phase contrast, (b) overlay of compound 15^2 PdLysCe$_6$ compound and phase contrast, (c) ER tracker Blue/White fluorescence (e) MitoTracker Green fluorescence, (g) BoDIPY Ceramide, (i) LysoSensor Green fluorescence, and (d, f, h, j) overlays of organelle tracers with compound fluorescence. Scale bar: 10 µm.

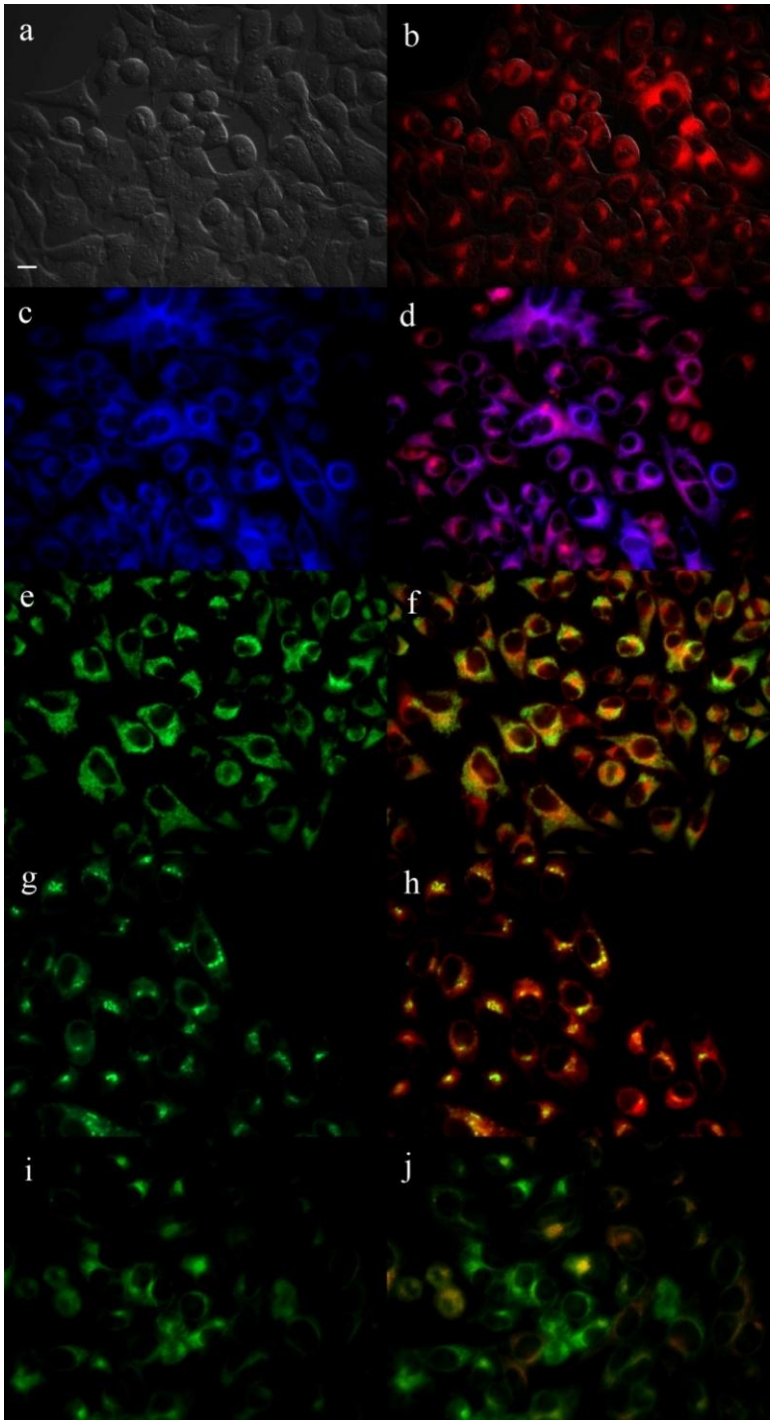

Figure 2.14: Subcellular localization of conjugate 17^3 LysCe_6TME in HEp2 cells at 10 µM for 18 h (a) phase contrast, (b) overlay of compound 17^3 LysCe_6 compound and phase contrast, (c) ER tracker Blue/White fluorescence (e) MitoTracker Green fluorescence, (g) BoDIPY Ceramide, (i) LysoSensor Green fluorescence, and (d, f, h, j) overlays of organelle tracers with compound fluorescence. Scale bar: 10 µm.

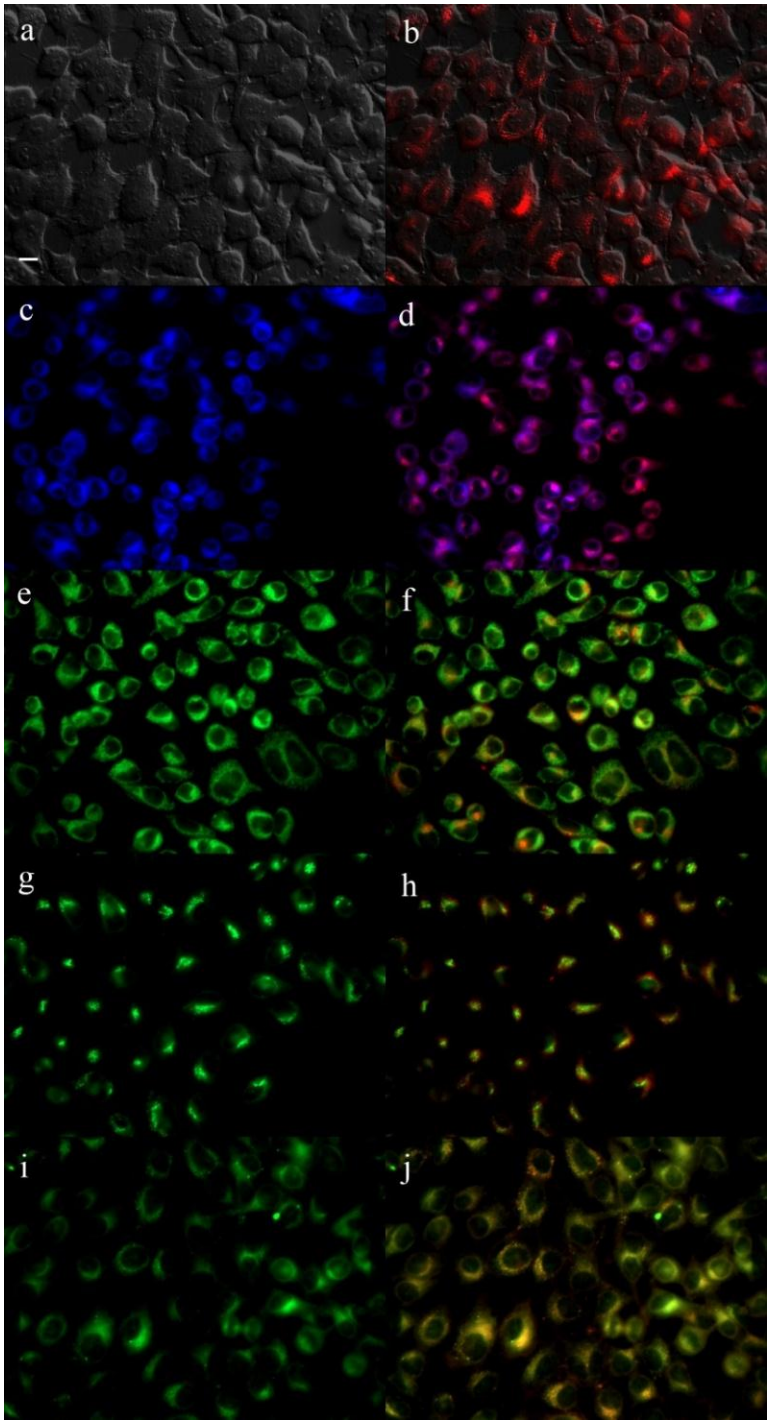

Figure 2.15: Subcellular localization of conjugate 13[1] ED-lysCe$_6$DME in HEp2 cells at 10 µM for 18 h (a) phase contrast, (b) overlay of compound 13[1] ED-lysCe$_6$ compound and phase contrast, (c) ER tracker Blue/White fluorescence (e) MitoTracker Green fluorescence, (g) BoDIPY Ceramide, (i) LysoSensor Green fluorescence, and (d, f, h, j) overlays of organelle tracers with compound fluorescence. Scale bar: 10 µm.

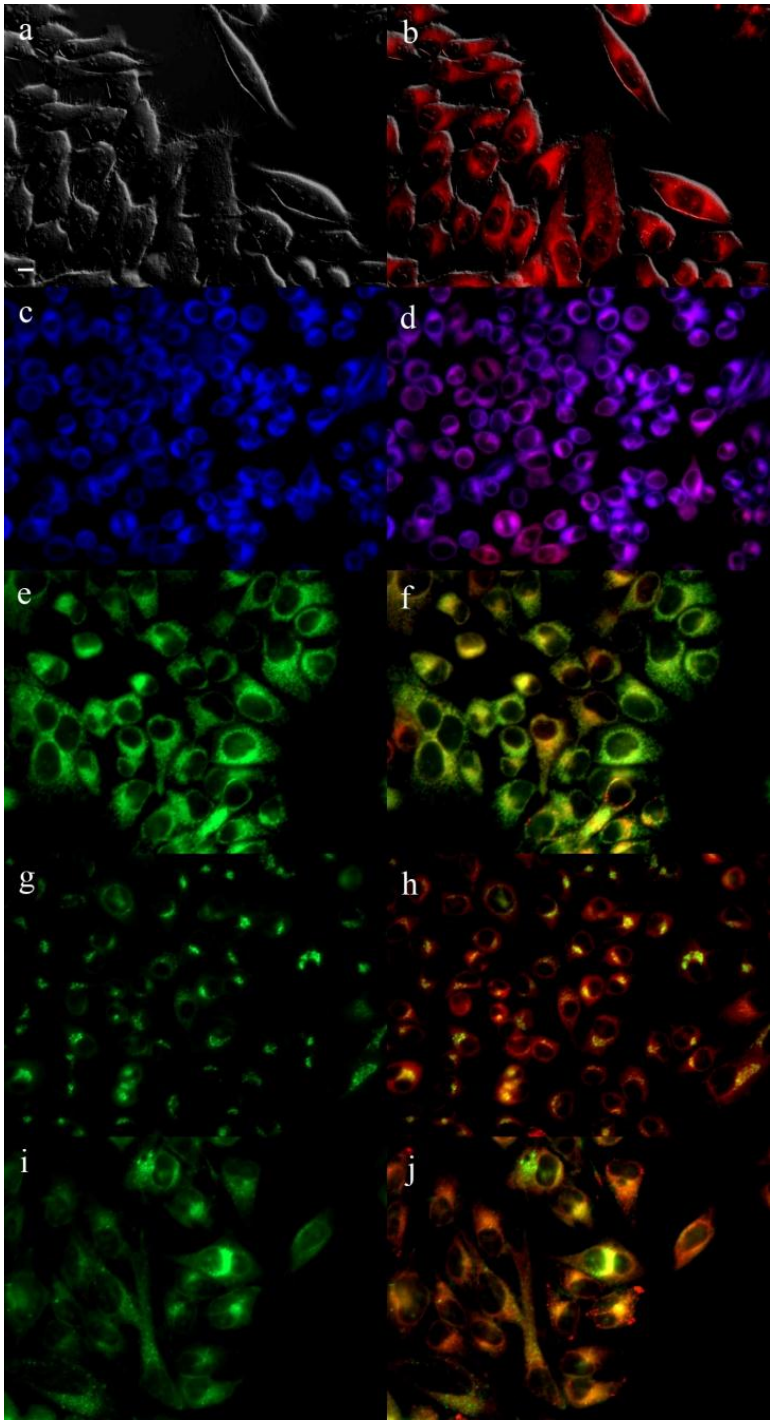

Figure 2.16: Subcellular localization of conjugate 13[1] $AspCe_6DME$ in HEp2 cells at 10 µM for 18 h (a) phase contrast, (b) overlay of compound 13[1] $AspCe_6$ compound and phase contrast, (c) ER tracker Blue/White fluorescence (e) MitoTracker Green fluorescence, (g) BoDIPY Ceramide, (i) LysoSensor Green fluorescence, and (d, f, h, j) overlays of organelle tracers with compound fluorescence. Scale bar: 10 µm.

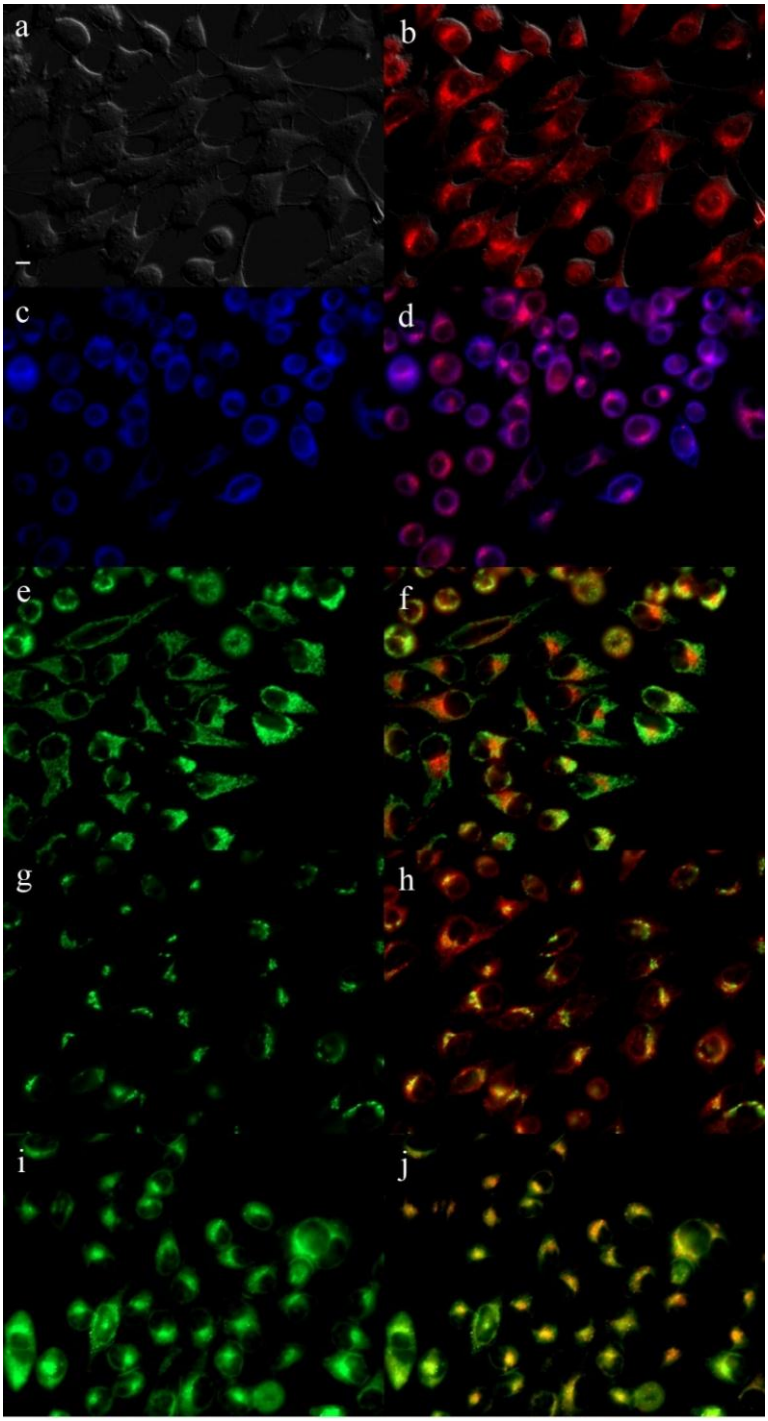

Figure 2.17: Subcellular localization of conjugate 13^1 β-Ala-AspCe_6DME in HEp2 cells at 10 µM for 18 h (a) phase contrast, (b) overlay of compound 13^1 β-Ala-AspCe_6 compound and phase contrast, (c) ER tracker Blue/White fluorescence (e) MitoTracker Green fluorescence, (g) BoDIPY Ceramide, (i) LysoSensor Green fluorescence, and (d, f, h, j) overlays of organelle tracers with compound fluorescence. Scale bar: 10 µm.

2.8 References

(1) Usuda, J.; Kato, H.; Okunaka, T.; Furukawa, K.; Tsutsui, H.; Yamada, K.; Suga, Y.; Honda, H.; Nagatsuka, Y.; Ohira, T.; Tsuboi, M.; Hirano, T. *J. Thorac. Oncol.* **2006**, *1*, 489.

(2) Light Sciences Oncology Inc: Bellevue, 2012.

(3) Hargus, J. A. Master's Thesis, Louisiana State University, 2005.

(4) Gomi, S.; Nishizuka, T.; Ushiroda, O.; Takahashi, H.; Sumi, S. *Heterocycles* **1998**, *48*, 2231.

(5) Hargus, J. A.; Fronczek, F. R.; Vicente, M. G.; Smith, K. M. *Photochem. Photobiol.* **2007**, *83*, 1006.

(6) Shiah, J.-G.; Sun, Y.; Peterson, C. M.; Straight, R. C.; Kopeček, J. *Clin. Cancer Res.* **2000**, *6*, 1008.

(7) Liu, W.; Jensen, T. J.; Fronczek, F. R.; Hammer, R. P.; Smith, K. M.; Vicente, M. G. H. *J. Med. Chem.* **2005**, *48*, 1033.

(8) Wender, P. A.; Mitchell, D. J.; Pattabiraman, K.; Pelkey, E. T.; Steinman, L.; Rothbard, J. B. *Proc. Natl. Acad. Sci. U S A.* **2000**, *97*, 13003.

(9) Ol'shevskaya, A. V.; Savchenko, A. N.; Zaitsev, A. V.; Kononova, E. G.; Petrovskii, P. V.; Ramonova, A. A.; Tatarskiy Jr, A.; Uvarov, O. V.; Moisenovich, M. M.; Kalinin, V. N.; Shtil, A. A. *J. Organomet. Chem.* **2009**, *694*, 1632.

(10) Wiehe, A.; Stollberg, H.; Runge, S.; Paul, A.; Senge, M. O.; Roder, B. *J. Porphyrins Phthalocyanines* **2001**, *5*, 853.

(11) Szaciłowski, K.; Macyk, W.; Drzewiecka-Matuszek, A.; Brindell, M.; Stochel, G. *Chem. Rev.* **2005**, *105*, 2647.

(12) Hargus, J. A.; Fronczek, F. R.; Vicente, M. G.; Smith, K. M. *Photochem. Photobiol.* **2007**, *83*, 1006.

(13) Smith, K. M.; Goff, D. A.; Simpson, D. J. *J. Am. Chem. Soc.* **1985**, *107*, 4946.

(14) Wasielewsi, M. R.; Svec, W. A. *J. Org. Chem..* **1980**, *45*, 1969.

(15) Hynninen, P. H.; Wasielewski, M. R.; Katz, J. J. *Acta Chem. Scand.* **1979**, *33*, 637.

(16) Pandey, R. K.; Sumlin, A. B.; Constantine, S.; Aoudla, M.; Potter, W. R.; Bellnier, D. A.; Henderson, B. W.; Rodgers, M. A.; Smith, K. M.; Dougherty, T. J. *Photochem. Photobiol.* **1996**, *64*, 194.

(17) Michalski, T. J.; Hunt, J. E.; Bradshaw, C.; Wagner, A. M.; Norris, J. R.; Katz, J. J. *J. Am. Chem. Soc.* **1988**, *110*, 5888.

(18) DiNello, R. K.; Chang, C. K., in "*The Porphyrins"* Dolphin, D Eds.; Academic Press: New York, 1978; Vol. 1.

(19) Mironov, A. F.; Nechaev, A. V. *Russian J. Bioorg. Chem.* **2003**, *29*, 110.

(20) Mironova, A. F.; Efremova, A. V.; Efremovaa, O. A.; Bonnet, R. *Tetrahedron Lett.* **1997**, *38*, 6775.

(21) *The Chlorophylls*; Seely, G. R.; Vernon, L. P., Eds.; Academic Press: London, 1966.

(22) Lötjönen, S.; Hynninen, P. H. *Synthesis* **1980**, 541.

(23) Hynninen, P. H.; Hyvarinen, K. *J. Org. Chem.* **2002**, 4055.

(24) Pennington, F. C.; Strain, H. H.; Svec, W. A.; Katz, J. J. *J. Am. Chem. Soc.* **1964**, *86*, 1418.

(25) *Protection Reactions, Medicinal Chemistry, Combinatorial Synthesis*; Hughes, A. B., Ed.; WILEY-VCH Verlag GmbH & Co. KGaA: Weinheim, 2011; Vol. 4.

(26) Kenner, G. W.; McCombie, S. W.; Smith, K. M. *J. Chem. Soc., Perkin Trans. 1* **1973**, 21.

(27) Green, T. W.; Wuts, P. G. M. *Protective Groups in Organic Synthesis*; Wiley-Interscience: New York, 1999.

(28) Manchand, P. S. *Chem. Commun.* **1971**, 667.

(29) Yazawa, H.; Tanaka, K.; Kariyone, K. *Tetrahedron Lett.* **1974**, 3995.

(30) Lovric, M.; Cepanec, I.; Vinkovic, V. *Croat. Chem. Acta* **2007**, *80*, 109.

(31) Bryan, D. B.; Hall, R. F.; Holden, K. G.; Huffman, W. F.; Gleason, J. G. *J. Am. Chem. Soc.* **1977**, *99*, 2353.

(32) Kaul, R.; Brouillette, Y.; Sajjadi, Z.; Hansford, K. A.; Lubell, W. D. *J. Org. Chem.* **2004**, *69*, 6131.

(33) Smith, K. M.; Lewis, M. W. *Tetrahedron Lett.* **1981**, *37*, 399.

(34) Ol'shevskaya *et al*. *Bioorgan. Med. Chem.* **2009**, *17*, 1297.

(35) Kessel, D. *J. Porphyrins Phthalocyanines* **2008**, *8*, 1009.

(36) Kessel, D. *Photochem. Photobiol.* **2008**, *49*, 447.

CHAPTER 3: SYNTHESIS AND CHARACTERIZATION OF WATER SOLUBLE CHLORIN e_6 DERIVATIVES FOR PHOTODYNAMIC THERAPY

3.1 Introduction

In the previous chapter the importance of chlorin e_6 derivatives in photodynamic therapy was discussed. The main goal was to increase the selectivity towards cancer cells over the normal cells. To increase the selectivity, different amino acids such as aspartic acid, which has negatively charged side chains, and lysine which has positively charged side chains at physiological pH were introduced to find out how these positively and negatively charged photosensitizers accumulate in different organelles in the cell. Also the positions of the amino acids were changed and a series of regioisomers was prepared to find how this affects the cell penetration. Cell studies revealed that all amino acid derivatives readily accumulated within human HEp2 cells in comparison with chlorin e_6 (**1**). However, the most phototoxic compounds were found to be the 13^1-regioisomers, bearing either an aspartic acid or a lysine residue directly conjugated to position-13 of the chlorin macrocycle, or connected via a β-alanine or ethylene diamine spacer. The most phototoxic compound of this series, and the most promising for PDT applications, is 13^1-aspartylchlorin e_6. But poor solubility of these molecules was one of the major drawbacks in the cellular studies. Apart from that some of these molecules tend to self-aggregate easily and result in lower cell uptake. To overcome these major shortcomings, a new series of chlorin e_6 derivatives which hold two amino acids in a single chlorin e_6 molecule were synthesized (Figure 3.1). The increase in the overall charge of the molecule and amphiphilicity, might increase the water solubility[1,2] and decrease the self-aggregation in biological media.[3]

Recent literature reported that increasing water solubility of photosensitizers helps to increase the cell uptake[4,5] and hence increase the phototoxicity.[6,7] Kimani and coworkers had synthesized mono-, di- and tri-PEGylated chlorin e_6 photosensitizers with tri(ethylene glycol) attached at three carboxylic positions in chlorin e_6.[6] These were tested for solubility and hydrolytic stability and also phototoxicity,

cell uptake and localization in ovarian OVCAR-5 cancer cells. Their results confirmed that the increasing number of PEG groups increased the water solubility and uptake into the cancer cells. Computational studies also indicated that PEG groups will increasingly resist formation of aggregates by π-π stacking. These PEG chains can wrap across the chlorin ring to prevent π-π stacking. Most significantly an increased number of PEG groups increased the phototoxicity, and the increase was parallel to the cell uptake.

Our hypothesis was that a higher number of charged substituents will increase the phototoxicity by increasing cell uptake. As in the previous project, all possible regioisomers of diamino acid chlorin e_6 derivatives were synthesized (Figure 3.1). It was found from our previous study, that the position of the amino acid plays a vital role in determining the conformation of the molecule.[8] New synthetic routes were developed to synthesize all three regioisomers. Both the 15^2,17^3-diamino and 13^1,17^3-diamino derivatives were synthesized starting from chlorin e_6 (**1**) and the 13^1,15^2-diamino derivatives were synthesized from pheophytin a.

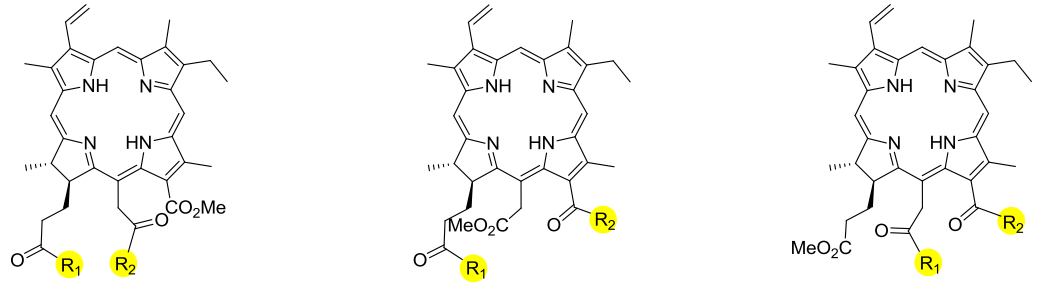

15^2,17^3-Chlorin e_6 derivative 13^1,17^3-Chlorin e_6 derivative 13^1,15^2-Chlorin e_6 derivative

Figure 3.1: Di-amino acid regioisomers of chlorin e_6

The aims of the present work were to determine: 1) the degree to which diaminochlorin e_6 derivatives were taken up and localized in cancer cells, 2) the main site of accumulation (which cell organelle), and 3) whether the position and charge of the amino acid substituents influenced the photo and dark toxicity.

3.2 Synthesis

3.2.1 Synthesis of 15^2,17^3-diaspartylchlorin e_6 derivative

A major side product in the synthesis of 15^2-mono-aspartylchlorin e_6 derivatives was the 15^2,17^3-diaspartylchlorin e_6 derivative **5**.[9] The yield of the byproduct **5** can be increased by changing the number of equivalents of coupling reagent and amino acid. According to the proposed mechanism, DCC and DMAP activated the acetic side chain and formed the anhydride intermediate **2**. The excess coupling reagent can activate the propionic acid side chain to form O-acylisourea anhydride intermediate **3** (Scheme 3.1).

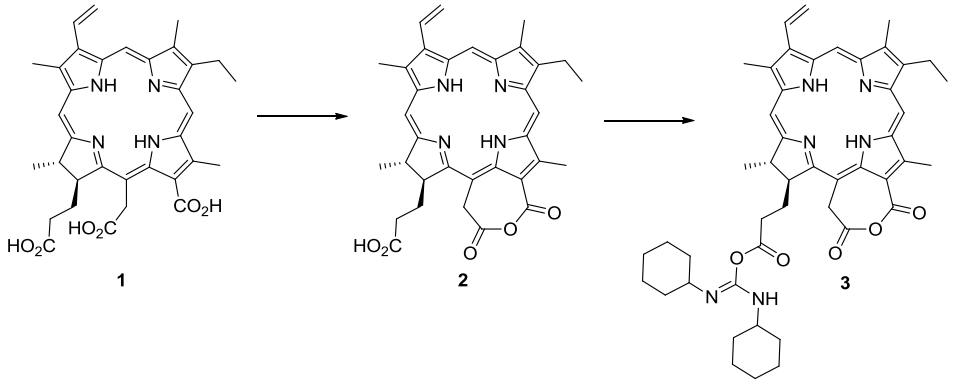

Scheme 3.1: Proposed intermediates in the formation of 15^2-17^3 di-amino acid derivative **4**.

Then, the free amine group of the amino acid can attack both carbonyl groups in intermediate **3**, one in the anhydride ring and the other one in the O-acylisourea group. Mechanistic studies revealed the nucleophile first attacks the more reactive 15^2 position of the anhydride ring instead of the 13^1 position, regardless of the size or nucleophilicity of the molecule. Then the second equivalent can react with the O-acylisourea group to form diaminochlorin e_6 derivative **4**.

The detailed synthetic route to 15^2,17^3-diaspartylchlorin e_6 methyl ester (**6**) is shown in Scheme 3.2. It was possible to obtain diaspartyl methyl ester **6** in 33% overall yield from chlorin e_6 (**1**). The optimal yield of diaspartyl chlorin e_6 **6** (26%) was obtained with activation of chlorin e_6 with three

equivalents of DCC and DMAP in CH_2Cl_2 at room temperature for two hours followed by coupling with 2.5 equivalents of di-*tert*-butyl protected aspartic acid for 24 hours.

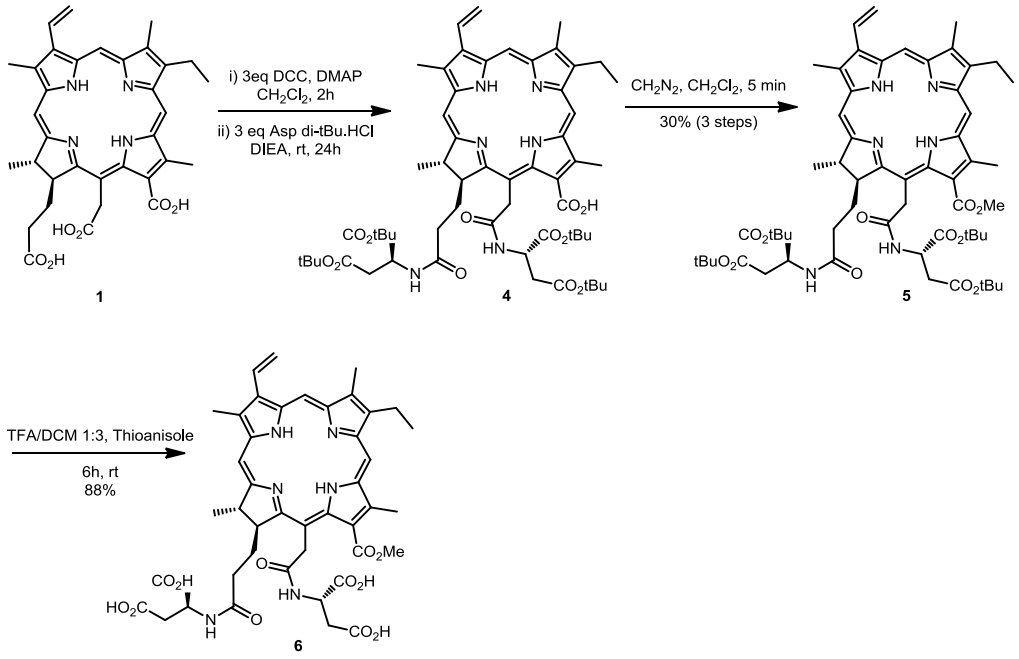

Scheme 3.2: Synthesis of 15^2,17^3-diaspartylchlorin e_6 methyl ester (**6**)

Less than three equivalents of DCC and aspartic acid tend to form significant amounts of the 15^2-monoaspartic acid conjugate as a side product. When the number of equivalents of either DCC or aspartic acid was increased, the yield of diaspartyl chlorin e_6 **4** improved. But it was not possible to stop the formation of the mono-aspartyl conjugate as a side product. Longer reaction times also helped to increase the yield of diaspartyl derivative **4**. After confirming the formation of tert-butyl protected diaspartyl chorin e_6 **4** by mass spectrometry, freshly prepared diazomethane gas was bubbled through the mixture for five minutes to convert remaining free acid groups into methyl esters. This reaction was monitored by TLC. It was possible to see two new spots in the TLC plate. A brighter spot with lower R_F value belongs to the desired product 15^2,17^3-diaspartylchlorin e_6 **5** and the second spot, which has a higher R_F value similar to 15^2-monoaspartlychlorin e_6. Purification was achieved via silica gel column chromatography and the identity of the esterified product **5** was confirmed using ^{1}H NMR and mass

spectrometry. ^{1}H NMR spectroscopy shows four singlets around 3.0 to 4.5 ppm which integrated to three protons each. Out of four, three peaks belong to the methyl groups directly connected to the macrocycle and the remaining peak belongs to the 13^2 methyl ester group. The most downfield singlet at δ 4.25 confirmed the formation of the 13^1 methyl ester because this peak is unique to the methyl group on the formic side chain of chlorin e_6 (**1**). That observation confirmed that aspartic acid coupled with the acetic and propionic side chains of the molecule.

In the final step, all four *tert*-butyl ester protections in molecule **5** were removed in a TFA/CH_2Cl_2 mixture for six hours at room temperature. The solvent was evaporated and aqueous work-up was performed to neutralize the remaining TFA. But basic aqueous work-up was unsuccessful due to the higher water solubility of these compounds. To avoid the aqueous work-up, TFA and CH_2Cl_2 was first removed by blowing nitrogen over the solution and the sample was placed in a high vacuum for four hours. Finally the product was freeze-dried by dissolving it in water/acetonitrile mixture. Once the sample was neutralized the color changed from purple to dark green. The identity of product **6** was confirmed by ^{1}H NMR, ^{13}C NMR and mass spectrometry.

3.2.2 Synthesis of 13^1,17^3-diaspartylchlorin e_6 derivative

There are two possible routes to synthesize the 13^1,17^3 chlorin e_6 conjugate **10**: 1) coupling of the first amino acid to the propionic acid chain of pheophorbide **8** and subsequent isocyclic ring opening of pheophorbide **8** with ethylenediamine followed by coupling of the second amino acid to the free amine group of the resulting chlorin derivative (Scheme 3.3), or 2) selective esterification of the acetic acid side chain (15^2 ester) of chlorin e_6 (**1**) followed by coupling with two equivalents of an amino acid to afford the 13^1,17^3-di(amino acid) derivative (Scheme 3.4).

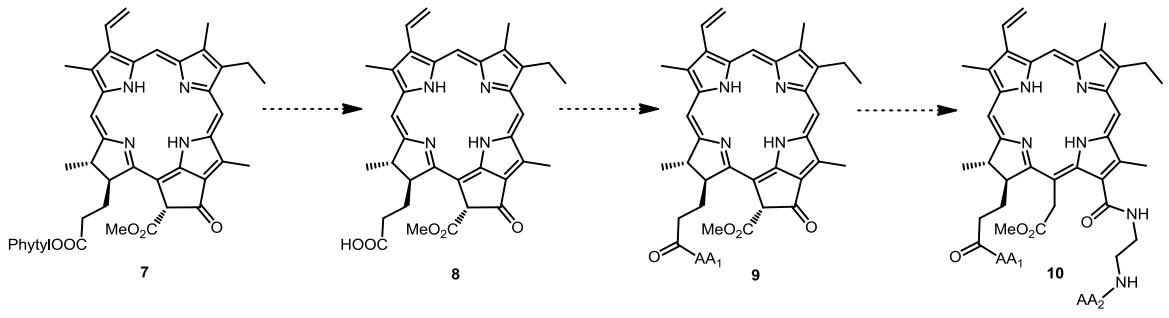

Scheme 3.3: Proposed route to obtain 13^1,17^3-di(amino acid) derivative

In the first method, pheophorbide a (**8**) can be obtained by selective hydrolysis of the phytyl ester group of pheophytin a (**7**) using the Wasielewski and Svec procedure as mentioned in the previous chapter.[10] Then the amino acid can be coupled to the propionic side chain to obtain the pheophorbide derivative **9**. Then the isocyclic ring can be cleaved using ethylene diamine as accomplished in the previous chapter.[11] That will provide a free amine group to couple the second amino acid to the 13^1 position to obtained 13^1,15^2 derivative **10**.

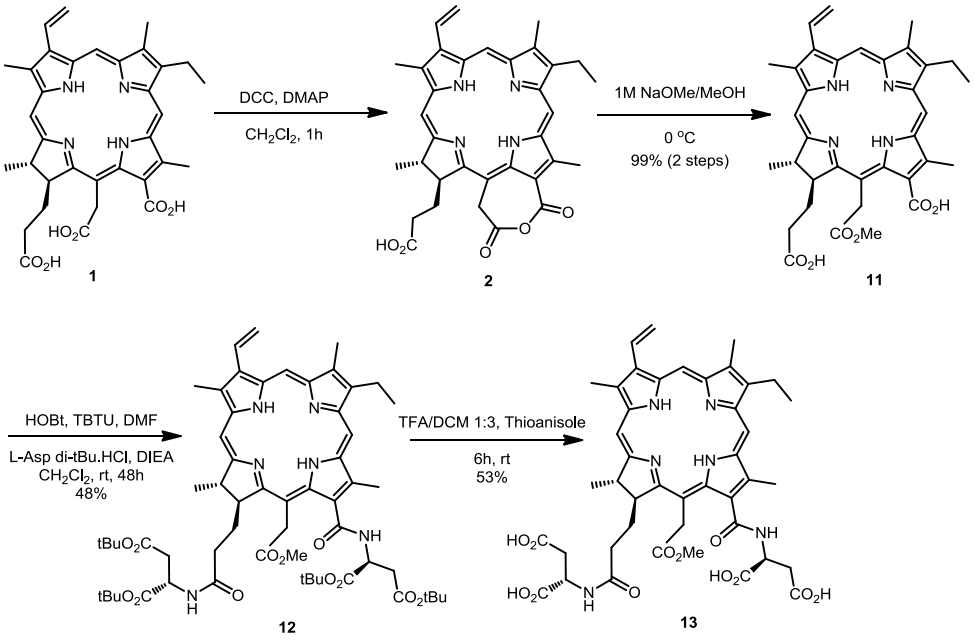

Scheme 3.4: Synthesis of 13^1,17^3-diaspartyl chlorin e_6 methyl ester (**13**)

The key step in the second method is the selective protection of the acetic acid side chain of chlorin e_6 (**1**) in the presence of the formic and propionic carboxylic side chains. From the previous work,

it was found that the acetic acid group of chlorin e_6 can be activated selectively by forming a cyclic anhydride. Chlorin e_6 was activated using one equivalent of DCC and DMAP to form the anhydride intermediate (**2**).[9] Formation of cyclic anhydride **2** can be confirmed by using UV-Vis spectroscopy. Then freshly prepared 0.5 M sodium methoxide was added until the color of the reaction mixture change from brown-purple to dark green. Mass spectroscopy confirmed the formation of desired product **11**. Purification of di-acid **11** was challenging due to its high polarity. After work-up it was possible to obtain a ^{1}H NMR spectrum of the crude product and it was clear enough to identify the unique peak for the 15^2 methyl ester, and sufficiently pure for the next step. Appearance of a new peak at 3.7 ppm for 3 protons provided evidence that esterification took place at the acetic acid side chain. Then *tert*-butyl-protected aspartic acid was coupled with crude 15^2-chlorin e_6 monomethyl ester. The optimal yield was obtained with HOBt and TBTU as coupling reagents at room temperature for 48 hours.[12] This reaction was monitored by TLC. The product was purified via silica gel column chromatography and the first moving band with 5% methanol/DCM was collected. The structure of product **12** was confirmed by mass and ^{1}H NMR spectroscopy. Purified *tert*-butyl protected diaspartyl chlorin e_6 **12** was treated with TFA/CH_2Cl_2 mixture for six hours at room temperature to deprotect all four carboxylic acid groups. Pure compound **13** was obtained after removal of TFA. The final product, 13^1,17^3-diaspartyl chlorin e_6 **13**, was obtained in 28% yield over four steps.

3.2.3 Synthesis of 13^1,15^2-di(amino acid) chlorin e_6 derivatives

Previous studies revealed that the formic and acetic acid derivatives of chlorin e_6 have more photosensitizing ability compared to propionic acid conjugates.[8] So it was assumed that the 13^1,15^2 di(amino acid) derivatives may show more potent photosensitizing ability in this diamino acid series compared to the two other regioisomers. Therefore two different amino acid conjugates of 13^1,15^2 regioisomer were synthesized.

The main challenge was to protect the propionic side chain in the presence of other two carboxyl groups. There is no known chemical method to selectively methylate the propionic side chain of chlorin e_6 without methylating the acetic side chain. Esterification with methanol under acidic conditions will form the 15^2,17^3-chlorin e_6 dimethyl ester.[13] Diazomethane will methylate all three carboxylic group to form chlorin e_6 trimethyl ester.[14] But in the recent literature there is reported a chemoselective aminolysis of the β-keto ester of methyl pheophorbide a.[15-17] This opens up a new route to synthesize 13^1,15^2 chlorin e_6 derivative from methyl pheophorbide a.

Previously, Shinoda and coworkers reported a facile transesterification of the β-keto ester of methyl pheophorbide a.[18] These authors were able to introduce various alcohols and steroid groups in the presence of 2-chloro-1-methylpyridinium iodide (CMPI) and of 4-(*N*,*N*-dimethylamino)pyridine (DMAP) to the 13^2 position of pheophorbide. Recently Haavikko and coworkers also reported a selective aminolysis of β-keto ester of the methyl pheophorbide a.[15] They used various primary, secondary and aromatic amines for the aminolysis of the β-keto ester. It is known that aminolysis of the β-keto ester is usually facile compared to unactivated esters.[19,20] In the previous literature the formation of β-enaminoesters by reaction between secondary amines and β-ketoesters under low temperatures is described.[21] It was noticed that at higher temperatures they tend to form substantial amounts of the corresponding β-ketoamide along with the expected enaminoester.

We have observed the same behavior with pheophorbide a. In the previous work, it was possible to open the isocyclic ring of pheophorbide a (by cleaving the β-keto ester) using ethylene diamine at room temperature. This time it was noticed at higher temperatures (90 ^{o}C in toluene) that reaction with ethylene diamine tended to form two major products (two new very close spots in TLC). Both products were isolated using preparative TLC and characterized by ^{1}H NMR and mass spectroscopy. One of the products still clearly shows the peak unique for the pheophorbide isocyclic ring: the proton

appears as a sharp singlet at δ 6.26. The disappearance of the peak for the methyl group of the β-ketoester and new peaks for the ethylene diamine methylene groups confirmed the formation of β-ketoamide **24**. The second product was identified as the expected chlorin e_6 derivative **26**. As reported in the literature, temperature and the concentration of the amine play vital roles in deciding the major product.[15] A large excess of amine and mild heating always produced the classical ring-opened product **26**, and a slight excess of amine in refluxing toluene yielded β-ketoamide **24** as the major product.

The exact mechanism for this reaction is still unclear. However Gravel and coworkers had proposed two possible mechanisms to form β-ketoamide at high temperature (Scheme 3.5).[21] Their first possible path involves an internal amine transfer from hemiaminal intermediate **15** to the ester carbonyl group through a four membered transition state. Another possible mechanism involves formation of a four membered β-lactone **18** followed by cleavage of this lactone by amine to yield the β-ketoamide **19**. These two mechanisms are also consistent with the reported high diastereomeric excess of the R-isomer of pheophorbide **24** (at $C13^2$).[15] Indeed the R-isomer is more stable compared to the S-isomer due to steric interaction between the 13^2 and 17 side chains of pheophorbide. However, if the reaction goes through an enol intermediate, the $C13^2$ position can be epimerized and end up as a mixture of isomers.

At low temperature, the reaction follows a different mechanism, as shown in Scheme 3.5. The first step is the same as in the previous mechanisms. Free amine will attack at the more nucleophilic keto group of molecule **14** to form hemiaminal **20**. Then the isocyclic ring will cleave between the $C13^1$-$C13^2$ atoms and form the chlorin e_6 derivative **21**. The ease of opening of the isocyclic ring is due to the release of the strain in the ring upon opening. It is clear that at higher temperatures reaction goes through a high energy transition state and forms the keto amide **19**, but at lower temperature it follows the low energy path and forms more stable ring-opened product **22**.

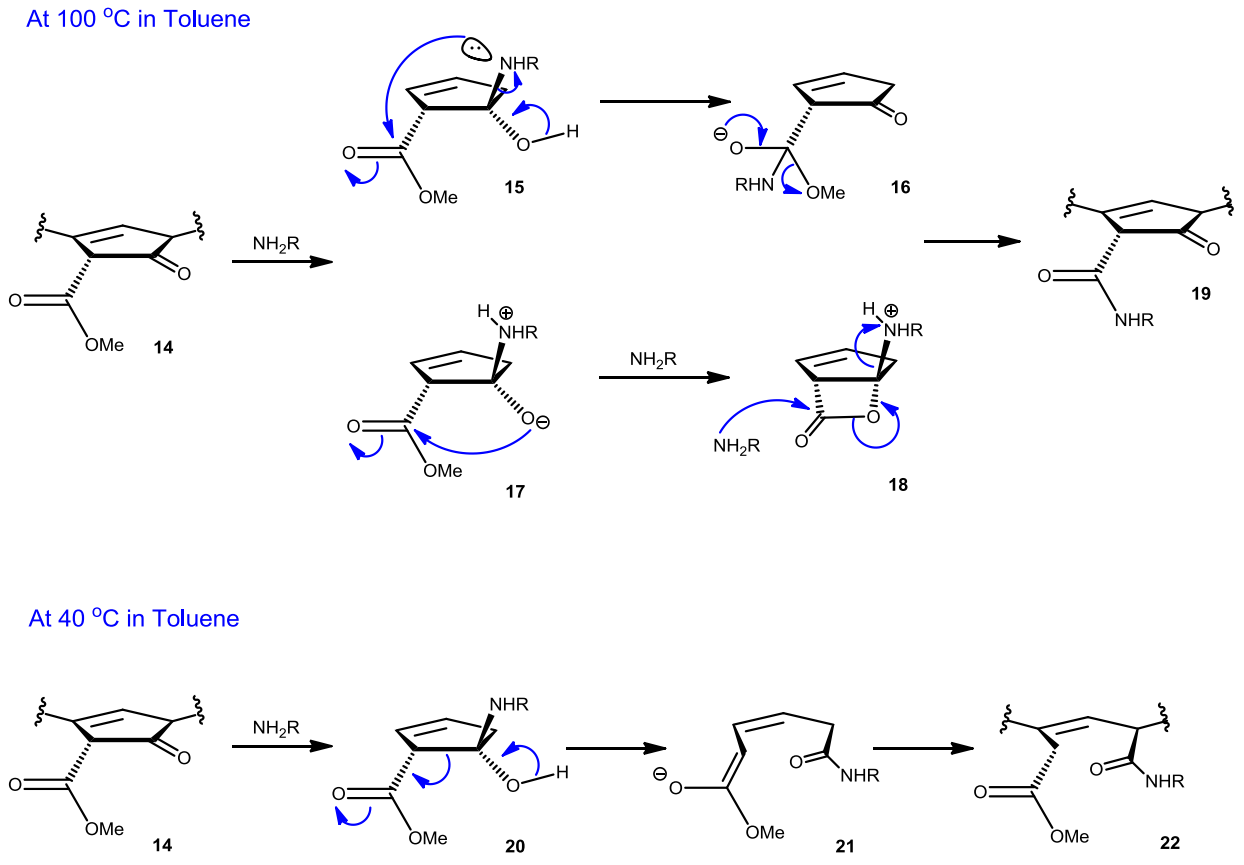

Scheme 3.5: Suggested mechanism for aminolysis of the β-keto ester of methyl pheophorbide a at high temperature (top), and the corresponding ring-opening reaction of methyl pheophorbide a at low temperature (bottom).

The first attempt to introduce the ethylene diamine to both ester and keto groups of the pheophorbide **23** to form 13[1] and 15[2] substituted chlorine e_6 derivative **25** was unsuccessful (Scheme 3.6). Both β-keto ester aminolysis and ring-opening reactions were attempted in one pot. First pheophorbide **23** and ethylene diamine were refluxed in toluene until disappearance of the starting material **23**, as monitored by TLC. Then excess amine was added and the mixture was stirred at 40 °C for 12 hours to complete the ring cleavage reaction. Unfortunately, this process resulted in a mixture of compounds, including the desired product **25**. Mass spectrometry revealed three major compounds in

this mixture, as shown in Scheme 3.6. Purification of these compounds was challenging due to high polarity of the free amine groups.

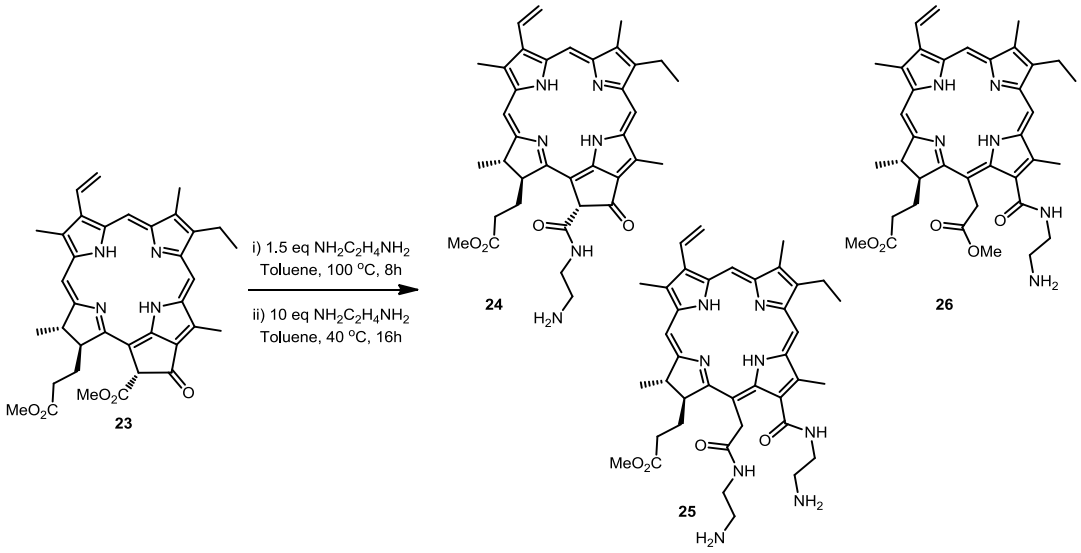

Scheme 3.6: Attempted synthesis of 13[1] and 15[2] ethylenediamine substituted chlorine e_6 derivative **25**

Then it was decided to use half protected ethylene diamine to simplify the purification process. As indicated by TLC, aminolysis of the β-keto-ester of pheophorbide **23** with protected ethylene diamine was completed after 12 hours. But the second step, ring-cleavage was unsuccessful with Boc protected ethylene diamine, possibly due to steric bulkiness of the amine. Next it was decided to purify the product **27** before going on to the ring cleavage reaction. As it was possible to achieve the isocyclic ring cleavage using free ethylene diamine, unprotected ethylene diamine was used for the second step and the diethylene diamine substituted product **28** was obtained. Product **28** was purified using a short silica gel column and its identity was confirmed using mass and ^{1}H NMR spectroscopy. Boc deprotection was achieved using TFA to obtain the free amines for the coupling reaction. Subsequent coupling with protected aspartic acid followed by deprotection produced the desired product **30**, in 15% yield over 5 steps from pheophorbide a (**23**, Scheme 3.7).

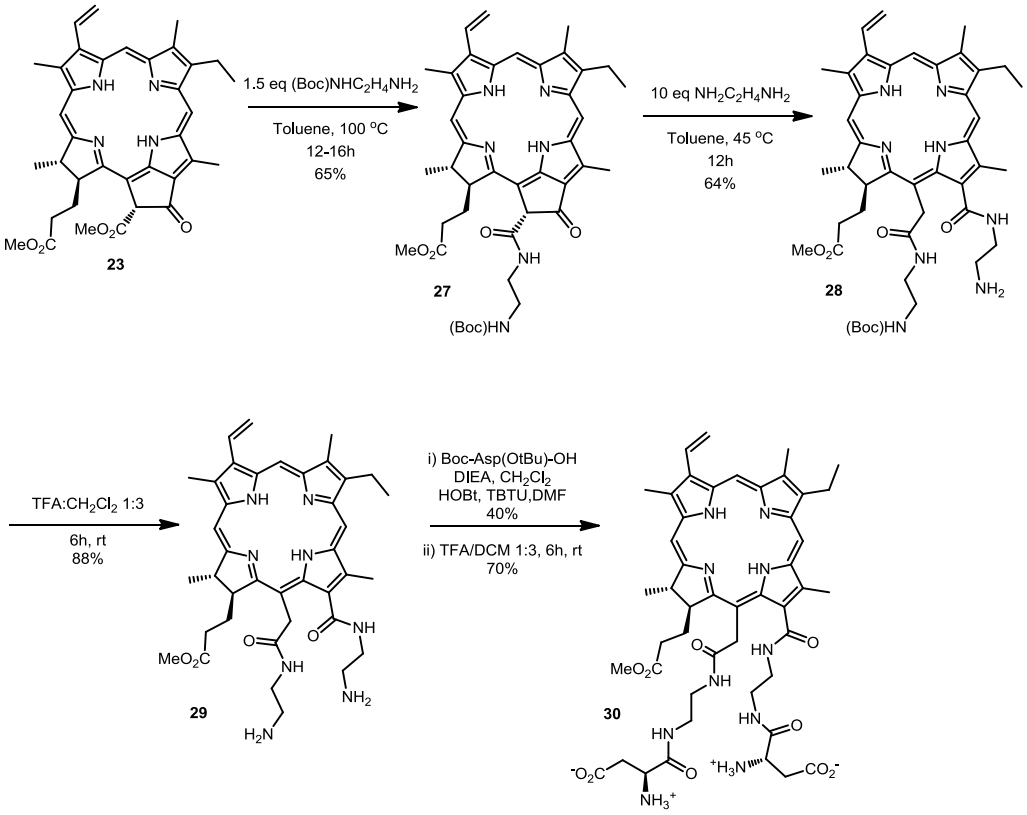

Scheme 3.7: Synthesis of 13^1,15^2-diethylenediaminylaspartylchlorin e_6 **30**

Advantage was taken of a previous route to introduce two types of amino acids to the 13^1 and 15^2 positions. Protected β-alanine was used for the aminolysis reaction as it greatly reduces the unwanted ring-opened product and creates a carboxylic end to couple aspartic acid through its amino group. Subsequent aminolysis with protected β-alanine followed by deprotection of the *tert*-butyl ester provided free acid **31**. Its identity was confirmed by mass spectroscopy. Free acid **31** was activated and coupled with protected aspartic acid to obtain pheophorbide derivative **32**. This was purified and characterized by ^{1}H NMR and mass spectroscopy. A classical ring-opening reaction was performed with excess ethylene diamine in toluene at 40 ^{o}C to provide the chlorine e_6 derivative **33**. The reaction was monitored using UV-Vis spectroscopy, and the color changed from dark green to bright green during isocyclic ring-opening. ^{1}H NMR spectroscopy shows the new peaks for ethylene diamine and mass spectroscopy confirmed the identity of the product. Then boc protected lysine was coupled with free

amine group of chlorin e_6 derivative **33** to produce the desired 13^1-ethylenediaminyllysinyl-15^2-β-alanylaspartylchlorine e_6 *tert*-butyl methyl ester. This product was purified using silica gel chromatography. Finally, global deprotection with TFA in DCM produced the final product **34** in 9% yield over six steps starting from pheophorbide a (Scheme 3.8).

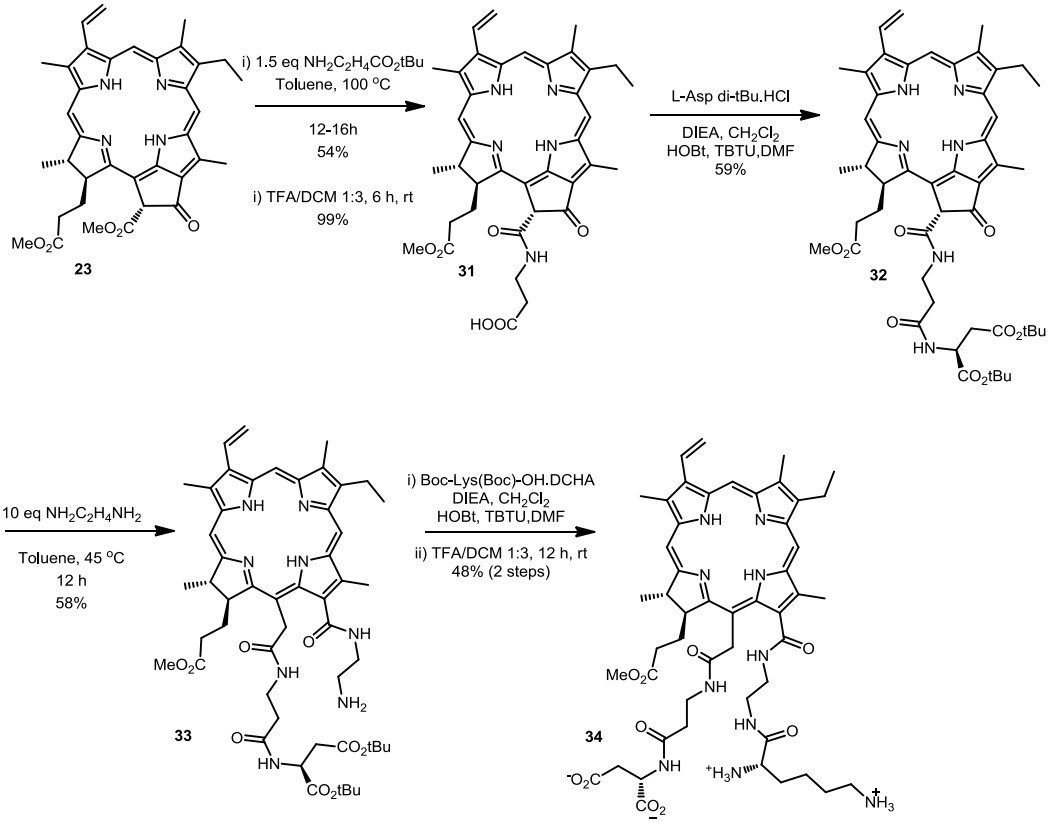

Scheme 3.8: Synthesis of 13^1,15^2-di(amino acid) derivative **34**

3.3 Cell Culture Studies

3.3.1 Time-dependent Cellular Uptake

The results obtained for the time-dependent uptake of chlorin e_6 and its derivatives at a concentration of 10 μM in human HEp2 cells are shown in Figure 3.2. The 13^1 amino acid conjugates of chlorin e_6 **34**, **30** and 13^1-AspCe_6DME were readily taken up by cells compared to unconjugated chlorin e_6 (**1**). However, the 15^2,17^3-di(Asp)Ce_6 MME (**6**) and 13^1,17^3-di(Asp)Ce_6 MME (**13**) showed the similar uptake kinetics to unconjugated chlorin e_6 (**1**). The 13^1-EDLys-15^2-β-AlaAspCe_6 MME (**34**) which is a zwitterion at physiological pH, showed the highest cell uptake compared to the other derivatives. In comparison with unconjugated chlorin e_6 (**1**), compounds **34** and **30** showed 5-fold and 4-fold cellular uptake after 24 hours, respectively. This is probably due to the high amphiphilicity and the linear extended conformation compared to other amino acid derivatives. The uptake of derivative **34** and **30** continues to increase over the 24 hour period investigated, therefore one can expect much higher uptake for these derivative with time. However di-amino acid derivative **13** and **6** showed similar uptake to unconjugated chlorin e_6; this might be due to the conjugation at the propionic side chain resulting in non-linear conformations for these molecules.[8] Previous computational studies of mono-conjugated chlorine e_6 derivatives revealed that the 17^3-conjugated chlorin e_6 derivatives assume a L-shape conformation with the side chain positioned perpendicular to the macrocyclic plane.[8] However in the case of the 15^2- and 13^1-conjugated derivatives, the amino acid side chain extends away from the macrocycle resulting in nearly linear conformations compared to 17^3-conjugated derivatives. A similar conformational change can be expected in the di-conjugated series. Amino acid conjugation at propionic side chain (compound **13** and **6**) makes it difficult for them to pass through the cell membrane, resulting the lower cellular uptake.

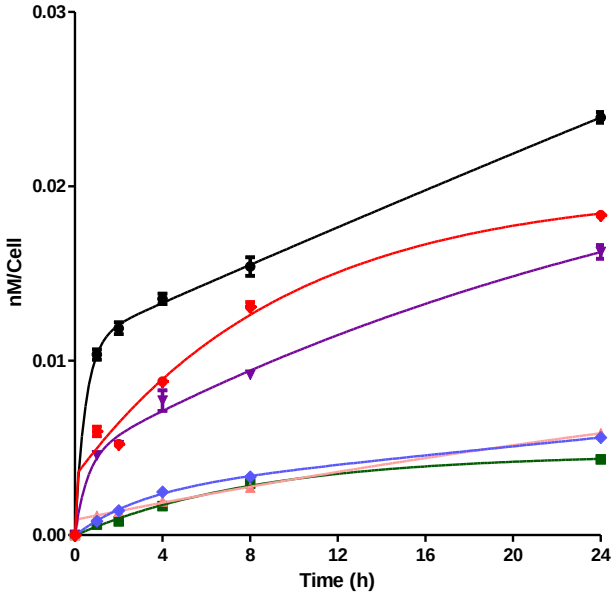

Figure 3.2: Time-dependent uptake of chlorin e_6 (**1**, green line) and its derivatives 15^2,17^3-di(Asp)Ce_6 MME (**6**, blue line), 13^1,17^3-di(Asp)Ce_6 MME (**13**, light pink line), 13^1,15^2-di(EDAsp)Ce_6 MME (**30**, purple line), 13^1-EDLys-15^2-β-AlaAspCe_6 MME (**34**, black line), 13^1-AspCe_6DME (red line), at 10 μM by HEp2 cells.

3.3.2 Cytotoxicity

The dark cytotoxicity and phototoxicity of chlorin e_6 and its amino acid conjugated derivatives was evaluated in HEp2 cells exposed to increasing concentrations of each compound, up to 400 μM. Toxicity of 13^1 AspCe_6 DME, which showed the highest phototoxicity in the mono conjugated amino acid series, was compared with the toxicity of di-conjugated chlorin e_6 series. The 13^1 lysine isomer 13^1-LysCe_6 DME was also tested with the new series and the dark and phototoxicity results are shown in Figures 3.3 and 3.4, respectively, and summarized in Table 3.1. Chlorin e_6 (**1**), 15^2,17^3-di(Asp)Ce_6 MME (**6**) and 13^1,17^3-di(Asp)Ce_6 MME (**13**) were found to be the least toxic in the dark and also in the presence of light. But all other mono- and di-substituted derivatives showed significant toxicity, even in the absence of light. After expose to light, all these derivatives were highly toxic to HEp2 cells. Mono substituted derivatives 13^1-LysCe_6 DME and 13^1-AspCe_6 DME were found to be most toxic compared to the di-substituted derivatives. The estimated IC_{50} values of the most phototoxic 13^1-chlorin e_6 derivatives 13^1-

$AspCe_6$ DME and 13^1-$LysCe_6$ DME, are 0.8 and 0.7 μM, respectively, and this is comparable to our previous cytotoxicity results of mono-conjugated derivatives. Surprisingly, our results revealed that the introduction of a second amino acid decreased the cytotoxicity of the compound. For example, the 13^1,15^2-di(EDAsp)Ce_6 MME (**30**) and 13^1,17^3-di(Asp)Ce_6 MME (**13**) were less phototoxic than its 13^1 mono substituted derivative 13^1-$AspCe_6$ DME by approximately 10-fold and 27-fold, respectively. As was expected, among the di-substituted series, the 13^1,17^3-di(Asp)Ce_6 MME (**13**) and 15^2,17^3-di(Asp)Ce_6 MME (**6**) showed the least cytotoxicity, probably due to conjugation at the propionic side chain (17^3 position). On the other hand the 13^1-EDLys -15^2-β-AlaAspCe_6 MME (**34**) and 13^1,15^2-di(EDAsp) Ce_6 MME (**30**) showed the highest phototoxicity with IC_{50} of 5.1 and 7.6 μM, respectively, but still more than 5-fold lower than the mono-conjugated derivatives 13^1-$AspCe_6$ DME and 13^1-$LysCe_6$ DME. These results show that the conjugation at the propionic and/or acetic acid chains of 13^1 $AspCe_6$ MME derivative greatly reduces its cytotoxicity. Cell uptake results of di-conjugated compounds also complemented the phototoxicity results. 13^1-EDLys-15^2-β-AlaAspCe_6 MME (**34**) has the highest cell uptake and the highest phototoxicity of the di-amino acid derivatives and 15^2,17^3-di(Asp)Ce_6 MME (**6**) and 13^1,17^3-di(Asp)Ce_6 MME (**13**) showed the lowest cell uptake and lowest phototoxicity in the di-amino acid conjugated series.

Table 3.1: Cytotoxicity (HEp2 cells) for chlorin e_6 and its derivatives using the MTT assay

Compound	**Dark toxicity (IC_{50}, μM)**	**Phototoxicity (IC_{50}, μM)**	**Ratio**
Chlorin e_6 (**1**)	330	10.6	31
15^2,17^3-di(Asp)Ce_6 MME (**6**)	>400	21	>19
13^1,17^3-di(Asp)Ce_6 MME (**13**)	286	22	13
13^1,15^2-di(EDAsp)Ce_6 MME (**30**)	76	7.6	10
13^1-EDLys-15^2-β-AlaAspCe_6 MME (**34**)	58	5.1	11
13^1-$AspCe_6$ DME	58	0.7	35

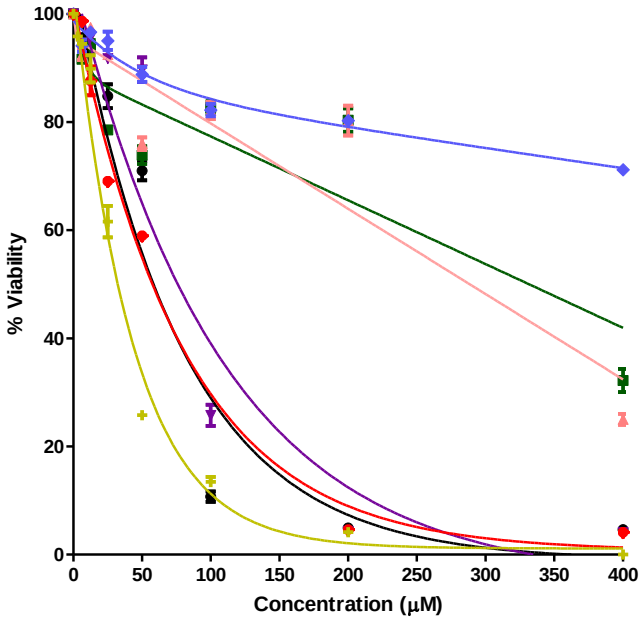

Figure 3.3: Dark toxicity of chlorin e_6 (**1**, green line) and its derivatives 15^2,17^3-di(Asp)Ce_6 MME (**6**, blue line), 13^1,17^3-di(Asp)Ce_6 MME (**13**, light pink line), 13^1,15^2-di(EDAsp)Ce_6 MME (**30**, purple line), 13^1-EDLys-15^2-β-AlaAspCe_6 MME (**34**, black line), 13^1-AspCe_6 DME (red line), 13^1-LysCe_6 DME (yellow line) toward HEp2 cells using 1 J/cm2 light dose and the Cell Titer Blue assay.

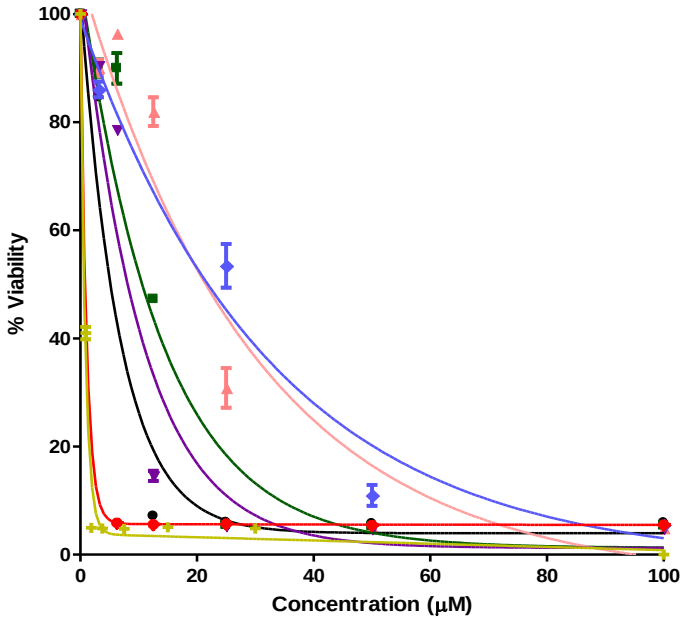

Figure 3.4: Phototoxicity of chlorin e_6 (**1**, green line) and its derivatives 15^2,17^3-di(Asp)Ce_6 MME (**6**, blue line), 13^1,17^3-di(Asp)Ce_6 MME (**13**, light pink line), 13^1,15^2-di(EDAsp)Ce_6 MME (**30**, purple line), 13^1-EDLys-15^2-β-AlaAspCe_6 MME (**34**, black line), 13^1-AspCe_6 DME (red line), 13^1-LysCe_6 DME (yellow line) toward HEp2 cells using 1 J/cm2 light dose and the Cell Titer Blue assay.

3.4 Experimental

15^2,17^3-Diaspartylchlorin e_6 tetra(*tert)*butyl methyl ester (**5**):

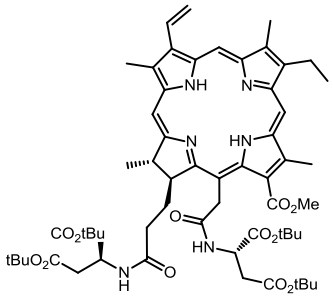

Chlorin e_6 (**1**, 100 mg, 0.168 mmol) was dissolved in dry CH_2Cl_2 (7 ml) and DIEA (0.06 ml, 0.34 mmol) was added. A mixture of DCC (105 mg, 0.51 mmol) and DMAP (163 mg, 0.51 mmol) in CH_2Cl_2 (8 ml) was added and the mixture was allowed to stir for 2 h. Then aspartic acid di(*tert*)butyl ester hydrochloride (125 mg, 0.445 mmol) and DIEA (0.075 ml) were mixed in CH_2Cl_2 and added to the reaction mixture. The solution was allowed to stir overnight at room temperature and after 12 h it was treated with ethereal diazomethane. Then the mixture was diluted with CH_2Cl_2 and washed with 5% aqueous citric acid, followed by a wash with brine and water. It was dried over anhydrous Na_2SO_4 and the solvent was evaporated. The residue was dissolved in 5% methanol/CH_2Cl_2 and purified via silica gel column chromatography with the same mobile phase to afford 15^2,17^3-diaspartylchlorin e_6 tera(*tert*)butyl methyl ester (**5**, $C_{59}H_{80}N_6O_{12}$, 54 mg, 0.051 mmol, 30%); UV-Vis (acetone): λ_{max} (rel. inten.) 664 nm (0.305), 608 (0.023), 528 (0.021), 500 (0.075), 400 (1.000); ^{1}H NMR (acetone-d_6, 400 MHz): δ 9.80 (s, 1H), 9.63 (s, 1H), 9.06 (s, 1H), 8.15 (dd, *J* = 17.9, 11.6 Hz, 1H), 7.37 (d, *J* = 7.9 Hz, 1H), 7.23 (d, *J* = 8.0 Hz, 1H), 6.37 (dd, *J* = 17.9, 1.5 Hz, 1H), 6.10 (dd, *J* = 11.6, 1.4 Hz, 1H), 5.37 (d, *J* = 12.0 Hz, 2H), 4.67 (s, 2H), 4.26 (s, 3H), 3.77 (d, *J* = 7.6 Hz, 2H), 3.57 (s, 3H), 3.48 (s, 4H), 3.25 (s, 3H), 2.83 – 2.63 (m, 3H), 2.52 – 2.28 (m, 2H), 2.14 (s, 2H), 1.89 – 1.79 (m, 2H), 1.78 (d, *J* = 7.1 Hz, 3H), 1.69 (t, *J* = 7.6 Hz, 3H), 1.43 (s, 9H), 1.35 (s, 9H), 1.26 (s, 9H), 1.16 (s, 9H), -1.36 (s, 1H), -1.57 (s, 1H); MS (MALDI-TOF) *m/z* 1065.591 $[M+H]^+$, calcd. for $C_{59}H_{81}N_6O_{12}$ 1065.591.

15^2,17^3-Diaspartylchlorin e_6 methyl ester (**6**):

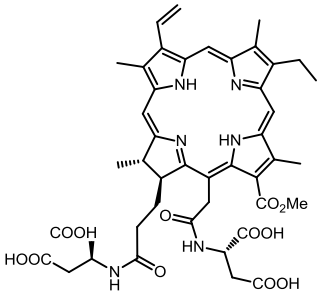

15^2,17^3-Diaspartylchlorin e_6 tetra(*tert*)butyl methyl ester (**5**, 54 mg, 0.051 mmol) was dissolved in 2 ml of dry CH_2Cl_2 and TFA (1 ml) was added in an ice bath under argon and the reaction mixture was allowed to stir overnight. Solvent was rotavaporated several times with diethyl ether to remove TFA. The residue was washed with CH_2Cl_2 several times. The final product was redissolved in a water/acetonitrile mixture and freeze dried to afford 15^2,17^3-diaspartylchlorin e_6 methyl ester (**6**, $C_{43}H_{48}N_6O_{12}$, 38 mg, 0.045 mmol, 88%); UV-Vis (MeOH): λ_{max} ($\varepsilon/M^{-1}cm^{-1}$) 661 nm (71,600), 607 (11,000), 527 (9,300), 499 (22,400), 399 (172,300); ^{1}H NMR (acetone-d_6, 400 MHz): δ 9.88 (s, 1H), 9.66 (s, 1H), 9.21 (s, 1H), 8.11 (dd, *J* = 17.8, 11.6 Hz, 1H), 6.35 (d, *J* = 17.8 Hz, 1H), 6.14 (d, *J* = 11.6 Hz, 1H), 5.35 (t, *J* = 22.7 Hz, 2H), 4.81 (br. s, 1H), 4.65 (br. s, 1H), 4.63 (br. S, 1H), 4.25 (s, 3H), 3.70 (d, *J* = 7.9 Hz, 2H), 3.54 (s, 3H), 3.46 (s, 3H), 3.18 (s, 3H), 3.06 – 2.60 (m, 5H), 2.27 (s, 3H), 1.81 (d, *J* = 7.1 Hz, 3H), 1.55 (t, *J* = 7.4 Hz, 3H). 2.00 – 1.50 (m, 4H); ^{13}C NMR (acetone-d_6, 100 MHz) δ 193.10, 192.75, 191.97, 191.93, 191.86, 191.81, 191.02, 188.70, 164.12, 160.40, 158.09, 157.49, 155.66, 155.24, 155.18, 151.90, 150.00, 149.02, 145.81, 142.62, 124.87, 121.05, 117.58, 115.99, 73.49, 73.03, 69.42, 69.24, 68.91, 68.68, 59.56, 55.70, 53.43, 52.59, 50.75, 45.56, 44.90, 42.86, 39.10, 36.79, 31.75, 31.58, 30.41. MS (MALDI-TOF) *m/z* 841 $[M+H]^+$, calcd. for $C_{43}H_{49}N_6O_{12}$ 841.340.

15^2-Chlorin e_6 monomethyl ester (**11**):

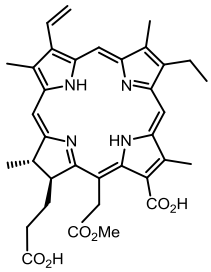

Chlorin e_6 (**1**, 100 mg, 0.168 mmol) was dissolved in methanol (5 ml). DCC (35 mg, 0.17 mmol) and DMAP (21 mg, 0.17 mmol) were added and the mixture was stirred until the anhydride intermediate was observed in the TLC. After 1 h, freshly prepared sodium methoxide (0.34 mL of a 0.5 M solution) was added into the reaction mixture dropwise until the color changed from brown to light green. The reaction was followed by UV-Vis spectroscopy. The solution changes from brown to light green as the anhydride ring opens. The mixture was diluted with ethyl acetate and then washed with 5% aqueous citric acid, followed by a wash with brine and water. It was dried over anhydrous Na_2SO_4 to afford 15^2-chlorin e_6 monomethyl ester (**11**, $C_{35}H_{39}N_4O_6$, 101 mg, 0.165 mmol, 100 %). Purification was challenging due to the two free acid groups. Thus, the crude product was subjected to the next reaction without purification. ^{1}H NMR spectrum of the crude product confirmed the methylated acetic side chain. MS (MALDI-TOF) *m/z* 611 $[M+H]^+$, calcd. for $C_{35}H_{39}N_4O_6$ 611.287.

13^1,17^3-Diaspartylchlorin e_6 tetra(*tert*)butyl methyl ester (**12**):

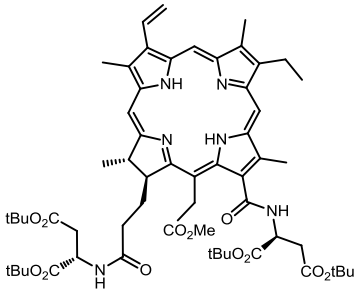

Chlorin e_6 monomethyl ester (**11**, 101 mg, 0.165 mmol) was dissolved in dry DMF (5 ml). A mixture of HOBt (46 mg, 0.34 mmol), TBTU (109 mg, 0.34 mmol) and DIEA (0.06 ml, 0.34 mmol) in DMF was added

and the mixture was allowed to stir for 30 min at room temperature. Then aspartic acid di(*tert*)butyl ester hydrochloride (125 mg, 0.445 mmol) and DIEA (0.08 ml, 0.445 mmol) were mixed in CH_2Cl_2 (2 ml) and added to the reaction mixture. The solution was allowed to stir for 48-72 h until formation of the desired product was confirmed by TLC. Then the reaction mixture was washed with 5% aqueous citric acid, followed by a wash with brine and water. It was dried over anhydrous Na_2SO_4 and solvent was evaporated. The residue was dissolved in 5% methanol/ CH_2Cl_2 and purified via a short silica gel column chromatography with the same mobile phase to afford 15^2-17^3-diaspartylchlorin e_6 tera(*tert*)butyl methyl ester (**12**, $C_{59}H_{81}N_6O_{12}$, 85 mg, 0.079 mmol, 48% of); UV-Vis (acetone): λ_{max} (rel. inten.) 663 nm (0.328), 607 (0.023), 528 (0.019), 500 (0.081), 399 (1.000); ^{1}H NMR (acetone-d_6, 400 MHz): δ 9.79 (d, *J* = 6.1 Hz, 1H), 9.65 (s, 1H), 9.10 (s, 1H), 8.42 (d, *J* = 7.9 Hz, 1H), 8.12 (dd, *J* = 17.8, 11.6 Hz, 1H), 7.29 (d, *J* = 8.2 Hz, 1H), 6.32 (d, *J* = 17.8 Hz, 1H), 6.06 (d, *J* = 11.4 Hz, 1H), 5.73 (d, *J* = 18.9 Hz, 1H), 5.50 – 5.21 (m, 2H), 4.76 – 4.61 (m, 2H), 4.61 – 4.48 (m, 1H), 3.76 (s, 3H), 3.74 – 3.68 (m, 1H), 3.65 (s, 3H), 3.47 (s, 3H), 3.42 (s, 1H), 3.22 (s, 3H), 3.20 – 3.11 (m, 2H), 2.66 (d, *J* = 5.2 Hz, 2H), 2.46 – 2.27 (m, 1H), 2.24 – 2.14 (m, 1H), 1.83 – 1.72 (m, 2H), 1.66 (s, 9H), 1.55 (s, 9H), 1.41 (s, 9H), 1.35 (s, 9H), 1.72-1.2 (m, 6H); MS (MALDI-TOF) *m/z* 1065 $[M+H]^+$, calcd. for $C_{59}H_{81}N_6O_{12}$ 1065.591.

13^1,17^3-Diaspartylchlorin e_6 methyl ester (**13**):

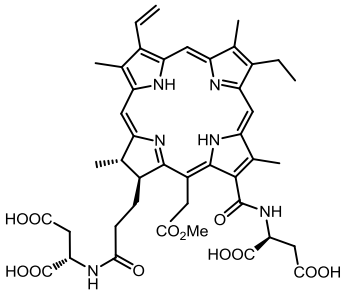

15^2,17^3-Diaspartylchlorin e_6 tetra(*tert*)butyl methyl ester (**12**, 50 mg, 0.047 mmol) was dissolved in 2 ml of dry CH_2Cl_2 in an ice bath under argon. TFA (1 ml) was added and the reaction mixture was allowed to stir overnight. The mixture was rotavaporated several times with diethyl ether to remove TFA. The

residue was dissolved in water/acetonitrile mixture and freeze dried to obtain 13^1,17^3-diaspartylchlorin e_6 methyl ester (**13**, $C_{43}H_{48}N_6O_{12}$, 21 mg, 0.025 mmol, 53%). UV-Vis (MeOH): λ_{max} ($\varepsilon/M^{-1}cm^{-1}$) 662 nm (75,300), 607 (23,000), 529 (10,000), 500(8,300), 400 (165,200); ^{13}C NMR (methanol-d_4, 100 MHz) δ 175.47, 175.04, 174.87, 174.17, 174.03, 173.97, 173.81, 169.50, 144.08, 143.10, 142.62, 140.72, 140.57, 138.37, 138.15, 136.27, 135.61, 134.11, 132.76, 131.44, 129.62, 124.84, 107.17, 100.27, 98.96, 97.91, 55.09, 53.20, 51.40, 50.70, 50.31, 47.32, 39.03, 37.01, 35.50, 34.82, 33.92, 31.99, 30.83, 26.82, 26.17, 24.34, 23.85, 20.15, 17.13, 12.36, 11.05, 9.26. MS (MALDI-TOF) *m/z* 841 $[M+H]^+$, calcd. for $C_{43}H_{49}N_6O_{12}$ 841.340.

Ethylenediaminyl(boc) pheophorbide a (**27**):

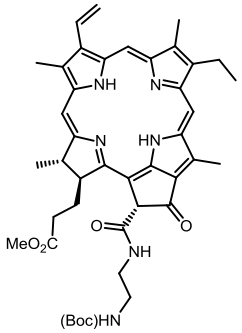

Methyl pheophorbide a (**23**, 100 mg, 0.165 mmol) was dissolved in dry toluene and the mixture was heated to 100 ^oC under nitrogen. Then mono-boc protected ethylene diamine (32 mg, 0.20 mmol) was added. The reaction mixture was allowed to stir overnight at 100 ^oC while monitoring by TLC. Then the solvent was removed and the residue was dissolved in CH_2Cl_2 and washed with 5% aqueous citric acid, followed by water and brine. It was dried over anhydrous Na_2SO_4 and the solvent was evaporated. The residue was dissolved in 3% methanol/CH_2Cl_2 and purified via a silica gel column chromatography with the same mobile phase to afford ethylenediaminyl(boc) pheophorbide a (**27**, $C_{42}H_{51}N_6O_6$, 80 mg, 0.109 mmol, 65%); UV-Vis (DCM): λ_{max} (rel. inten.) 667 nm (0.463), 609 (0.066), 535 (0.079), 505 (0.101), 413 (1.000); ^{1}H NMR (acetone-d_6, 400 MHz) δ 9.58 (s, 1H), 9.30 (s, 1H), 8.87 (s, 1H), 8.13 – 7.92 (m, 2H), 6.27 (dd, *J* = 17.9, 1.5 Hz, 1H), 6.18 (s, 1H), 6.12 (dd, *J* = 11.5, 1.4 Hz, 1H), 4.77 – 4.55 (m, 1H), 4.37 (dt, *J* = 9.3,

2.5 Hz, 1H), 3.59 (s, 3H), 3.52 (s, 3H), 3.42 – 3.36 (m, 2H), 3.35 (d, *J* = 6.5 Hz, 3H), 3.08 (s, 3H), 2.74 – 2.57 (m, 2H), 2.46 – 2.33 (m, 1H), 2.31 – 2.19 (m, 1H), 1.84 (d, *J* = 7.3 Hz, 3H), 1.76 – 1.64 (m, 1H), 1.58 (t, *J* = 7.6 Hz, 3H), 1.35 (s, 9H), -1.77 – -2.11 (m, 2H); MS (MALDI-TOF) *m/z* 841 $[M+H]^+$, calcd. for $C_{42}H_{51}N_6O_6$ 735.387.

15^2-Ethylenediaminyl(boc)-13^1-ethylenediaminylchlorin e_6 methyl ester (**28**):

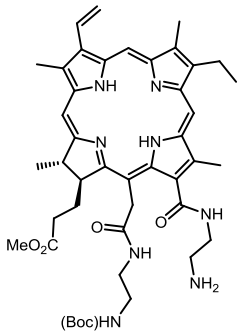

Ethylenediaminyl(boc) pheophorbide-*a* (**27**, 80 mg, 0.109 mmol) was dissolved in toluene (10 ml) and ethylene diamine (30 mg, 0.5 mmol) was added. The reaction mixture was heated at 40 ^oC overnight. Progress was monitored by TLC and UV-Vis spectrometry. After the reaction was complete by TLC, the solvent was removed and the residue was dissolved in CH_2Cl_2 and washed with 5% aqueous citric acid to remove excess amine, followed by a wash with brine. It was dried over anhydrous Na_2SO_4 and the solvent was evaporated. The residue was dissolved in 5% methanol/CH_2Cl_2 and eluted with the same mobile phase. Then the methanol percentage of the mobile phase was gradually increased up to 20% to elute the pure product from the column. The solvent was evaporated and the residue was re-dissolved in 5% acetone/CH_2Cl_2 and filtered to remove silica from the sample. After evaporation of the solvent pure 15^2-ethylenediaminyl(boc)-13^1-ethylenediaminylchlorin e_6 methyl ester was obtained (**28**, $C_{44}H_{58}N_8O_6$, 55 mg, 0.069 mmol, 64%); UV-Vis (acetone): λ_{max} (rel. inten.) 663 nm (0.325), 607 (0.015), 528 (0.008), 500 (0.072), 399 (1.000); ^{1}H NMR (acetone-d_6, 400 MHz) δ 9.74 (s, 1H), 9.73 (s, 1H), 9.13 (s, 1H), 8.36 (br. s, 1H), 8.23 (dd, *J* = 17.8, 11.5 Hz, 1H), 7.46 (br. s, 1H), 6.64 (br. s, 1H), 6.40 (dd, *J* = 17.9, 1.5 Hz, 1H), 6.12 (dd, *J* = 11.7, 1.5 Hz, 1H), 5.55 (d, *J* = 18.0 Hz, 1H), 5.09 (d, *J* = 9.3 Hz, 1H), 4.76 – 4.51

(m, 2H), 4.28 (s, 1H), 4.01 – 3.83 (m, 1H), 3.80 – 3.67 (m, 4H), 3.58 (s, 3H), 3.54 (s, 3H), 3.52 (s, 3H), 3.29 (s, 3H), 3.25 – 3.16 (m, 2H), 3.08 (dd, *J* = 9.1, 4.9 Hz, 1H), 2.78 – 2.64 (m, 1H), 2.43 – 2.21 (m, 2H), 2.00 (d, *J* = 8.0 Hz, 1H), 1.76 (d, *J* = 7.1 Hz, 3H), 1.68 (t, *J* = 7.6 Hz, 3H), 1.20 (s, 9H), -1.66 (s, 1H), -2.02 (s, 1H); MS (MALDI-TOF) *m/z* 841 $[M+H]^+$, calcd. for $C_{44}H_{59}N_8O_6$ 795.447.

13^1,15^2-Diethylenediaminylchlorin e_6 methyl ester (**29**):

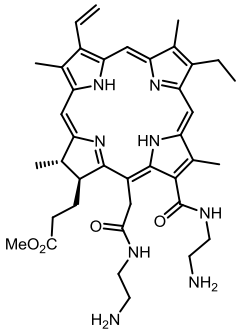

15^2-Ethylenediaminyl(boc)-13^1-ethylenediaminylchlorin e_6 methyl ester (**28**, 55 mg, 0.069 mmol) was dissolved in 3 ml of dry CH_2Cl_2 in an ice bath under argon and 1 ml of TFA was added. Then the reaction mixture was allowed to stir overnight. The mixture was rotavaporated several times with diethyl ether to remove TFA. The residue was dissolved in water/acetonitrile mixture and and freeze dried. Without any further purification the crude product was taken to the next step. (**29**, $C_{39}H_{50}N_8O_4$, 42 mg, 0.06 mmol, 88%) MS (MALDI-TOF) *m/z* 695 $[M+H]^+$,calcd. for $C_{39}H_{51}N_8O_4$ 695.403.

13^1,15^2-Diethyleneaminylaspartylchlorin e_6 di(*tert*)butyl di(boc) methyl ester:

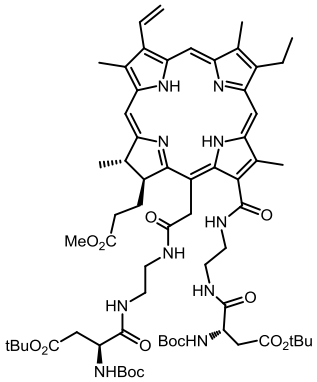

(Boc)Asp(tBu)OH (70 mg, 0.24 mmol) was dissolved in dry DMF (5 ml). A mixture of HOBt (32 mg, 0.24 mmol), TBTU (77 mg, 0.24 mmol) and DIEA (0.05 ml, 0.29 mmol) in DMF (3 ml) was added and the

mixture was allowed to stir for 1 h. 13^1,15^2-Diethylenediaminylchlorin e_6 methyl ester (**29**, 42 mg, 0.060 mmol) was added to the reaction mixture and stirring was continued for 48 h. The mixture was diluted with CH_2Cl_2 and then washed with 5% aqueous citric acid, followed by washes with brine and water. The organic layer was dried over anhydrous Na_2SO_4 and the solvent was evaporated. The residue was dissolved in 6% MeOH/CH_2Cl_2 and purified via silica gel column chromatography using the same mobile phase to afford 13^1,15^2-diethyleneaminyl-diaspartylchlorin e_6 di(*tert*)butyl di(boc) methyl ester ($C_{65}H_{92}N_{10}O_{14}$, 30 mg, 0.024 mmol, 40%); UV-Vis (acetone): λ_{max} (rel. inten.) 663 nm (0.319), 607 (0.014), 528 (0.011), 500 (0.070), 399 (1.000); ^{1}H NMR (chloroform-*d*, 400 MHz) δ 9.68 (s, 1H), 9.61 (s, 1H), 8.79 (s, 1H), 8.07 (dd, *J* = 17.9, 11.5 Hz, 1H), 7.97 (d, *J* = 5.7 Hz, 1H), 7.74 (s, 1H), 6.34 (d, *J* = 17.8 Hz, 1H), 6.13 (d, *J* = 11.5 Hz, 1H), 5.81 (d, *J* = 8.3 Hz, 1H), 5.47 (d, *J* = 18.1 Hz, 1H), 5.28 – 4.88 (m, 2H), 4.67 – 4.30 (m, 3H), 4.10 – 3.68 (m, 6H), 3.54 (s, 3H), 3.48 (s, 3H), 3.31 (s, 3H), 2.93 – 2.69 (m, 2H), 2.67 – 2.53 (m, 1H), 2.23 (d, *J* = 9.3 Hz, 1H), 2.04 (s, 1H), 1.90 – 1.55 (m, 6H), 1.31 (d, *J* = 3.9 Hz, 18H), 1.14 (d, *J* = 8.0 Hz, 18H), 0.94 – 0.80 (m, 1H), -1.62 (s, 1H), -1.80 (s, 1H); MS (MALDI-TOF) *m/z* 1237.651 $[M+H]^+$, calcd. for $C_{65}H_{93}N_{10}O_{14}$ 1237.687.

13^1,15^2-Diethyleneaminyl-diaspartylchlorin e_6 methyl ester (**30**):

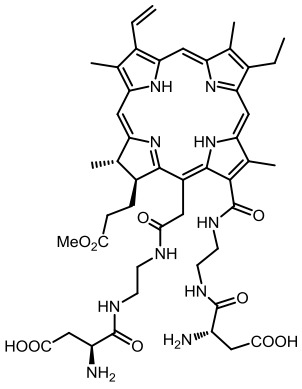

13^1,15^2-Diethyleneaminyl-diaspartylchlorin e_6 di(*tert*)butyl di(boc) methyl ester (30 mg, 0.024 mmol) was dissolved in 2 ml of dry CH_2Cl_2 in an ice bath under argon. TFA (1 ml) was added and the reaction mixture was allowed to stir overnight. The reaction mixture was rotavaporated several times with

diethyl ether to remove TFA. The residue was washed with CH_2Cl_2 several times. The final product was dissolved in water and freeze dried to obtain 13^1-15^2-diethyleneaminyl-diaspartylchlorin e_6 methyl ester (**30**, $C_{48}H_{59}N_9O_{12}$, 16 mg, 0.016 mmol, 70%). UV-Vis (MeOH): λ_{max} ($\varepsilon/M^{-1}cm^{-1}$) 661 nm (74,700), 606 (8,400), 527 (6200), 500 (20,500), 400 (190,200); ^{1}H NMR (methanol-d_4, 400 MHz) δ 10.18 (s, 1H), 10.03 (s, 1H), 9.47 (s, 1H), 8.20 (dd, *J* = 17.7, 11.6 Hz, 1H), 6.39 (d, *J* = 17.8 Hz, 1H), 6.29 (d, *J* = 11.5 Hz, 1H), 5.59 (d, *J* = 18.7 Hz, 1H), 5.42 (d, *J* = 18.7 Hz, 1H), 4.79 (d, *J* = 7.2 Hz, 1H), 4.54 (d, *J* = 10.8 Hz, 1H), 4.44 (ddd, *J* = 24.1, 8.5, 4.2 Hz, 1H), 4.25 – 4.05 (m, 1H), 4.03 – 3.83 (m, 4H), 3.74 (s, 3H), 3.67 (s, 3H), 3.56 (s, 3H), 3.49 (td, *J* = 10.6, 9.5, 4.6 Hz, 2H), 3.41 – 3.26 (m, 5H), 3.23 – 3.00 (m, 2H), 2.99 – 2.82 (m, 2H), 2.70 (dd, *J* = 17.9, 9.0 Hz, 1H), 2.59 – 2.47 (m, 1H), 2.46 – 2.31 (m, 1H), 1.83 (d, *J* = 7.1 Hz, 3H), 1.68 (t, *J* = 7.3 Hz, 3H); ^{13}C NMR (methanol-d_4, 100 MHz) δ 174.40, 173.96, 173.73, 172.85, 171.54, 171.38, 169.04, 168.71, 168.03, 143.06, 142.09, 141.75, 139.02, 138.75, 137.66, 136.96, 135.22, 134.57, 132.80, 131.32, 130.48, 128.32, 123.53, 105.18, 99.19, 97.42, 97.05, 53.89, 51.07, 49.95, 49.13, 39.50, 39.30, 39.19, 39.12, 38.70, 34.67, 34.46, 30.47, 29.64, 29.30, 22.82, 22.37, 18.95, 15.79, 11.06, 10.88, 9.85; MS (MALDI-TOF) *m/z* 947 $[M+Na]^+$, calcd. for $C_{48}H_{59}N_9NaO_{12}$ 947.438.

β-Alanylpheoporbide a (*tert*)butyl methyl ester:

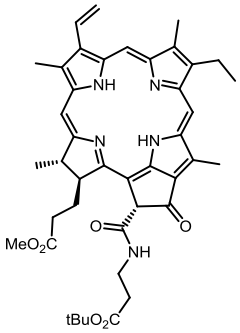

Methyl pheophorbide a (**23**, 100 mg, 0.165 mmol) was dissolved in dry toluene (10 ml) and the mixture was heated to 100 ^oC under nitrogen. Then β-alanine(tBu).HCl (45 mg, 0.25 mmol) and DIEA (0.06 ml, 0.33 mmol) were added. The reaction mixture was allowed to stir overnight at 100 ^oC in an oil bath and was monitored by TLC. Then the solvent was removed and the residue was dissolved in CH_2Cl_2 and

washed with 5% aqueous citric acid followed by water and with brine. The organic layer was dried over anhydrous Na_2SO_4 and the solvent was evaporated. The residue was dissolved in 5% methanol/CH_2Cl_2 and purified via silica gel chromatography with the same mobile phase and to afford β-alanylpheoporbide a (*tert*)butyl methyl ester (**31**, $C_{42}H_{49}N_5O_6$, 65 mg, 0.090 mmol, 54%); UV-Vis (DCM): λ_{max} (rel. inten.) 667 nm (0.420), 609 (0.060), 535 (0.071), 505 (0.098), 412 (1.000); ^{1}H NMR (acetone-d_6, 400 MHz) δ 9.33, 9.23* (s, 1H), 8.99, 9.93* (s, 1H), 8.79, 8.77* (s, 1H), 7.97*, 7.92 (t, *J* = 6.0 Hz, 1H), 7.80 (m, 1H), 6.16, 6.13* (s, 1H), 6.07 (d, *J* = 9.7 Hz, 1H), 5.99 (dd, *J* = 11.6, 1.5 Hz, 1H), 4.65*, 4.57 (qd, *J* = 7.4, 2.0 Hz, 1H), 4.38 (tt, *J* = 9.7, 2.2 Hz, 1H), 3.68 (qd, *J* = 6.6, 2.3 Hz, 1H), 3.61 (q, *J*=6.4, 1H) 3.59*, 3.53 (s, 3H), 3.49, 3.41* (s, 3H), 3.28*, 3.27 (s, 3H), 2.86*, 2.84 (s, 3H), 2.71 – 2.52 (m, 3H), 2.49 – 2.12 (m, 1H), 1.85 (d, *J* = 7.3 Hz, 2H), 1.64 (d, *J* = 7.3 Hz, 1H), 1.48*, 1.49 (s, 9H), -2.08 (d, *J* = 66.3 Hz, 1H).(* Minor 13^2 epimer); MS (MALDI-TOF) *m/z* 720 $[M+H]^+$, calcd. for $C_{42}H_{50}N_5O_6$ 720.368.

β-Alanylpheoporbide a methyl ester (**31**):

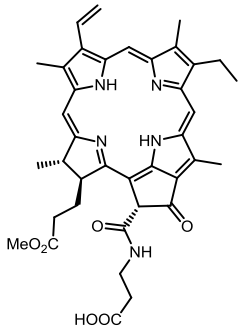

β-Alanylpheophorbide a (*tert*)butyl methyl ester (65 mg, 0.090 mmol) was dissolved in 2 ml of dry CH_2Cl_2 in an ice bath under argon. TFA (1 ml) was added and the reaction mixture was allowed to stir for 6 h. The reaction mixture was diluted with CH_2Cl_2 and washed with water and then with saturated sodium bicarbonate. This formed a precipitate while washing with sodium bicarbonate then citric acid solution was added until the precipitate dissolved in the organic phase. Then the solution was washed with brine and dried over anhydrous Na_2SO_4 to give β-alanylpheoporbide a methyl ester (**31**, $C_{38}H_{41}N_5O_6$, 60 mg, 0.09 mmol, 100%). MS (MALDI-TOF) *m/z* 686 $[M+H]^+$, calcd. for $C_{38}H_{41}N_5NaO_6$ 686.295.

β-Alanylaspartylpheoporbide a di(*tert*)butyl methyl ester (**32**):

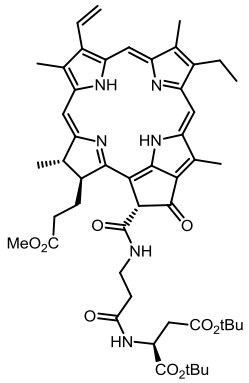

β-Alanylpheoporbide a methyl ester (**31**, 60 mg, 0.090 mmol) was dissolved in dry DMF (5 ml). A mixture of HOBt (18 mg, 0.135 mmol), TBTU (43 mg, 0.135) and DIEA (0.03 ml, 0.18 mmol) in DMF (3 ml) was added and the mixture was allowed to stir for 30 min. Then a mixture of aspartic acid di(tert)butyl ester hydrochloride (101 mg, 0.36 mmol) and DIEA (0.06 ml, 0.36 mmol) in CH_2Cl_2 (3 ml) was added to the reaction mixture. The mixture was allowed to stir for 24 h. The mixture was diluted with CH_2Cl_2 and then washed with 5% aqueous citric acid, followed by with water and brine. The organic layer was dried over anhydrous Na_2SO_4 and the solvent was evaporated. The residue was dissolved in 5% methanol/CH_2Cl_2 and purified via silica column chromatography with the same mobile phase to afford β-alanyl aspartyl pheophorbide a di(*tert*)butyl methyl ester (**32**, $C_{50}H_{62}N_6O_9$, 48 mg, 0.053 mmol, 59%); UV-Vis (DCM): λ_{max} (rel. inten.) 667 nm (0.401), 609 (0.055), 535 (0.069), 505 (0.097), 413 (1.000); ^{1}H NMR (acetone-d_6, 400 MHz) δ 9.06, 8.98* (s, 1H), 8.70, 8.59* (s, 1H), 8.69 (s, 1H), 8.2* 8.06 (t, *J* = 5.9 Hz, 1H), 7.70 – 7.45 (m, 2H), 6.17, 6.08* (s, 1H), 5.93 (dt, *J* = 17.7, 2.3 Hz, 1H), 5.85 (dd, *J* = 11.5, 1.4 Hz, 1H), 4.82*, 4.76 (dt, *J* = 8.3, 5.8 Hz, 1H), 4.64*, 4.55 (tt, *J* = 9.0, 4.5 Hz, 1H), 4.42*, 4.35 (dt, *J* = 9.7, 2.5 Hz, 1H), 3.77 (q, *J* = 6.5 Hz, 2H), 3.63*, 3.59 (s, 3H), 3.42, 3.31* (s, 3H), 3.14 (s, 3H), 3.05 (h, *J* = 6.8, 6.3 Hz, 3H), 2.78 (dd, *J* = 5.9, 4.7 Hz, 2H), 2.74 – 2.66 (m, 4H), 2.63 (s, 3H), 2.49 – 2.37 (m, 1H), 2.20 (td, *J* = 9.0, 3.3 Hz, 1H), 1.85, 1.65* (d, *J* = 7.3 Hz, 3H), 1.45 (s, 9H), 1.42 (s, 9H), 1.35 (t, *J* = 7.5 Hz, 2H), -2.17*, -2.33 (s, 2H).).(* Minor 13^2 epimer); MS (MALDI-TOF) *m/z* 891 $[M+H]^+$, calcd. for $C_{50}H_{63}N_6O_9$ 891.465.

13^1-Ethylenediaminyl-15^2-β-alanylaspartylchlorin e_6 di(*tert*)butyl methyl ester (**33**):

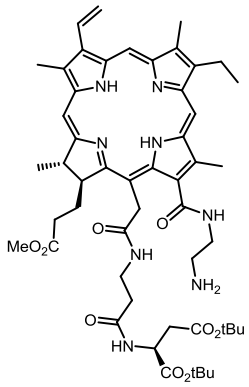

β-Alanylaspartylpeoporbide a di(*tert*)butyl methyl ester (**32**, 48 mg, 0.053 mmol) was dissolved in toluene and ethylenediamine (15 mg, 0.26 mmol) was added. The reaction mixture was heated at 40 ^oC for 24-36 h. It was monitored by TLC and UV-Vis spectroscopy. After reaction was complete as monitored by TLC, the solvent was removed and the residue was dissolved in CH_2Cl_2 and washed with 5% aqueous citric acid to remove excess amine, followed by a wash with brine. It was dried over anhydrous Na_2SO_4 and the solvent was evaporated. The residue was dissolved in 5% methanol/CH_2Cl_2 and chromatographed on a silica gel column with the same mobile phase. Then the methanol percentage of the mobile phase was gradually increased up to 20% to elute the pure product from the column. The solvent was evaporated and re-dissolved in 5% acetone/CH_2Cl_2 and filtered to remove silica from the sample. After evaporation of solvent 13^1-ethylenediaminyl-15^2-β-alanyl aspartylchlorin e_6 di(*tert*)butyl methyl ester was obtained (**33**, $C_{52}H_{70}N_8O_9$, 30 mg, 0.031 mmol, 58 %). UV-Vis (acetone): λ_{max} (rel. inten.) 664 nm (0.322), 607 (0.015), 528 (0.012), 500 (0.070), 400 (1.000); It was not possible to obtain the ^1H NMR spectrum and so the crude product was subjected to next step. MS (MALDI-TOF) *m/z* 951 $[M+H]^+$, calcd. for $C_{52}H_{71}N_8O_9$ 951.534.

13^2-Ethylenediaminyllysinyl-15^2-β-alanylaspartylchlorin e_6 di(*tert*)butyl di(boc) methyl ester:

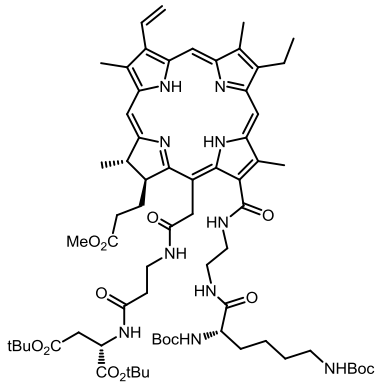

Boc-Lys(Boc)OH.DCHA (61 mg, 0.116 mmol) was dissolved in dry DMF (5 ml). A mixture of HOBt (16 mg, 0.116 mmol), TBTU (37 mg, 0.116 mmol) and DIEA (0.024 ml, 0.14 mmol) in DMF (3 ml) was added and the mixture was stirred for 30 min. 13^1-Ethylenediaminyl-15^2-β-alanylaspartylchlorin e_6 di(*tert*)butyl methyl ester (**33**, 30 mg, 0.031 mmol) was added to the reaction mixture and it was stirred for 72 h. After the reaction was deemed complete by TLC, the mixture was diluted with CH_2Cl_2 and then washed with 10% sodium bicarbonate, 5% aqueous citric acid, then followed by washing with brine. The organic phase was dried over anhydrous Na_2SO_4 and the solvent was evaporated. The residue was dissolved in 10% MeOH/CH_2Cl_2 and purified via silica gel column chromatography using the same mobile phase to afford 13^1-ethylenediaminyllysinyl-15^2-β-alanylaspartylchlorin e_6 di(*tert*)butyl di(*tert*)butyl carbamates methyl ester ($C_{68}H_{98}N_{10}O_{14}$, 24 mg, 0.018 mmol, 61%); UV-Vis (acetone): λ_{max} (rel. inten.) 663 nm (0.320), 607 (0.021), 528 (0.019), 500 (0.075), 400 (1.000); ^{1}H NMR (acetone-d_6, 400 MHz) δ 9.67 (s, 1H), 9.65 (s, 1H), 9.10 (s, 1H), 8.71 (s, 1H), 8.26 (d, *J* = 5.5 Hz, 1H), 8.17 (dd, *J* = 17.8, 11.5 Hz, 1H), 7.05 (s, 2H), 6.34 (d, *J* = 17.8 Hz, 1H), 6.23 (d, *J* = 8.0 Hz, 1H), 6.07 (d, *J* = 11.5 Hz, 1H), 5.95 (s, 1H), 5.56 (d, *J* = 18.9 Hz, 1H), 5.22 (d, *J* = 19.2 Hz, 1H), 4.68 (q, *J* = 7.1 Hz, 1H), 4.54 (d, *J* = 9.6 Hz, 1H), 4.29 (q, *J* = 3.6 Hz, 1H), 3.98 – 3.62 (m, 9H), 3.57 (s, 3H), 3.48 (s, 6H), 3.25 (s, 3H), 3.02 (d, *J* = 6.0 Hz, 2H), 2.56 – 2.40 (m, 2H), 2.40 – 2.26 (m, 2H), 2.26 – 2.17 (m, 1H), 1.91 (dt, *J* = 23.0, 8.6 Hz, 2H), 1.74 (d, *J* = 7.1 Hz, 3H), 1.66 (t, *J* = 7.2 Hz,

3H), 1.57 – 1.44 (m, 4H), 1.37 (s, 18H), 1.34 (s, 18H), -1.65 (s, 1H), -1.94 (s, 1H); MS (MALDI-TOF) *m/z* 1279.775 $[M+H]^+$, calcd. for $C_{68}H_{99}N_{10}O_{14}$ 1279.734.

13^1-Ethylenediaminyllysinyl-15^2-β-alanylaspartylchlorin e_6 methyl ester (**34**):

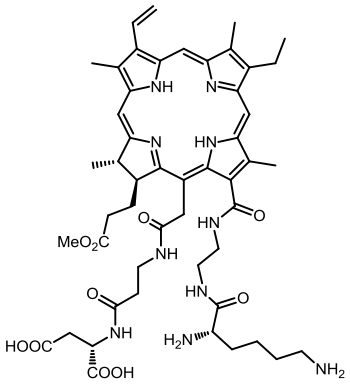

13^1-Ethylenediaminyllysinyl-15^2-β-alanylaspartylchlorin e_6 di(*tert*)butyl di(boc) methyl ester (24 mg, 0.018 mmol) was dissolved in 2 ml of dry CH_2Cl_2 in an ice bath under argon. TFA (1 ml) was added and the reaction mixture was allowed to stir overnight. The mixture was rotavaporated several times with diethyl ether to remove TFA and the residue was washed with CH_2Cl_2 several times. The final product was dissolved in water and then freeze dried to obtain 13^1-ethylenediaminyllysinyl-15^2-β-alanylaspartylchlorin e_6 methyl ester (**34**, $C_{50}H_{66}N_{10}O_{10}$, 14 mg, 0.014 mmol; 79%). UV-Vis (MeOH): λ_{max} ($\varepsilon/M^{-1}cm^{-1}$) 658 nm (18,900), 635 (67,800), 594 (14,000), 511 (10,000), 411 (150,800); ^{13}C NMR (methanol-d_4, 100 MHz) δ 174.29, 173.52, 173.43, 173.36, 172.48, 172.40, 172.37, 171.98, 169.48, 169.39, 169.22, 143.32, 143.11, 141.31, 141.27, 138.82, 138.71, 138.37, 138.20, 136.41, 134.92, 134.80, 134.48, 132.41, 130.82, 130.22, 130.20, 128.61, 128.35, 128.12, 125.99, 125.06, 123.04, 121.12, 118.95, 118.21, 115.29, 112.38, 109.04, 104.87, 104.84, 99.37, 96.89, 96.86, 53.87, 53.19, 51.06, 49.15, 48.72, 39.85, 39.27, 39.14, 38.98, 37.50, 36.18, 35.26, 34.82, 30.76, 30.52, 29.82, 26.79, 22.43, 21.66, 18.72, 15.78, 11.06, 10.83, 9.62..MS (MALDI-TOF) *m/z* 967.602 $[M+H]^+$, calcd. for $C_{50}H_{67}N_{10}O_{10}$ 967.50

3.5 Supporting information

^{1}H NMR spectrum of 15^{2},17^{3}-di(Asp)Ce$_{6}$ (tBu)$_{4}$ MME **5** in acetone-d_{6} at 400 MHz

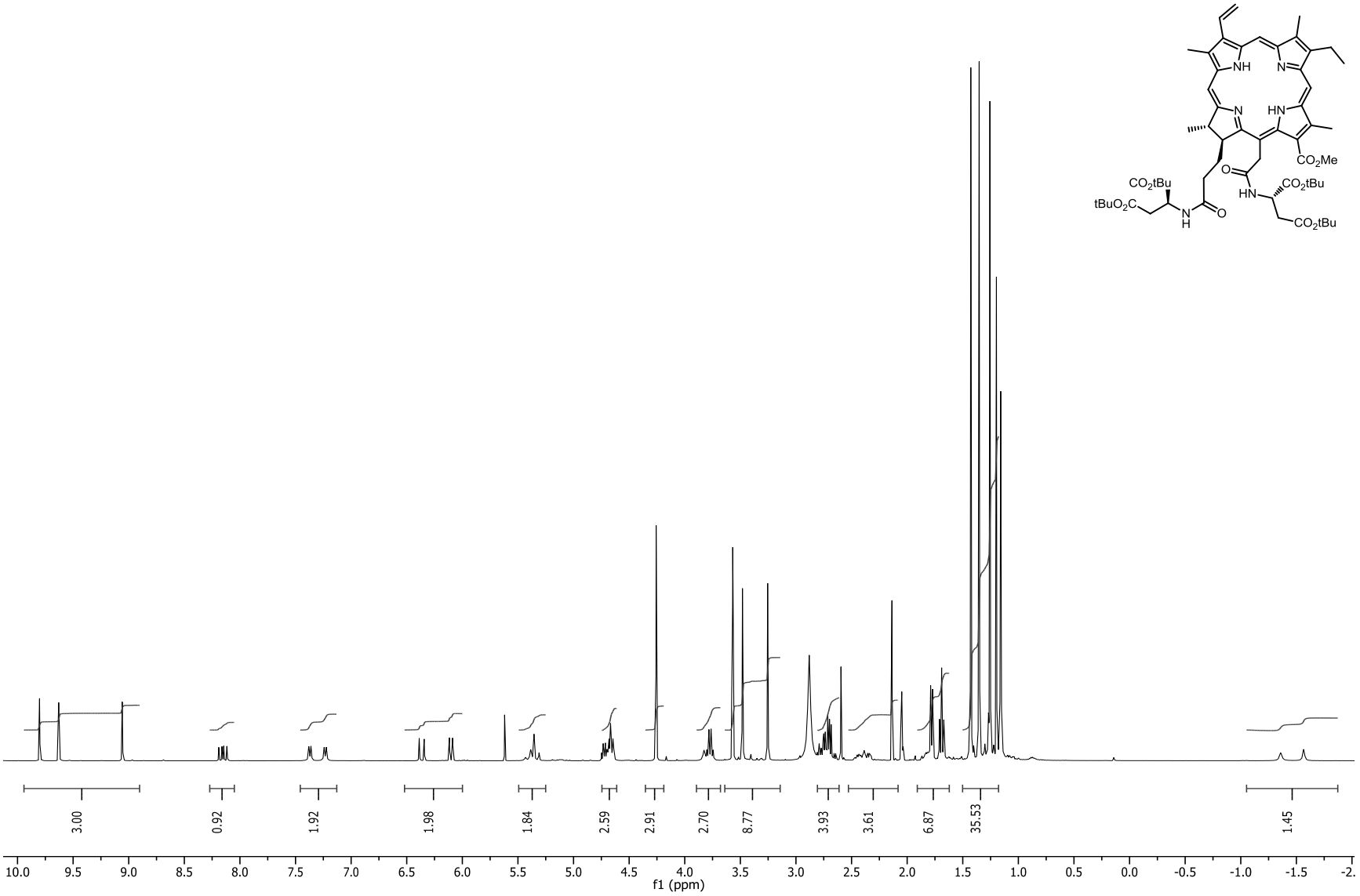

^{1}H NMR spectrum of 15^{2},17^{3}-di(Asp)Ce$_{6}$ MME **6** in acetone-d_{6} at 400 MHz

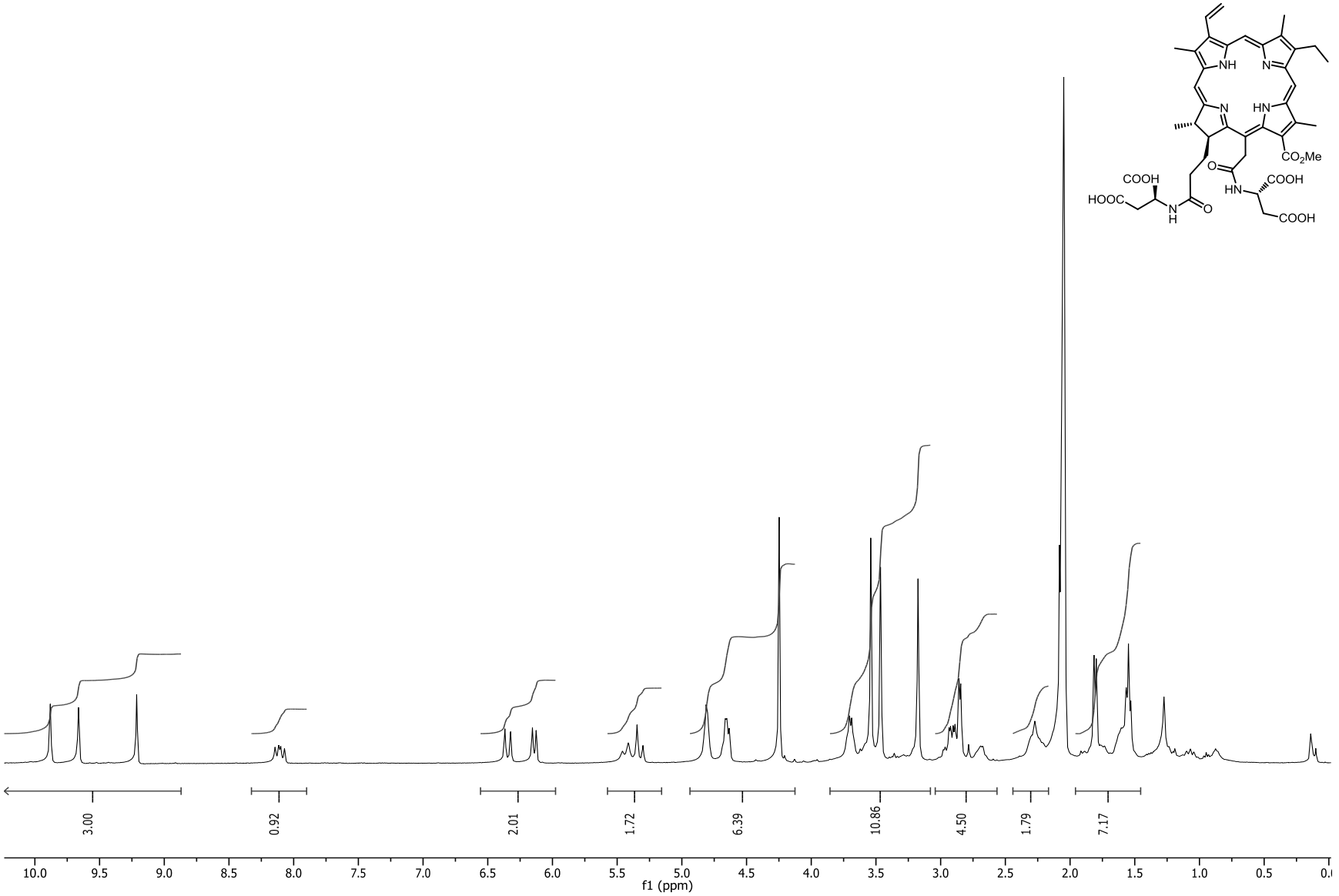

^{1}H NMR spectrum of 13^{1},17^{3}-di(Asp)Ce$_6$ (*t*Bu)$_4$ MME **12** in acetone-d_6 at 400 MHz

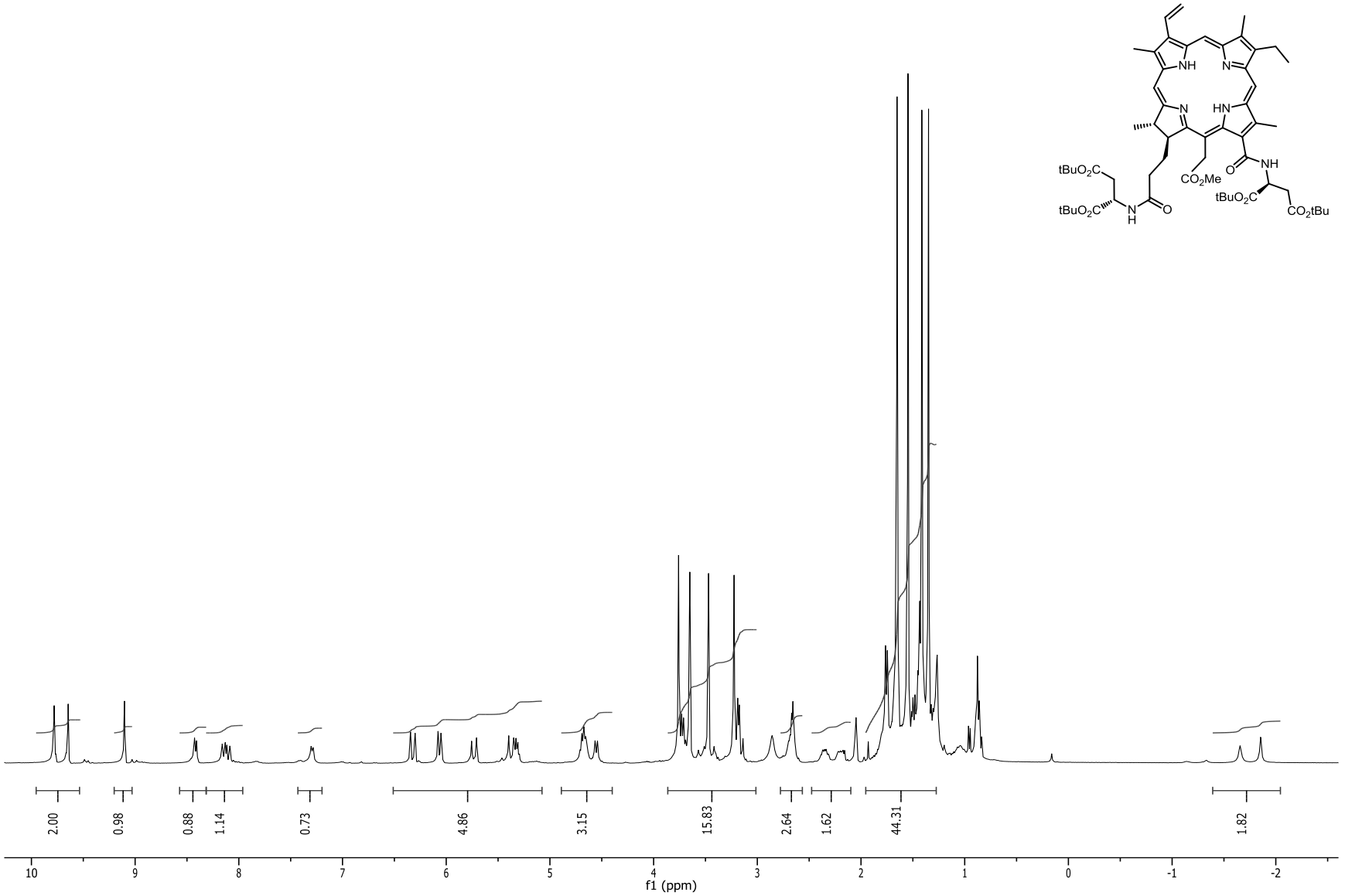

^{1}H NMR spectrum of 13^{1}-ED 15^{2}-ED(boc)Ce$_6$ MME **28** in acetone-d_6 at 400 MHz

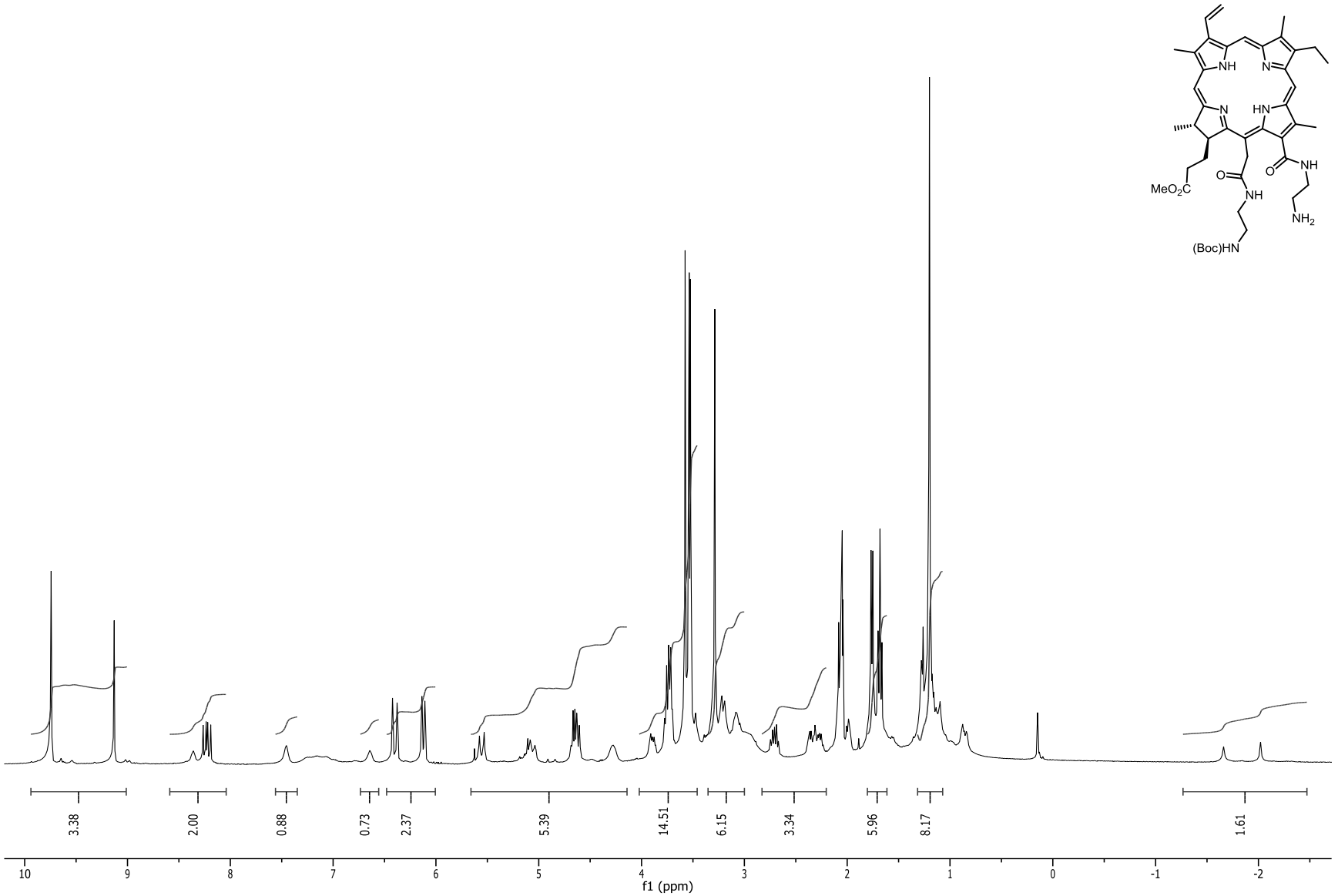

^{1}H NMR spectrum of 13^{1},15^{2}-ED-AspCe$_{6}$ (*t*Bu)$_{2}$ (boc)$_{2}$ MME in chloroform-*d* at 400 MHz

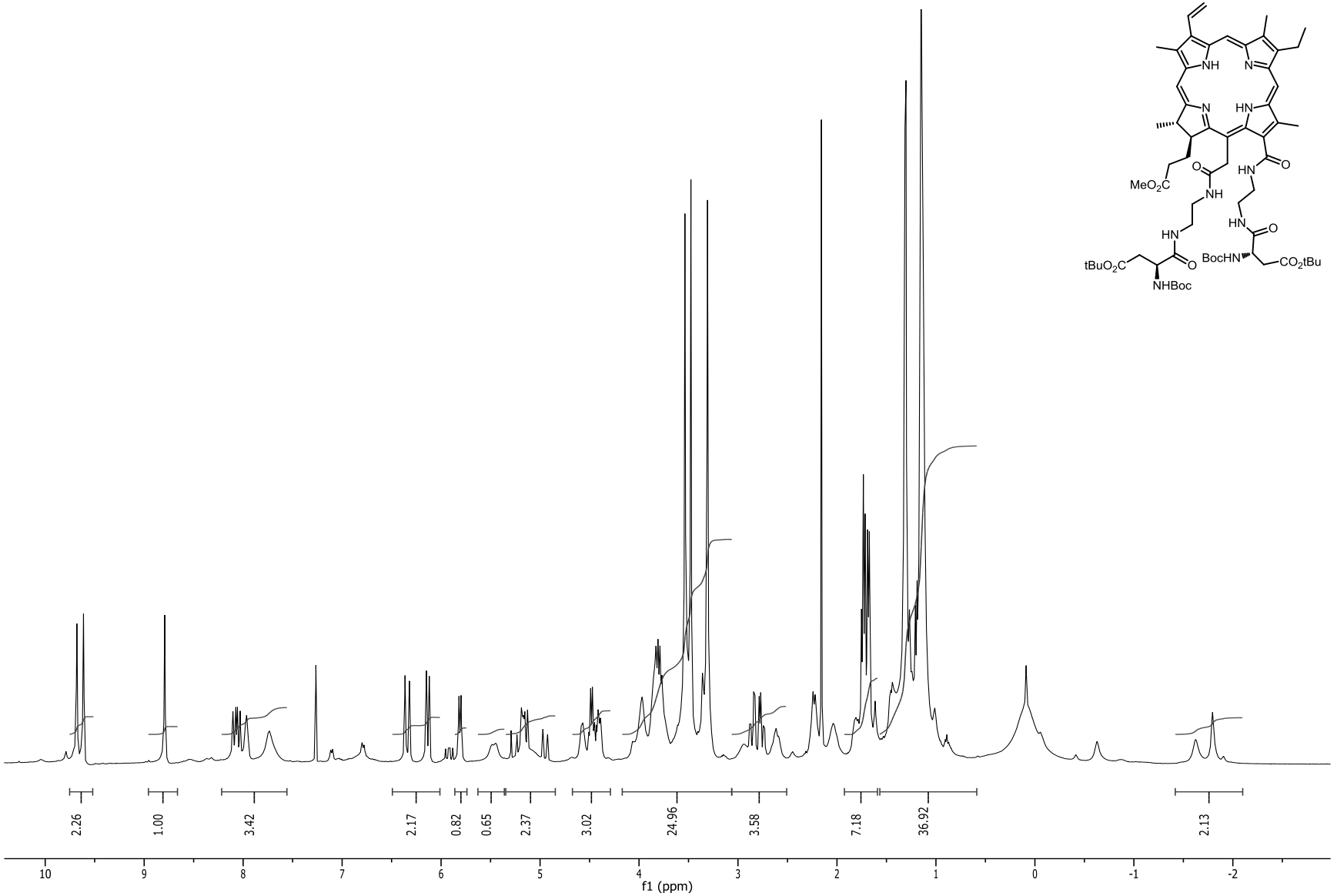

^{1}H NMR spectrum of 13^{1},15^{2}-ED-AspCe$_{6}$ MME **30** in methanol-d_4 at 400 MHz

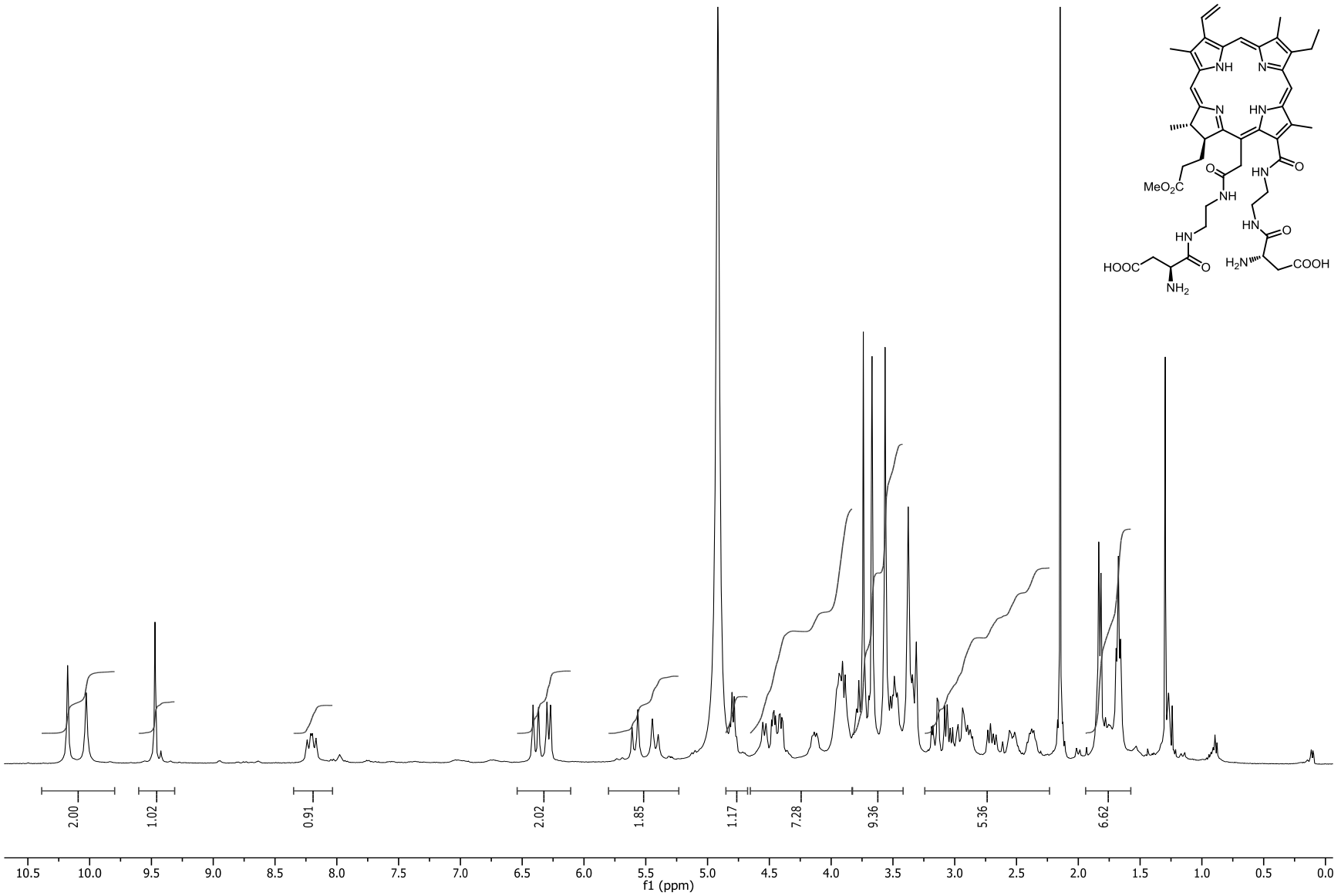

^{1}H NMR spectrum of β-Ala-pheoporbide a *t*Bu MME in acetone-d_6 at 400 MHz

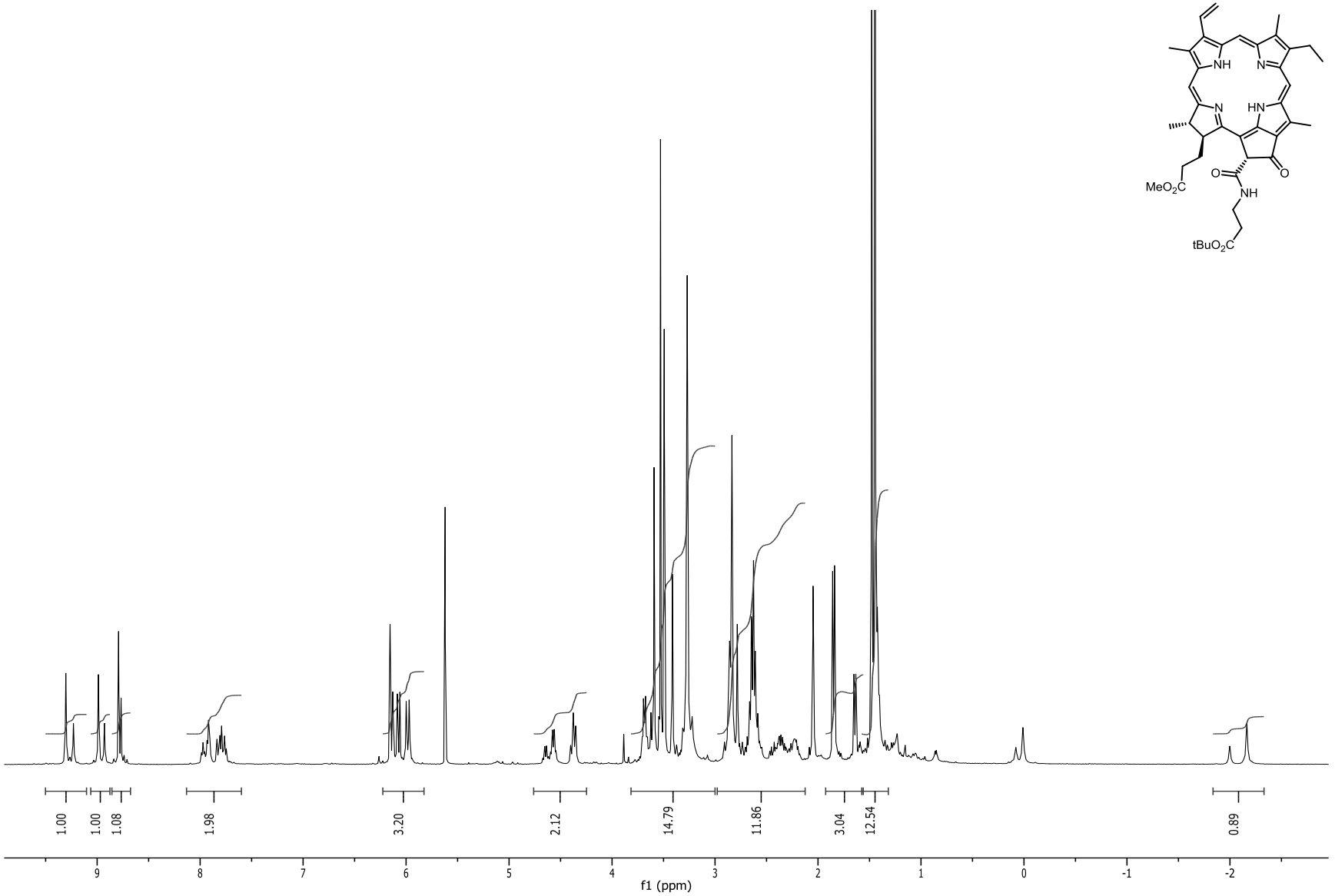

^{1}H NMR spectrum of β-Ala-Asp-pheoporbide a (tBu)$_2$ MME **32** in acetone-d_6 at 400 MHz

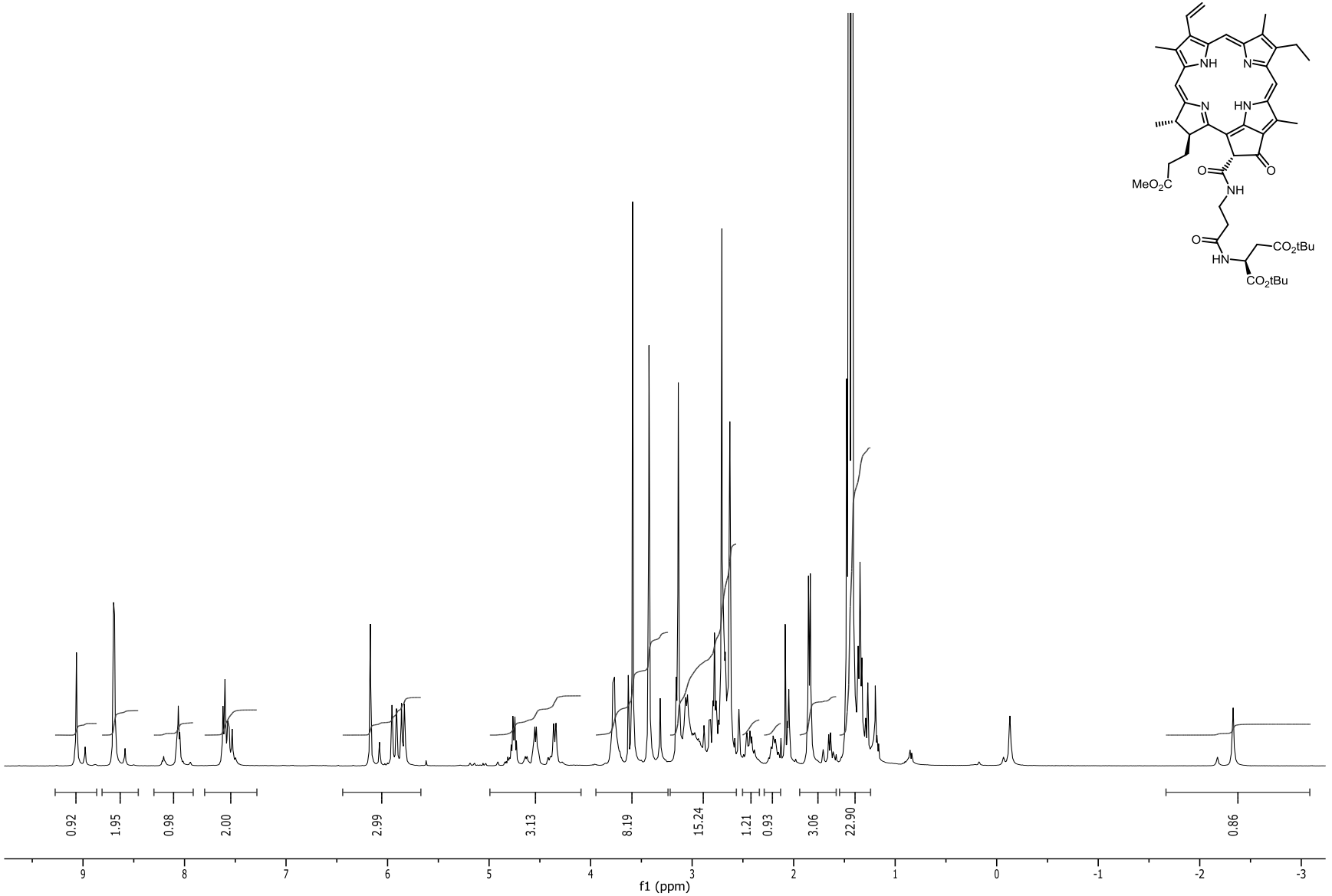

^{1}H NMR spectrum of 13^{2}-EDLys -15^{2}-β-AlaAspCe$_6$ (*t*Bu)$_2$ (boc)$_2$ MME in acetone-d_6 at 400 MHz

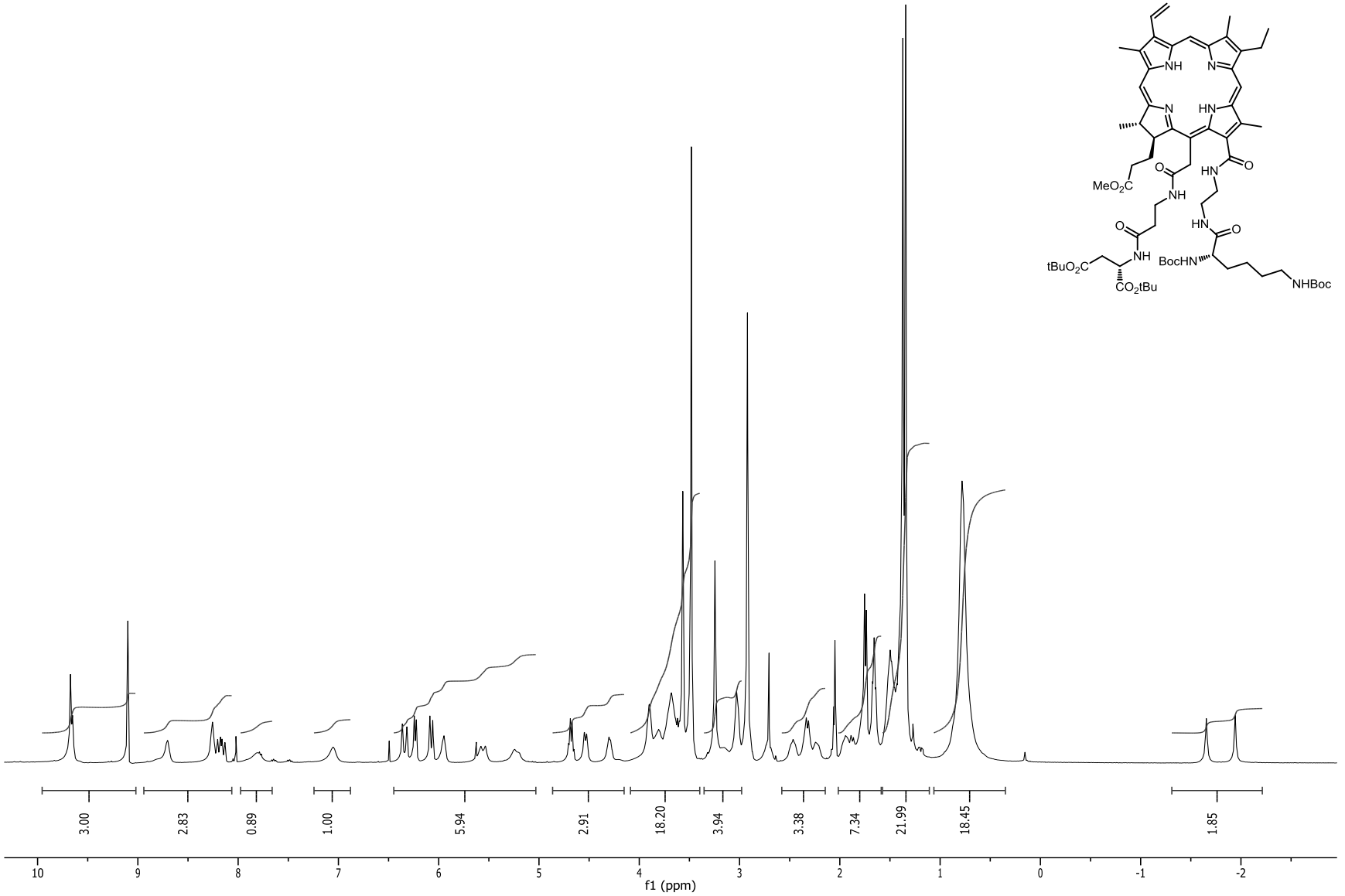

^{13}C NMR spectrum of 15^{2},17^{3}-di(Asp)Ce$_6$ MME **6** in methanol-d_4 at 100 MHz

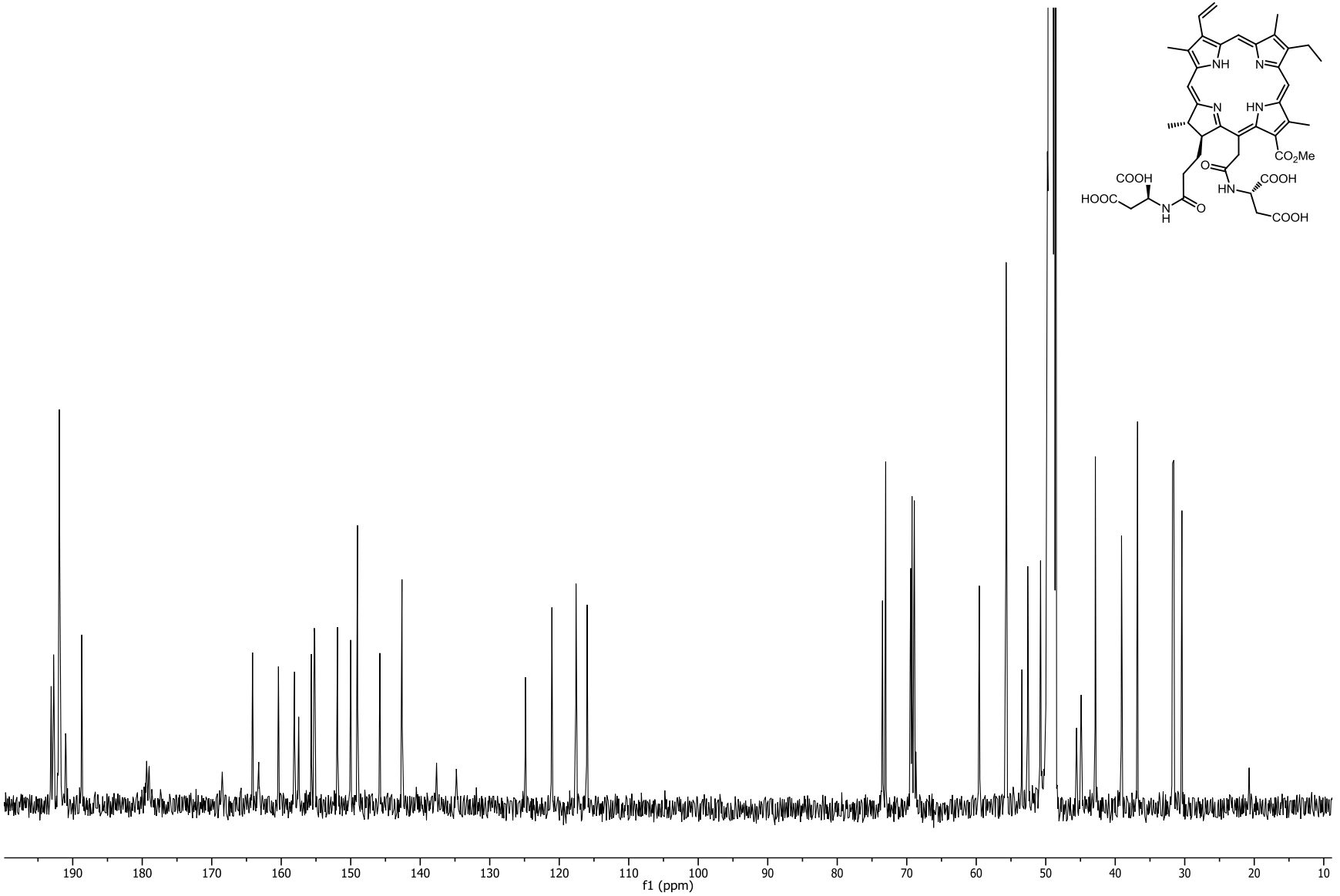

^{13}C NMR spectrum of 13^{1},15^{2}-ED-AspCe$_6$ MME **30** in methanol-d_4 at 400 MHz

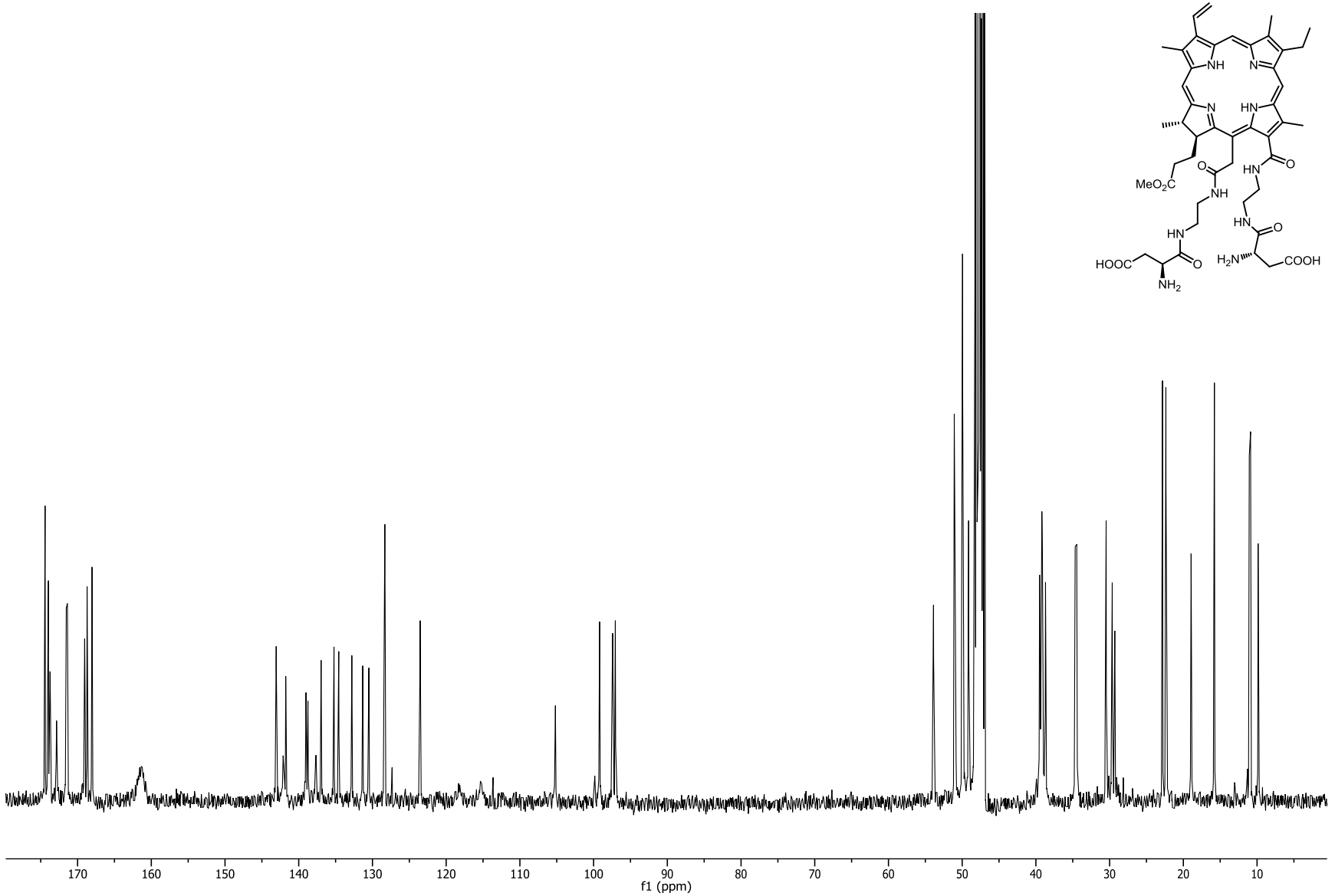

^{13}C NMR spectrum of 13^{2}-EDLys -15^{2}-β-AlaAspCe$_6$ MME **34** in methanol-d_4 at 100 MHz

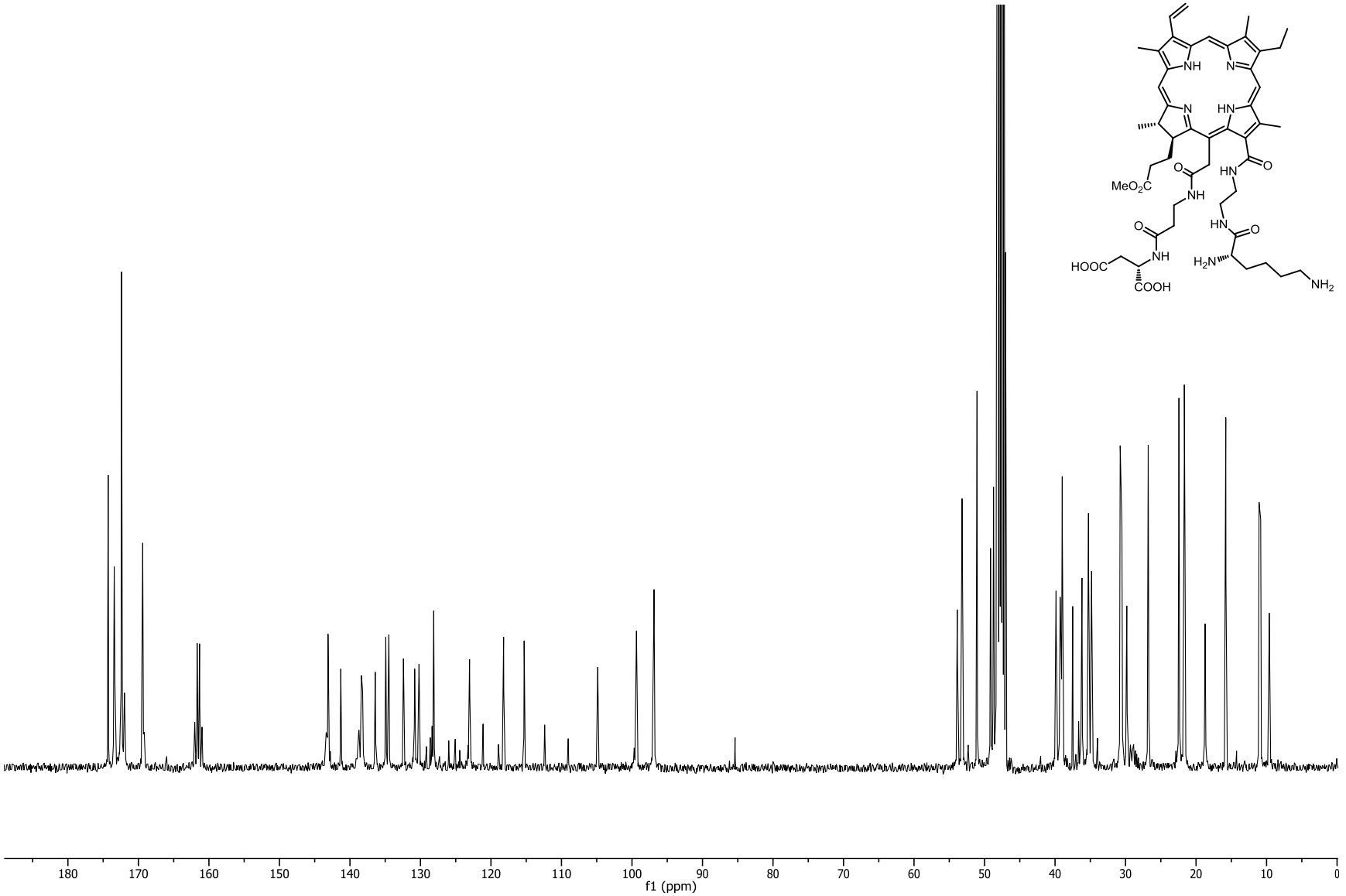

3.6 References

(1) Pegaz, B.; Debefve, E.; Borle, F.; Ballini, J. P.; Wagnières, G.; Spaniol, S.; Albrecht, V.; Scheglmann, D.; Nifantiev, N. E.; van den Bergh, H.; Konan, Y. N. *Photochem. Photobiol.* **2005**, *81*, 1505.

(2) Hamblin, M. R.; Miller, J. L.; Rizvi, I.; Ortel, B.; Maytin, E. V.; Hasan, T. *Cancer Res.* **2001**, *61*, 7155.

(3) Kuimova, M. K.; Collins, H. A.; Balaz, M.; Dahlstedt, E.; Levitt, J. A.; Sergent, N.; Suhling, K.; Drobizhev, M.; Makarov, N. S.; Rebane, A.; Anderson, H. L.; Phillips, D. *Org. Biomol. Chem.* **2009**, *7*, 889.

(4) Jensen, T. J.; Vicente, M. G.; Luguya, R.; Norton, J.; Fronczek, F. R.; Smith, K. M. *J. Photochem. Photobiol. B* **2010**, *100*, 100.

(5) Kim, W. J.; Kang, M. S.; Kim, H. K.; Kim, Y.; Chang, T.; Ohulchanskyy, T.; Prasad, P. N.; Lee, K. S. *J. Nanosci. Nanotechnol.* **2009**, *9*, 7130.

(6) Kimani, S.; Ghosh, G.; Ghogare, A.; Rudshteyn, B.; Bartusik, D.; Hasan, T.; Greer, A. *J. Org. Chem.* **2012**, 10638.

(7) Park, H.; Na, K. *Biomaterials* **2013**, *34*, 6992.

(8) Jinadasa, R. G. W.; Hu, X.; Vicente, M. G. H.; Smith, K. M. *J. Med. Chem.* **2011**, *54*, 7464.

(9) Hargus, J. A.; Fronczek, F. R.; Vicente, M. G. H.; Smith, K. M. *Photochem. Photobiol. B* **2007**, *83*, 1006.

(10) Wasielewski, M. R.; Svec, W. A. *J . Org. Chem.* **1980**, *45*, 1969.

(11) Ol'shevskaya, V. A.; Savchenko, A. N.; Zaitsev, A. V.; Kononova, E. G.; Petrovskii, P. V.; Ramonova, A. A.; Tatarskiy Jr, V. V.; Uvarov, O. V.; Moisenovich, M. M.; Kalinin, V. N.; Shtil, A. A. *J. Organomet. Chem.* **2009**, *694*, 1632.

(12) Meseguer, B.; Alonso-Díaz, D.; Griebenow, N.; Herget, T.; Waldmann, H. *Chem. Eur. J.* **2000**, *6*, 3943.

(13) Smith, K. M.; Lewis, W. M. *Tetrahedron* **1981**, *37, Supplement 1*, 399.

(14) Hudlicky, M. *J. Org. Chem.* **1980**, *45*, 5377.

(15) Haavikko, R.; Kavakka, J. S.; Helaja, J. *Tetrahedron Lett.* **2010**, *51*, 714.

(16) Belykh, D. V.; Kopylov, E. A.; Gruzdev, I. V.; Kuchin, A. V. *Russ. J. Org. Chem* **2010**, *46*, 577.

(17) Dugin, N. O.; Zavialova, M. G.; Novikov, R. A.; Timofeev, V. P.; Misharin, A. Y.; Ponomarev, G. V. *Macroheterocycles* **2012**, *5*, 146.

(18) Shinoda, S.; Osuka, A. *Tetrahedron Lett.* **1996**, *37*, 4945.

(19) Cossy, J.; Thellend, A. *Synthesis* **1989**, 753.

(20) Garcia, M. J.; Rebolledo, F.; Gotor, V. *Tetrahedron Lett.* **1993**, *34*, 6141.

(21) Labelle, M.; Gravel, D. *Chem. Commun.* **1985**, 105.

CHAPTER 4: SYNTHESIS OF ELECTRON DEFICIENT PORPHYRINS FOR A SYNTHETIC CYTOCHROME

4.1 Introduction

A large number of enzymes contain redox centers, which comprise metal-associated tetrapyrrolic precursors that are important for their function. These cofactors accomplish electron transportation in biological systems. They display a wide range of reduction midpoint potentials. The magnitude of the redox potential of cofactors needs to be tuned depending on their function. These different values of redox potential are dictated by the oxidation state of metal ion, protein environment, axial ligation to the metal ion and the nature of the substituents on the porphyrin ring.[1-3]

Cytochromes, which contain one or several heme groups in their active sites, are an important subgroup of electron transfer proteins. They are primarily responsible for ATP production via electron transfer processes where the heme centers serve as one-electron carriers. The iron in the cytochrome cycles between Fe^{2+} (reduced) and Fe^{3+}(oxidized). The protein environment mainly determines the redox potential of the ion in the cytochrome and provides the direction of electron flow in the electron transfer chain. In the past, cytochromes were classified into cytochrome a, b and c depending on their lowest energy absorption band in the reduced state.[4] But now they are labeled using the wavelength (in nm) of an absorption band in the reduced state, for example, cytochrome c_{559}.[5] The reduced form of cytochromes show three peaks in their UV-Vis spectra. Peaks are named α, β, and ϒ (the last of which is also known as the Soret band) and these bands are positioned around 570 nm (α band), around 530 nm (β band) and around 400 nm (Soret Band).

In the past few years numerous studies have reported the preparation of model systems that mimic characteristics of the cytochromes.[6-8] De novo design of such hemoproteins is now possible using modern peptide synthesis and assembly techniques.[9,10] The binding of heme to an antiparallel four-α-helix bundle (as in native cytochrome b, Figure 4.1) was investigated in detail and structural properties,[7]

electronic properties[10] and redox potentials[11] of heme cofactors in a synthetic cytochrome were examined experimentally and computationally by our collaborators.[2]

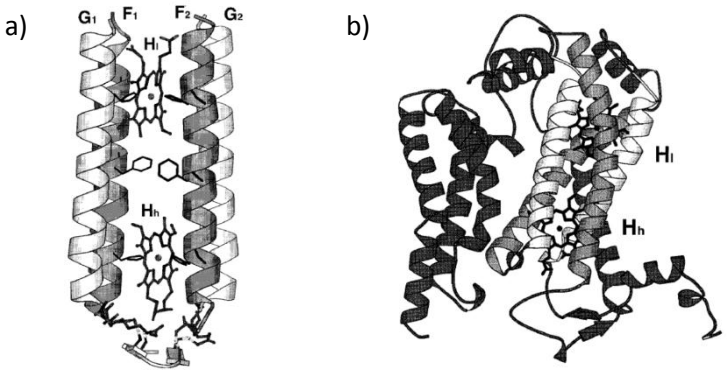

Figure 4.1: The side view of the artificial cytochrome-b (a) is the same as the view of the native cytochrome-b (b). [Adapted with permission from reference 1. Copyright (2010) American Chemical Society.]

The importance of the construction of artificial hemoproteins is to understand the relationship between the structure and the redox chemistry, the minimal requirements for function and the mechanism and the factors on which the electron transfer processes depend in the proteins.[12] These investigations may be useful in bioelectronic[13] and biocatalytic[14,15] applications by constructing artificial proteins that are smaller, cheaper to produce, more efficient than natural counterparts, and more stable under hostile environments compared to the natural protein.[1,5]

Previous studies on synthetic cytochrome-b revealed that there are significant differences in redox potentials of hemes in synthetic cytochromes compared with natural cytochromes. As has been reported, the redox potentials of two heme groups in synthetic cytochrome-b are -106 and -170 meV compared to the heme in the native cytochrome-b subunit +93 meV and -34 meV.[8] Even though both artificial and native cytochromes contain the same cofactor and same axial ligation by histidine, the native protein showed more positive values than did the synthetic protein.[8] Later studies showed that incorporation of electron donating and electron-withdrawing porphyrin substituents can alter the redox

potential by as much as 200 mV within a single four-α-helix bundle. Then the incorporation of strong electron-withdrawing groups resulted in a dramatic increase of the redox potential.[3,11] This may be due to decrease in donor ability of the lone pair of nitrogen in the porphyrin (equatorial ligands) upon addition of electron withdrawing substituents to the macrocycle. This not only affects the equatorial ligands but also changes the donor power of axial ligands through a cis-effect. Therefore, introducing electron withdrawing substituents to a synthetic heme group will help to increase the reduction potential of synthetic cytochromes to move the value closer to natural cytochromes redox potentials.

The main goal of this research is to synthesize a series of electron deficient porphyrins in order to investigate the effect of their iron complexes (heme cofactors) in a synthetic cytochrome. It is necessary to maintain the unnatural C_2 symmetry of the heme group to minimize the number of isomers that can form while binding with a synthetic four-α-helix bundle. The propionic acid side chains of heme groups are vital in their coordination with protein as they can make salt bridges with arginine residues the in synthetic protein.[1] By considering these factors, a symmetric porphyrin **1** (Figure 4.2) was designed which holds two strong electron-withdrawing groups at the β-position of one end, and propionic acid chains at the other end, closely resembling the native heme group.

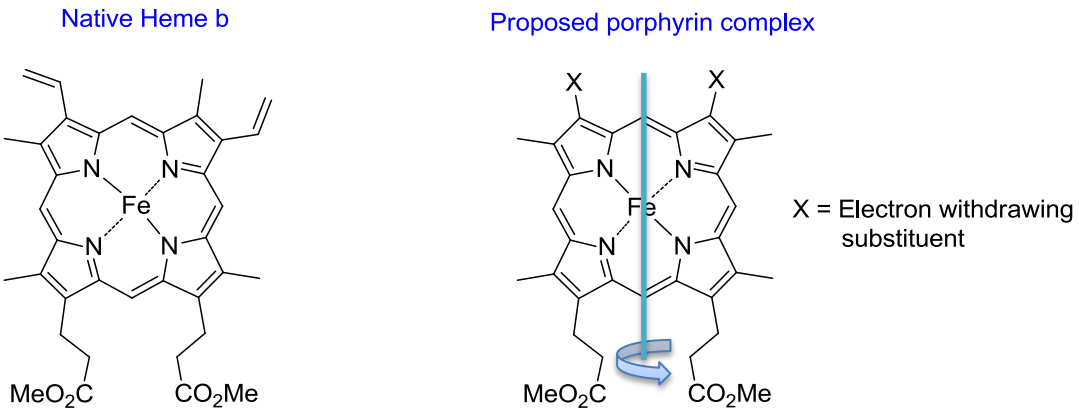

Figure 4.2: Comparison of porphyrin in native heme group and proposed porphyrin for a synthetic cytochrome.

In this research, the synthesis of a series of porphyrins, bearing electronegative nitrile groups, nitro groups, and halogens was attempted, starting from simple building blocks. After completing the syntheses of these electron deficient porphyrins, the magnitude of redox activity in synthetic proteins induced by the factors of heme peripheral substitution will be investigated by our collaborators.

4.1.1 Synthesis of Porphyrins

There are numerous methods available for synthesis of porphyrins, but the most suitable route depends on the structure of porphyrin, and most importantly the symmetry and the nature of the substituents in the target porphyrin.[16] For example, fully symmetric porphyrins can be synthesized conveniently from polymerization of monopyrrole units (Scheme 4.1).

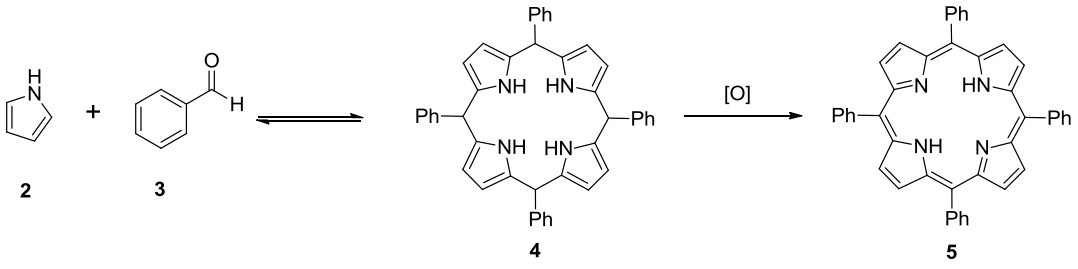

Scheme 4.1: Condensation of pyrrole and benzaldehyde to form TAPs

The most widely used methods for porphyrin synthesis are 1) cyclotetramerization of pyrroles; 2) condensation of two dipyrrolic intermidiates using 2+2 MacDonald cyclization; 3) the Fischer porphyrin synthesis via dipyrromethenes; 4) condensation of tripyrrolic intermediates with a monopyrrole unit (“3+1” methodology); and 5) cyclization of open chain tetrapyrroles such as b-bilenes and a,c biladienes. Apart from these methods porphinoid compounds can be synthesized by modification of readily accessible naturally occurring tetrapyrroles such as chlorophyll and heme.

4.1.1.1 Cyclotetramerization of Monopyrroles

Cyclotetramerization of monopyrroles is the most convenient approach to prepare porphyrins and has been used numerous times in the synthesis of simple symmetric porphyrins.[17] But the usage of this method is limited to symmetric porphyrins. β-Substituents of the pyrrole must be identical, otherwise the approch leads to a mixture of structural isomers. This method is most commonly used in synthesis of symmetric *meso*-substituted porphyrin.[18] It involves the formation of porphyrinogen **4** from the condensation between an aldehyde **3** and pyrrole **2** in the presence of a catalytic amount of acid, and subsequent oxidation affords the desired porphyrin (Scheme 4.1). Asymmetrically *meso*-substituted porphyrins can also be synthesized using mixed aldehyde condensation, but this results in a mixture of compounds. By varying the stoichiometry of the reactants the yield of the desired product can be maximized.

4.1.1.2 Fischer Porphyrin Synthesis via Dipyrromethenes

This 2+2 condensation method was first developed by Fisher in 1934.[19] It involves the condensation of two dipyrromethene units in an organic melt at very high temperature (Scheme 4.2). High temperature is probably needed to convert dipyrromethene **6** in to its enamine counterpart **7** before condensation. The major limitation of this method is that only a few substituted dipyrromethenes are able to withstand the severe reaction conditions. In the 1960s MacDonald and coworkers developed a method to synthesize porphyrins using dipyrromethanes under milder conditions.[20]

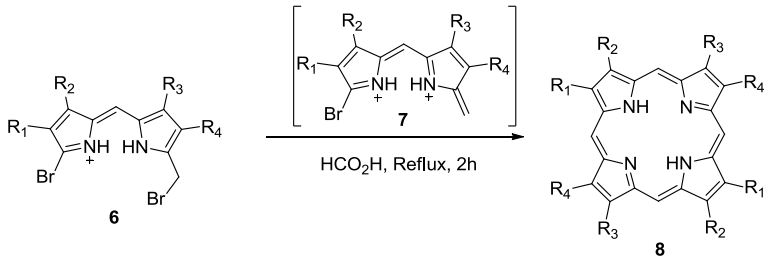

Scheme 4.2: 2+2 Condensation of dipyrromethenes – Fischer method

4.1.1.3 Condensation of Two Dipyrrolic Intermediates Using 2+2 MacDonald Cyclization

This is the most widely used method for the synthesis of porphyrins. But the principal limitation to this method is the necessity to use at least one dipyrromethane which has a symmetric β substitution pattern to avoid formation of constitutional isomers (Scheme 4.3). In situ decarboxylation of dipyrromethane dicarboxylic acid **10** will form an α free dipyrromethane, which acts as a nucleophile in the condensation reaction.[20] Condensation of α free dipyrromethane with diformyldipyrromethane **9** is catalyzed by acid. Then the intermediate porphodimethane **11a** is oxidized by air to afford the desired porphyrin **11b**.

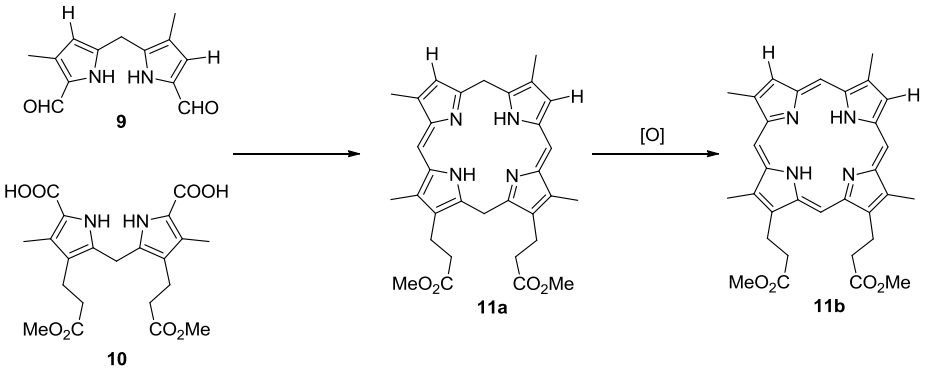

Scheme 4.3: 2+2 Condensation of Dipyrromethane – MacDonald Method

4.1.1.4 Condensation of Tripyrrolic Intermediates with a Monopyrrole Unit

To overcome limitations in the 2+2 cyclization, the 3+1 synthetic route was developed. This involves condensation of an α free tripyrrole with a diformylpyrrole, followed by oxidation to obtain the desired porphyrin (Scheme 4.4). To avoid constitutional isomers, one of the two units, tripyrrane or diformylpyrrole should be symmetrical. Molecules such as **17** can be easily obtained using the 3+1 method, where 2+2 method condensation needs a significantly large number of steps. New developments in the direct synthesis of tripyrranes such as compound **15** by condensation of two

equivalents of an acetoxymethylpyrrole **12** with one equivalent of a diunsubstituted pyrrole **13** vastly reduce the number of steps needed for synthesis of the desired pyrrole **17**.[21]

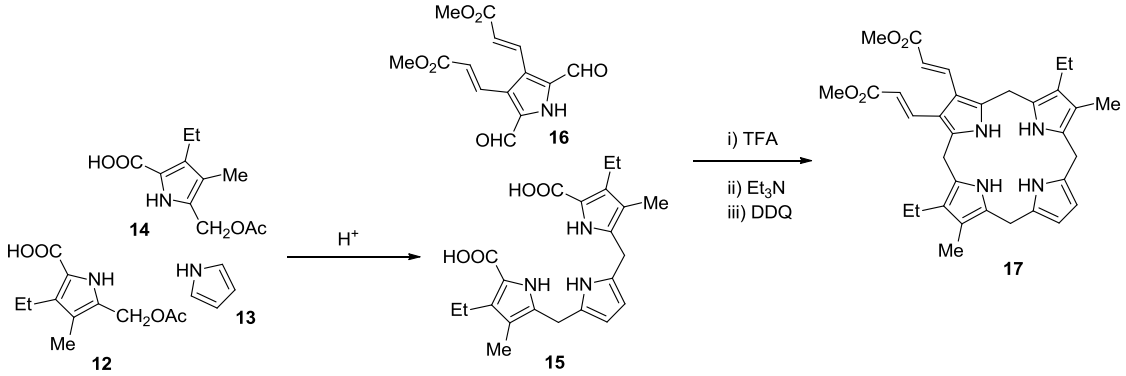

Scheme 4.4: 3+1 Condensation of Tripyrrane with Diformylpyrrole

4.1.1.5 Cyclization of Open Chain Tetrapyrroles such as b-Bilenes and a,c-Biladienes

This strategy is very useful in the synthesis of a porphyrin which is asymmetric and has a variety of substituents at the β positions. Linear tertrapyrroles can be cyclized using transition metals by oxidative cyclization to obtain the desired porphyrin. The most widely used tetrapyrroles are 1,19-dicarboxylic-b-bilenes (**18**) and 1,19-dimethy-a,c-biladienes (**19**, Scheme 4.5).

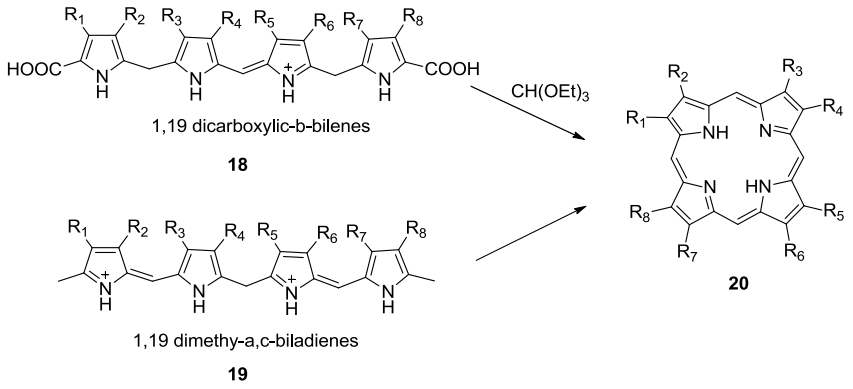

Scheme 4.5: Synthesis of porphyrin by cyclization of tetrapyrroles

Condensation of 1,19-dicarboxylic-b-bilenes (**18**) requires orthoformate, which provides the methylene bridge carbon. b-Bilenes **18** are in a lower oxidation state compared to a,c-biladiene **19**. This results in lower yield in the synthesis of porphyrin using b-bilene compared to a,c-biladiene. However both these cyclizations suffer from side reactions, such as poor yields, and sometimes, lack of reproducibility.[22] Cyclization of 1,19-dimethy-a,c-biladienes (**19**) involves the formation of a so-called "valley" substituted intermediate (**24**) and subsequent loss of a carbon function to afford the desired porphyrin (Scheme 4.6).[23,24] Cyclization usually takes place in DMF or ethanol under reflux conditions in the presence of a copper salt. The resulting copper porphyrin is treated with strong acid to obtain the free porphyrin. As shown in the mechanism in the first step, the fairly acidic methylene proton of the a,c-biladiene **21** is lost to produced more conjugated bilatriene **22**. Then the bilatriene **22** is oxidized to an enamine intermediate **23**, which is cyclized by attack of the enamine at the electrophilic carbon of the terminal pyrrole ring, forms the macrocycle **24** bearing a methyl group at the α position of the pyrrole. This will undergo oxidation to give macrocycle **25** followed by nucleophilic displacement of the "valley" methyl group which results in the porphyrin **26**.

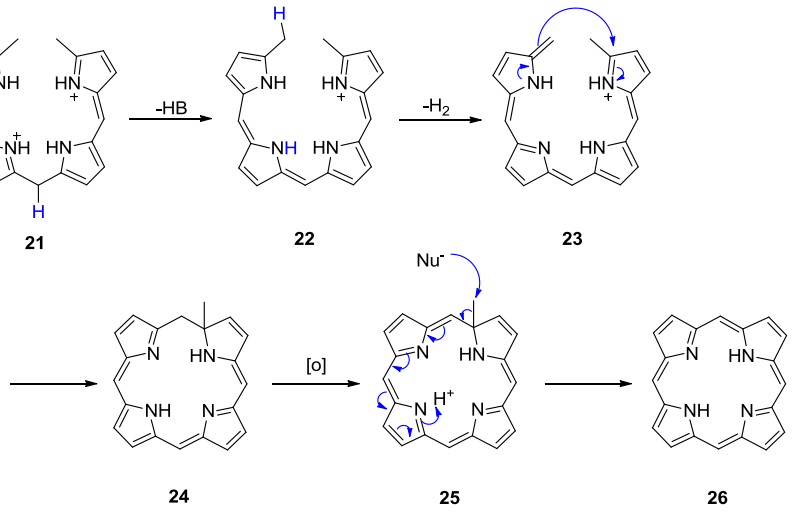

Scheme 4.6: Mechanism of a,c biladiene oxidative cyclization

4.2 Synthesis

4.2.1 Retrosynthetic Analysis of Porphyrin 1

In our retrosynthesis (Scheme 4.7), the first disconnections were made at meso positions of the porphyrin in order to get symmetric dipyrromethanes **27** and **28**. These dipyrromethanes can be cyclized using the 2+2 MacDonald cyclization.[20] Then these symmetric dipyrromethanes can be synthesized from the analogous pyrroles using self-condensation. Self-condensation of β substituted pyrrole **32** will form β substituted dipyrromethane **27**. β-Substituted pyrrole **32** can be obtained from acetylpyrrole **33**. The β position of acetylpyrrole **33** can be functionalized through formation of β-free pyrrole. The Knorr pyrrole synthesis can be used, which is widely used in the synthesis of substituted pyrroles, to obtain acetylpyrrole **33**.[25] In the same way the lower lobe of the targeted molecule can be synthesized. Dipyrromethane **28** can be synthesized by self-condensation of pyrrole **29**, which can be synthesized by the Knorr pyrrole route, namely by condensation between diketone **31** with oximinoacetate **30**.

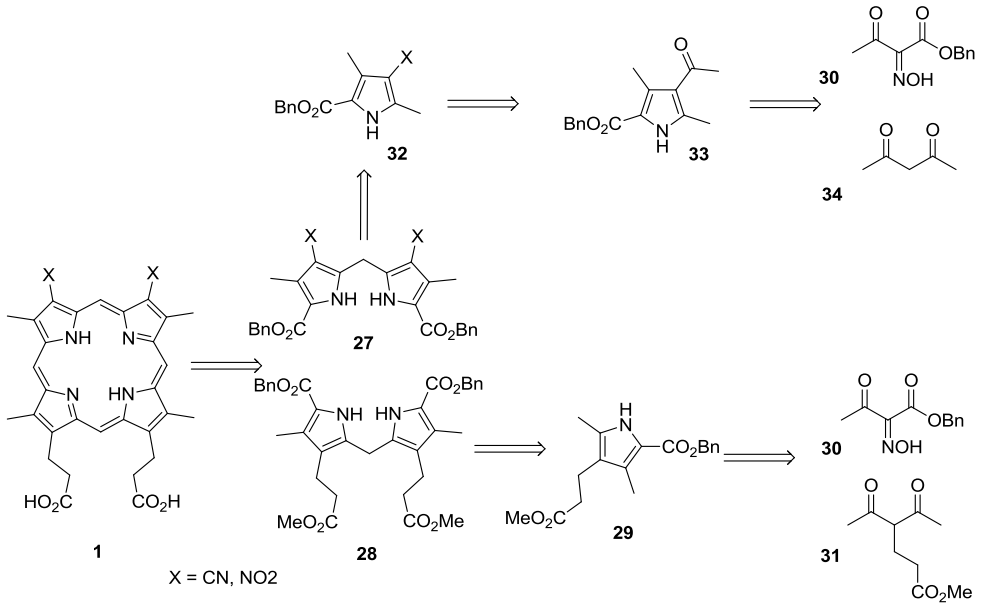

Scheme 4.7: Retrosynthesis of porphyrin **1**

4.2.2 Synthesis of the Lower Lobe 28

Synthesis of dipyrromethane **28** was previously reported and gave a good yield (Scheme 4.8).[26] Treatment of benzyl acetoacetate (**35**) with aqueous sodium nitrite in acetic acid formed benzyl oximinoacetate **30** which was condensed with diketone **31** in acetic acid under Johnson conditions in the presence of Zn dust to obtain the benzyl pyrrole carboxylate **29**.[27] After precipitation and recrystallization, it was possible to obtain the pure product **29** in 43% yield. Prior to condensation, the α-methyl group of the pyrrole **29** required activation. The most widely used activation methods are 1) bromination of an α-methyl group followed by condensation;[28] or 2) oxidation of an α-methyl group with lead tetra-acetate.[26] The lead tetra-acetate oxidation was followed first. The pyrrole **29** was treated with lead tetraacetate to afford acetoxymethylpyrrole **36**. The product was purified via recrystallization in methanol. This purified product **36** was heated in methanol under acidic conditions to form the desired dipyrromethane **28**, which was characterized by ^{1}H NMR and mass spectroscopy.

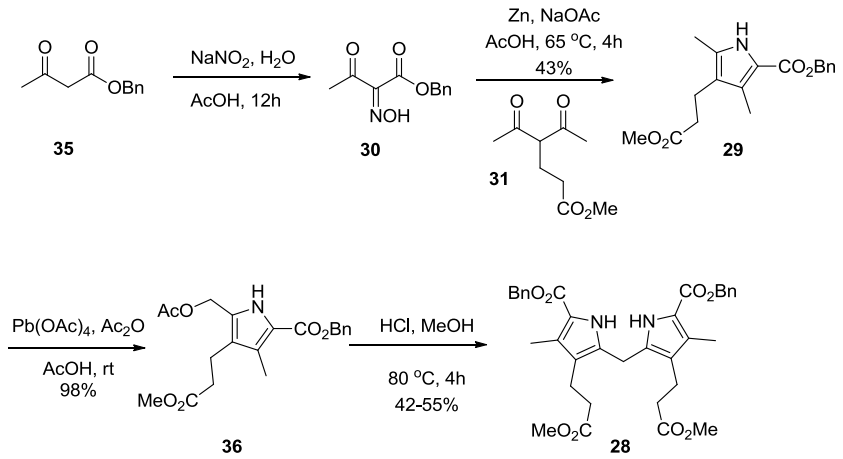

Scheme 4.8: Synthesis of benzyl dipyrromethane **28**

4.2.3 Synthesis of the Upper Lobe 27

The other precursor pyrrole **33** for the synthesis of the β-substituted dipyrromethane **27** was prepared using the same Johnson conditions (Scheme 4.9).[27,29] Oximinoacetate **30** was synthesized from the reaction between benzyl acetoacetate (**35**) with sodium nitrite in acetic acid and then condensed with pentanedione **34** in the presence of Zn dust to obtain acetylpyrrole carboxylate **33**.

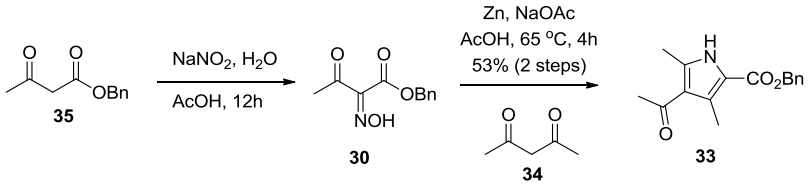

Scheme 4.9: Synthesis of acetylpyrrole **33**

The next step was to oxidize the α-methyl group of the acetylpyrrole **33** in order to facilitate the self-condensation to obtain the desired dipyrromethane **39**. But the oxidation of acetylpyrrole **33** with lead tetra-acetate failed. Only the starting material was recovered after 20 hours. Different reaction conditions were employed but it was impossible to obtain the desired product **37**. Then it was decided to try the α-bromination route in order to obtain α-bromomethylpyrrole **38**, which can be self-condensed to give the dipyrromethane **39**. After the bromination, the crude product was subjected to the self-condensation reaction. But again it was not possible to obtain the desired dipyrromethane **39**. The mass spectrum of the crude material, obtained after the bromination step, showed a peak for mono-brominated compound. But bromination could in theory happen on either the α-methyl group on the pyrrole or at the α-methyl group on acetyl group. Purification of brominated product was unsuccessful due to its low yield (Scheme 4.10).

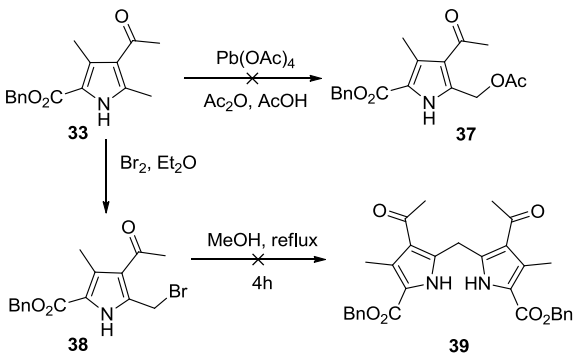

Scheme 4.10: Attempted synthesis of acetyldipyrromethane **39**

It was then decided to replace the acetyl group with a formyl group to eliminate the competition in the bromination step (Scheme 4.11). To obtain formylpyrrole **33**, first it was required to synthesize the β-free pyrrole **40**. In the literature a versatile high yielding method for deacylation of pyrrole is reported.[30] The authors were able to deacylate pyrroles with ethylene glycol and *p*-toluenesulfonic acid under reflux in benzene. When this procedure was followed a 95% yield of β-free pyrrole **40** was obtained. Reaction progress was monitored through TLC. After completion of the reaction, solvent was removed to obtain the pure crystalline product. ^{1}H NMR and mass spectroscopy confirmed the identity of the product **40**.

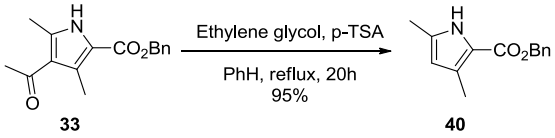

Scheme 4.11: Deacylation of the acetylpyrrole **33**

As the authors discussed in the paper, the mechanism involves initial ketal formation (**41**) in a classical carbonyl protection reaction (Scheme 4.12). Then electrophilic substitution (protonation) at the ketal substituted carbon followed by elimination of the bulky protected acetyl group will help to regain the aromaticity of pyrrole **42**.

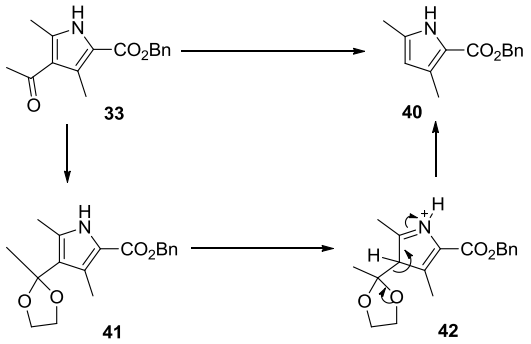

Scheme 4.12: Mechanism of deacylation

The next step required formylation of the free β-position of pyrrole **40**. Formylation can be accomplished either using triethyl orthoformate[31] or under Vilsmeier-Haack conditions.[32] Triethyl orthoformate worked best in the formylation of this pyrrole. β-Free pyrrole **40** was treated with a slight excess of triethyl orthoformate in TFA to obtain formylpyrrole **41** in 70% yield (Scheme 4.13). A very short silica gel column was used to purify the product, which was characterized by ^{1}H NMR and mass spectrometry. Some difficulty was encountered in the formylation under Vilsmeier-Haack conditions, and the yield was always lower than the yield of the triethyl orthoformate reaction.

Scheme 4.13: Formylation of β-free pyrrole **40**

Self-condensation of formylpyrrole **41** was attempted by initial bromination followed by condensation in methanol under acidic conditions (Scheme 4.14). After two hours of reflux a white color precipitate was formed in the reaction mixture. This precipitate refused to dissolve in common solvents tested. It seems under reflux, the pyrrole **41** tends to polymerize to give this white precipitate. Oxidation of the α-methyl group of formylpyrrole **41** with lead tetra-acetate (LTA) was also unsuccessful, as with its acetyl precursor **43**.

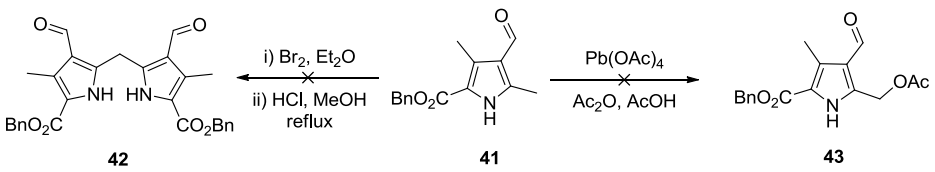

Scheme 4.14: Attempted synthesis of formyldipyrromethane **42**

Then it was decided to perform chlorination of the α-methyl group instead of bromination in order to prevent the polymerization during the condensation reaction. Formylpyrrole **41** was treated with sulfuryl chloride to obtain the chloromethylpyrrole **44**. Mass spectrometry showed a peak for mono chlorinated product but purification was unsuccessful. Then the crude product was used for the condensation reaction in methanol. But again it was not possible to obtain the desired dipyrromethane **42**. Our next approach was to convert chloromethylpyrrole **44** to acetoxymethylpyrrole **45** using a S_N2 type reaction. Previous literature has reported conversion of chloromethylpyrrole into acetoxymethylpyrrole using sodium acetate.[33] But with acetylpyrrole **44** only a trace amount of product **45** was isolated. The yield of this reaction was very low and it was not possible to prepare enough material for the next condensation reaction (Scheme 4.15).

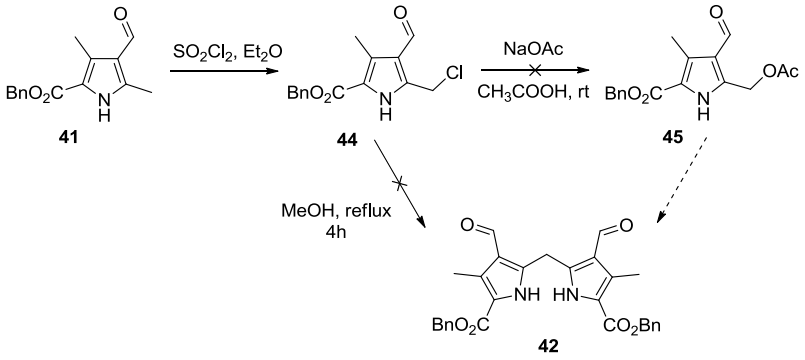

Scheme 4.15: Atempted synthesis of acetyldipyyromethane **42** by chlorination

Both acetyl and formyl groups can significantly lower the electron density in the pyrrole by removing electrons from the system by resonance. Lower electron density in the pyrrole makes it

unreactive towards electrophilic substitution reactions. To overcome electron deficiency in the pyrrole, the next approach employed was to synthesize β-free dipyrromethane **46** and then functionalize it with electron withdrawing substituents (Scheme 4.16). Removal of formyl and acetyl substituents from the pyrrole can increase the electron density in the pyrrole. Hence, it will increase the reactivity of α-methyl group of the pyrrole **40**.

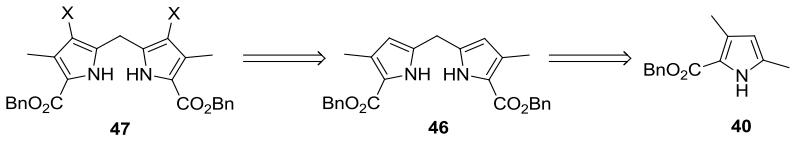

Scheme 4.16: Retrosynthesis of dipyrromethane **47**

The synthesis was started with the previously synthesized β-free pyrrole **40**. The first attempt to synthesize acetoxymethylpyrrole with lead tetraacetate failed to achieve the desired product (Scheme 4.17). ^{1}H NMR and mass spectrometry showed the addition of an extra acetoxymethyl group to the product. Absence of the peak for β-hydrogen confirmed the additional substitution of hydrogen with an acetoxy group had taken place at β-position. Excess lead tetraacetate was reacted with both β-position and α-methyl group of pyrrole **40**. It was not possible to obtain the desired dipyrromethane **47** even by changing the number of equivalents of LTA or by changing the reaction conditions. Then it was decided to do the condensation reaction with acetoxypyrrole **48** to obtain dipyrromethane **49**, which can be converted into the desired dipyrromethane. But this acetoxypyrrole **48** was easily polymerized in methanol under acidic conditions. Bromination followed by condensation of pyrrole **40** also provided no success. As expected, bromination leads to di-brominated pyrrole **50**. The crude mixture was refluxed in methanol under acidic conditions to obtain di-bromodipyrromethane **51**, but only polymerized product was observed.

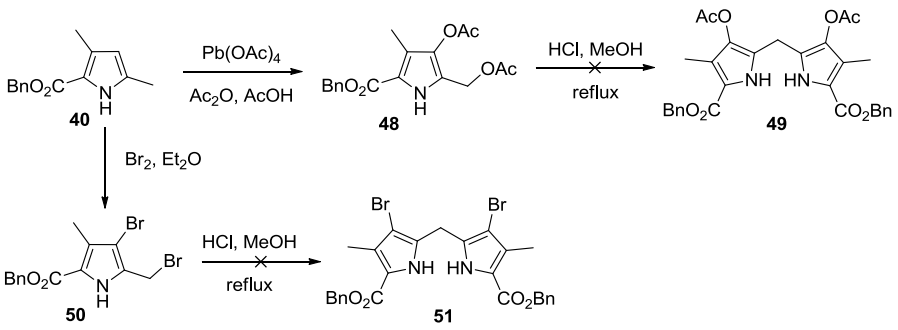

Scheme 4.17: Attempted self-condensation of β free pyrrole **40**

It was not possible to synthesize the starting material for the MacDonald cyclization. The retrosynthesis (Scheme 4.7) involved synthesis of two symmetric dipyrromethanes followed by a 2+2 MacDonald tetramerization to give the macrocycle **1**. Synthesis of dipyrromethane **28** has previously been reported and gave a good yield (Scheme 4.8). However using various synthetic paths, synthesis of the upper lobe of the molecule **27** that bears either electron-withdrawing groups or hydrogens at the β-positions failed. The electron-withdrawing groups at the β-positions of pyrrole **32** significantly reduced the reactivity of the α-methyl group. For the condensation of two pyrroles, one needs an activated acetoxymethylpyrrole or bromomethylpyrrole.[27] But in the presence of an electron-withdrawing group at the β-position, it was not possible to synthesize the desired acetoxymethylpyrole **37** or bromomethylpyrrole **38** from acetylpyrrole **33** or from formylpyrrole **41**. Another possible route, self-condensation of β-free pyrrole **40**, provided a polymerized product rather than the desired dipyrromethane **46**. This led to the design of a different retrosynthetic path.

4.2.4 Revised Retrosynthesis

The designed alternate strategy is shown in Scheme 4.18; it involves an a,c-biladiene **53** synthesis, followed by cyclization to construct the β-free porphyrin **52**. Functionalization of the β-positions of porphyrin **52** will be done to get the target molecules **1**. a,c-Biladiene **53** can be synthesized from two different starting materials. Either reacting the dipyrromethane dicarboxylate **54a** with

formylpyrrole **55a** or the diformyldipyrromethane **54b** can be react with pyrrole carboxylate **55b** to obtain a,c-biladiene **53**. Both formylpyrrole **55a** and pyrrole carboxylic acid **55b** can be synthesized from previously synthesized benzyl pyrrole carboxylate **40**. Likewise diformyldipyrromethane **54b** and dipyrromethane dicarboxylic acid **54a** can be synthesized from benzyl dipyrromethane dicarboxylate **28** which was already synthesized in good yield.

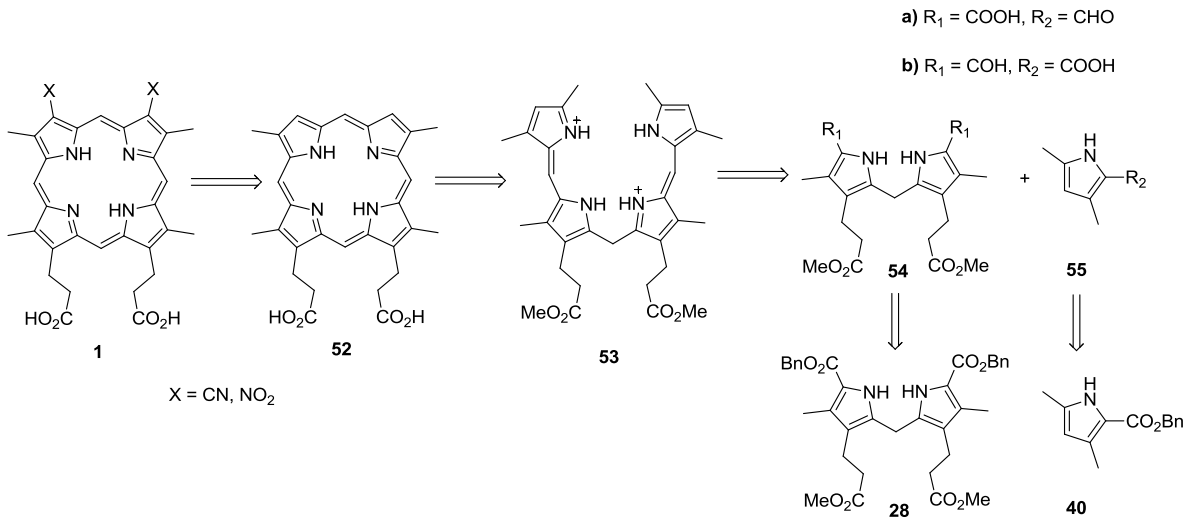

Scheme 4.18: Revised retrosynthesis of porphyrin **1**

4.2.5 Synthesis of a,c Biladiene

As was mentioned earlier, a,c biladienes **53** can be synthesized using two different starting materials. The best overall yield is obtained by reaction between a formylpyrrole **55a** and a dipyrromethane di-carboxylic acid **54a**. As shown in Scheme 4.19, first pyrrole carboxylic acid **57** was obtained from benzyl deprotection of benzyl pyrrole **40**. Then formypyrrole **59** was obtained by decarboxylation followed by formylation of pyrrole **57**. Pyrrole carboxylate **57** was stirred in TFA in an ice bath to accomplish the decarboxylation and then treated with excess triethyl orthoformate to selectively formylate the α-position of the α,β-unsubstituted pyrrole **58**. Pyrrole undergoes electrophilic

aromatic substitution predominantly at the α-positions. Once formylated at the α-position, this will prevent the addition of a second formyl group to the β-position by deactivating the pyrrole ring through resonance. The desired formylpyrrole **59** was purified via a short silica gel column and characterized by ^{1}H NMR and mass spectrometry.

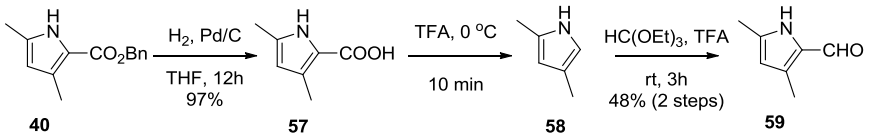

Scheme 4.19: Synthesis of β-free formylpyrrole **59**

Dipyrromethane dicarboxylic acid **60** was synthesized by benzyl deprotection of the previously synthesized dipyrromethane **28**. After de-benzylation by hydrogenolysis, the first attempt at formylation with triethyl orthoformate was unsuccessful, but formylation using the modified Vilsmeier-Haack procedure gave the diformyldipyrromethane **61** in a relatively good yield (Scheme 4.20). The modified Vilsmeier-Haack reaction uses benzoyl chloride (**63**) and dimethylformamide (**62**), which forms the reactive chloromethyleneiminium **64** salt that will react at the α-position of pyrrole by electrophilic substitution followed by hydrolysis of the imine to produce the formyl group.

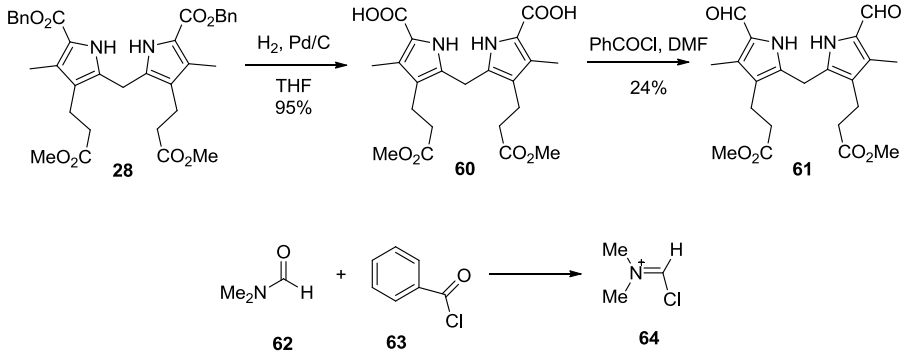

Scheme 4.20: Formylation of dipyrrolmethane using modified Vilsmeier-Haack reaction

Condensation of formylpyrrole **59** with dipyrromethane dicarboxylic acid **60** in trifluoroacetic acid afforded the corresponding a,c-biladiene salt **53** (Scheme 3.21). This involves in situ generation of α-free dipyrromethane by decarboxylation of the dipyrromethane dicarboxylic acid **60** in TFA. Then the a,c-biladiene was converted into the hydrochloride salt by bubbling HCl gas through the reaction mixture and there was a noticeable color change from orange to dark red. The reaction was monitored by UV-Vis throughout (Figure 4.3). Once the reaction was complete, the absorption spectrum showed two characteristic absorption bands at around 440 and 507 nm as shown in Figure 4.3. a,c-Biladiene **53** was purified via precipitation, i.e. adding petroleum ether into a concentrated solution of a,c-biladiene **53** in MeOH, and Figure 4.4 shows its proton NMR spectrum in $CDCl_3$. As an alternate method, condensation of diformyldipyrromethane **54b** with pyrrole carboxylic acid **55b** was carried out but the overall yield was always lower than the previous method.

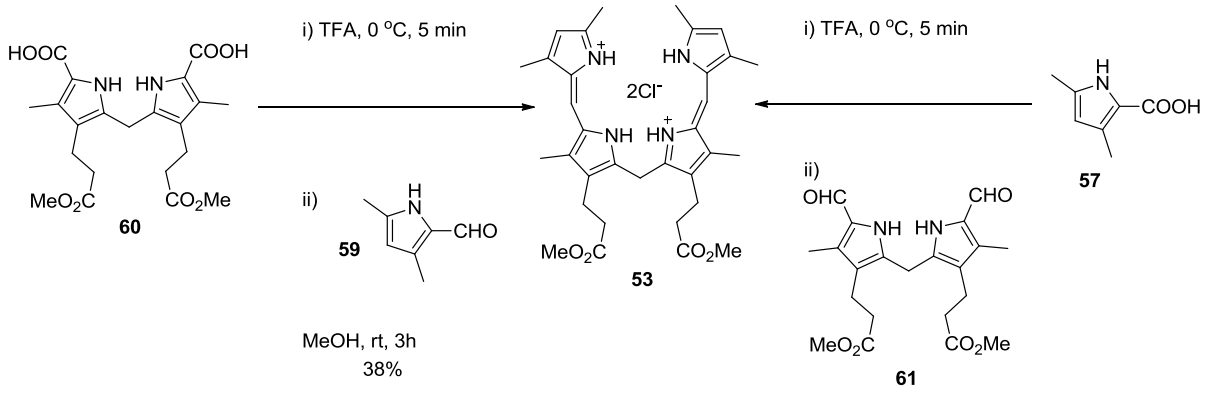

Scheme 4.21: Syntheis of a,c-biladiene

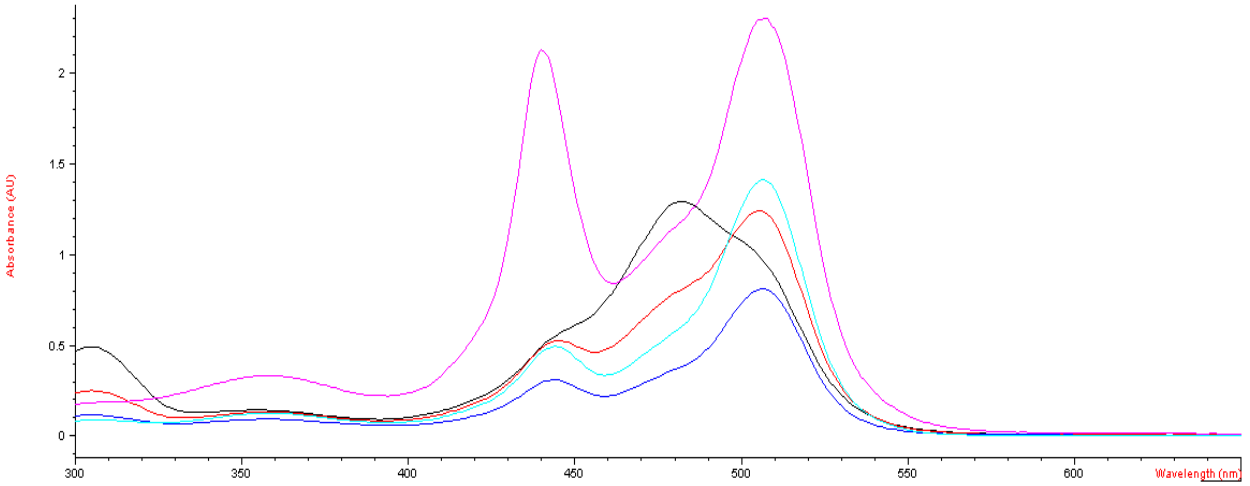

Figure 4.3: UV-Vis spectroscopic progression of the a,c-biladiene synthesis in CH_2Cl_2 and UV-Vis spectrum of pure a,c biladiene dihydrochloride **53** (pink) in CH_2Cl_2.

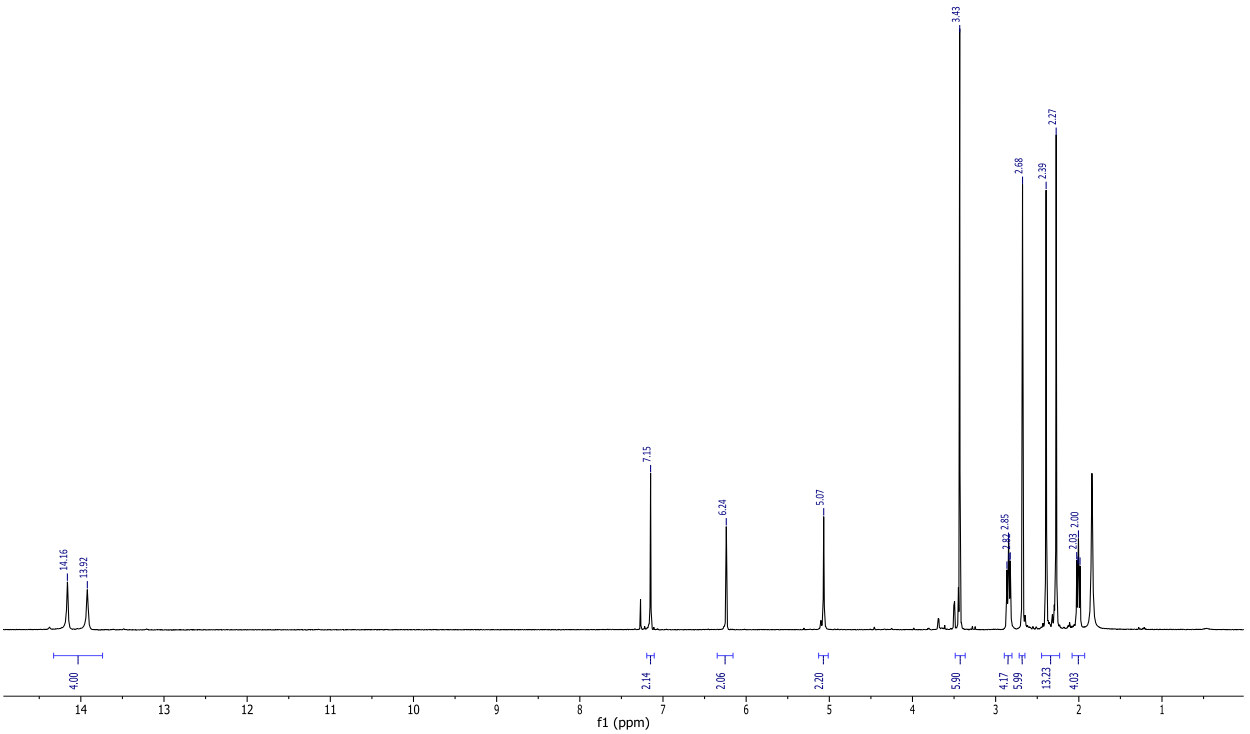

Figure 4.4: ^{1}H NMR spectrum of a,c-biladiene dihydrochloride **53** in $CDCl_3$

4.2.6 Synthesis of β-Free Porphyrin 52

The literature reports two main methods for cyclization of a,c-biladiene salts to give the corresponding porphyrin. 1) Metal catalyzed oxidative cyclization;[23] and 2) electrochemical cyclization.[34] Various metals [Cu(II), Cr(III), Ru(III) and Rh(III)] have been used in the metal catalyzed oxidative cyclizations.[35] According to the literature, the cyclization of a,c-biladiene salts catalyzed by copper ions has proved to be one of the most successful syntheses of porphyrins.[35] The reactions were generally carried out in DMF and the resulting products are the corresponding copper porphyrinates. If acid-labile substituents are present on the macrocycles, the removal of the metal ion can be quite difficult, as it requires a strong acid to remove copper from the copper porphyrinates; also, unpredictable yields of porphyrins have sometimes been reported. Cyclization using Cr(III), Ru(III) and Rh(III) provide the porphyrin free base and eliminate the harsh acidic conditions necessary for removal of copper. But the cyclization yields were significantly lower than those using the copper mediated oxidative cyclization.[35] After considering all these facts it was decided to use Cu(II) for the oxidative cyclization step.

Oxidative cyclization of a,c biladiene dihydrochloride **53** was carried out in DMF using $Cu(OAc)_2$ and the reaction was monitored by UV-Vis spectroscopy (Scheme 4.22). The reaction mixture was heated at 100 ^{o}C until reaction was completed as indicated by UV-Vis spectrometry. Once reaction was completed, the UV-Vis spectrum showed the Soret band (400 nm) that is characteristic of porphyrins (Figure 4.5). After workup, the crude product was taken to the next step. Crude copper porphyrin **65** was demetalated in the presence of ice cold H_2SO_4/ TFA for six hours. The final product was purified using a silica gel column and the porphyrin was characterized by X-ray crystallography (Figure 4.6), ^{1}H NMR (Figure 4.7) and mass spectrometry. Unfortunately, the yield of these two steps was highly variable as reported in the literature and the maximum yield obtained was 13%.

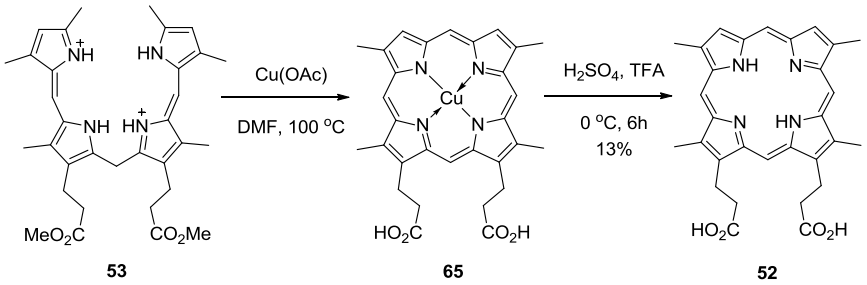

Scheme 4.22: Synthesis of β-free porphyrin **52** by oxidative cyclization of a,c-biladiene **53**.

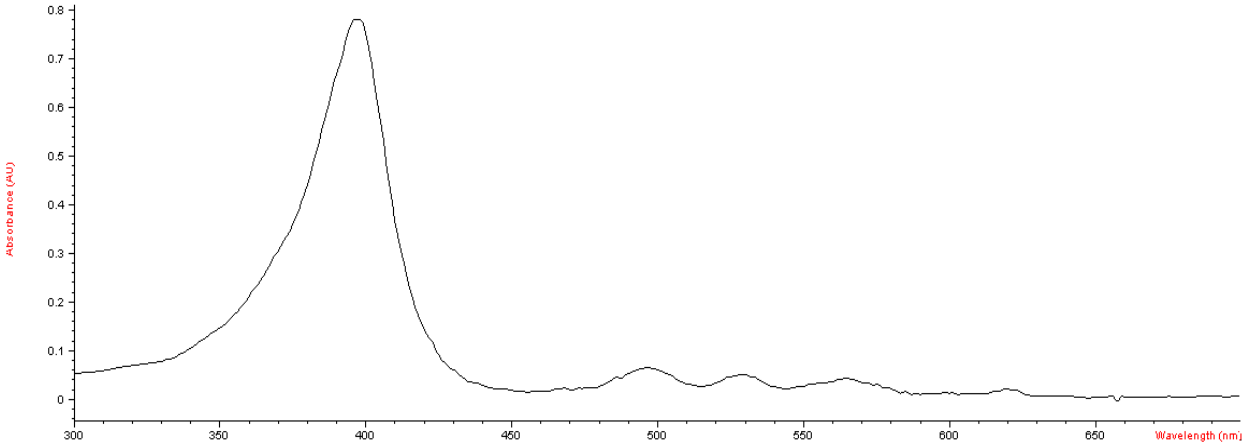

Figure 4.5: UV-Vis spectrum of β-free porphyrin **52** in CH_2Cl_2

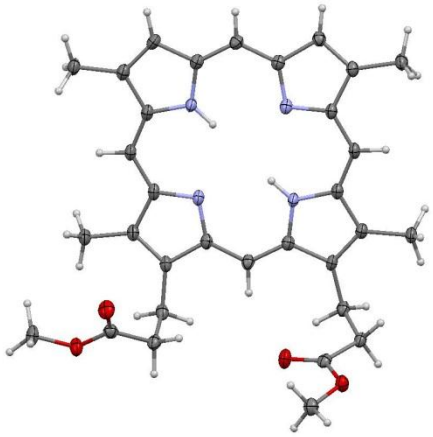

Figure 4.6: X-ray crystal structure of β-free porphyrin **52**

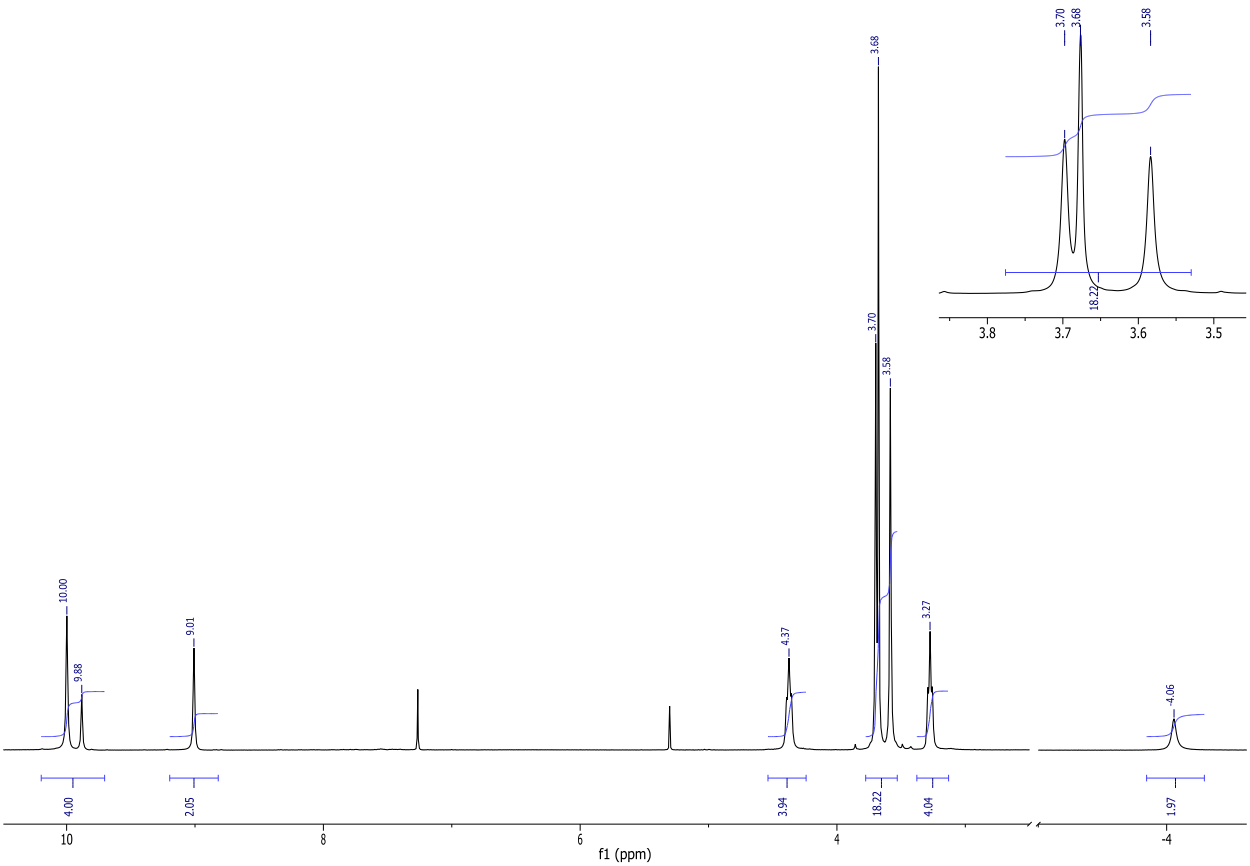

Figure 4.7: ^{1}H NMR spectrum of β-free porphyrin **52** in $CDCl_3$

As proposed in the revised retrosynthesis, the last step is to functionalize the β-position of the porphyrin **52**. The plan is to functionalize it with electron withdrawing groups such as nitriles, halides, formyl and nitro groups. As shown in Scheme 4.23, several reactions to introduce electron-withdrawing substituents to the porphyrin **52** were attempted. Formylation with triethyl orthoformate, the Vilsmeier complex, or with the modified Vilsmeier-Haack reaction were unsuccessful and the starting material was recovered. Nitration of the β-position using $PPh_3/Br_2/AgNO_3$, as reported in the literature,[36] was also attempted. But it was not possible to obtain the desired product **67**. Bromination was unsuccessful with Br_2 in ether but the peak for the desired di-bromoporphyrin **68** was visible in the mass spectrum when NBS was used for bromination. However, the amount of product was not sufficient to characterize by ^{1}H NMR.

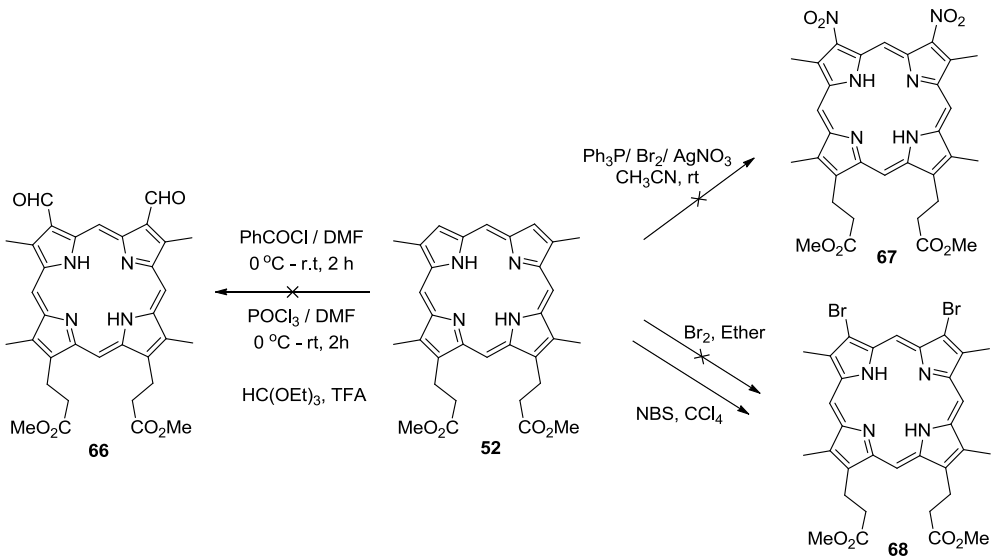

Scheme 4.23: Attempted β functionalization of β free porphyrin **52**

As can be seen from the literature, under acidic conditions the basic inner nitrogens of porphyrins can be easily protonated, and this deactivates the ring towards electrophilic substitution reactions. Therefore, formylation of free base porphyrins is not possible under acidic conditions. But protonation of the inner nitrogens can be prevented by inserting a metal ion into the porphyrin core. The best choice is to use copper complex porphyrin **65** as it forms during the synthesis as an intermediate. Then formylation of copper porphyrin **65** was done under Vilsmeier conditions (Scheme 4.24). Mass spectrometry confirmed the formation of monoformylated product. But increasing the reaction time, temperature or number of equivalents of Vilsmeier complex did not show any sign of formation of the diformyl derivative **69**. Reaction with triethyl orthoformate was also unsuccessful in giving the diformyl derivative **69**.

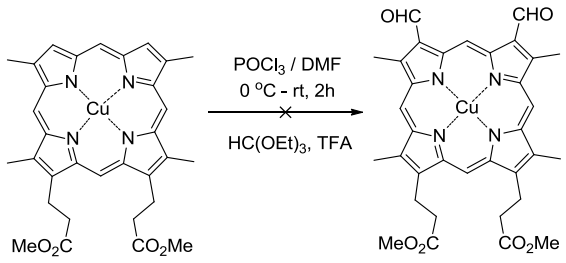

Scheme 4.24: Attempted diformylation of copper porphyrin **69**

To test each one of these functionalization reactions, the cyclization of a,c-biladiene **53** was the starting point. The yield of the cyclization step of a,c biladiene **53** was very low and highly variable. Also, selective functionalization of the β-position of the *meso* unsubstituted porphyrin is extremely challenging due to high reactivity of the *meso* positions compared to the β-positions. However, the functionalization of β-positions of porphyrin may require preparation of β-activated porphyrins over *meso* position prior to functionalization. This led to the conclusion that addition of electron withdrawing groups to the β-free pyrrole **40** should be done before the cyclization step. The next approach therefore was to synthesize a pyrrole **71** bearing an electron-withdrawing group such as nitrile and halides at the β-position. This can be synthesized from the previously synthesized β-free pyrrole **40**. Then a,c biladiene synthesis followed by oxidative cyclization should result in the final product **1** (Scheme 4.25).

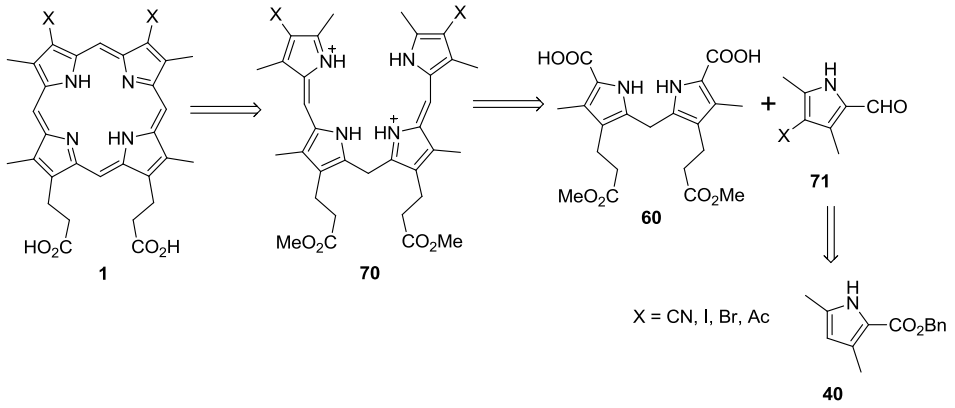

Scheme 4.25: New approach to synthesize porphyrin **1** from electron deficient pyrrole **71**

4.2.7 Synthesis of Electron Deficient Pyrrole

Synthesis was started from formylpyrrole **41**, which was synthesized by deacylation of acetylpyrrole **33** followed by formylation with triethyl orthoformate. The next step was to convert the formyl group into a nitrile group. Recently, Veisi reported an efficient procedure for the one-pot conversion of various alcohols, aldehydes and primary amines into the corresponding nitriles in excellent yields using trichloroisocyanuric acid (TCCA) and aqueous ammonia.[37] But this oxidative

conversion was unsuccessful in conversion of formylpyrrole **41** to its nitrile counterpart **72** (Scheme 4.26).

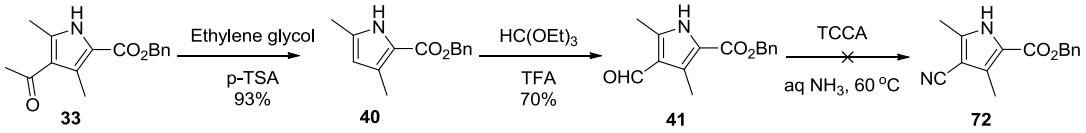

Scheme 4.26: Attempted synthesis of 3-cyanopyrrole **72**

The next approach was to convert the formyl group into an oxime followed by dehydration to give the desired cyanopyrrole **72**. Before that, models studies were performed using ethyl formylpyrrole carboxylate **73** which was readily available in the laboratory (Scheme 4.27). Formylpyrrole **73** was reacted with hydroxylamine hydrochloride to afford aldoxime **74** in high yield.[38] For the dehydration of aldoxime **74**, first a traditional dehydrating agent chlorosulfonic acid was used.[39] After dehydration, the product was purified via a silica gel column to afford 31% yield, along with large number of by products (in the TLC).

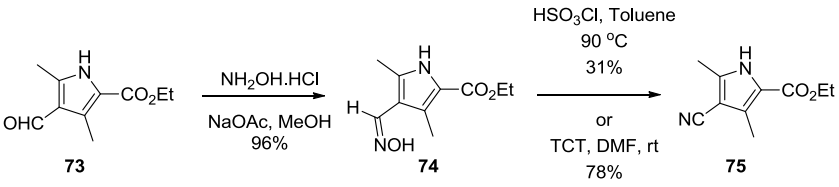

Scheme 4.27: Conversion of formylpyrrole **73** to cyanopyrrole **75**

Previous literature has reported a two-step method to convert a variety of ketones and aldehydes into amide and nitriles, respectively, under mild conditions.[40] In this method, the first step involves formation of the corresponding oxime and then a rearrangement to nitrile using cyanuric chloride (trichlorotriazine, TCT) in DMF. As shown in Scheme 4.28, TCT and DMF forms a Vilsmeier-Haack type active complex **76** and then the hydroxyl group of the oxime **77** will add to the complex in a

type of Mannich addition. A subsequent Beckman rearrangement to the intermediate **78** will afford the final product; cyanopyrrole **75**. The TCT/DMF complex was prepared by dissolving one equivalent of TCT in DMF at room temperature. During the reaction the complex precipitated as a white solid. After confirming complete disappearance of free TCT by TLC, one equivalent of aldoxime **77** in DMF was added and the reaction was monitored by TLC. After completion of the reaction, the product was purified via column chromatography. It was possible to isolate the desired cyanopyrrole **75** in 78% yield and X-ray crystallograpy (Figure 4.7), ^{1}H NMR, and mass spectrometry confirmed the identity of the product **75**.

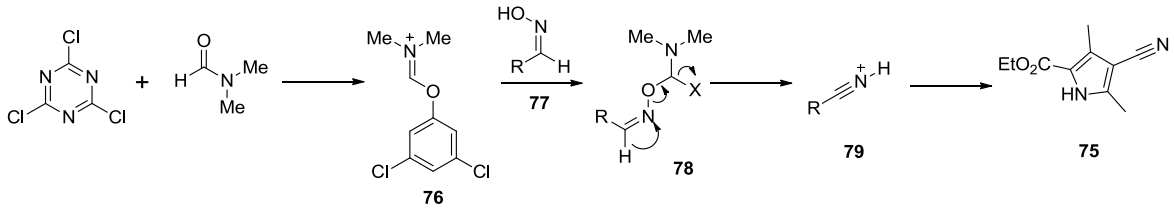

Scheme 4.28: Mechanism of dehydration by TCT

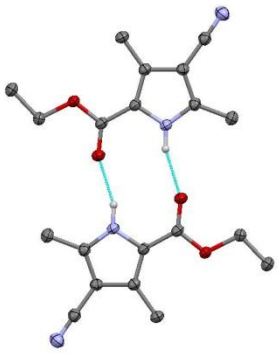

Figure 4.7: X-ray crystal structure of cyanopyrrole **75**

As the targeted conversion of formyl to nitrile in good yield by using model compound **73** had been achieved, the same conversion was carried out with benzyl formylpyrrole carboxylate **41**. The formyl group of the benzyl pyrrole **41** was transformed into nitrile by oximation followed by dehydration with TCT in good yield. Next it was necessary to formylate the cyanopyrrole **73** in order to do the condensation with a dipyrromethane dicarboxilic acid **60**. Hydrogenolysis of cyanopyrrole **73** afforded

pyrrole carboxylic acid **81** in quantitative yield. Formylation was attempted with triethyl orthoformate in TFA but it was not possible to obtain the formypyrrole **82**. Formylation with the Vilsmeier complex also provided no success (Scheme 4.29).

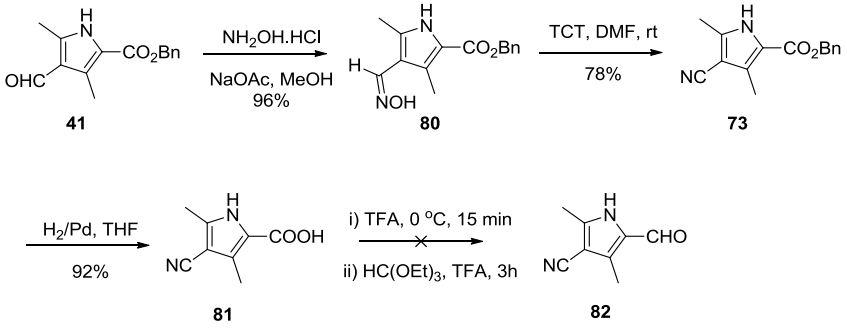

Scheme 4.29: Synthesis of 3-cyano-1-formylpyrrole **82**

The next approach was to synthesize α-free β-cyanopyrrole **86** which can condense with diformyldipyrromethane **61** directly. β-Formylpyrrole **84** has been synthesized from ethyl formylpyrrole carboxylate **73** by ester hydrolysis under basic conditions followed decarboxylation. Then it was converted into the corresponding oxime **85** in good yield, but dehydration to nitrile **86** was unsuccessful (Scheme 4.30).

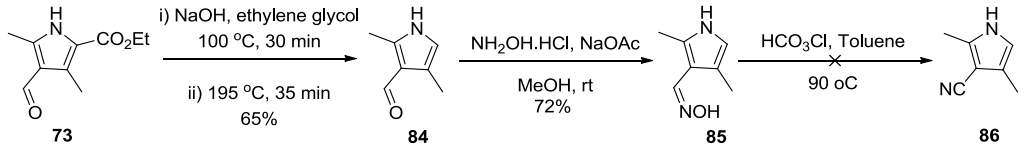

Scheme 4.30: Attempted synthesis cyanopyrrole **86**

As the synthesis of both formylpyrrole **82** and α-free cyanopyrrole **86** were unsuccessful, it was decided to condense pyrrole carboxylic acid **81** with diformyldipyrromethane **61** to obtain the a,c-biladiene **87** (Scheme 4.31). The reaction was monitored by UV-Vis spectroscopy over three hours, which showed no a,c-biladiene absorption peak. After treatment with HCl gas, petroleum ether was

added. If a,c-biladiene salt was present it should precipitate in the medium, but no precipitate was obtained. Thus, the electron withdrawing ability of the cyano group may reduce the nucleophilicity at the α-carbon of the pyrrole. That is most likely the reason for the failure of both formylation and condensation reactions.

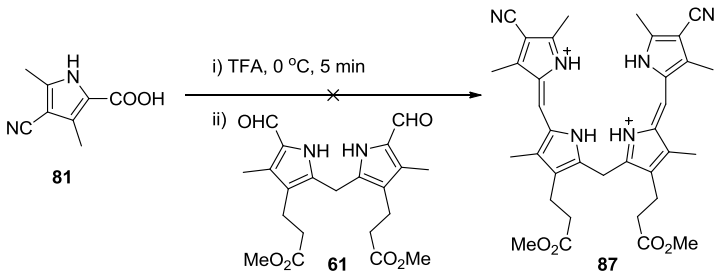

Scheme 4.31: Attempted synthesis of a,c biladiene **87** from cyanopyrrole **81**

Then it was decided to introduce a less electron withdrawing substituent at the β-position to determine its effect on the formylation. Iodo was selected as an ideal substituent as it can be used for further coupling reactions to introduce various substituents at the β-position. Iodination of pyrrole **40** was archived by direct action of I_2 in aqueous KI, which maintains a low concentration of free I_2 in the reaction medium by equilibration with triiodide ion (I_3^-). Sodium bicarbonate was used to neutralize the starting material and prevent the formation of HI. Iodopyrrole **88** was afforded in high yield and was characterized by ^{1}H NMR and mass spectrometry (Scheme 4.32). Unfortunately, debenzylation of iodobenzene **88** afforded a polymerized product.

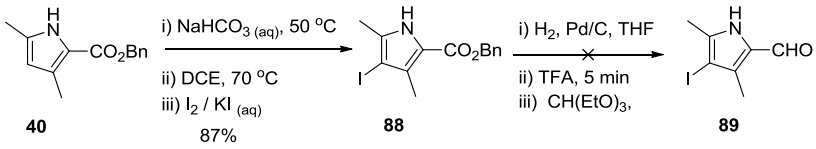

Scheme 4.32: Attempted synthesis of iodopyrrole **89**

The next approach was to reduce the carboxylic acid group of the cyanopyrrole **81** to a formyl group because its α-carbon no longer acts as a nucleophile in the condensation reaction. The resulting formylpyrrole **82** can potentially be condensed with dipyrromethane dicarboxylic acid **60** to obtain a,c-biladiene **87**. The main challenge is to reduce the carboxyl without reducing the nitrile group. Strong reducing agents such as lithium aluminum hydride will reduce both functional groups. With this in mind a mild and selective reducing agent to convert carboxyl group to formyl in good yield without occurrence of overreduction was sought. Burns and coworkers reported a mild and selective method to reduce carboxyl group to formyl in the presence of an electron withdrawing β-acetyl functional group.[41] The reaction involves formation of an acid chloride in the presence of oxalyl chloride and a catalytic amount of trimethylphosphine followed by reduction of the acid chloride to aldehyde with sodium triacetoxyborohydride and trimethylphosphine (Scheme 4.33). Cyanopyrrole **81** was dissolved in CH_2Cl_2 as it refused to dissolve in benzene, and was then added to the freshly distilled oxalyl chloride in CH_2Cl_2 and a few drops of trimethylphosphine were added. After one day the temperature was lowered to 0 ^oC and 1.2 equivalents of sodium triacetoxyborohyride were added and the mixture was stirred for another one day. Mass spectrometry showed the peak for the desired formylpyrrole **82**. Crude ^1H NMR spectroscopy confirmed the formation of the aldehyde. However the yield of purified product was less than satisfactory. Unfortunately, the use of other solvents such as THF, CH_3CN and CH_2Cl_2/THF or different phosphine reagents, such as tributylphosphine, did not improve the yield.

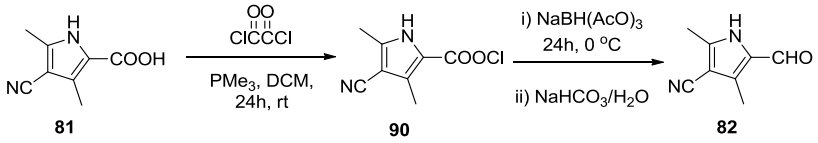

Scheme 4.33: Reduction of cyanopyrrole carboxylic acid **81** to formylpyrrole **82**

As was mentioned earlier, iodination followed by formylation of pyrrole was unsuccessful. Attention then focused on doing the iodination on formylpyrrole **59**. It was possible to obtain

iodopyrrole **89** from β-free formylpyrrole **59** in good yield using *N*-iodosuccinimide in carbon tetrachloride (Scheme 4.34). Then the condensation of iodopyrrole **89** with dipyrromethane dicarboxylic acid was performed to afford a,c-biladiene **91**. Mass spectroscopy confirmed the formation of a,c-biladiene **91**. Oxidative cyclization with copper acetate followed by demetalation with sulfuric acid afforded the desired iodoporphyrin **92** in only trace amount. The compound was characterized by high-resolution mass spectrometry.

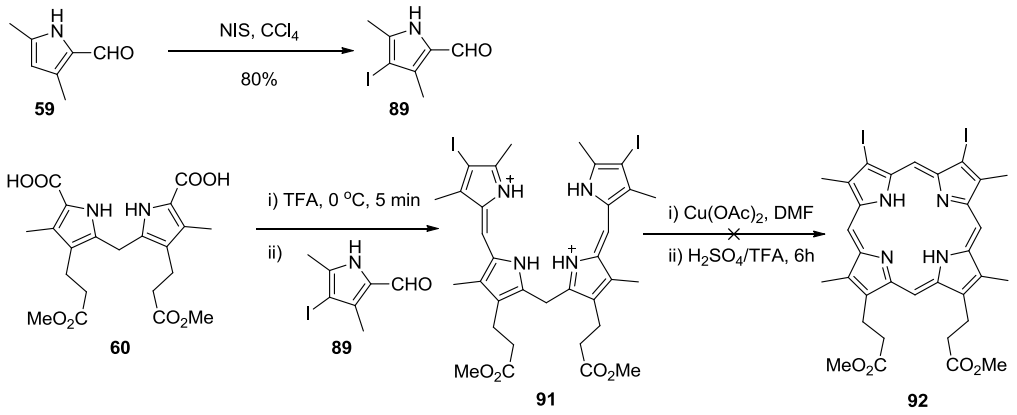

Scheme 4.34: Attempted cyclization of 2,18-diiodo-a,c-biladiene **91**

4.2.8 Synthesis of Electron Rich Pyrrole

Since the difficulty encountered in the decarboxylation and formylation was probably due to electron-withdrawing β-substituents, the same reaction sequence was attempted with a pyrrole bearing a neutral or electron donating substituents at the β-position which can later be converted into electron withdrawing substituents. As shown in Scheme 4.35, after cyclization of a,c-biladiene **94**, hydroxymethyl substituents can be converted into nitriles in one step.[37] a,c-Biladiene **94** will be synthesized from pyrrole carboxylic acid **95**, condensed with diformyldipyrromethane **61**. Hydroxymethylpyrrole carboxylic acid **95** can be synthesized from reduction of formylpyrrole **83**.

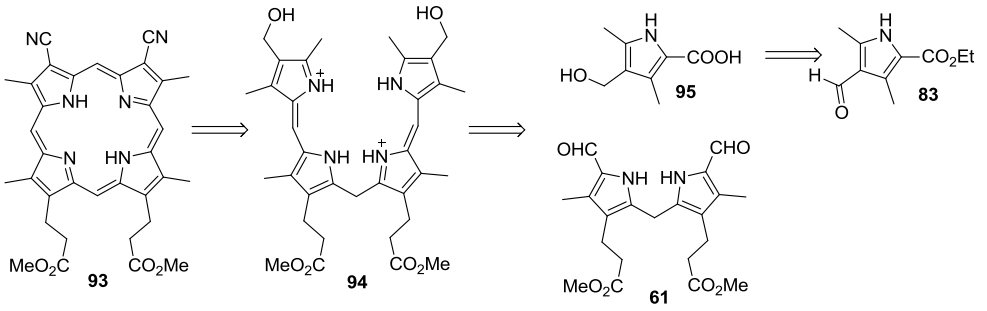

Scheme 4.35: Retrosynthesis of porphyrin **93**

Hydroxymethylpyrrole **96** was synthesized in high yield, by reduction of formylpyrrole **73** using lithium borohydride (Scheme 4.36). The product was purified via silica gel column chromatography and characterized by ^{1}H NMR and mass spectrometry. Pyrrole carbocyclic acid **95** was obtained by hydrogenolysis of hydroxymethylpyrrole **96** in quantitative yield. Then crude carboxylic acid **95** was dissolved in TFA in an ice bath. Within a few minutes the reaction mixture turned red in color before addition of diformyldipyrromethane **61**. It seems in the presence of an acid that the hydroxyl group can protonate and leave as a water molecule to afford a methylene pyrrole intermediate, which is no longer a nucleophile in the condensation reaction. As an alternate method, decarboxylation was attempted with a catalytic amount of *p*-TSA but the final result was the same. Next it was attempted to dissolve both pyrrole carboxylic acid **95** and diformyldipyrromethane **61** in CH_2Cl_2/methanol and *p*-TSA in methanol was added dropwise into the reaction mixture. By doing that, it was thought that the decarboxylated pyrroles will readily react with diformyldipyrromethane **61** to afford a,c-biladiene **94** before dehydration. After thirty minutes there were no a,c-biladiene absorption peaks in the UV-Vis spectrum.

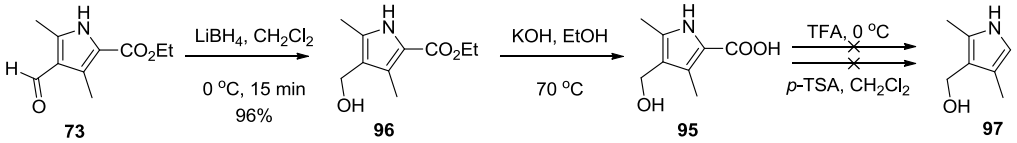

Scheme 4.36: Attempted synthesis of β-hyroxymethylpyrrole **97**

It was also a struggle to make dipyrromethane using hydroxymethylpyrrole **96**. Activation of the α-methyl group of pyrrole **96** with lead tetraacetate formed an unexpected product **98** (Scheme 4.37). After purification ^{1}H NMR showed addition of two extra methyls to the pyrrole **96**. The molecular weight of this compound was equal to addition of two acetate groups to pyrrole **96**. This product **98** was self-condensed to afford dipyrromethane **99** but the product could not be characterized.

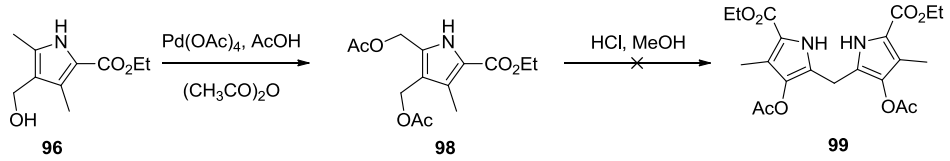

Scheme 4.37: Attempted synthesis of dipyrromethane **99**

4.3 Future work

Recent literature has reported a total synthesis of protoporphyrin IX using a new alternate method to the well-known MacDonald condensation (Scheme 4.38).[42] The key step is the condensation of diiododipyrromethane **100** with known diformyldipyrromethane **61** to obtain the desired porphyrin **101** in a single step in 76% yield. In the classical MacDonald condensation, diformyldipyrromethane reacts with α-free dipyrromethane to give dihydroporphyrin as the product. Then it needs to oxidize to get the desired porphyrin using either air[43] or DDQ.[44]

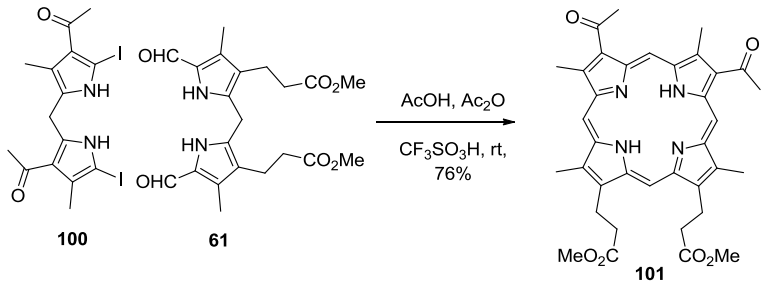

Scheme 4.38: Reported synthesis of protoporphyrin IX

Our previous attempts to synthesize benzyl 5-acetoxymethyl-4-acetyl-3-methylpyrrole carboxylate (**37**) were unsuccessful as mentioned earlier. But the authors reported a new one pot

synthetic procedure to obtain molecule **37** in 45% yield from benzyl 4-acetyl-3,5-dimethylpyrrole carboxylate (**33**, Scheme 4.39).

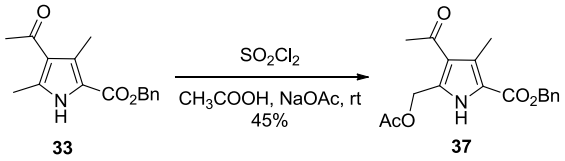

Scheme 4.39: Reported synthesis of acetoxymethylpyrrole **37**

The new approach is to synthesize diiododipyrromethane **106** starting from formylpyrrole **33** (Scheme 4.39). First formylpyrrole **33** will be acetoxylated using the new synthetic procedure. Reaction between pyrrole **33** and sulfuryl chloride will form the chloromethylpyrrole intermediate that will readily react with acetate to form the desired acetoxymethylpyrrole **37**. Self-condensation of acetoxypyrrole **37** will lead to the desired dipyrromethane **42**. But the formyl group at the β-position may diminish the nucleophilicity of the α-carbon of the pyrrole by resonance. As alternate route, deformylation of acetoxymethylpyrrole **37** can be achieved prior to the self-condensation reaction. That will help to keep the α-carbon more nucleophilic in the condensation reaction. After the self-condensation, formyl groups can be reinserted using formylation with triethyl orthoformate. As mentioned earlier, formyl groups can be easily converted into nitriles using oximation followed dehydration, to obtain dipyrromethane **104**.

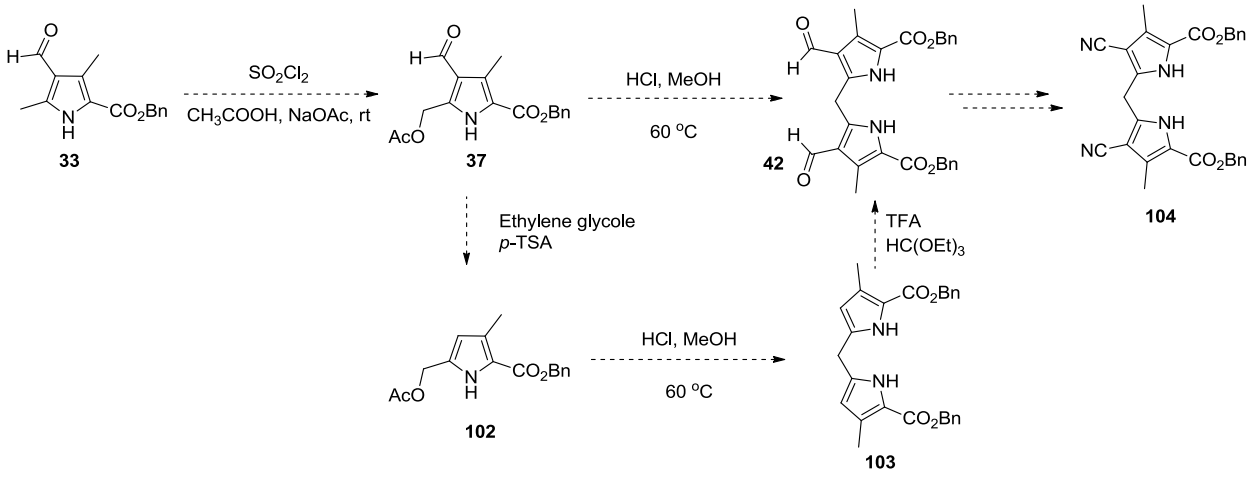

Scheme 4.40: Proposed synthesis of dicyanodipyrromethane **104**

Removal of benzyl protection via hydrogenolysis with Pd/C will form the diacid **105** which can be converted into the desired diiododypyrromethane **106** using decarboxylation followed by iodination. With the previously synthesized diformyldipyrromethane **61** and diiododiyromethane **106** in hand, the condensation will be carried out in a mixture of acetic anhydride and trifluoromethyl sulfonic acid in acetic acid under anhydrous conditions to obtain the desired porphyrin **1** (Scheme 4.41). But there is a possibility for hydrolysis of nitrile group in the condensation step with strong acids.[45] As an alternate route, condensation can be done with diformyldipyrromethane to obtain diformylporphyrin which can be converted into the desired product.

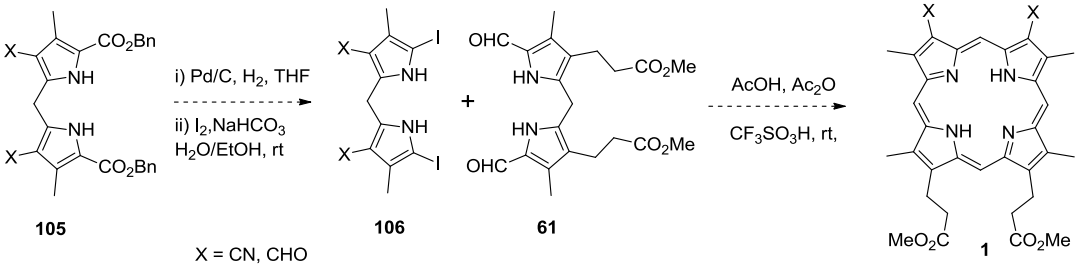

Scheme 4.41: Proposed synthesis of porphyrin **1**

4.4 Experimental

Benzyl 4-(2-methoxycarbonylethyl)-3,5-dimethylpyrrole (**29**):

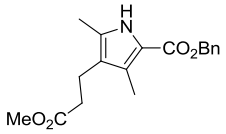

Benzyl acetoacetate (**35**, 33.5 g, 171 mmol) was dissolved in acetic acid (40 ml) and placed in an ice bath. Then it was treated with solution of sodium nitrite (13 g, 188 mmol) in water and the temperature was controlled around 10 ^{o}C throughout. Then the reaction mixture was stirred for another 3 h and stored in a refrigerator overnight to complete the formation of benzyl oximinoacetate **30**. This solution was added to the solution of methyl 4-acetyl-5-oxohexanoate (**31**, 19 g, 102 mmol) in acetic acid (65 ml) during 2 h

at 65 ^{o}C. Simultaneously, an intimate mixture of zinc dust (19 g, 287 mmol) and sodium acetate (19g, 231 mmol) was added while keeping zinc dust always excess in the reaction mixture. The resulting mixture was stirred for 1 h at 65 ^{o}C. Then it was poured into chilled water (1.5 L) while stirring. The resulting precipitate was filtered off and dissolved in CH_2Cl_2 and washed with water and brine. It was dried over anhydrous Na_2SO_4 and the solvent was removed. Crude product was recrystallized from a methanol/water mixture to afford benzyl 4-(2-methoxycarbonylethyl)-3,5-dimethylpyrrole (**29**, $C_{18}H_{21}NO_4$, 14g, 44 mmol, 43%); m.p. 98-102 ^{o}C, Lit m.p. 99-101 ^{o}C.[46] ^{1}H NMR (chloroform-*d*, 400 MHz): δ 8.56 (s, 1H), 7.53-7.23 (m, 5H), 5.29 (s, 2H), 3.66 (s, 3H), 2.71 (t, *J* = 8.6, 7.0 Hz, 2H), 2.43 (t, *J* = 8.7, 6.8 Hz, 2H), 2.29 (s, 3H), 2.21 (s, 3H). MS (ESI) m/z 136.15 $[M+H]^+$, calcd. for $C_{18}H_{22}NO_4$ 136.14.

Benzyl 5-acetoxymethyl-4-(2-methoxycarbonylethyl)-3-methylpyrrole-2-carboxylate (**36**):

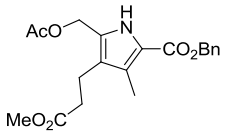

benzyl 4-(2-methoxycarbonylethyl)-3,5-dimethylpyrrole (**29**, 5.0 g, 15 mmol) was dissolved in acetic acid (50 ml) and acetic anhydride (1.5 ml, 15 mmol) was added. Then lead tetraacetate (7.5 g, 17 mmol) was added in small portions over a period of 1.5 h to the reaction mixture. It was stirred overnight at room temperature under argon and the resulting solution was added dropwise to chilled water (200 ml) while continuous stirring. The resulting precipitate was filtered off and dissolved in CH_2Cl_2 and washed with water and brine. It was then dried over anhydrous Na_2SO_4 and the solvent was removed. The crude product recrystallized from CH_2Cl_2/hexane mixture to afford benzyl 5-acetoxymethyl-4-(2-methoxycarbonylethyl)-3-methylpyrrole-2-carboxylate (**36**, $C_{20}H_{23}NO_6$, 5.5g, 14.7 mmol, 98%); m.p. 106-109 ^{o}C, Lit m.p. 109.5-110.[46] ^{1}H NMR (chloroform-*d*, 400 MHz): δ 9.05 (br. s, 1H), 7.51-7.29 (m, 3H), 5.31 (s, 2H), 5.06 (s, 2H), 3.67 (s, 3H), 2.79 (t, *J* = 7.7 Hz, 2H), 2.47 (t, *J* = 7.6 Hz, 2H), 2.29 (s, 3H), 2.07 (s, 3H). MS (ESI) m/z 374.1603 $[M+H]^+$, calcd. for $C_{20}H_{24}NO_6$ 374.1604.

Dibenzyl 3,3'-di(2-methoxycarbonylethyl)-4,4'-dimethylpyrromethane-5,5'-dicarboxylate (**28**):

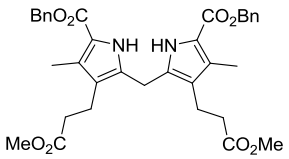

Method a

Benzyl 5-acetoxymethyl-4-(2-methoxycarbonylethyl)-3-methylpyrrole-2-carboxylate (**36**, 5.5 g, 14.7 mmol) was dissolved in methanol (30 ml) and HCl (2 ml). The reaction mixture was heated at 70 ^{o}C for 4 h or until a precipitate formed. Then the mixture was stirred at room temperature and placed in an ice bath to complete the precipitation of the product. The titled product **28** was collected by filtration ($C_{35}H_{38}N_2O_8$, 3.8 g, 6.2 mmol, 42%).

Method b

Benzyl 4-(2-methoxycarbonylethyl)-3,5-dimethylpyrrole (**29**, 5.2 g, 16.5 mmol) was dissolved in diethyl ether (200 ml) by heating the mixture at 40 ^{o}C. Then bromine (1.1 ml, 21.4 mmol) was added dropwise and the mixture was stirred for 1.5 h at room temperature. Then the solvent was evaporated and a pink solid residue was dissolved in methanol (35 ml). Then concentrated hydrochloric acid (0.2 ml) was added and the mixture was refluxed for 9 to 11 h. While cooling down to room temperature, the product precipitated. The precipitated product was isolated by filtration and washed with cold methanol. Then it was recrystallized from hot methanol to give the titled product **28** ($C_{35}H_{38}N_2O_8$, 3.17g, 5.2 mmol, 31%); m.p. 103 ^{o}C, Lit m.p. 102-103 ^{o}C.[47] ^{1}H NMR (chloroform-*d*, 400 MHz): δ 9.06 (s, 2H), 7.44-7.23 (m, 10H), 5.26 (s, 4H), 3.97 (s, 2H), 3.57 (s, 6H), 2.76 (t, *J* = 7.0 Hz, 4H), 2.52 (t, *J* = 7.0 Hz, 4H), 2.29 (s, 6H). MS (ESI) m/z 615.6908 $[M+H]^+$, calcd. for $C_{35}H_{39}N_2O_8$ 615.6928.

3,3'-Di(2-methoxycarbonylethyl)-4,4'-dimethylpyrromethane-5,5'-dicarboxylate (**60**):

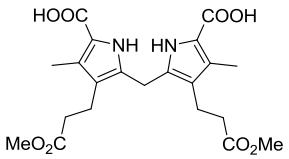

Dibenzyl 3,3'-di(2-methoxycarbonylethyl)-4,4'-dimethylpyrromethane-5,5'-dicarboxylate (**28**, 2.5 g, 4.1 mmol) was dissolved in dry THF (20 ml) and degassed with argon for 10 min. Then 10% Pd/C (500 mg) and 1-2 drops of TEA were added and the flask was sealed. Then the flask was evacuated of air by using a syringe and filled with hydrogen gas using a hydrogen gas filled balloon. The reaction mixture was stirred for 12 h. After completion of reaction (monitored by TLC), the solvent was evaporated and the residue was dissolved in 2 M ammonium hydroxide and filtered through a Celite cake to remove the catalyst. 2 M acetic acid solution was added dropwise to the filtrate while stirring until a precipitate was fully formed. The product was collected by filteration, washed with water and dried in a desiccator to obtain compound **60** ($C_{21}H_{26}N_2O_8$, 1.7 g, 3.9 mmol, 95%); MS (ESI) m/z 457.1577 $[M+Na]^+$, calcd. for $C_{21}H_{26}N_2O_8Na$ 457.1578.

Benzyl 4-acetyl-3,5-dimethylpyrrole carboxylate (**33**):

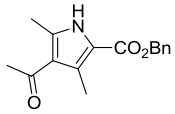

Benzyl acetoacetate (**35**, 33.5 g, 174 mmol) was dissolved in acetic acid (40 ml) and placed in an ice bath. Then it was treated with a solution of sodium nitrite (13 g, 188 mmol) in water and the temperature was controlled around 10 ^oC throughout. The mixture was stirred for another 3 h and stored in a refrigerator overnight. This solution was added to a solution of 2,4-pentandione (**34**, 10.2 g, 102 mmol) in acetic acid (65 ml) during 2 h at 65 ^oC. Simultaneously, an intimate mixture of zinc dust (19 g, 287 mmol) and sodium acetate (19g, 231 mmol) was added while keeping zinc dust always excess in the reaction mixture. The resulting mixture was stirred for 1 h at 65 ^oC. Then it was poured into chilled water (1.5 L)

while stirring. The resulting precipitate was filtered off and dissolved in CH_2Cl_2 and washed with water and brine. It was then dried over anhydrous Na_2SO_4 and the solvent was evaporated. The crude product was recrystallized from a methanol/water mixture to afford benzyl 4-(2-methoxycarbonylethyl)-3,5-dimethylpyrrole (**33**, $C_{16}H_{17}NO_3$, 15 g, 55 mmol, 53 % of); m.p. 134-136 ^oC, Lit m.p. 134.5 ^oC.[48] ^1H NMR (chloroform-*d*, 400 MHz): δ 9.06 (s, 1H), 7.73-7.22 (m, 5H), 5.33 (s, 2H), 2.62 (s, 3H), 2.51 (s, 3H), 2.45 (s, 3H); MS (ESI) m/z 272.1266 $[M+H]^+$, calcd. for $C_{16}H_{18}NO_3$ 272.1287.

Benzyl 3,5-dimethylpyrrole carboxylate (**40**):

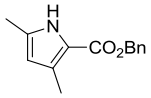

Benzyl 4-acetyl-3,5-dimethylpyrrole carboxylate (**33**, 1.0 g, 3.7 mmol) in dry benzene was treated with *p*-toluenesulfonic acid (0.02 g, 0.12 mmol). Then dry ethylene glycol (4 ml) was added and the mixture was refluxed under argon for 15 h until reaction completion was confirmed by TLC. After the reaction was completed, water (16 ml) was added the mixture was washed with CH_2Cl_2, which was then washed with saturated $NaHCO_3$, water and brine. The organic layer was dried over anhydrous Na_2SO_4. The product was purified via a silica gel column chromatography to obtain benzyl 3,5-dimethylpyrrole carboxylate (**40**, $C_{14}H_{15}NO_2$, 0.8 g, 3.5 mmol, 95%); m.p. 100-102 ^oC, Lit m.p. 99 ^oC.[49] ^1H NMR (chloroform-*d*, 400 MHz): δ 8.57 (br. s, 1H), 7.63-7.29 (m, 5H), 5.82 (s, 1H), 5.30 (s, 2H), 2.33 (s, 3H), 2.25 (s, 3H); MS (ESI) m/z 230.1179 $[M+H]^+$, calcd. for $C_{14}H_{16}NO_2$ 230.1181.

Benzyl 4-formyl-3,5-dimethylpyrrole carboxylate (**41**):

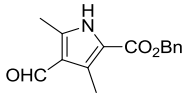

Benzyl 3,5-dimethylpyrrole carboxylate (**40**, 1.0 g, 4.3 mmol) was dissolved in TFA under argon in an ice bath. Then triethyl orthoformate was added slowly and the reaction mixture was allowed to stir an additional 3 h while it reached room temperature. The reaction mixture was diluted with CH_2Cl_2 and

extracted with several portions of water to remove the TFA. Then the organic layer was neutralized with saturated $NaHCO_3$, washed with brine and dried over anhydrous Na_2SO_4. After removal of the solvent, the resulting crude product was dissolved in a minimum amount of CH_2Cl_2 and eluted through a silica gel column. The first fraction was collected and shown to be the title compound **41** ($C_{15}H_{15}NO_3$, 0.85 g, 3.0 mmol, 70%); m.p. 151-153 ^oC, Lit m.p. 151 ^oC.[49] ^1H NMR (chloroform-*d*, 400 MHz): δ 10.00 (s, 1H), 9.37 (br. s, 1H), 7.64-7.29 (m, 5H), 5.34 (s, 2H), 2.59 (s, 3H), 2.53 (s, 3H); MS (ESI) m/z 258.1115 $[M+H]^+$, calcd. for $C_{15}H_{16}NO_3$ 258.1130.

3,5-dimethylpyrrole carboxylic acid (**57**):

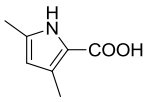

Benzyl 3,5-dimethylpyrrole-2-carboxylate (**40**, 2.2 g, 9.6 mmol) was dissolved in dry THF (10 ml) and degassed with argon. Then 10% Pd/C was added and the flask was sealed. Then the flask was evacuated of air and filled with hydrogen gas using a balloon filled with hydrogen. The reaction mixture was stirred overnight. Then the catalyst was filtered off using a Celite cake and the solvent was evaporated. This product **57** (1.3 g, 9.3 mmol, 97%) was not purified or characterized, and was directly subjected to the next step.

2-Formyl-3,5-dimethylpyrrole (**59**):

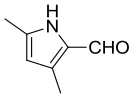

3,5-Dimethylpyrrole carboxylic acid (**57**, 1.3 g, 9.3 mmol) was treated with TFA (10 ml) in an ice bath and stirred for 15 min. in a open flask to complete the decarboxylation to form pyrrole **58**. Then triethyl orthoformate (5 ml) was added slowly into the reaction mixture and it was stirred for an additional 3 h under argon. Once at room temperature, the solution was partitioned between CH_2Cl_2 and water. The organic layer washed with saturated $NaHCO_3$ to neutralize TFA. The resulting organic layer was washed

with brine and dried over anhydrous Na_2SO_4 and then evaporated to give a dark brown product. Crude product was purified via a silica gel column to afford 3,5-dimethyl-2-formylpyrrole (**59**, C_7H_9NO, 0.55 g, 4.5 mmol, 48%); m.p. 87-89 ^oC, Lit m.p. 91 ^oC.[50] ^1H NMR (chloroform-*d*, 400 MHz): δ 9.45 (s, 1H), 9.37 (br. s, 1H), 5.86 (s, 1H), 2.32 (s, 3H), 2.29 (s, 3H); MS (ESI) m/z 122.0500 $[M-H]^-$, calcd. for C_7H_8NO 122.0606.

3,3'-Di(2-methoxycarbonylethyl)-4,4'-dimethyl-5,5'-diformylpyrromethane (**61**):

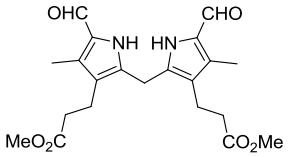

3,3'-Di(2-methoxycarbonylethyl)-4,4'-dimethylpyrromethane-5,5'-dicarboxylic acid (**60**, 0.6 g, 1.38 mmol) was dissolved in CH_2Cl_2 (10 ml) and *p*-toluenesulfonic acid (0.1 g) was added. The reaction mixture was stirred for 1 h while monitoring by TLC. After completion of the decarboxylation, a saturated solution of $NaHCO_3$ was added to neutralize the acid, and the mixture was washed with water, brine and dried over anhydrous Na_2SO_4. Without any purification, the crude product was dissolved in dimethylformamide (2 ml) and placed in an ice bath. Then Vilsmeier complex **64** was prepared by adding benzoyl chloride (1.2 ml, 10 mmol) dropwise to dry dimethylformamide (1.6 ml, 20 mmol) at 0 ^oC over 30 min. The Vilsmeier complex was added dropwise into the solution of decarboxylated dipyrromethane in dimethylformamide and stirred for 15 min in an ice bath and another 1 h at room temperature. Then benzene (10 ml) was added to the reaction mixture to precipitate the iminium salt. The resulting precipitate was collected by filtration and redissolved in a saturated solution of NaOAc in methanol (12 ml) and water (12 ml). The mixture was heated at 60 ^oC for 8 h until it formed a precipitate. The reaction mixture was extracted with CH_2Cl_2 and dried over anhydrous Na_2SO_4. Then the resulting brown solid, after removal of the solvent, was purified via a silica gel column eluting with 2.5% methanol/CH_2Cl_2 to afford the titled compound **61**($C_{21}H_{26}N_2O_6$, 0.12g, 3.1 mmol, 24%); m.p. 179-182 ^oC, Lit m.p. 184-185 ^oC.[51]

^{1}H NMR (chloroform-*d*, 400 MHz): δ 10.46 (d, *J* = 23.5 Hz, 2H), 9.44 (s, 2H), 4.05 (s, 2H), 3.70 (s, 6H), 2.79 (t, *J* = 7.4 Hz, 4H), 2.51 (t, *J* = 8.9, 4H), 2.29 (s, 6H). MS (ESI) m/z 403.1888 $[M+H]^+$, calcd. for $C_{21}H_{27}N_2O_6$ 403.1896.

a,*c*-Biladiene dihydrochloride (**53**):

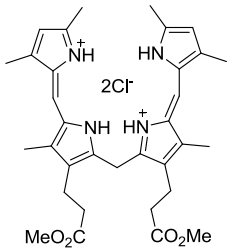

Method a:

Dipyrromethane dicarboxylic acid (**60**, 0.17 g, 0.4 mmol) was treated with TFA (8 ml) in an ice bath and stirred under argon for 15 min to complete the decarboxylation. Then formylpyrrole (**59**, 0.10 g, 0.81 mmol) in methanol (5 ml) was added to the mixture of decarboxylated dipyrromethane. During the addition of formylpyrrole, the color of the reaction mixture changed from yellow to red. The reaction was monitored by UV-Vis spectrometry and the appearance of absorption bands around 440 and 507 nm confirmed the formation of the a,c-biladiene **53**. After 2 h, freshly prepared HCl gas was bubbled through the reaction mixture for 5 min and the color of the reaction mixture changed from red to dark red. Then chilled ether was added to the mixture until the a,c-biladiene salt precipitated. Then the flask was sealed and kept in the refrigerator overnight. The precipitate was collected by filtration to afford a,c-biladiene **53** ($C_{33}H_{42}Cl_2N_4O_4$, 0.096 g, 0.15 mmol, 38%).

Method b:

3,5-dimethylpyrrole carboxylic acid (**57**, 0.17 g, 1.2 mmol) was dissolved in TFA and kept in an ice bath for 10 min under argon. Then diformyldipyrromethane (**61**, 0.24 g, 0.6 mmol) in methanol was added to the decarboxylated pyrrole. A color change from yellow to red was observed over time and reaction was monitored by UV-Vis spectrometry. After completion of the reaction, freshly prepared HCl gas was

bubbled through the reaction mixture for 5 min. Then chilled ether was added to the mixture until a precipitate of the a,c-biladiene dihydrochloride salt **53** was observed. Then the flask was sealed and kept in the refrigerator overnight. The precipitate was collected by filtration to afford a,c-biladiene **53** ($C_{33}H_{42}Cl_2N_4O_4$, 0.11g, 1.9 mmol, 32%); UV-Vis (MeOH): λ_{max} (rel. inten.) 507 nm (1.00), 440 (0.92); ^{1}H NMR (acetone-d_6, 400 MHz): δ 14.16 (s, 2H), 13.92 (s, 2H), 7.15 (s, 2H), 6.24 (s, 2H), 5.07 (s, 2H), 3.43 (s, 6H), 2.84 (t, *J* = 9.3 Hz, 4H), 2.68 (s, 6H), 2.39 (s, 6H), 2.27 (s, 6H), 2.05 (t, *J*=7.98, 4H).

Copper(II) Porphyrin (**65**):

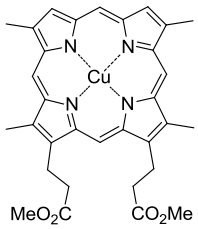

The a,c-biladiene dihydrochloride salt (**53**, 96 mg, 0.15 mmol) was dissolved in dimethylformamide and treated with excess copper acetate in dimethylformamide. The reaction mixture was heated at 100 ^oC while monitoring with UV-Vis spectrometry. Appearance of a sharp absorption band at 399 nm (Soret band) in the UV-Vis spectrum confirmed the formation of porphyrin. After 40 min the mixture was partitioned between water and CH_2Cl_2. The organic layer was washed with Na_2CO_3 and brine. It was dried over anhydrous Na_2SO_4 to afford crude titled product ($C_{32}H_{32}CuN_4O_4$); MS (MALDI-TOF) m/z 600.182 $[M+H]^+$, calcd. for $C_{32}H_{33}CuN_4O_4$ 600.180, which was immediately demetalated.

Demetalation of Copper(II) Porphyrin (**52**):

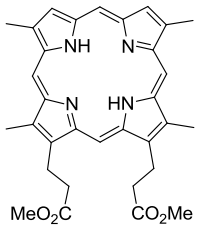

The crude copper(II) porphyrin **65** was demetalated using ice cold sulfuric acid/TFA (1:4) mixture. The mixture was stirred in an ice bath for 6 h. Then CH_2Cl_2 was added to the reaction mixture and it was washed with water 2 times to remove the acid. Then it was washed with 10% NaOH to neutralize any acids remaining and then again with water and brine. After drying over anhydrous Na_2SO_4, the solvent was evaporated and the resulting residue was redissolved in CH_2Cl_2 and treated with ethereal diazomethane gas for 5 min. The solvent was evaporated and the crude product was placed on a silica gel column and eluted with 1% methanol/CH_2Cl_2. The first band (red color) was collected and crystallized to afford the title compound **52** ($C_{33}H_{34}N_4O_4$, 11 mg, 0.02 mmol, 13%); UV-Vis (DCM): λ_{max} (rel. inten.) 564 nm (0.054), 529 (0.064), 496 (0.083), 468 (0.030), 397 (1.000); m.p. >260 ^{o}C, Lit m.p. 224-225 ^{o}C.[52] ^{1}H NMR (chloroform-*d*, 400 MHz): δ 10.05 (s, 3H), 9.92 (s, 1H), 9.04 (s, 2H), 4.40 (t, *J* = 7.8 Hz, 4H), 3.72 (s, 6H), 3.67 (s, 6H), 3.62 (s, 6H), 3.29 (t, *J* = 7.6 Hz, 4H), -3.97 (s, 2H). MS (MALDI-TOF) m/z 539.287 $[M+H]^+$, calcd. for $C_{32}H_{35}N_4O_4$ 539.266.

Ethyl 4-(hydroxyimino)methyl-3,5-dimethylpyrrole carboxylate (**74**):

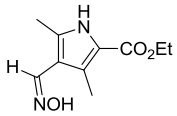

Ethyl 4-formyl-3,5-dimethylpyrrole carboxylate (**73**, 0.61 g, 3.14 mmol) was dissolved in dry methanol (10 mL). Sodium acetate (0.31 g, 3.77 mmol) and hydroxylamine hydrochloride (0.26 g, 3.77 mmol) were added and mixture was refluxed for 2 h. Then the mixture was allowed to cool to room temperature and diluted with ethyl acetate (20 mL). 2M NaOH (2.14 mL) was added and the solvent was removed. The crude product was dissolved in ethyl acetate and washed with water several times and then with brine (50 mL). It was dried over anhydrous Na_2SO_4 and filtration through cotton, followed by concentration *in vacuo* furnished an off-white solid shown to be titled compound **74** ($C_{10}H_{14}N_2O_3$, 0.64 g, 3.04 mmol, 97%); ^{1}H NMR (chloroform-*d*, 400 MHz): δ 8.81 (br. s, 1H), 8.17 (s, 1H), 4.33 (q, *J* = 7.6 Hz, 2H), 2.43 (s, 3H), 2.39 (s, 3H), 1.37 (t, *J* = 7.7 Hz, 3H). MS (ESI) m/z 211.1084 $[M+H]^+$, calcd. for $C_{10}H_{15}N_2O_3$ 211.1083

Ethyl 4-cyano-3,5-dimethylpyrrole carboxylate (**75**):

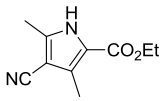

Method a

Ethyl 4-(hydroxyimino)methyl-3,5-dimethylpyrrole carboxylate (**74**,0.30 mg, 1.5 mmol) was placed in a two neck round-bottomed flask with a condenser attached, and toluene (2 ml) was added. Then the mixtue was heated to 90 ^{o}C while stirring. Once it reached 90 ^{o}C, chlorosulfonic acid (0.05 ml, 0.75 mmol) was added dropwise through the other mouth of the round-bottomed flask. The reaction mixture was further stirred for 30 min at 90 ^{o}C. The reaction mixture cooled to room temperature, sodium hydroxide (2M, 1.5 mmol) was added to neutralize the acid. Toluene (15 ml) was added to dissolve the product. Then it was washed with water and brine and dried over anhydrous Na_2SO_4. The crude product was purified via a silica gel column eluted with a 7% acetone/CH_2Cl_2 solvent system to obtain ethyl 4-cyano-3,5-dimethylpyrrole carboxylate (**75**, $C_{10}H_{12}N_2O_2$, 0.090 g, 0.046 mmol, 31%)

Method b

2,4,6-Trichloro-[1,3,5]-triazine (**74**, 0.22 g, 1.2 mmol) was added to DMF (2 mL) and stirred at room temperature for 1 h. During the reaction a white precipitate (Vilsmeier-Haack-type complex) was formed and the reaction was monitored by TLC until complete disappearance of 2,4,6-trichloro-[1,3,5]-triazine. Then ethyl 4-(hydroxyimino)methyl-3,5-dimethylpyrrole (0.21 g, 1.0 mmol) in DMF (5 ml) was added and the reaction mixture was stirred at room temperature until complete disappearance of ethyl 4-(hydroxyimino)methyl-3,5-dimethylpyrrole in the TLC. The mixture was diluted with water and extracted with CH_2Cl_2. Then the organic phase was washed with saturated Na_2HCO_3 followed by 1M hydrochloric acid and brine. Then it was dried over anhydrous Na_2SO_4 and the solvent was evaporated. The crude product was purified using a short silica gel column and eluted with 8% acetone/CH_2Cl_2 to afford ethyl 4-cyano-3,5-dimethylpyrrole carboxylate (**75**, $C_{10}H_{12}N_2O_2$, 0.15 g, 0.78 mmol, 78%); m.p. 170-172 ^{o}C. ^{1}H

NMR (chloroform-*d*, 400 MHz): δ 9.36 (br. s, 1H), 4.34 (q, *J* = 7.1 Hz, 2H), 2.43 (s, 3H), 2.40 (s, 3H) 1.38 (t, *J*=7.1 Hz, 3H). MS (ESI) m/z 193.2183 $[M+H]^+$, calcd. for $C_{10}H_{13}N_2O_2$ 193.2145

Benzyl 4-(hydroxyimino)methyl-3,5-dimethylpyrrole carboxylate (**80**):

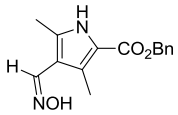

Benzyl 4-formyl-3,5-dimethylpyrrole carboxylate (**33**, 0.57 g, 2.21 mmol) was dissolved in dry methanol (10 mL). Sodium acetate (0.22 mg, 2.7 mmol) and hydroxylamine hydrochloride (0.20 g, 2.8 mmol) were added and mixture was refluxed for 2 h. Then the reaction mixture was allowed to cool to room temperature and it was diluted with ethyl acetate (20 mL). Then 2M NaOH (1 mL) was added and the solvent was removed. The crude product was dissolved in ethyl acetate and washed with water several times and then with brine (50 mL). It was then dried over anhydrous Na_2SO_4 and filtration through cotton, followed by concentration in *vacuo* furnished the titled product **80** ($C_{15}H_{16}N_2O_3$, 0.58 g, 2.13 mmol, 96% yield); m.p. 195-198 ^oC, Lit m.p. 199-200 ^oC.[53] ^1H NMR (acetone-d_6, 400 MHz): δ 10.71 (br. s, 1H), 9.72 (s, 1H), 8.11 (s, 1H), 7.55-7.25 (m, 5H), 5.27 (s, 2H), 2.42 (s, 3H), 2.36 (s, 3H). MS (ESI) m/z 173.2140 $[M+H]^+$, calcd. for $C_{15}H_{17}N_2O_3$ 173.2139

Benzyl 4-cyano-3,5-dimethylpyrrole carboxylate (**73**):

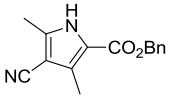

2,4,6-Trichloro-[1,3,5]-triazine (0.18 g, 1.0 mmol) was added to DMF (2 mL) and it was stirred at room temperature for 1 h. During the reaction a white precipitate (Vilsmeier-Haack-type complex) was formed and the reaction was monitored by TLC until complete disappearance of 2,4,6-trichloro-[1,3,5]-triazine. Then benzyl 4-(hydroxyimino)methyl-3,5-dimethylpyrrole (**80**, 0.25 g, 0.91 mmol) in DMF was added and the reaction mixture was stirred at room temperature until complete disappearance of ethyl 4-

(hydroxyimino)methyl-3,5-dimethylpyrrole in the TLC. The mixture was diluted with water and extracted with CH_2Cl_2. Then the organic phase was washed with saturated Na_2HCO_3 followed by 1M hydrochloric acid and brine. Then it was dried over anhydrous Na_2SO_4 and the solvent was evaporated. The crude product was purified using a short silica gel column and eluted with 8% acetone/CH_2Cl_2 to afford benzyl 4-cyano-3,5-dimethylpyrrole carboxylate (**73**, $C_{15}H_{14}N_2O_2$, 0.18 g, 0.71 mmol, 78%); m.p. 173-175 ^oC. ^1H NMR (chloroform-*d*, 400 MHz): δ 9.16 (s, 1H), 7.57 – 7.22 (m, 5H), 5.32 (s, 2H), 2.41 (s, 6H). MS (ESI) m/z 255.1127 $[M+H]^+$, calcd. for $C_{15}H_{15}N_2O_2$ 255.1134.

4-Formyl-3,5-dimethylpyrrole (**64**):

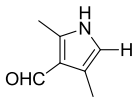

Ethyl 4-formyl-3,5-dimethylpyrrole carboxylate (**73**, 0.30 g, 1.5 mmol) and NaOH (0.48 g, 1.2 mmol) were added to ethylene glycol (10 ml) and heated at 100 ^oC for 30 min until it dissolved completely. Then the temperature was increase to 195 ^oC for the decarboxylation reaction. After half an hour the reaction mixture was allowed to cool to room temperature. Then the product was extracted with CH_2Cl_2 and purified via a silica gel column to afford 4-formyl-3,5-dimethylpyrrole (**64**, C_7H_9NO, 0.12 g, 0.97 mmol, 65%); m.p. 124-126 ^oC, Lit m.p. 126 ^oC.[54] ^1H NMR (chloroform-*d*, 400 MHz): δ 9.89 (s, 1H), 9.68 (br. s, 1H), 6.40 (s, 1H), 2.50 (s, 3H), 2.28 (s, 3H). MS (ESI) m/z 124.1604 $[M+H]^+$, calcd. for $C_7H_{10}NO$ 124.0684.

4-(Hydroxyimino)methyl-3,5-dimethylpyrrole (**85**):

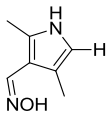

4-Formyl-3,5-dimethylpyrrole (**84**, 0.10 g, 0.81 mmol) was dissolved in dry methanol (10 mL). Sodium acetate (0.77 g, 94 mmol) and hydroxylamine hydrochloride (0.066 g, 0.94 mmol) were added and the mixture was refluxed for 2 h. Then the reaction mixture was allowed to cool to room temperature and

diluted with ethyl acetate (20 mL). 2M NaOH (1 mL) was added and the solvent was removed. The crude product was dissolved in ethyl acetate and washed with water several times and then with brine. Then it was dried over anhydrous Na_2SO_4 and filtration through cotton, followed by concentration in *vacuo* provided 4-(hydroxyimino)methyl-3,5-dimethylpyrrole **85** ($C_7H_{10}N_2O$, 0.08 g, 0.58 mmol, 72%); ^{1}H NMR (chloroform-*d*, 400 MHz): δ 8.18 (s, 1H), 7.82 (br. s, 1H), 6.41 (s, 1H), 2.33 (s, 3H), 2.18 (s, 3H). MS (ESI) m/z 139.0869 $[M+H]^+$, calcd. for $C_7H_{11}N_2O$ 139.0871

Benzyl 4-iodo-3,5-dimethylpyrrole carboxylate (**88**)**:**

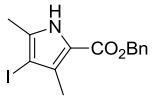

Benzyl 3,5-dimethylpyrrole carboxylate (**40**, 1.0 g, 4.35 mmol) was dissolved in dichloroethane (20 ml) and saturated Na_2HCO_3 (10 ml) was added. The mixture was heated at 50 ^oC for 15 min. Then a saturated solution of KI/I_2 in water (20 ml) was added and heating was continued at 70 ^oC for 1 h. Then saturated solution of sodium thiosulfate (20 ml) was added to quench the excess iodine. The reaction mixture was diluted with CH_2Cl_2 and the organic phase was washed with water followed by 1M hydrochloric acid and brine. After removal of the solvent, the crude product was chromatographed on a silica gel column and eluted with 1% methanol/CH_2Cl_2 to afford benzyl 4-iodo-3,5-dimethylpyrrole carboxylate (**88**, $C_{14}H_{14}INO_2$, 1.35 g, 3.8 mmol, 87%); ^{1}H NMR (chloroform-*d*, 400 MHz): δ 9.04 (s, 1H), 7.55 – 7.16 (m, 5H), 5.31 (s, 2H), 2.31 (s, 3H), 2.28 (s, 3H). MS (ESI) m/z 356.1787 $[M+H]^+$, calcd. for $C_{14}H_{15}INO_2$ 356.1789.

4-Iodo-3,5-dimethyl-1-formylpyrrole (**89**)**:**

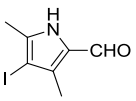

To a solution of benzyl 3,5-dimethylformylpyrrole carboxylate (**59**, 0.25 mg, 2.03 mmol) in carbon tetrachloride (15 ml), was added *N*-iodosuccinimide (0.68 mg, 3.0 mmol), which was recrystallized from

a mixture of 1,4-dioxane/CCl_4 before use. Then mixture was stirred at room temperature for 2 h. After confirming the formation of 4-iodo-3,5-dimethyl-1-formylpyrrole by mass spectrometry, the mixture was diluted with CH_2Cl_2 and washed with 1M NaOH and brine. The crude product was chromatograph on a silica gel column and eluted with 1% methanol/CH_2Cl_2 to give 4-iodo-3,5-dimethyl-1-formylpyrrole (**89**, C_7H_8INO, 0.42 mg, 1.7 mmol, 83%) ; m.p. 166-167 ^oC, Lit m.p. 167-170 ^oC.[55] ^1H NMR (chloroform-*d*, 400 MHz): δ 10.53 (s, 1H), 9.49 (s, 1H), 2.36 (s, 3H), 2.28 (s, 3H). MS (ESI) m/z 249.9721 $[M+H]^+$, calcd. for C_7H_9INO 249.9729.

4-Cyano-3,5-dimethyl-1-formylpyrrole (**82**)**:**

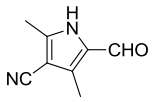

Benzyl 4-cyano-3,5-dimethylpyrrole carboxylate (**72**, 350 mg, 1.37 mmol) was dissolved in dry THF and 10% Pd/C (70 mg) was added. The reaction flask was sealed, evacuated of air and filled with hydrogen gas using a hydrogen filled balloon. The reaction mixture was stirred overnight at room temperature. After confirming the completion of the reaction by TLC, the catalyst was removed by filtration and the solvent was evaporated. Then the crude carboxylic acid **81** was dissolved in benzene (7 ml) and a solution of oxalyl chloride (0.35 ml, 4.11 mmol) in CH_2Cl_2 (7 ml) was added. A few drops of 1M trimethylphosphine in toluene were added as a catalyst and the reaction mixture was allowed to stir at room temperature for 24 h under argon. The solvent was evaporated and the crude acid chloride **90** was redissolved in a THF/CH_2Cl_2 1:1 mixture (15 ml) in an ice bath. A solution of trimethylphosphine in toluene (1.4 ml, 1.4 mmol) was added and the mixture was stirred for 1 h. Then sodium triacetoxyborohydride (0.46 g, 2.17 mmol) was added and strring was continued at 0 ^oC for 18 h. 5% $NaHCO_3$ solution was added to quench the reaction and was stired for another 2 h at room temperature. Then the reaction mixture was extracted with CH_2Cl_2 and the organic layer was washed with water, brine and dried over anhydrous Na_2SO_4. The solvent was removed and the residue was chromatographed on a

silica gel column to afford titled product **82** ($C_8H_8N_2O$); m.p. 218-221 ^oC. ^1H NMR (chloroform-*d*, 400 MHz): δ 10.53 (s, 1H), 9.51 (s, 1H), 2.40 (s, 3H), 2.36 (s, 3H). MS (ESI) m/z 149.0710 $[M+H]^+$, calcd. for $C_8H_9N_2O$ 249.0715.

3,7-Diiodoporphyrin-13,17-dipropionic methylester (**92**)**:**

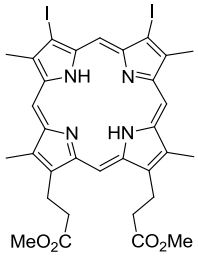

Dipyrromethane dicarboxylic acid **60** (355 mg) was treated with TFA (25 ml) in an ice bath and stirred under argon for 15 min to complete the decarboxylation. Then 4-iodo-3,5-dimethyl-1-formylpyrrole (**89**, 400 mg) in methanol was added to the mixture of decarboxylated dipyrromethane. During the addition of formylpyrrole **89**, the color of the reaction mixture changed from yellow to red. After 2 h, freshly prepared HCl gas was bubbled through the reaction mixture for 5 min and the color of the reaction mixture changed from red to dark red. Chilled ether was added to the mixture until the a,*c*-biladiene salt **91** precipitated. The flask was sealed and kept in the refrigerator overnight. The precipitate was collected by filtration to afford 2,18-diiodo-a,c-biladiene dihydrochloride (**91**, $C_{33}H_{40}Cl_2I_2N_4O_4$) m.p. >260 ^oC. The crude a,c-biladiene dihydrochloride salt **91** was dissolved in dimethylformamide and treated with excess copper acetate. The reaction mixture was heated at 100 ^oC while monitoring with UV-Vis spectrometry. Appearance of a sharp absorption band at 400 nm (Soret band) in the UV-Vis spectrum confirmed the formation of porphyrin. After 40 min the mixture was partitioned between water and CH_2Cl_2. The organic layer was washed with Na_2CO_3 and brine. It was dried over anhydrous Na_2SO_4 to afford the copper(II) porphyrin which was demetalated using ice cold sulfuric acid/TFA (2:8) (10 ml) mixture. The mixture was stirred in an ice bath for 5 h. Then CH_2Cl_2 was added to the reaction mixture and it was washed with water 2 times to remove the acid. Next it was washed with 10% NaOH to

neutralize any acids remaining and then again with water and brine. After drying over anhydrous Na_2SO_4, the solvent was evaporated and the resulting residue was redissolved in CH_2Cl_2 and treated with ethereal diazomethane gas for 5 min. The solvent was evaporated and the crude product was placed on a silica gel column and eluted with 1% methanol/CH_2Cl_2. The titled product **92** was characterized by mass spectrometry. Unfortunately, the amount was not enough to characterize by ^{1}H NMR. ($C_{32}H_{32}I_2N_4O_4$); MS (MALDI-TOF) m/z 791.051 $[M+H]^+$, calcd. for $C_{32}H_{33}I_2N_4O_4$ 791.051.

Ethy 4-hydroxymethyl-3,5-dimethylpyrrole carboxylate (**96):**

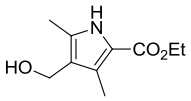

Ethyl 4-formyl-3,5-dimethylpyrrole (**83**, 0.10 g, 0.52 mmol) was dissolved in dry CH_2Cl_2 (5 ml) in an ice bath under argon. Then a solution of sodium borohydride in THF (1.00 ml, 2.50 mmol) was added dropwise. After 15 min the reaction was completed as indicated by TLC. An aqueous solution of ammonium chloride was added slowly to quench the excess sodium borohydride. The product was extracted with CH_2Cl_2 and washed with water and brine. It was then dried over anhydrous Na_2SO_4. The crude product was chromatographed on a silica gel column and eluted with 2.5% methanol/CH_2Cl_2 to afford the titled product **96** ($C_{10}H_{16}NO_3$, 0.098 g, 0.50 mmol, 96%); m.p. 125 ^{o}C. ^{1}H NMR (chloroform-*d*, 400 MHz): δ 8.78 (br. s, 1H), 4.50 (s, 2H), 4.31 (q, *J* = 7.1 Hz, 2H), 2.36 (s, 3H), 2.30 (s, 3H), 1.36 (t, *J* = 7.1 Hz, 3H). MS (ESI) m/z 198.1126 $[M+H]^+$, calcd. for $C_{10}H_{17}NO_3$ 198.1130.

4.5 Supporting Information

^{1}H NMR spectrum of benzyl pyrrole carboxylate **29** in chloroform-*d* at 400

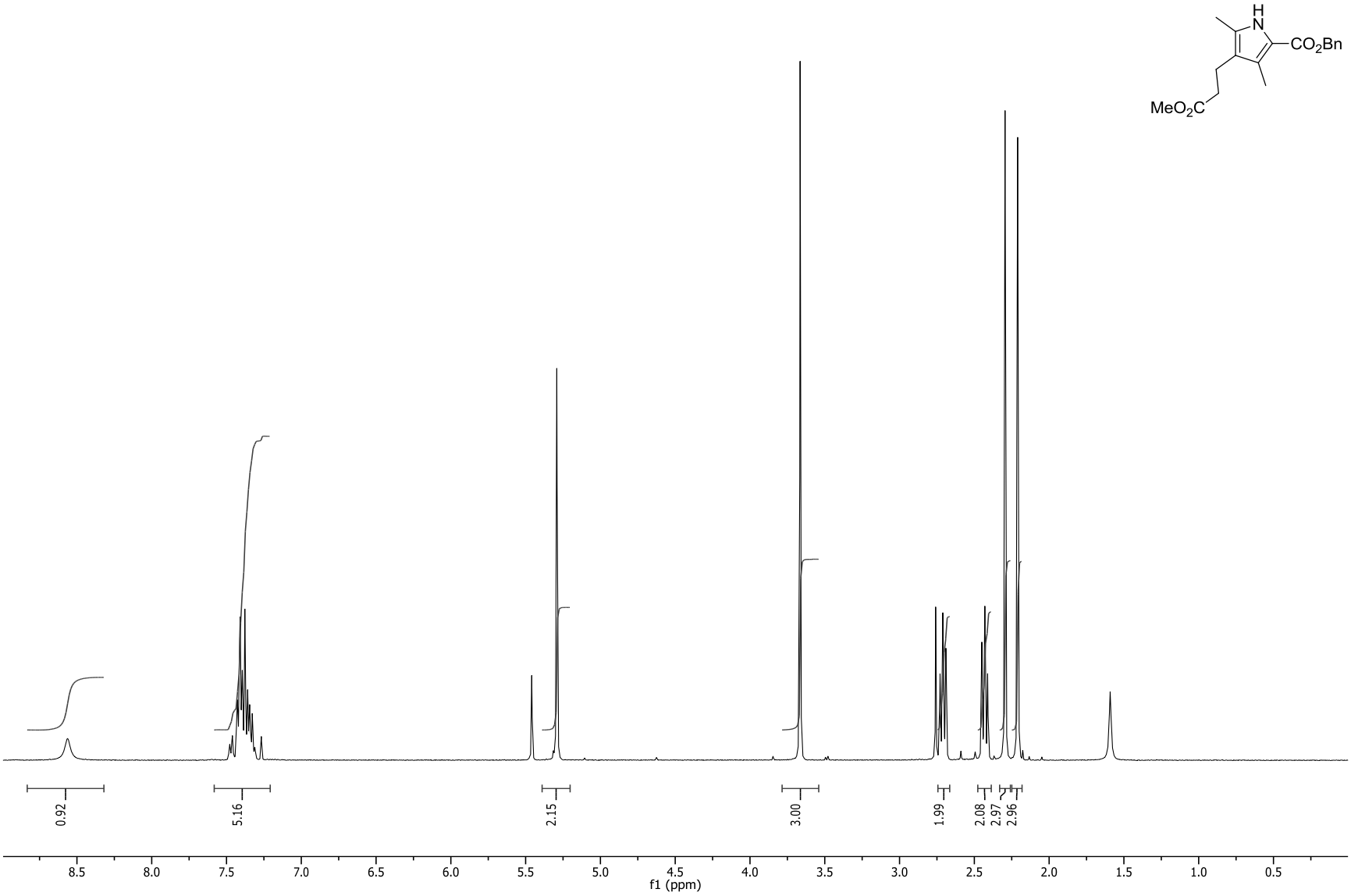

^{1}H NMR spectrum of acetoxymethylpyrrole carboxylate **36** in chloroform-*d* at 400 MHz

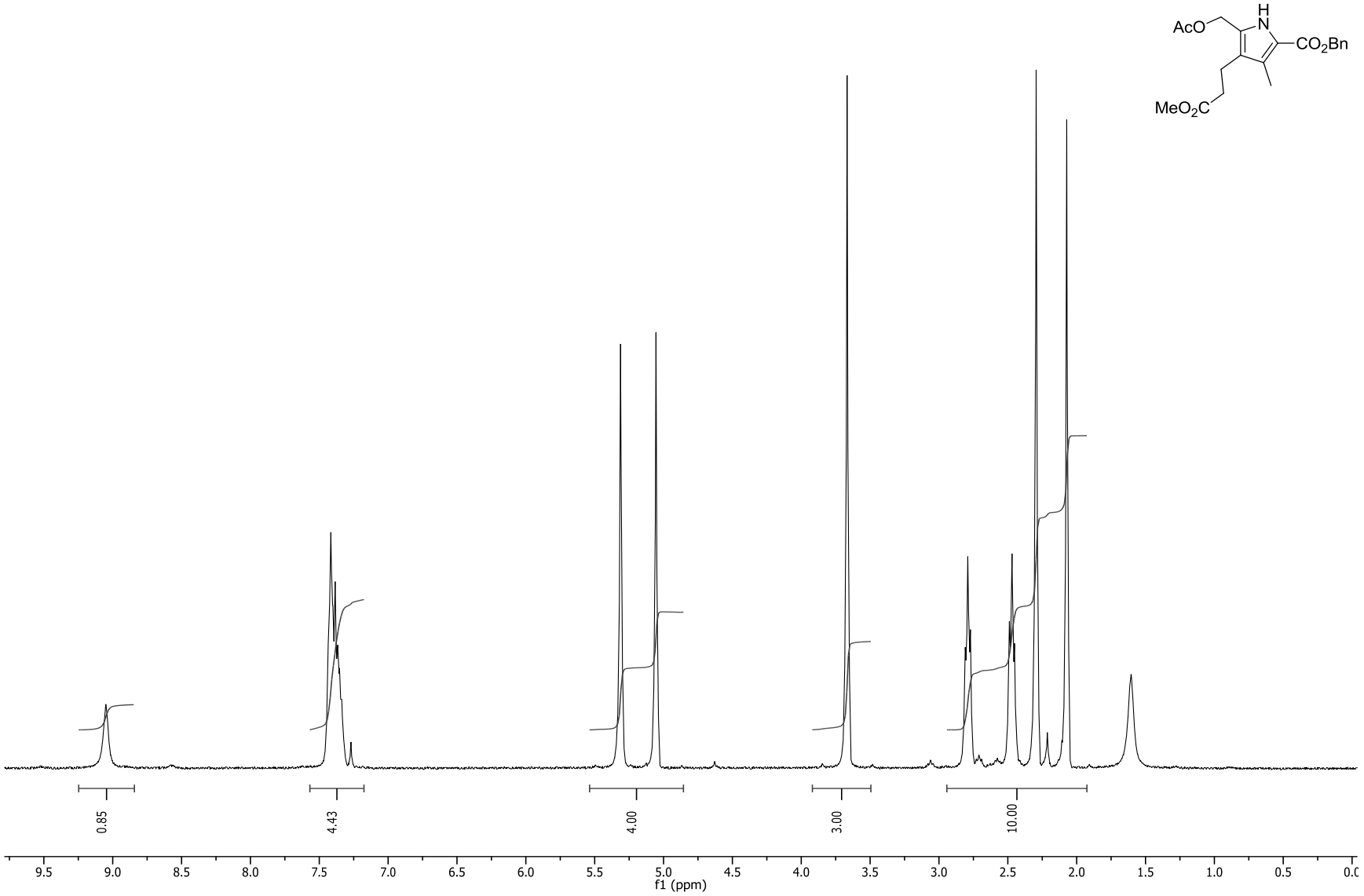

^{1}H NMR spectrum of benzyl dimethylpyrromethane dicarboxylate **28** in chloroform-*d* at 400 MHz

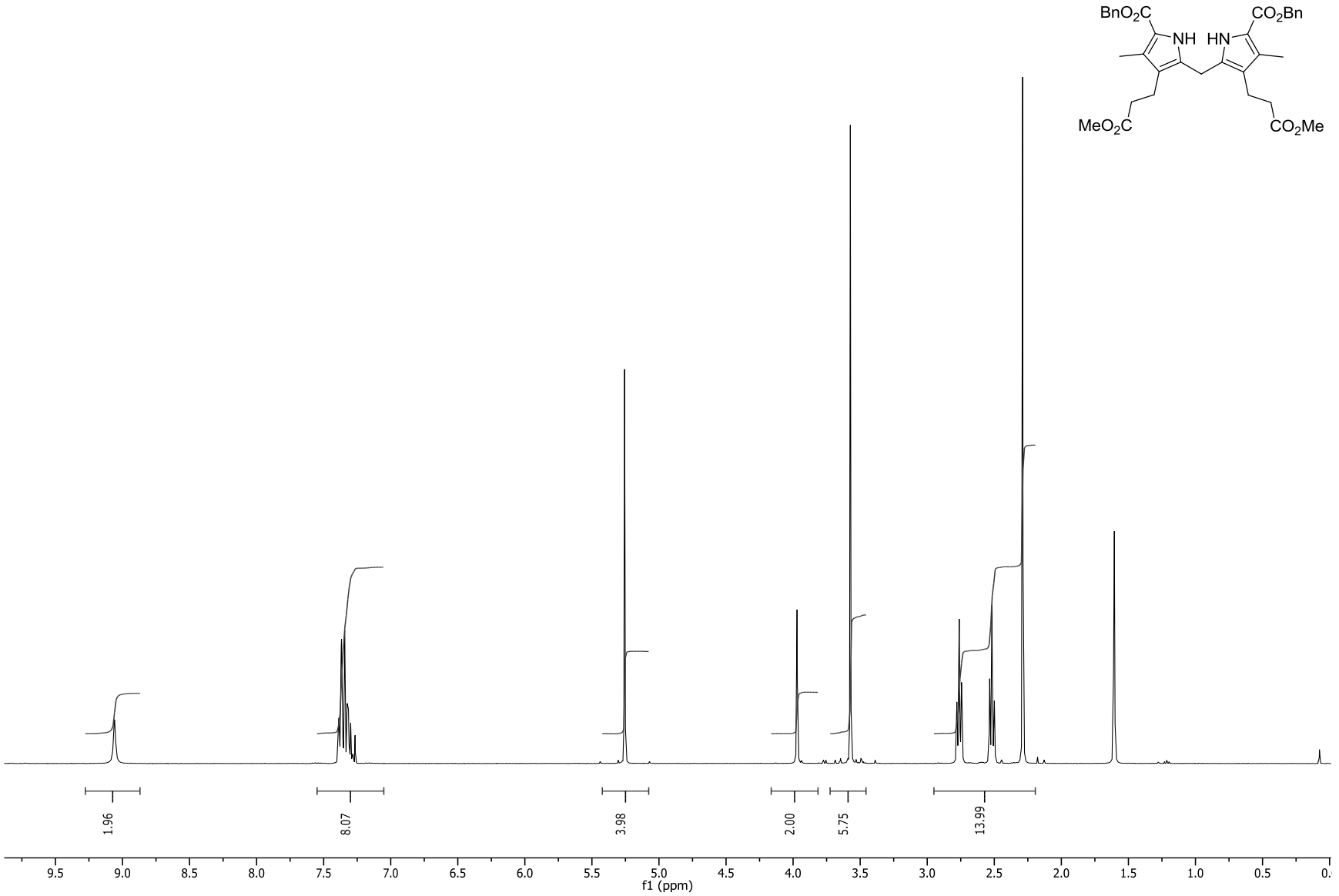

^{1}H NMR spectrum of benzyl acetylpyrrole carboxylate **33** in chloroform-*d* at 400 MHz

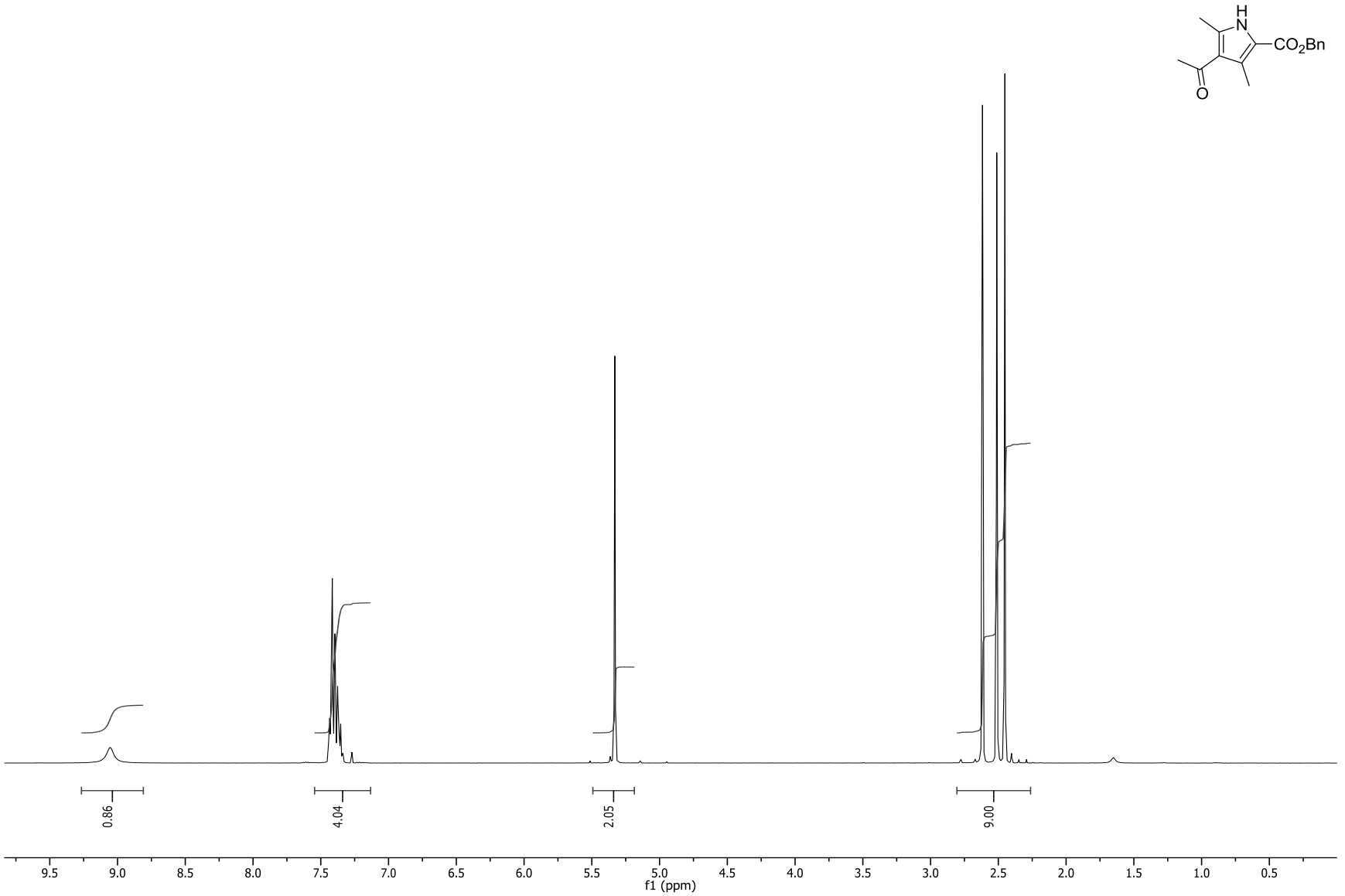

^{1}H NMR spectrum of benzyl 3,5-dimethylpyrrole carboxylate **40** in chloroform-*d* at 400 MHz

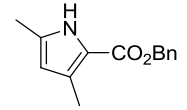

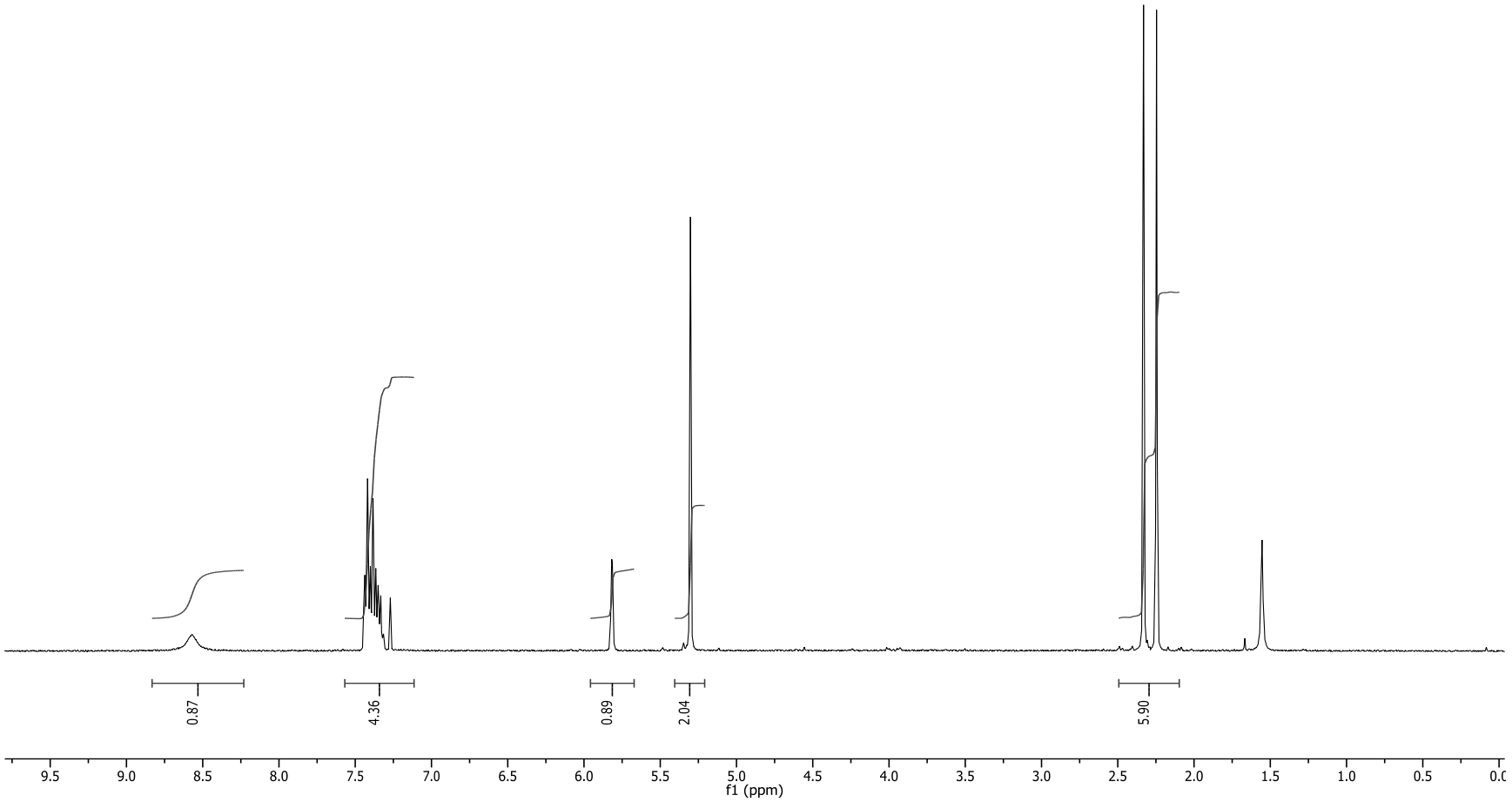

^{1}H NMR spectrum of benzyl formylpyrrole carboxylate **41** in chloroform-*d* at 400 MHz

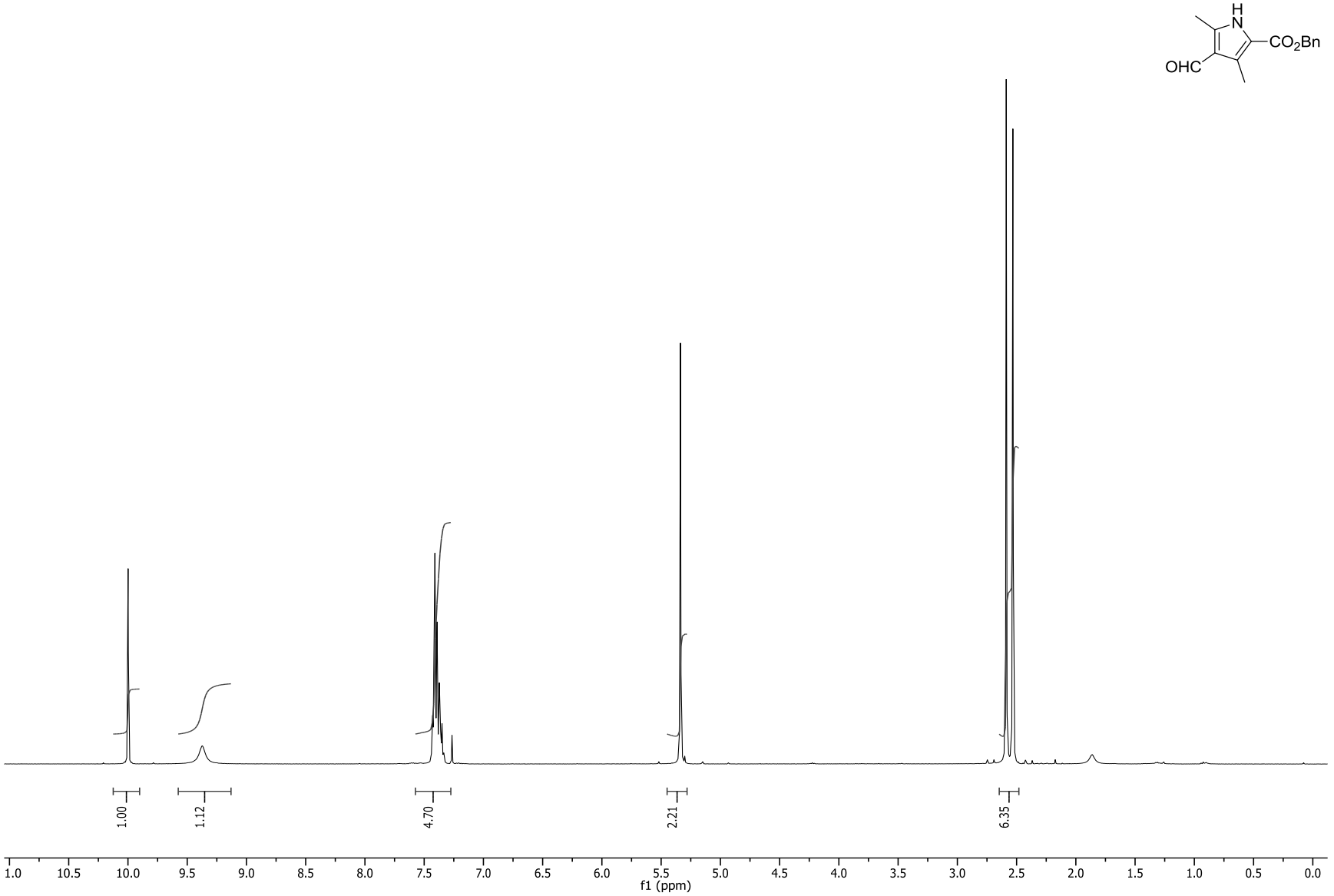

^{1}H NMR spectrum of formylpyrrole **59** in chloroform-*d* at 400 MHz

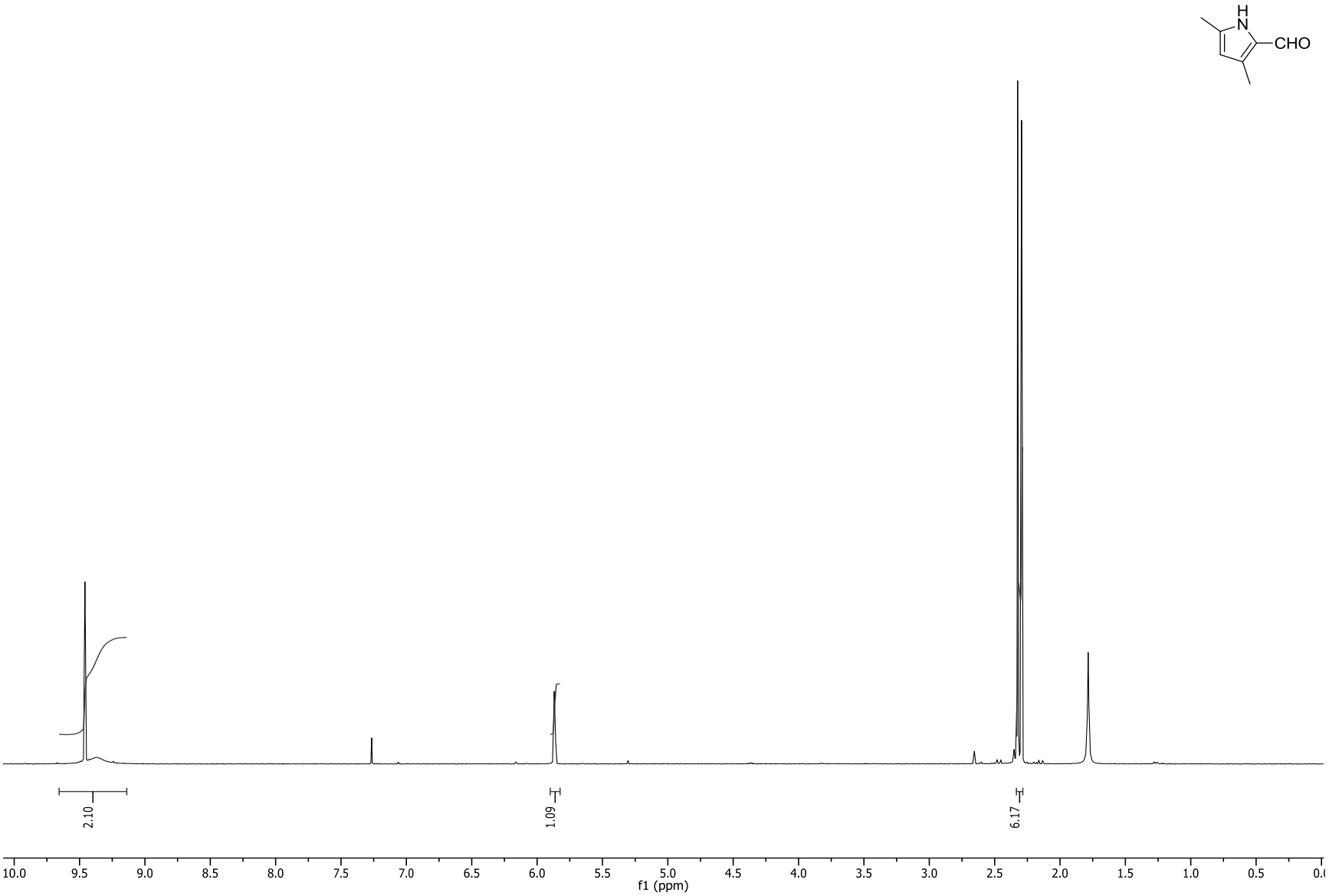

^{1}H NMR spectrum of diformylpyrromethane **61** in chloroform-*d* at 400 MHz

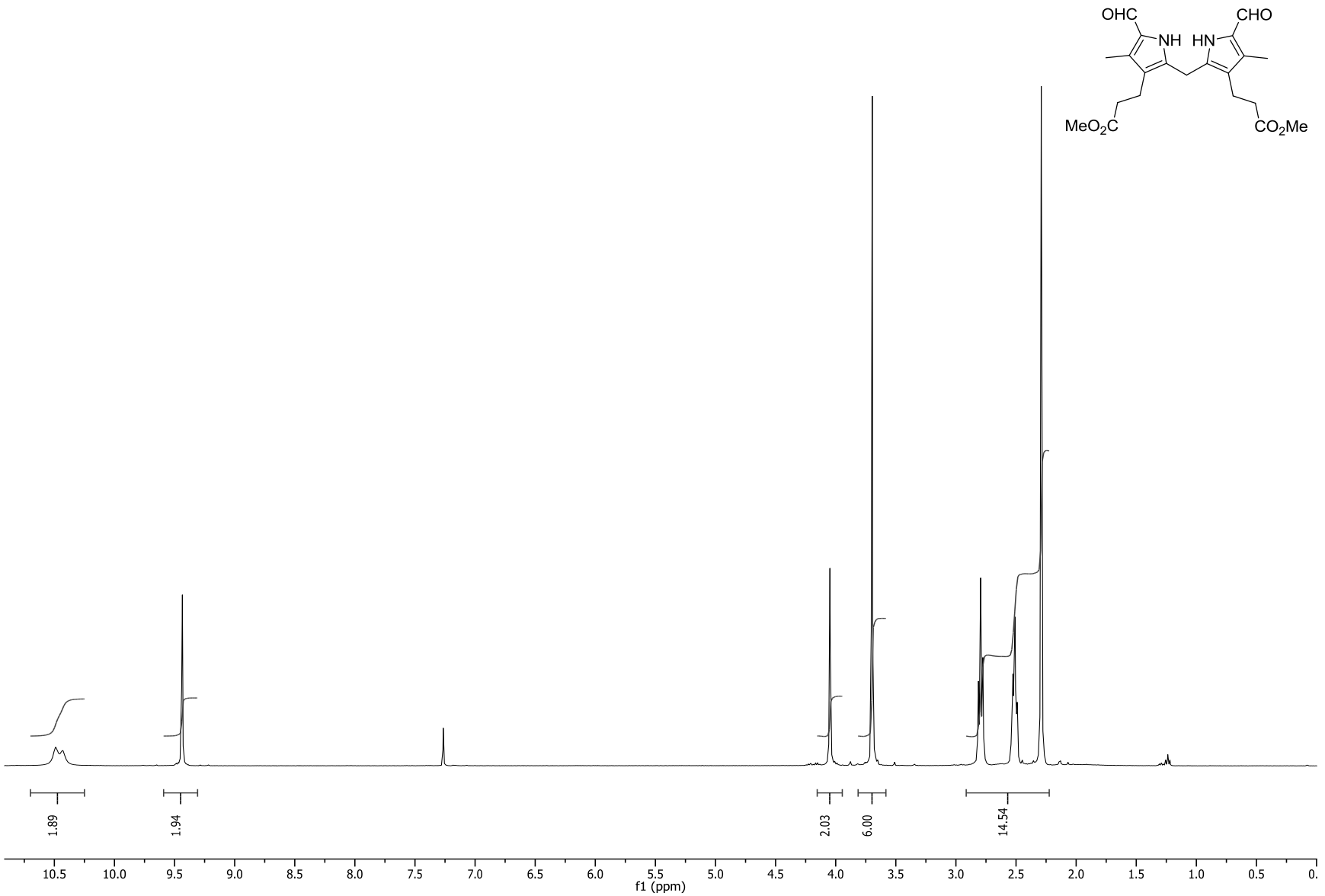

^{1}H NMR spectrum of a,c-biladiene dihydrochloride **53** in acetone-d_6 at 400 MHz

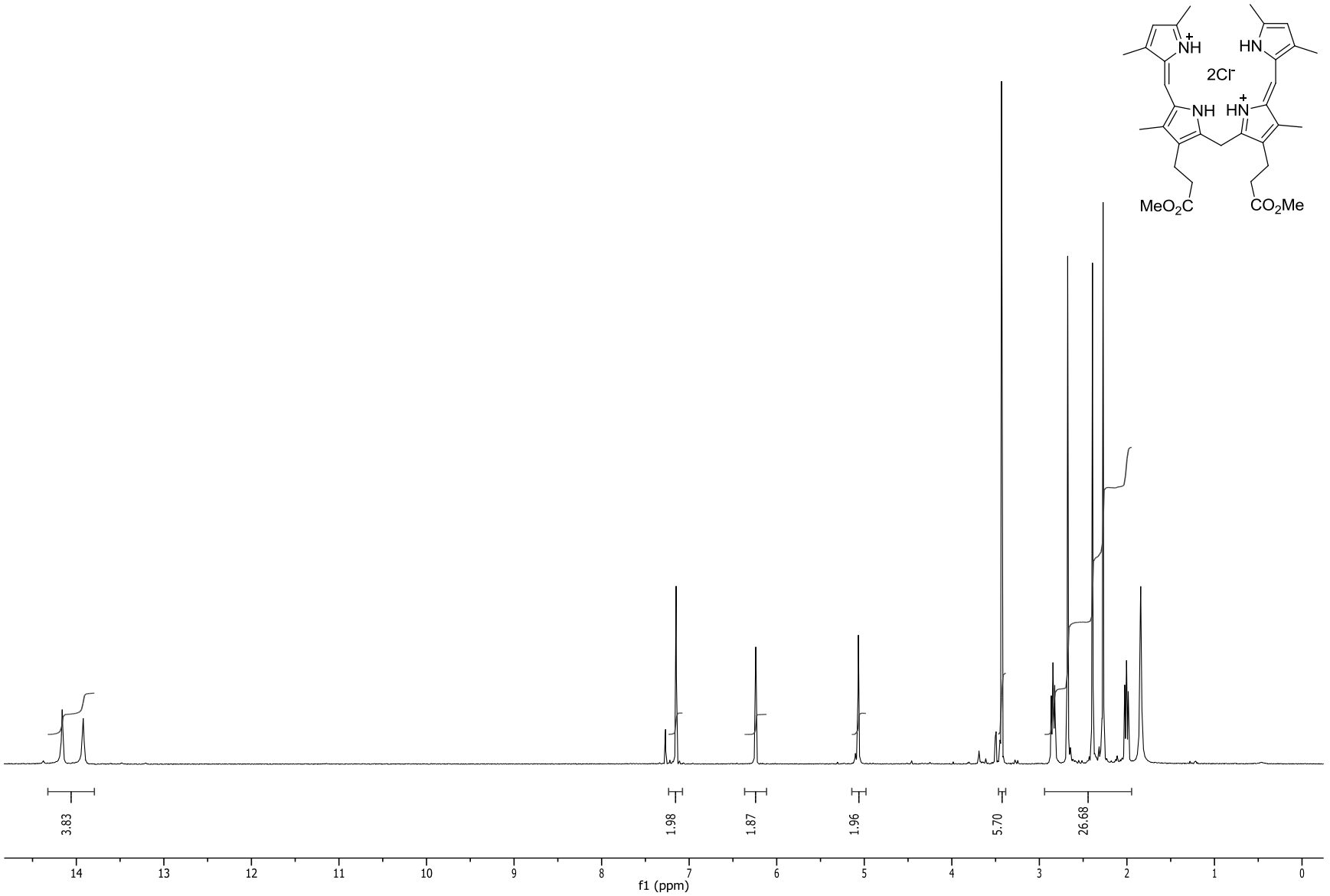

^{1}H NMR spectrum of porphyrin **52** in chloroform-*d* at 400 MHz

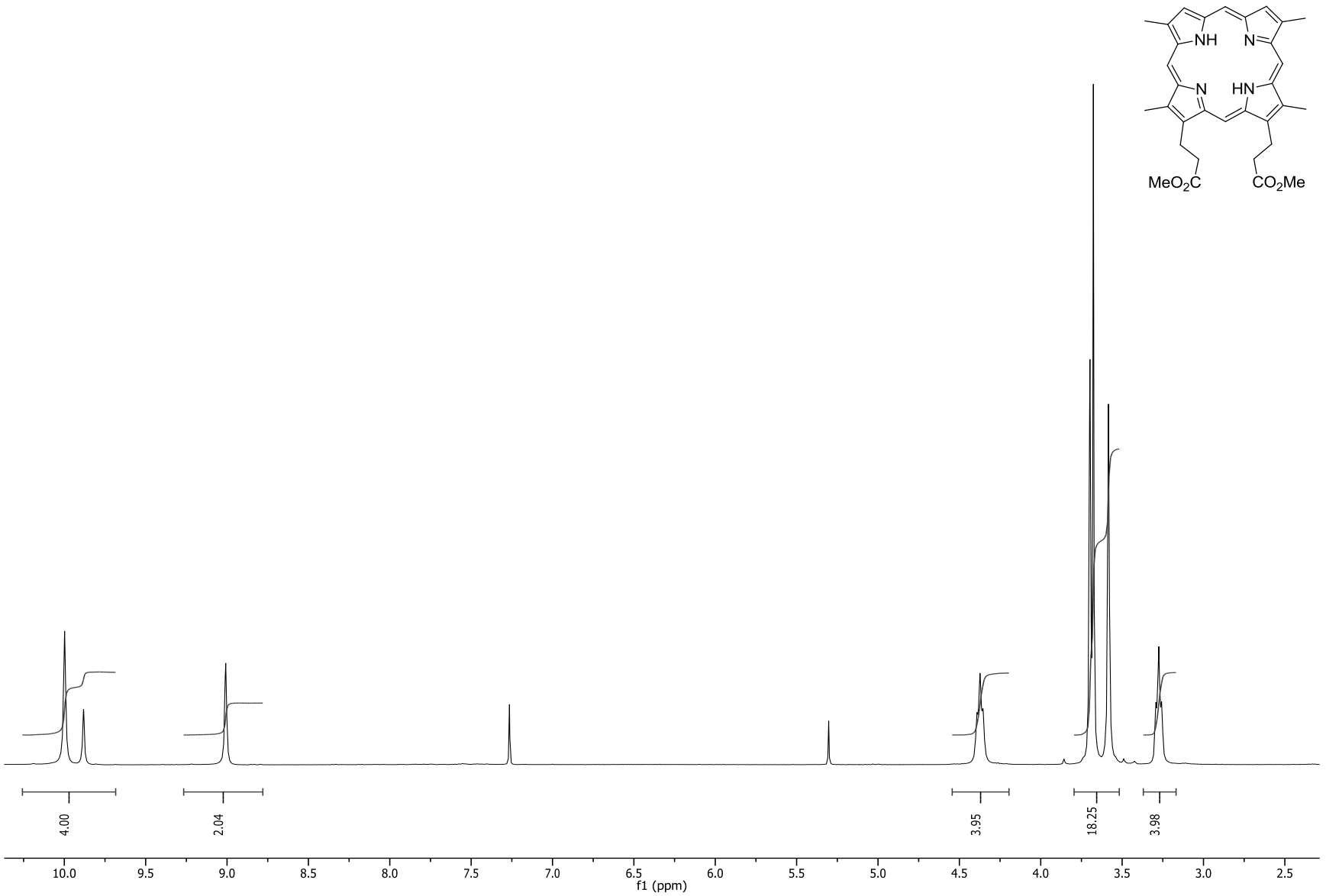

^{1}H NMR spectrum of ethyl cyanopyrrole carboxylate **75** in chloroform-*d* at 400 MHz

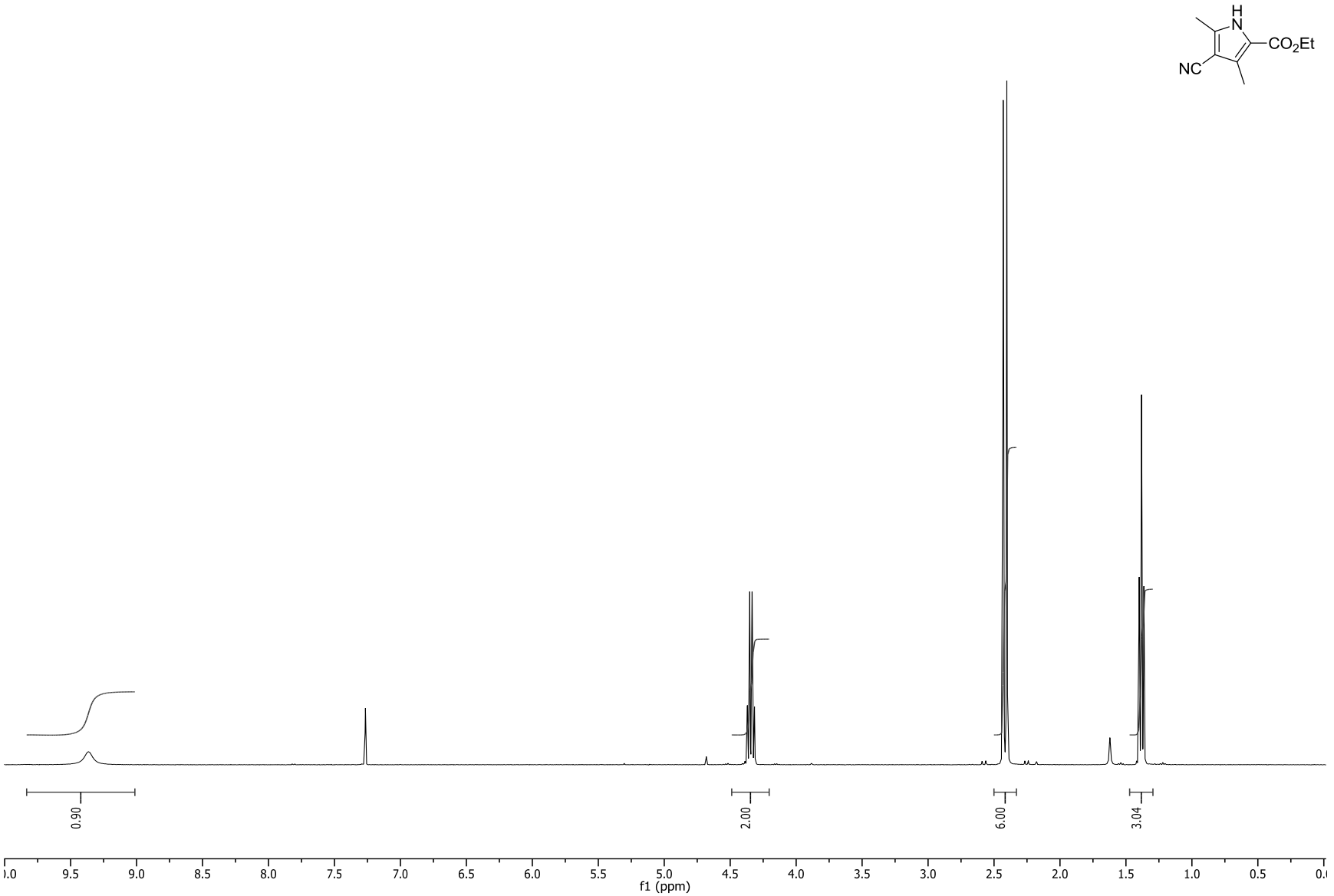

^{1}H NMR spectrum of benzyl hydroxyiminopyrrole carboxylate **80** in acetone-d_6 at 400 MHz

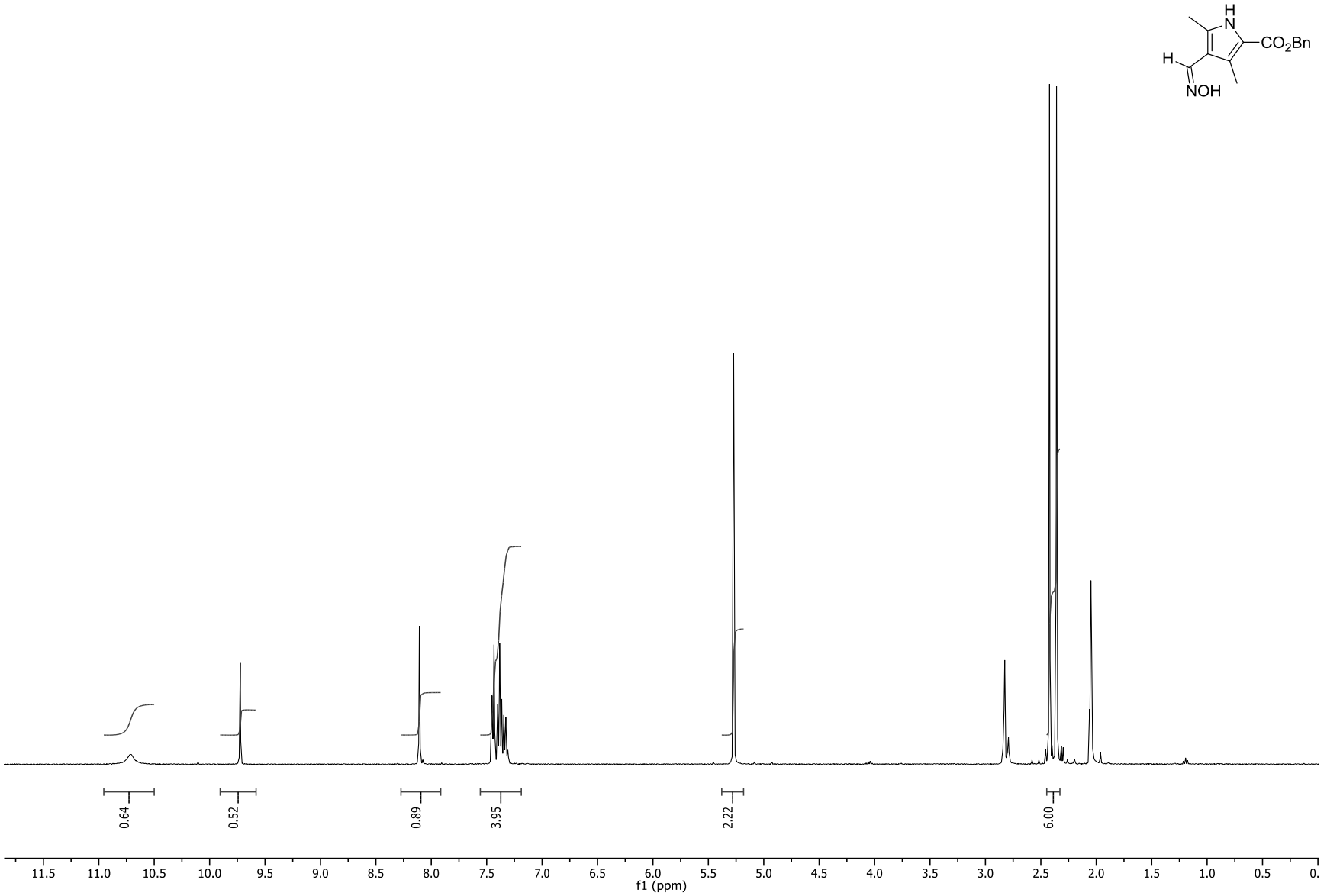

^{1}H NMR spectrum of benzyl cyanopyrrole carboxylate **73** in chloroform-*d* at 400 MHz

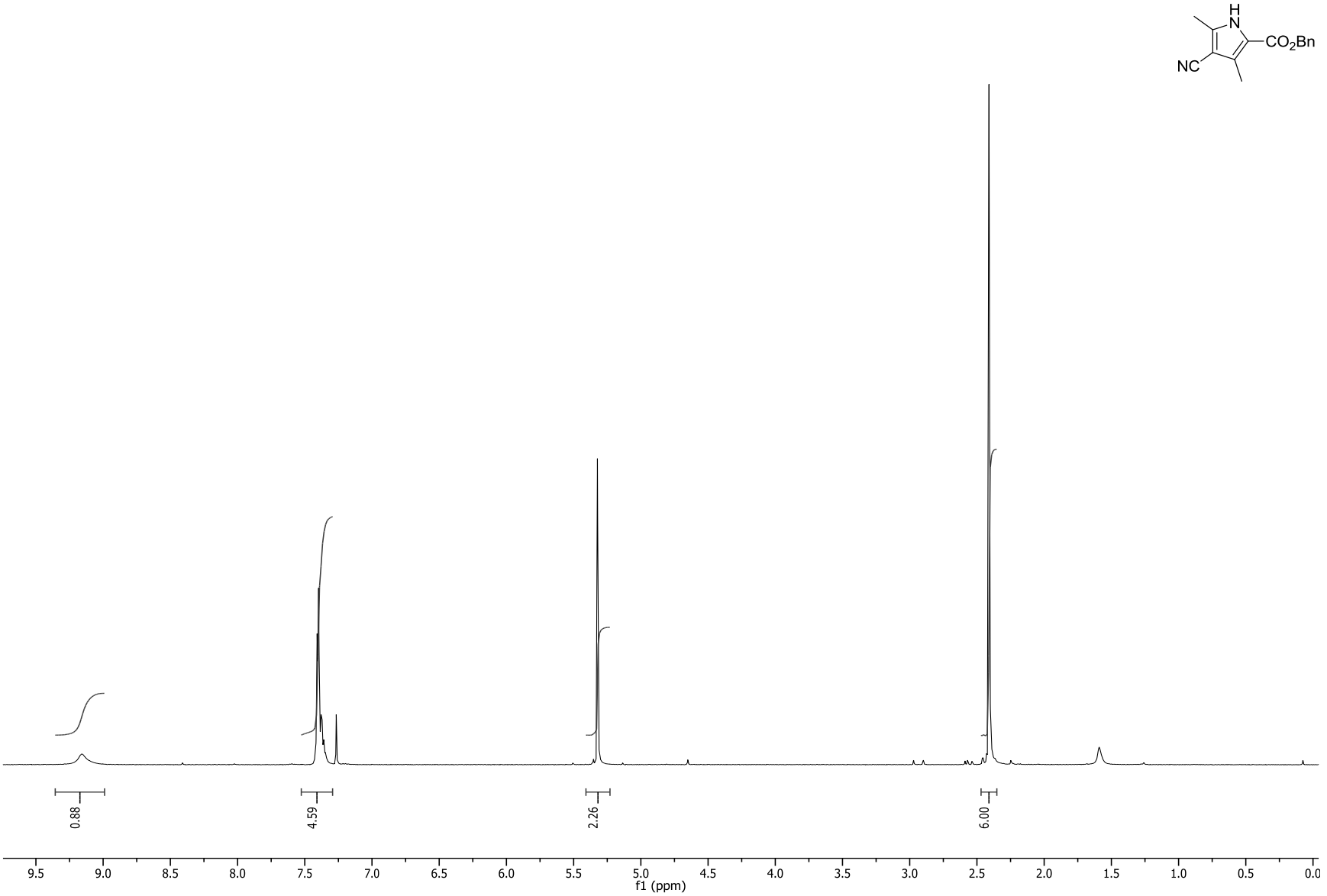

^{1}H NMR spectrum of 4-formylpyrrole **64** in Chloroform-*d* at 400 MHz

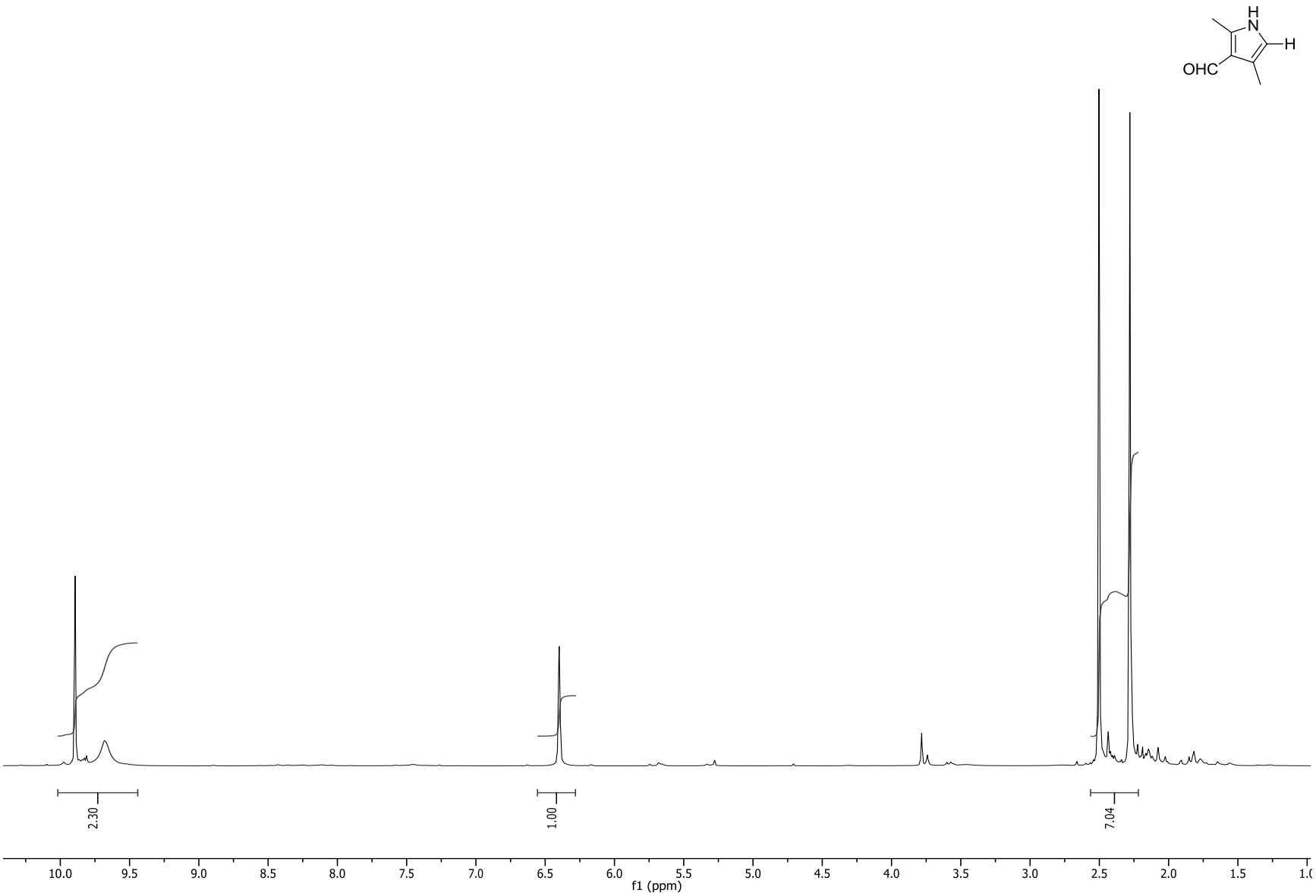

^{1}H NMR spectrum of 4-(hydroxyimino)methylpyrrole **85** in chloroform-*d* at 400 MHz

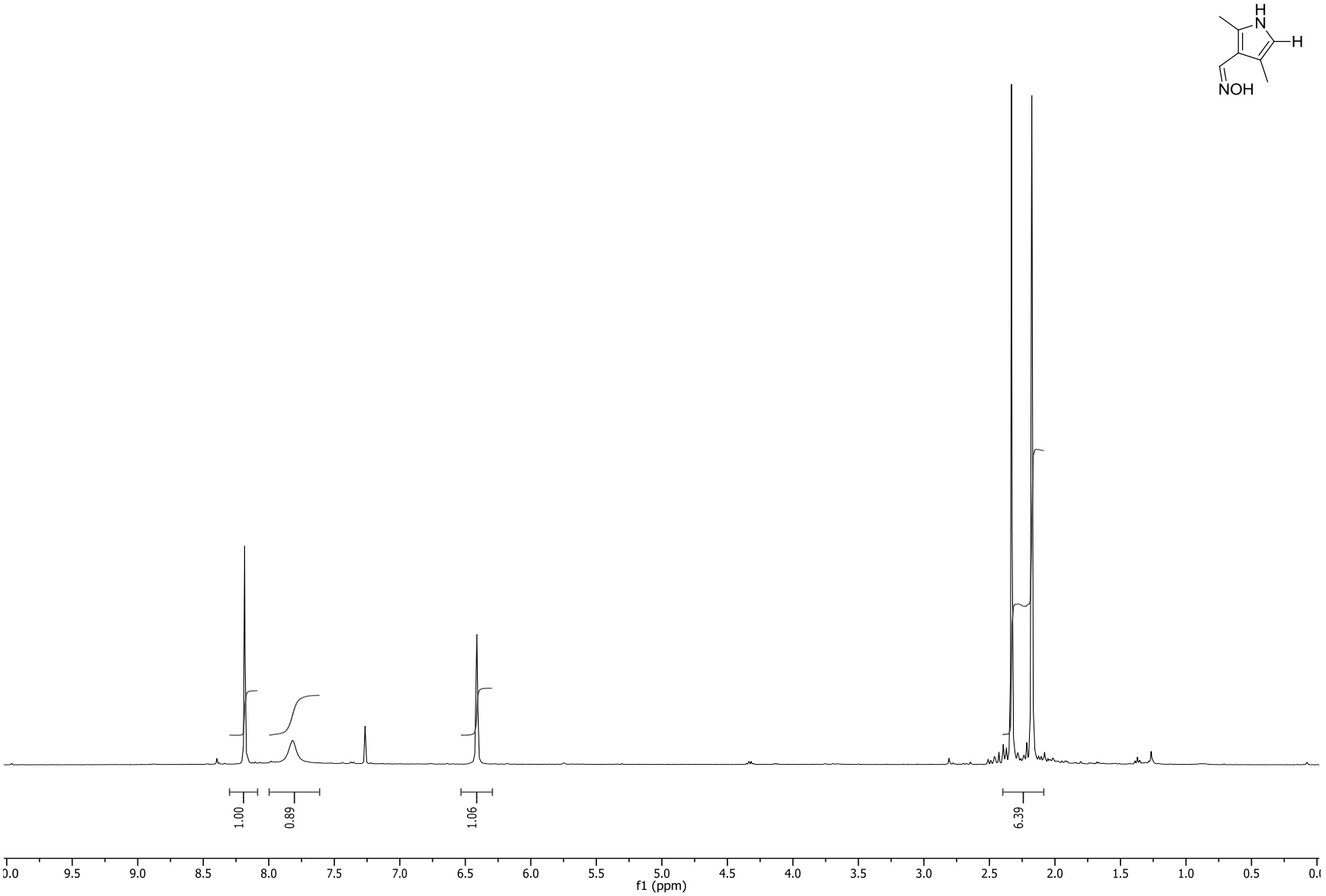

^{1}H NMR spectrum of benzyl 4-iodopyrrole carboxylate **88** in chloroform-*d*, 400 MHz

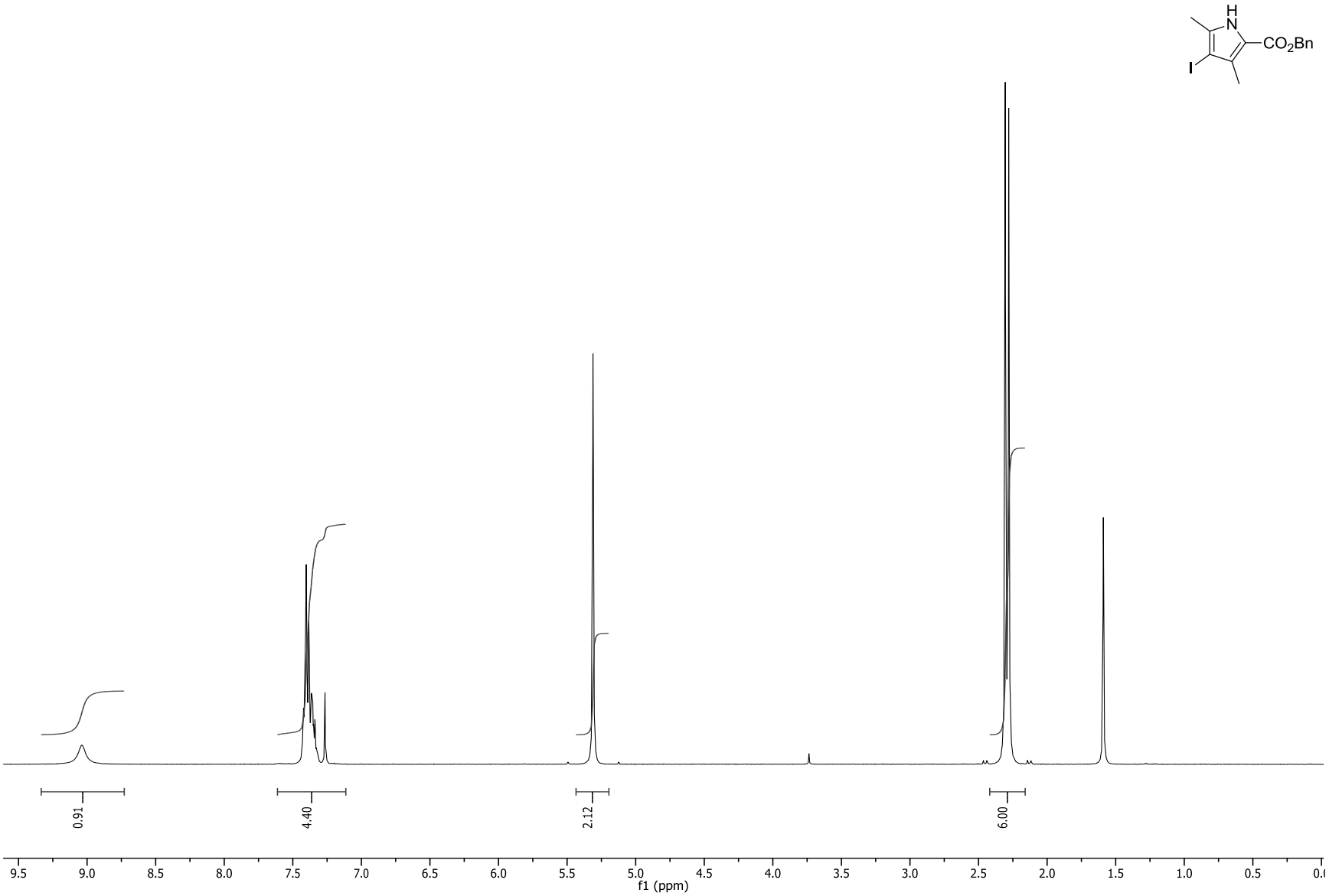

^{1}H NMR spectrum of 4-iodo-formylpyrrole **89** in chloroform-*d* at 400 MHz

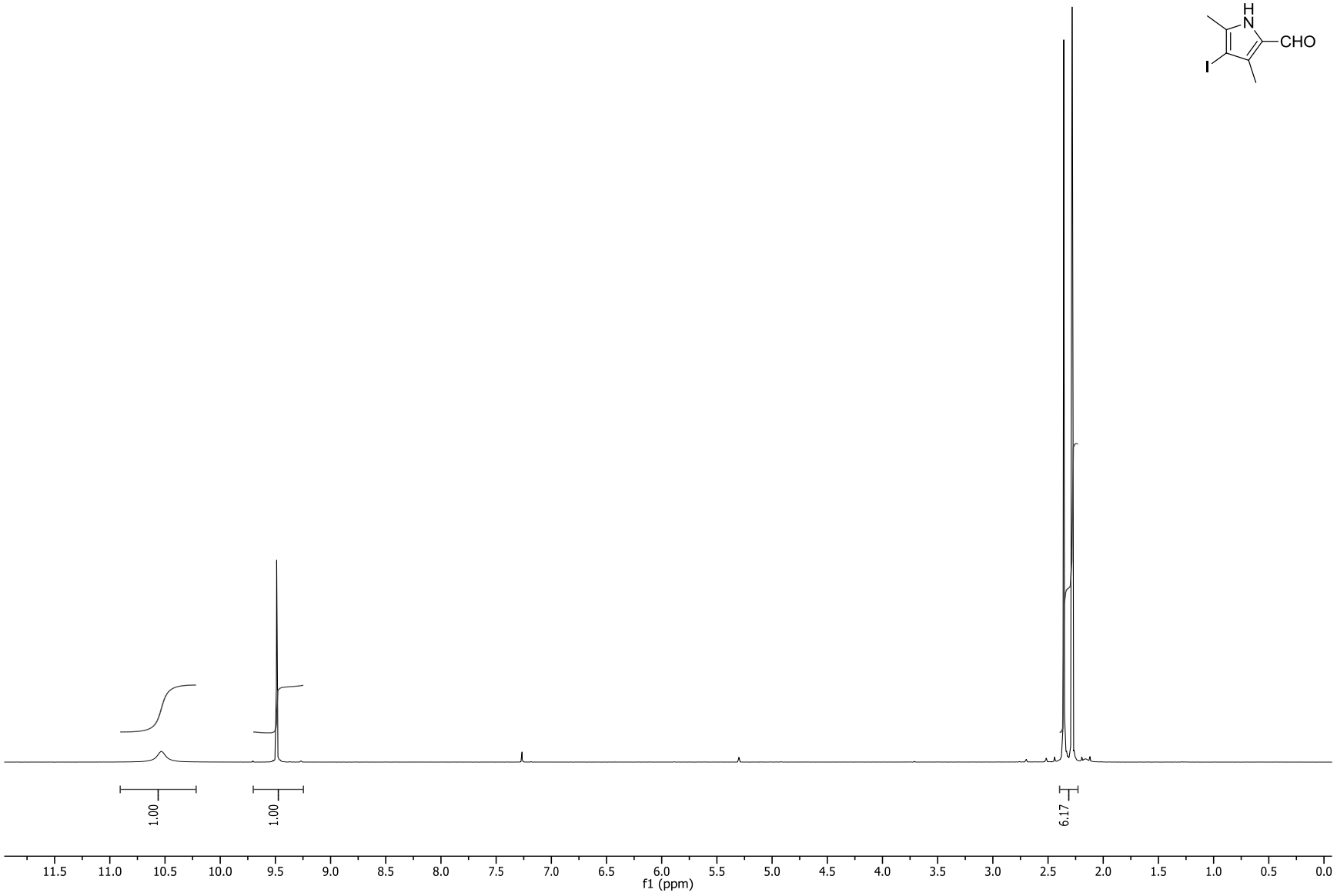

^{1}H NMR spectrum of ethylhydroxymethylpyrrole carboxylate **96** in chloroform-*d* at 400 MHz

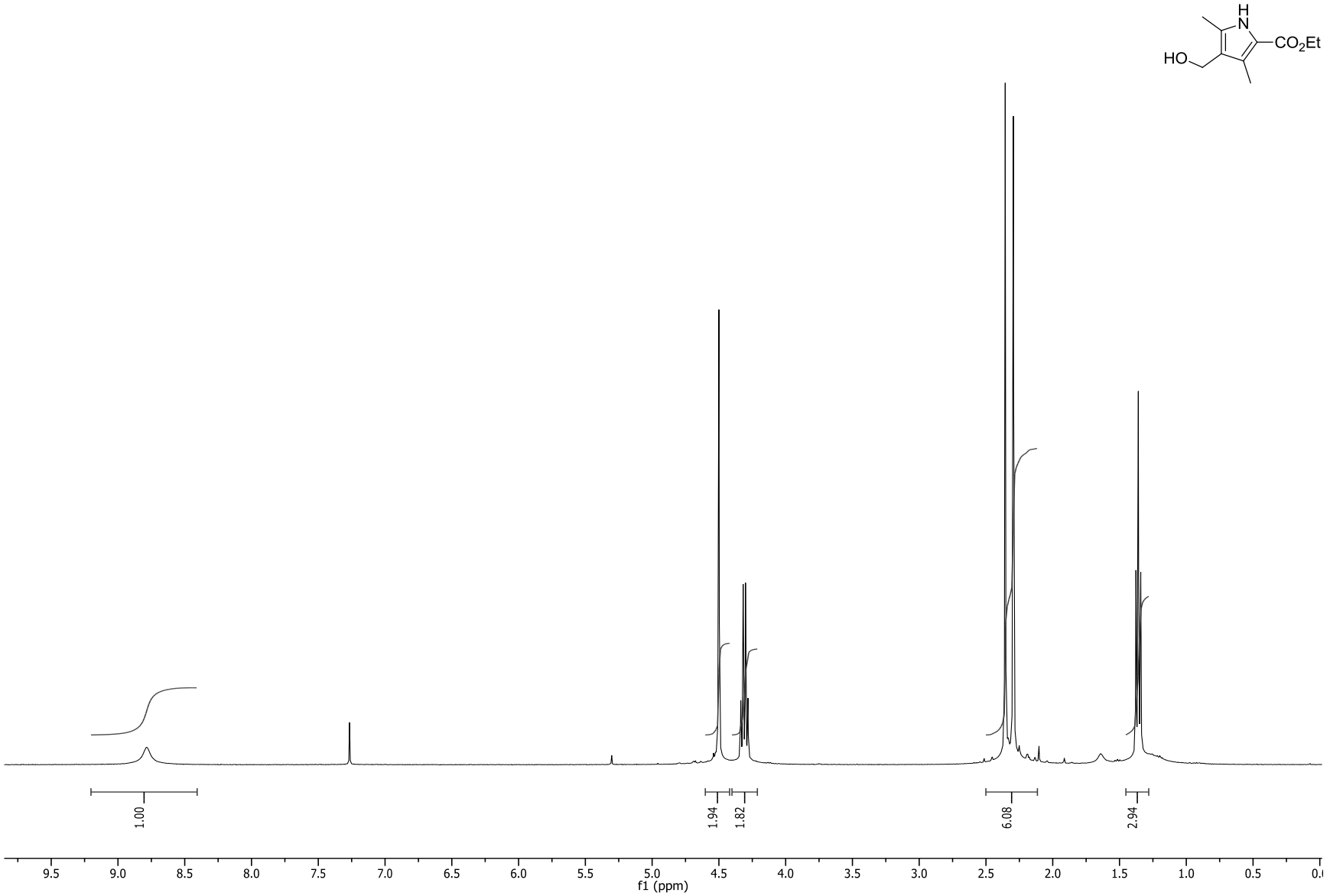

4.6 References

(1) Popovic´, D. M.; Zaric´, S. D.; Rabenstein, B.; Knapp, E. W. *J. Am. Chem. Soc.* **2001**, *123*, 6040.

(2) Shifman, J. M.; Gibney, B. R.; Sharp, R. E.; Dutto, P. L. *Biochemistry* **2000**, *39*, 14813.

(3) Gámiz-Hernández, A. P.; Kieseritzky, G.; Galstyan, A. S.; Demir-Kavuk, O.; Knapp, E. *ChemPhysChem* **2010**, *11*, 1196.

(4) Keilin, D. *Nature* **1927**, *119*, 670.

(5) Reedy, C. J.; Gibney, B. R. *Chem. Rev.* **2004**, *104*, 617.

(6) Koder, R. L.; Valentine, K. G.; Cerda, J.; Noy, D.; Smith, K. M.; Wand, A. J.; Dutton, P. L. *J. Am. Chem. Soc.* **2006**, *128*, 14450.

(7) Ghirlanda, G.; Osyczka, A.; Liu, W.; Antolovich, M.; Smith, K. M.; Dutton, P. L.; Wand, A. J.; DeGrado, W. F. *J. Am. Chem. Soc.* **2004**, *126*, 8141.

(8) Rau, H. K.; Haehne, W. *J. Am. Chem. Soc.* **1998**, *120*, 468.

(9) *Organized Monolayers and Assemblies: Structure, Processes, and Function.*; 1 ed.; Romero, M. T.; Miller, R., Eds.; Elsevier B.V: Amsterdam, 2002; Vol. 16.

(10) Kalsbeck, W. A.; Robertson, D. E.; Pandey, R. K.; Smith, K. M.; Dutton, P. L.; Bocian, D. F. *Biochemistry* **1996**, *35*, 3429.

(11) Cavaleiro, J. A. S.; Gonsalves, A. M. d. A. R.; Kenner, G. W.; Smith, K. M. *J. Chem. Soc., Perkin Trans. 1* **1974**, 1771.

(12) Ullman, G. M.; Knapp, E. W.; Kostic, N. *J. Am. Chem. Soc.* **1997**, *119*, 42.

(13) Hulko, M.; Hospach, I.; Krasteva, N.; Nelles, G. *Sensors (Basel)* **2011**, *11*, 5968.

(14) Vazquez-Duhalt, R. *J. Mol. Catal. B: Enzym.* **1999**, *7*, 241.

(15) Bernhardt, R. *J. Biotechnol.* **2006**, *124*, 128.

(16) *Hetarenes and Related Ring Systems*; Weinreb, S. M., Ed.; Thieme Medical Publishers: New York, 2004; Vol. 17.

(17) Lindsey, J. S.; Schreiman, I. C.; Hsu, H. C.; Kearney, P. C.; Marguerettaz, A. M. *J. Org. Chem.* **1987**, *52*, 827.

(18) *Synthesis and Organic Chemistry*; Lindsey, J., Ed.; Academic Press: Boston, 2000; Vol. 1.

(19) Paine, J. B.; Chang, C. K.; Dolphin, D. *Heterocycle* **1977**, *7*.

(20) Tarlton, E. J.; MacDonald, S. F.; Baltazzi, E. *J. Am. Chem. Soc.* **1960**, *82*, 4389.

(21) Lash, T. D. *Chem. Eur. J.* **1996**, *2*, 1197.

(22) *Aromatic and Heteroaromatic Large Rings*; Montforts, F. P.; Breiling, G. B.; Kusch, D., Eds.; Thieme: Stuttgart 1997; Vol. E9.

(23) Lin, J. J.; Gerzevske, K. R.; Liddell, P. A.; Senge, M. O.; Olmstead, M. M.; Khoury, R. G.; Weeth, B. E.; Tsao, S. A.; Smith, K. M. *J. Org. Chem.* **1997**, *62*, 4266.

(24) Liddell, P. A.; Gerzevske, K. R.; Lin, J. J.; Olmstead, M. M.; Smith, K. M. *J. Org. Chem.* **1993**, *58*, 6681.

(25) Fabiano, E.; Golding, B. T. *J. Chem. Soc., Perkin Trans. 1* **1991**, 3371.

(26) Cavaleiro, J. A. S.; Gonsalves, A. M. d. A. R.; Kenner, G. W.; Smith, K. M. *J. Chem. Soc., Perkin Trans. 1* **1974**, 1771.

(27) Johnson, A. W.; Markham, E.; Price, R.; Shaw, K. B. *J. Chem. Soc.* **1959**, 3416.

(28) Swanson, K. L.; Snow, K. M.; Jeyakumar, D.; Smith, K. M. *Tetrahedron* **1991**, *47*, 685.

(29) Johnson, A. W.; Markham, E.; Price, R.; Shaw, K. B. *J. Chem. Soc.* **1958**, 4254.

(30) Smith, K. M.; Miura, M.; Tabba, H. D. *J. Org. Chem.* **1983**, *48*, 4779.

(31) Clezy, P. S.; Fookes, C., J. R.; Liepa, A. J. *Aust. J. Chem.* **1972**, *25*, 1979

(32) Rajput, A. P.; Girase, P. D. *IJPCBS* **2012**, *3*, 25.

(33) Chunchatpraserta, L.; Raob, K. R. N.; Shannon, P. V. R. *J. Chem. Soc., Perkin Trans. 1* **1992**, 1979.

(34) Swanson, K. L.; Snow, K. M.; Jeyakumar, D.; Smith, K. M. *Tetrahedron* **1991**, *47*, 685.

(35) Boschi, T.; Paolesse, R.; Tagliatesta, P. *Inorg. Chim. Acta.* **1990**, *168*, 83.

(36) Iranpoor, N.; Firouzabadi, H.; Nowrouzi, N.; D., F. *Tetrahedron. Lett.* **2006**, *47*, 6879.

(37) Veisi, H. *Synthesis* **2010**, *15*, 2631.

(38) Zhao, H.; Koenig, S. G.; Sing, S. P.; Bakale, R. P. *Org. Lett.* **2008**, *10*, 505.

(39) Li, D.; Shi, F.; Guo, S.; Deng, Y. *Tetrahedron Lett.* **2005**, *46*, 671.

(40) Luca, L. D.; Giacomelli, G.; Porcheddu, A. *J. Org. Chem.* **2002**, *67*, 6272.

(41) Burns, D. H.; Burden, M. W.; Li, Y. H. *J. Porphyrins Phthalocyanines* **1998**, *2*, 295.

(42) Martin, P.; Mueller, M.; Flubacher, D.; Boudier, A.; Blaser, H.-U.; Spielvogel, D. *Org. Process Res. Dev.* **2010**, *14*, 799.

(43) Arsenault, G. P.; Bullock, E.; MacDonald, S. F. *J. Am. Chem. Soc.* **1960**, *82*, 4384.

(44) Lee, C.-H.; Li, F.; Iwamoto, K.; Dadok, J.; Bothner-By, A. A.; Lindsey, J. S. *Tetrahedron* **1995**, *51*, 11645.

(45) Pala Wilgus, C.; Downing, S.; Molitor, E.; Bains, S.; Pagni, R. M.; Kabalka, G. W. *Tetrahedron lett.* **1995**, *36*, 3469.

(46) Johnson, A. W.; Markham, E.; Price, R.; Shaw, K. B. *J. Chem. Soc.* **1958**, 4254.

(47) *Porphyrins and Metalloporphyrins*; Smith, K. M., Ed.; Elsevier: Amsterdam, 1975.

(48) Kenner, G. W.; Rimmer, J.; Smith, K. M.; Unsworth, J. F. *J. Chem. Soc., Perkin Trans. 1* **1977**, 332.

(49) Smith, K. M.; Bisset, G. M. F. *J. Org. Chem.* **1979**, *44*, 2077.

(50) Corwin, A. H.; Krieble, R. H. *J. Am. Chem. Soc.* **1941**, *63*, 1829.

(51) Jackson, A. H.; Kenner, G. W.; Wass, J. *J. Chem. Soc., Perkin Trans. 1* **1972**, 1475.

(52) Hu, B.; Zhou, W.; Tang, Y.; Huang, C.; Liu, Z. *Ultrasonics Sonochemistry* **2010**, *17*, 288.

(53) Chu, E. J.-H.; Chu, T. C. *J. Org. Chem.* **1954**, *19*, 266.

(54) *Die Chemie des Pyrrols*; Fischer, H., Ed.; Akad. Verlagsges: Leipzig, 1934; Vol. 1.

(55) Antina, E. V.; Guseva, G. B.; Loginova, A. E.; Semeikin, A. S.; V'yugin, A. I. *Rus. J. Gen. Chem.* **2010**, *80*, 2374.

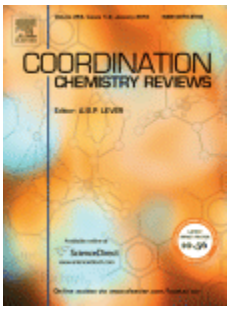

Title: Photosensitized singlet oxygen and its applications
Author: Maria C DeRosa,Robert J Crutchley
Publication: Coordination Chemistry Reviews
Publisher: Elsevier
Date: 1 November 2002

Order Completed

Thank you very much for your order.

This is a License Agreement between Raja W Jinadasa ("You") and Elsevier ("Elsevier"). The license consists of your order details, the terms and conditions provided by Elsevier, and the payment terms and conditions.

License Number	3247231468717
License date	Oct 13, 2013
Licensed content publisher	Elsevier
Licensed content publication	Coordination Chemistry Reviews
Licensed content title	Photosensitized singlet oxygen and its applications
Licensed content author	Maria C DeRosa,Robert J Crutchley
Licensed content date	1 November 2002
Licensed content volume number	233–234
Number of pages	21
Type of Use	reuse in a thesis/dissertation
Portion	figures/tables/illustrations
Number of figures/tables/illustrations	2
Format	both print and electronic
Are you the author of this Elsevier article?	No
Will you be translating?	No
Order reference number	
Title of your thesis/dissertation	Design Synthesis and Characterization of Porphyrin Derivatives for Biological Applications
Expected completion date	Dec 2013
Estimated size (number of pages)	250
Elsevier VAT number	GB 494 6272 12
Permissions price	0.00 USD
VAT/Local Sales Tax	0.00 USD / 0.00 GBP
Total	0.00 USD

Title:	Syntheses and Cellular Investigations of 17^3-, 15^2-, and 13^1-Amino Acid Derivatives of Chlorin e_6
Author:	R. G. Waruna Jinadasa, Xiaoke Hu, M. Graça H. Vicente, and Kevin M. Smith
Publication:	Journal of Medicinal Chemistry
Publisher:	American Chemical Society
Date:	Nov 1, 2011

PERMISSION/LICENSE IS GRANTED FOR YOUR ORDER AT NO CHARGE

This type of permission/license, instead of the standard Terms & Conditions, is sent to you because no fee is being charged for your order. Please note the following:

- Permission is granted for your request in both print and electronic formats, and translations.
- If figures and/or tables were requested, they may be adapted or used in part.
- Please print this page for your records and send a copy of it to your publisher/graduate school.
- Appropriate credit for the requested material should be given as follows: "Reprinted (adapted) with permission from (COMPLETE REFERENCE CITATION). Copyright (YEAR) American Chemical Society." Insert appropriate information in place of the capitalized words.
- One-time permission is granted only for the use specified in your request. No additional uses are granted (such as derivative works or other editions). For any other uses, please submit a new request.

THE VITA

R. G. Waruna E. Jinadasa was born in Colombo, Sri Lanka, to Mr. R. G. Jinadasa and Mrs. D. R. Latha Jinadasa. He had his secondary education at Royal College, Colombo. Then he entered the University of Colombo in year 2002 and graduated with an Honors Degree in chemistry in 2006.

After serving for a few months as a teaching assistant at the Department of Chemistry, University of Colombo, he was accepted to Graduate School Doctoral program at Louisiana State University (LSU) in the Department of Chemistry in 2008. He joined the laboratory of Prof. Kevin M. Smith in January 2009 where he carried out his doctoral research work on porphyrin derivatives of biomedical relevance. He is a candidate for the degree of Doctor of Philosophy in the Fall Commencement 2013.